Report No. FAA-RD-74-179, II

NASA TMX-62,396

A STOL AIRWORTHINESS INVESTIGATION USING A SIMULATION OF AN AUGMENTOR WING TRANSPORT

Volume II - Simulation Data and Analysis

Robert K. Heffley, Robert L. Stapleford, Robert C. Rumold, and John M. Lehman
Systems Technology, Inc.
Mountain View, Calif. 94043

Barry C. Scott
Federal Aviation Administration
Ames Research Center
Moffett Field, Calif. 94035

Charles S. Hynes
Ames Research Center
Moffett Field, Calif. 94035

October 1974

Final Report

Prepared for

U.S. DEPARTMENT OF TRANSPORTATION
FEDERAL AVIATION ADMINISTRATION
Systems Research & Development Service
Washington, D.C. 20590

1. Report No. TM X-62,396 FAA-RD-74-179-II	2. Government Accession No.	3. Recipient's Catalog No.
4. Title and Subtitle A STOL AIRWORTHINESS INVESTIGATION USING A SIMULATION OF AN AUGMENTOR WING TRANSPORT Volume II – Simulation Data and Analysis		5. Report Date October 1974 6. Performing Organization Code
7. Author(s) Robert K. Heffley, Robert L. Stapleford, Robert C. Rumold, and John M. Lehman Charles S. Hynes, Barry C. Scott		8. Performing Organization Report No. A-5798 10. Work Unit No. 182-530-035.2
9. Performing Organization Name and Address Systems Technology, Inc. Mountain View, Calif. 94043 Ames Research Center Moffett Field, Calif. 94035 Federal Aviation Administration Ames Research Center Moffett Field, Calif. 94035		11. Contract or Grant No. NAS2-7926 13. Type of Report and Period Covered Final Report
12. Sponsoring Agency Name and Address Department of Transportation Federal Aviation Administration Washington, D.C. 20590 and Ames Research Center Moffett Field, Calif. 94035		14. Sponsoring Agency Code
15. Supplementary Notes		

16. Abstract

A simulator study of STOL airworthiness criteria was conducted using a model of an augmentor wing transport. This study covered the approach, flare and landing, go-around, and takeoff phases of flight. The two volumes of this report document the results of that investigation.

Volume One (NASA TM X-62,395; FAA-RD-74-179-I) summarizes the results and discusses possible implications with regard to airworthiness criteria. The results provide a data base for future STOL airworthiness requirements and a preliminary indication of potential problem areas. The results are also compared to the results from an earlier simulation of the Breguet 941S. Where possible, airworthiness criteria are proposed for consideration.

Volume Two (NASA TM X-62,396; FAA-RD-74-179-II) contains a detailed description of the simulation and the data obtained. These data include performance measures, pilot commentary, and pilot ratings. This volume also contains a pilot/vehicle analysis of glide slope tracking and of the flare maneuver.

17. Key Words (Suggested by Author(s))

Short takeoff and landing
Powered lift
Airworthiness criteria

18. Distribution Statement

Document is available to the public through the National Technical Information Service, Springfield, Virginia 22151.

STAR Category – 02

19. Security Classif. (of this report)	20. Security Classif. (of this page)	21. No. of Pages	22. Price
Unclassified	Unclassified	222	

TABLE OF CONTENTS

		Page
I.	INTRODUCTION	1
II.	SIMULATION DESCRIPTION	4
	A. Piloting Tasks	4
	1. Approach Task	8
	2. Landing Task	10
	3. Go-Around Task	10
	4. Takeoff Task	11
	B. Cockpit Layout	12
	C. Simulator Apparatus	12
	D. Mathematical Model	19
	E. Subject Pilots	21
	F. Data Gathering	21
	1. Pilot Evaluation Information	21
	2. Pilot Performance Printout	21
	3. Analog Strip Chart Recordings	28
	4. Flare Maneuver Plots	28
III.	ILS TRACKING	31
	A. Tabulation of Results	31
	1. Pilot Comments	31
	2. Pilot Ratings	31
	3. Measured Performance Data	31
	B. Analysis of Results	33
	1. Approach Speed Variation	40
	2. Airframe Natural Response Variation	53
	3. Complementary Control Response Variation	53
	4. Complementary Control Orientation	54
	5. Piloting Technique Variation	58
	6. Augmentation Level Variation	59
	a. SAS Off	59
	b. Flight Director On	59
	c. Configuration SAS	61

Page

IV. FLARE AND LANDING 62
A. Types of Data 62
1. Pilot Comments 62
2. Pilot Ratings 63
3. Flare Profile 63
4. Touchdown Performance Data 63
B. Results 63
1. Approach Speed Variation 63
2. Complementary Control Variations 84
3. Ground Effects 85
4. Approach Speed Compensation for Tailwinds 86

V. GO-AROUND 92
A. AEO Go-Arounds 93
B. OEI Go-Arounds 93
C. OEI Continued Approaches 94

VI. TAKEOFF DATA 96
A. Test Conditions 96
B. V_{MU} Testing 96
C. Balanced Field Length 96
D. V_2 Variation 98
E. V_R Abuses 100
F. Engine Failures 100
1. Performance Effects, No Wind or Turbulence 100
2. Crosswind Effects 104
3. Turbulence Effects 104
G. Pilot Comments 104

VII. SUMMARY OF RESULTS 108
A. ILS Tracking 108
B. Flare and Landing 110
C. Go-Around 111
D. Takeoff 112

REFERENCES 113

Page

APPENDIX A - SIMULATION MODEL CHARACTERISTICS 114
1. Complementary Control Characteristics 114
2. Dimensional Airframe Stability Derivatives 116
3. Airframe Transfer Functions 116
4. Trim γ - V Curves 116
5. Step Control Input Time Histories 116

APPENDIX B - ANALYSIS OF GLIDE SLOPE TRACKING 136
1. Classification of Key Control Factors 136
a. Sensitivity 136
b. Control Power 137
c. Bandwidth 137
d. Cross Coupling 139
2. Analysis of Augmentor Wing 146
a. Baseline Case 150
b. Approach Speed Variation 151
c. Complementary Control Variation 151
d. Wind Variations 152

APPENDIX C - ANALYSIS OF THE FLARE AND LANDING 153
1. Flare Model Structure 153
2. Dynamics of the Flare 156
3. Pilot Adjustment of Flare Parameters 159
4. Criteria for Good Landing Characteristics 165
5. Factors Involved in Flare and Landing 165
6. Analysis of the Simulation Model 168

APPENDIX D - MATHEMATICAL MODEL 174
1. Engine Model Changes 174
2. Turbulence Model 175
3. Ground Effect 175
4. Landing Gear 175
5. Longitudinal Control System 179
6. Direct Lift/Drag Control 179

APPENDIX E - SUMMARY OF PILOT COMMENTS 181

LIST OF FIGURES

		Page
I-1	Augmentor Wing Jet STOL Research Aircraft, General Arrangement	2
II-1	Wind and Turbulence	6
II-2	Modified Cooper-Harper Rating Scale	7
II-3	Instrument Panel Layout	13
II-4	View From the Pilot's Station	15
II-5	Cockpit Instruments and Controls	16
II-6	Simulator Apparatus	17
II-7	Runway Geometry	20
II-8	Pilot Evaluation Sheet	25
II-9	Digital Printout of Approach and Landing Performance	26
II-10	Digital Printout of Takeoff Performance	27
II-11	Digital Plots Showing Vertical Flight Path	29
II-12	Digital Plots Showing Lateral Flight Path	30
III-1	ILS Tracking Task Relation of Test Cases to Baseline	39
III-2	Pilot Rating Versus Approach Speed	41
III-3	Pilot Rating Variation with Approach Speed	45
III-4	Localizer Error Versus Glide Slope Error at Various Approach Speeds in Turbulence	48
III-5	Overall Approach Speed Effect on Pilot Rating	49
III-6	G/S - IAS Coupling Parameter - Varying Approach Speed	51
III-7	G/S - IAS Coupling Parameter - Varying Wind Direction	52
III-8	Adjusted Pilot Opinion Versus Effective Frequency Response of Pilot Plus Engine	55
III-9	Adjusted Glide Slope Tracking Performance Versus Effective Frequency Response of Pilot Plus Engine	56

		Page
III-10	G/S - IAS Coupling Parameter	57
IV-1	Flare Pilot Rating Versus Approach Speed	66
IV-2	Measured Flare Profiles	67
IV-3	Landing Performance - $\dot{h}_{TD}$ vs x_{TD}	70
IV-4	Cumulative Touchdown Performance, x_{TD} and $\dot{h}_{TD}$	75
IV-5	Landing Performance vs Approach Speed	80
IV-6	General Effect of Approach Speed	82
IV-7	Margins vs Approach Speed and Steady Winds	89
IV-8	Flare Technique used in Tailwind Experiment	90
VI-1	Balanced Field Test	97
VI-2	V_2 Abuses - Variations	99
VI-3	Effects of Rotation Speed	101
VI-4	Effects of Engine Failure - No Wind or Turbulence	102
VI-5	Minimum Plane Penetrated - No Wind or Turbulence	103
VI-6	Effects of Crosswinds	105
VI-7	Effects of Turbulence	106
A-1	γ vs V Approach Configuration, δ_f = 65 deg, δ_ν = 75 deg	125
A-2	Effect of Power on V_{min}, α (V_{min})	126
A-3	γ vs V Approach Configuration, δ_f = 65 deg, δ_ν = 50 deg	127
A-4	γ vs V About Trim Point for Various Controls Used - V_{APP} = 33.5 m/s (65 kt)	128
A-5	γ vs V Takeoff Configuration: δ_f = 30 deg, δ_ν = 6 deg Max. Power (N_H = 101.7%)	129
A-6	Altitude Response to a 1-inch Column Step	130
A-7	Speed Response to a 1-inch Column Step	131
A-8	Altitude Response to a 1% Engine RPM Step	132

		Page
A-9	Velocity Response to a 1% Engine RPM Step	133
A-10	Altitude Response to a +20 Deg Nozzle Step	134
A-11	Speed Response to a +20 Deg Nozzle Step	135
B-1	G/S - IAS Coupling Parameter Varying Approach Speed . .	144
B-2	Comparison of Flight Path Response to Throttle Step Attitude vs Airspeed Constraint	145
C-1	Typical Flare Profiles - Calm Air	155
C-2	Landing Conditions vs Flare Height; $\Delta\theta/h_{FL}$ = .005 rad/sec	160
C-3	Linear Flare Solution for Varying h_{FL} and $\Delta\theta/h_{FL}$ . . .	161
C-4	Comparison of Linear Analysis to Exact	163
C-5	Touchdown Performance vs Flare Parameters; V_{APP} = 65 kt	166
C-6	Touchdown Performance vs Flare Parameters; V_{APP} = 60 kt	170
C-7	Touchdown Point vs Touchdown Airspeed Approach Speed Effect	171
C-8	Touchdown Performance vs Flare Parameters; V_{APP} = 65 kt with 10 kt Tailwind	172
D-1	Turbulence Distribution	177
D-2	Typical Turbulence Time History	178
D-3	Longitudinal Attitude Command SAS	180

LIST OF TABLES

		Page
II-1	Key to Instrument Panel Layout of Figure II-3	14
II-2	FSAA Motion Capability	18
II-3	Subject Pilot Background	22
III-1	ILS Pilot Rating Summary	32
III-2	Performance Data Versus Pilot and Configuration Flown . . .	34
III-3	Summary of Augmentation Effects (65 kt Approach Case) . . .	60
IV-1	Flare and Landing Pilot Rating Summary	64
IV-2	Results of Ground Effect Study	87
VI-1	Pilot Comments	107
A-1	K and τ Values for Complementary Controls used in Simulations	115
A-2	Longitudinal Stability Derivatives	117
A-3	Lateral-Directional Stability Derivatives	119
A-4	Longitudinal Transfer Functions - Approach Configuration .	120
A-5	Lateral-Directional Transfer Functions - Approach Configuration, SAS Off	123
A-6	Lateral-Directional Transfer Functions - Approach Configuration, SAS On	124
B-1	Interpretation of μ^{STOL}	147
B-2	Key Flight Path and Airspeed Control Parameters	148
B-3	Glide Slope Control Characteristics	149
D-1	Turbulence Parameters	176
E-1	Summary of Pilot Comments on ILS Tracking	182
E-2	Summary of Pilot Comments on Flare	195

LIST OF ABBREVIATIONS

AEO	All Engines Operating
A/C	Aircraft
ATC	Air Traffic Control
BR	Breguet
CTOL	Conventional Takeoff and Landing
DDC	Direct Drag Control
FAA	Federal Aviation Administration
FSAA	Flight Simulator for Advanced Aircraft
G/S	Glide Slope
IAS	Indicated Airspeed
IFR	Instrument Flight Rules
ILS	Instrument Landing System
MPP	Minimum Plane Penetrated
NAFEC	National Aviation Facilities Experimental Center
NASA	National Aeronautics and Space Administration
OEI	One Engine Inoperative
PIO	Pilot Induced Oscillation
POR	Pilot Opinion Rating
RMS	Root Mean Square
SAS	Stability Augmentation System
STOL	Short Takeoff and Landing
VFR	Visual Flight Rules
VASI	Visual Approach Slope Indicator

LIST OF SYMBOLS

C_ℓ	Rolling moment coefficient
C_L	Lift coefficient
$C_{L_{MAX}}$	Maximum value of lift coefficient
C_{L_α}	Lift curve slope (1/rad)
d	Glide slope deviation (ft)
g	Acceleration due to gravity
h	Altitude (ft)
$\dot{h}$	Rate of climb (ft/s)
K	Open loop gain
K_D	Drag ground effect factor
K_L	Lift ground effect factor
K_p	Open loop pilot gain
$\mathcal{L}$	Laplace operator
L_x	x scale length for turbulence model
M_λ	Partial derivative of pitch acceleration with respect to λ where λ = u, w, $\dot{w}$, q, or δ_e
n	Load factor
N_b^a	Transfer function numerator for "a" response due to "b" control
$N_{b\ d}^{a\ c}$	Coupling numerator
N_H	Engine RPM (% maximum)
n_{Z_α}	Normal load factor per unit angle of attack (g/rad)
q	Pitch rate (rad/s)
s	Laplace operator, second
S	Reference wing area (ft^2)

t	Time
T_p	Pilot lead time constant
u	x component of velocity
V	Airspeed (kt)
$\bar{V}$	Mean airspeed (kt)
V_{APP}	Target approach airspeed on the glide slope (kt)
V_{EC}	Engine out speed (kt)
V_{LOF}	Lift-off speed (kt)
V_{MC}	Minimum control speed
V_{MCG}	Ground minimum control speed
V_{min}	Minimum possible speed at given power setting (kt), $\frac{\partial \gamma}{\partial V} = \infty$ at V_{min}
V_{MU}	Minimum unstick speed (kt)
V_R	Target rotation speed (kt)
V_1	Critical engine failure speed (kt)
V_2	Takeoff safety speed (kt)
V_{35}	Speed at 35 ft height (kt)
w	z component of velocity
x_{LOF}	x distance at lift-off (ft)
x_{TD}	x distance at touchdown (ft)
x_{35}	x distance at 35 ft height (ft)
X_λ	Partial derivative of longitudinal acceleration with respect to λ where $\lambda = u, w$, or N_H
Y_p	Pilot transfer function
Y_x	Crossfeed
Z_λ	Partial derivative of vertical acceleration with respect to λ where $\lambda = u, \alpha, w, \dot{w}, q, \delta_e$, or N_H

SECTION I

INTRODUCTION

This volume presents the results of a simulator investigation of STOL airworthiness problems and criteria. This study is part of a long-range program to develop airworthiness standards for STOL aircraft. The program plan includes a series of simulation experiments using models of several different STOL design concepts, e.g. deflected slipstream, augmentor wing, and externally blown flap. This report covers the second simulation in that series. The first aircraft simulated was the French Breguet 941S, a deflected slipstream STOL transport. The results of that simulation are presented in Reference 1.

This report covers the simulation of the NASA Augmentor Wing Jet STOL Research Aircraft (AWJSRA). A three-view drawing is given in Figure I-1. The aircraft is a modified de Havilland DHC-5 BUFFALO. Augmentor-wing jet flaps, blown and drooped ailerons, and leading edge slats have been added. The wing span has been reduced to increase the wing loading. The original engines have been replaced with two Rolls Royce SPEY 801-SF turbofan engines. Cold air from the engines is ducted to the flaps and ailerons. Hot air is exhausted through vectorable PEGASUS nozzles.

The emphasis in this study has been on low-speed longitudinal flight path control since this is the area where STOL aircraft differ most from CTOL aircraft. Most of the simulation time was devoted to the approach and landing phases of flight as this was felt to be the most critical area. Considerably smaller amounts of time were spent on aborted landings (go-arounds) and takeoffs.

The report is organized generally by piloting tasks with simulator and analysis results contained within the body of the report. The analytical techniques which were utilized are described in the appendices.

Section II contains a detailed description of the simulation hardware and design of the experiment. Starting with Section III the individual piloting task results are discussed. Section III deals with the ILS approach, Section IV the flare and landing, Section V the go-around, and Section VI the takeoff. Findings are summarized in Section VII.

Figure I-1

AUGMENTOR-WING JET STOL RESEARCH AIRCRAFT

General Arrangement

Appendix A presents the characteristics of the airplane model. Appendix B describes the analytical techniques used to study glide slope tracking problems and Appendix C the techniques for flare and landing. Appendix D is a detailed description of math model changes from the basic AWJSRA model supplied by NASA. Finally, Appendix E contains a summary of pilot comments and ratings obtained during the simulation.

SECTION II

SIMULATION DESCRIPTION

This section describes the simulation experiment, the equipment and facilities used, and the nature of the data collected. This description is organized in the following sequence:

- Piloting Tasks
- Cockpit Layout
- Simulator Apparatus
- Mathematical Model
- Subject Pilots
- Data Gathered

A. PILOTING TASKS

The piloting tasks which made up the simulation experiment could be broken down into four general classifications:

- Approach
- Landing
- Go-Around
- Takeoff

In general, the first three tasks were performed during the course of a single run, that is, the pilot would fly an approach ending with either a landing or a go-around.

The adversity factors which could be introduced into these tasks consisted of:

- Wind and turbulence
- IFR conditions
- Engine failure

Figure II-1 depicts the combinations of winds and turbulence used during this simulator experiment. Wind speed is shown as a function of altitude (above 200 ft wind speed was held constant). The turbulence is more completely described in Appendix D, Mathematical Model.

Each pilot participating in the experiment was given substantial opportunity to acquaint himself with the simulator and the aircraft being simulated. Only after a pilot felt satisfied with his level of proficiency with each new configuration or approach speed was formal testing begun.

The ability of the pilot to perform a combination of tasks with a given configuration was generally evaluated under 3 different conditions or sets of adversities. Typically a pilot would fly and evaluate a given configuration on a combination of tasks such as approach and landing. Initially, the pilot would fly with minimum adversity, case 1 (no wind, no turbulence, VFR). After the pilot had performed the tasks a number of times and felt somewhat comfortable with the airplane, the pilot rated his ability to perform each of the assigned tasks. A modified Cooper-Harper Rating Scale was used. This scale was modified to eliminate ambiguities in addressing the question of airworthiness as opposed to handling qualities. A detailed description of the rating scale is shown in Figure II-2. For the calm air task a minimum acceptable rating for routine airline operations was a 3.5.

The level of adversity was then increased and the pilot again performed the combination of tasks; however, he now had to fly in IFR conditions (ceiling of 60 m [200 ft]), with wind and turbulence. The winds and turbulence used for the five runs that followed are defined in cases 2 through 6 of Figure II-1. After the completion of case 6, the pilot was again asked to rate his ability to perform each of the tasks in the presence of winds and turbulence under IFR conditions. The minimum acceptable rating for this was 6.5.

Wind shears were added in cases 7 through 11 (Figure II-1). For case 12 the ceiling was set to zero so the pilot would be called upon to perform a go-around task rather than the landing task he had been expecting. An engine might be failed during the performance of the tasks which would further add to the pilot workload. Engine failures and case-12 mandatory go-arounds were inserted randomly in each series of runs.

Notes:

1. Case 1 has no wind, no turbulence
2. Case 2 has zero mean wind but does have turbulence
3. Runway Heading = 090 deg
4. x/y → Surface Wind = x deg at y kt
5. Standard level of turbulence is σ_{ug} = 1.4 m/s (4.5 ft/sec)

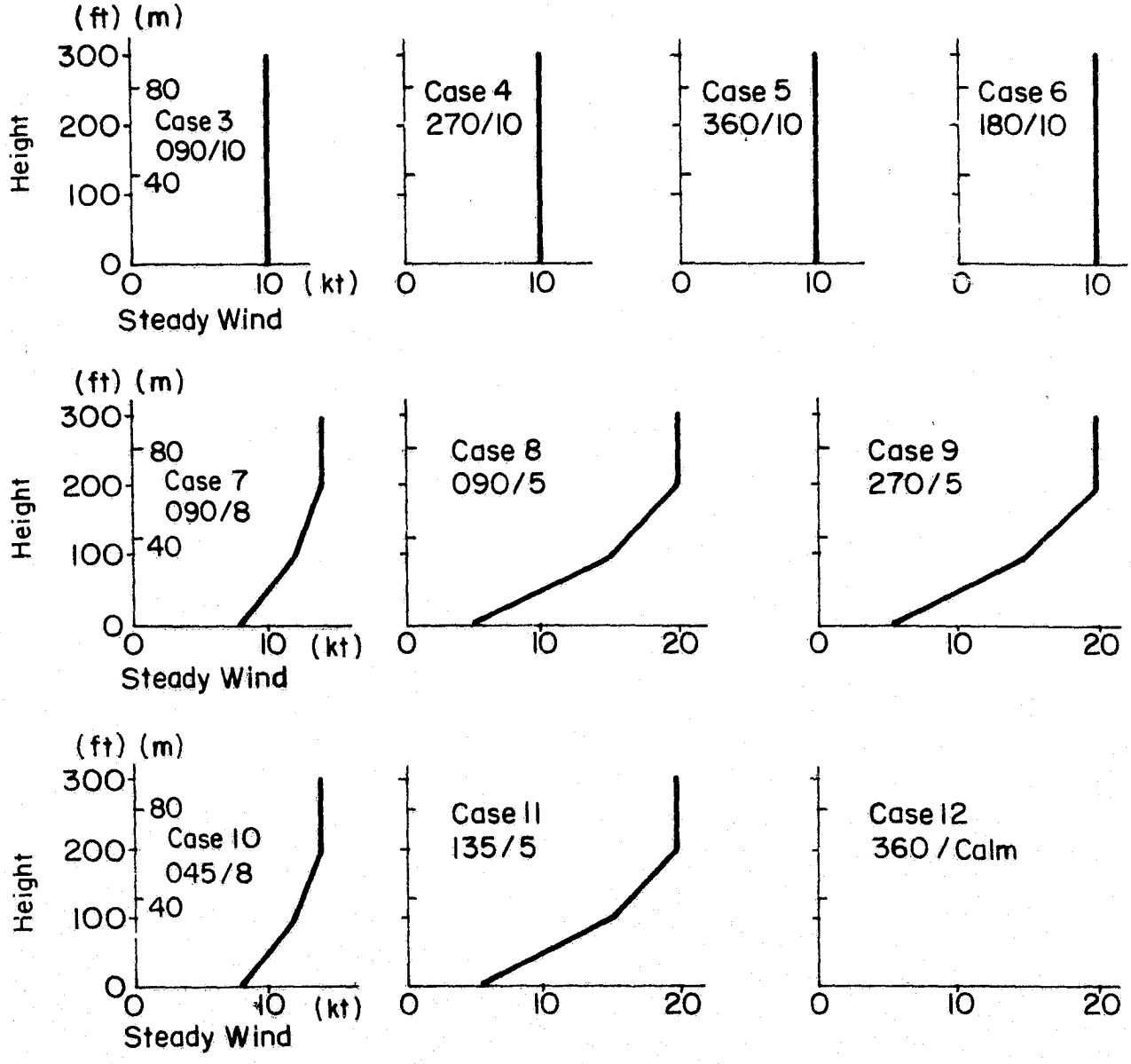

Figure II-1. Wind and Turbulence

Figure II-2

Modified Cooper-Harper Rating Scale

GENERAL CHARACTERISTICS	SAFETY MARGINS	DEMANDS ON THE PILOT	PILOT RATING
Excellent Highly desirable	Clearly adequate	Pilot compensation not a factor for desired performance	1
Good Negligible deficiencies	Clearly adequate	Pilot compensation not a factor for desired performance	2
Fair - Some mildly unpleasant deficiencies	Clearly adequate	Minimal pilot compensation required for desired performance	3
Minor but annoying deficiencies	Clearly adequate	Desired performance requires moderate pilot compensation	4
Moderately objectionable deficiencies	Adequate	Adequate performance requires considerable pilot compensation	5
Very objectionable but tolerable deficiencies	Marginal	Adequate performance requires extensive pilot compensation	6
Major deficiencies	Inadequate	Adequate performance not attainable with maximum tolerable pilot compensation Controllability not in question	7
Major deficiencies	Inadequate	Considerable pilot compensation is required for control	8
Major deficiencies	Inadequate	Intense pilot compensation is required to retain control	9
Major deficiencies	None	Control will be lost during some portion of required operation	10

At the conclusion of these six cases (7 through 12), the pilots were once again asked to rate their ability to perform the assigned tasks in the environment of the turbulence and shears. The minimum acceptable rating here was also 6.5. Although the turbulence and shears did not directly affect flight path control above 60 m (200 ft) they did force the pilot to fly to a smaller window prior to flare.

After the pilot had completed the formal testing of the configuration, he was able to repeat specific environmental conditions to aid in his evaluation. Once the pilot left the simulator cab he was asked to fill out the Pilot Evaluation Sheet described at the end of this section.

1. Approach Task

This was the most frequently performed task of the experiment. Nominally, the task consisted of flying a straight-in approach on a 7.5 deg glide slope.

The baseline condition about which the testing was done was: 18144 kg (40,000 lb); 65 kt; 65 deg flap; 75 deg nozzle; pitch, roll, and yaw SAS on; and flight director off. The conventional STOL technique (flight path with power, airspeed with attitude) was used by the pilots. After the baseline configuration was established the following alternate configurations were investigated:

- The approach speed was varied with data being taken at 75, 70, 60, and 55 kt trim flight conditions.
- The airframe natural response was altered by operating the airplane at 55 kt, 50 deg nozzle
- Thrust control response was investigated using 1.5 and 2.5 sec engine time constants (nominal was .7 sec)
- Effective thrust orientation was evaluated using DLC (vertical), nozzle (horizontal), and DDC (horizontal) instead of the normal power control
- The investigation of piloting technique was performed using nozzle control with CTOL and STOL techniques, DDC with CTOL

and STOL techniques, and throttle control using CTOL and STOL techniques

- The effects of augmentation were tested by operating without any SAS and by operating with the flight director on.

For the approach task, the airplane was initially trimmed in the landing configuration on the glide slope and localizer at an altitude of 335 m (1100 ft), about 2.5 km (1.3 miles) from the end of the runway. Typically, flaps were 65 deg and nozzles were 75 deg; for 65 kt the engines were at 91% RPM and the pitch angle was -2.3 deg. The pilot was given surface wind conditions.

The approach task was initiated as the pilot began flying the aircraft and continued until one of three events occurred:

- The pilot signaled that he was unable to fly this particular run and was, therefore, terminating the run
- The pilot initiated a landing flare
- The pilot initiated a go-around.

The pilot was told that the task consisted of tracking the localizer and glide slope at a target airspeed. Each pilot was aware of the glide path sensitivities and transmitter locations. Because of the depth of experience of the subject pilots, no weighting was given to the importance of one parameter versus another; each pilot divided his attention among the various tracking parameters as he considered appropriate. Tracking performance was measured between 300 m (1000 ft) and 100 m (300 ft) and the pilot was asked to rate the task.

Early in the experiment the approach task was initiated in a cruise configuration on a course intercepting the localizer at a 45 deg angle. The pilot would then have to transition to the landing configuration while slowing down. Once the deceleration was completed the pilot would capture the glide slope and localizer. Because of the relative ease of this sequence of maneuvers and the long period of simulator time required, the overall task was altered so that the pilot would start on the glide path at 335 m (1100 ft) altitude in the landing configuration.

A very preliminary investigation of operation of the aircraft in an ATC environment was also conducted. A curved decelerating descending path approach of the type under consideration by some of the air traffic systems groups at the National Aviation Facilities Experimental Center (NAFEC) was used. The commands for flying the curved approaches were programmed into the flight director. Flap and nozzle management was automatically accomplished by a speed control system. The results of this series of tests are described in Reference 10.

2. Landing Task

The landing task was also performed frequently because most data runs consisted of an approach task and a landing task combination. The landing task really consisted of three maneuvers - flare, touchdown, and rollout. There was no formally defined beginning to the landing task. The initial conditions for this task were determined by the end points of the approach task. The task begins as the pilot increases his pitch or other flight path control to reduce his sink rate for landing. The touchdown portion begins after the pilot reaches flare attitude and continues until all three landing gear have contacted the runway. The rollout begins after gear contact and continued until the velocity reaches 3 m/s (5 kt) or the pilot terminates the run.

Again, the depth of experience of the pilots made weighting of various landing parameters unnecessary; the pilots made their own trade-offs of touchdown sink rate versus landing distance. Ideal performance was .6 - .9 m/s (2 - 3 fps) touchdown sink rate, 90 - 150 m (300 - 500 ft) down the runway (touchdown zone).

While brakes and ground steering were available, no emphasis was placed on rollout performance. Landing performance (i.e., touchdown sink rate and touchdown distance) and pilot opinion were of primary concern during this task.

3. Go-Around Task

The go-around task was performed in conjunction with the approach task; about 5% of the data runs included go-around tasks. The go-around task could be initiated in three ways:

- The pilot would be told to execute a go-around
- The pilot was still IFR at decision height
- The pilot elected to go-around because it was his judgment that he would be unable to execute a successful landing.

Pilots were generally not warned in advance that they would be executing a go-around. Each pilot was allowed to develop his own go-around procedure. While the initial conditions were variable, the optimum go-around configuration was 70 - 75 kt, 30 deg flaps, and 6 deg nozzle. The go-around climb was made on a 90 deg heading to 335 m (1100 ft). During climb the pilots were instructed to hold a pitch angle not greater than 15 deg.

During all go-around tasks pilots were most concerned with the altitude lost, particularly after an engine failure. The go-arounds that were continued to 335 m (1100 ft) allowed the minimum departure obstacle clearance plane to be determined; however, not all go-arounds were continued to 335 m (1100 ft) because of time limitations. Pilots were asked to comment on the task.

4. Takeoff Task

The takeoff tasks were performed as a separate series of evaluations. The task consisted of acceleration to rotation, rotation, liftoff, and departure climb. The task began with the airplane rolling at 20 kt on the runway with full power, 30 deg flaps, and 6 deg nozzle.

An Engine failure was introduced during different portions of the task to determine its effect on the takeoff.

The data run was concluded when:

- The pilot signaled that he was finished
- The airplane reached 335 m (1100 ft)
- The pilot performed a maneuver which would be catastrophic if continued.

The pilot was given a V_R and a V_2; he was also told to rotate rapidly upon reaching V_R. During climb, the pilot was instructed to maintain an

airspeed (V_2) unless a pitch attitude greater than 15 deg was required. Engine cuts were made at various points during the takeoff roll. Also, the pilot was instructed to perform abuses of V_R and V_2. Crosswinds and turbulence were introduced as adversity factors.

B. COCKPIT LAYOUT

The cockpit layout used in this series of tests is shown in Figure II-3. This cockpit is similar to the one used in the April/May 1973 Breguet 941S simulation. Important features include:

- Conventional transport control column and wheel
- Overhead throttle and nozzle controllers (similar to actual aircraft)
- Standard "T" instrument arrangement.

Table II-1 provides a key to the layout of the cockpit arrangement used for the experiment. The accompanying key indicates any non-standard or unusual instrument sensitivities.

The view from the pilot's station of the primary instrument panel and accompanying visual scene are shown in Figure II-4. The aircraft was at 30 m (100 ft) altitude on the glide path when the photograph was taken.

The engine instruments, engine controls, and co-pilot station are pictured in Figure II-5.

C. SIMULATOR APPARATUS

The simulator apparatus was composed of three primary elements: The simulator cab, the visual display system, and the digital computer. Figure II-6 shows the relationship of these in block diagram form.

The Ames Research Center Flight Simulator for Advanced Aircraft (FSAA) was used in this experiment. This is a six-degree-of-freedom moving base simulator with an especially long lateral travel. Table II-2 describes the basic characteristics of the motion system.

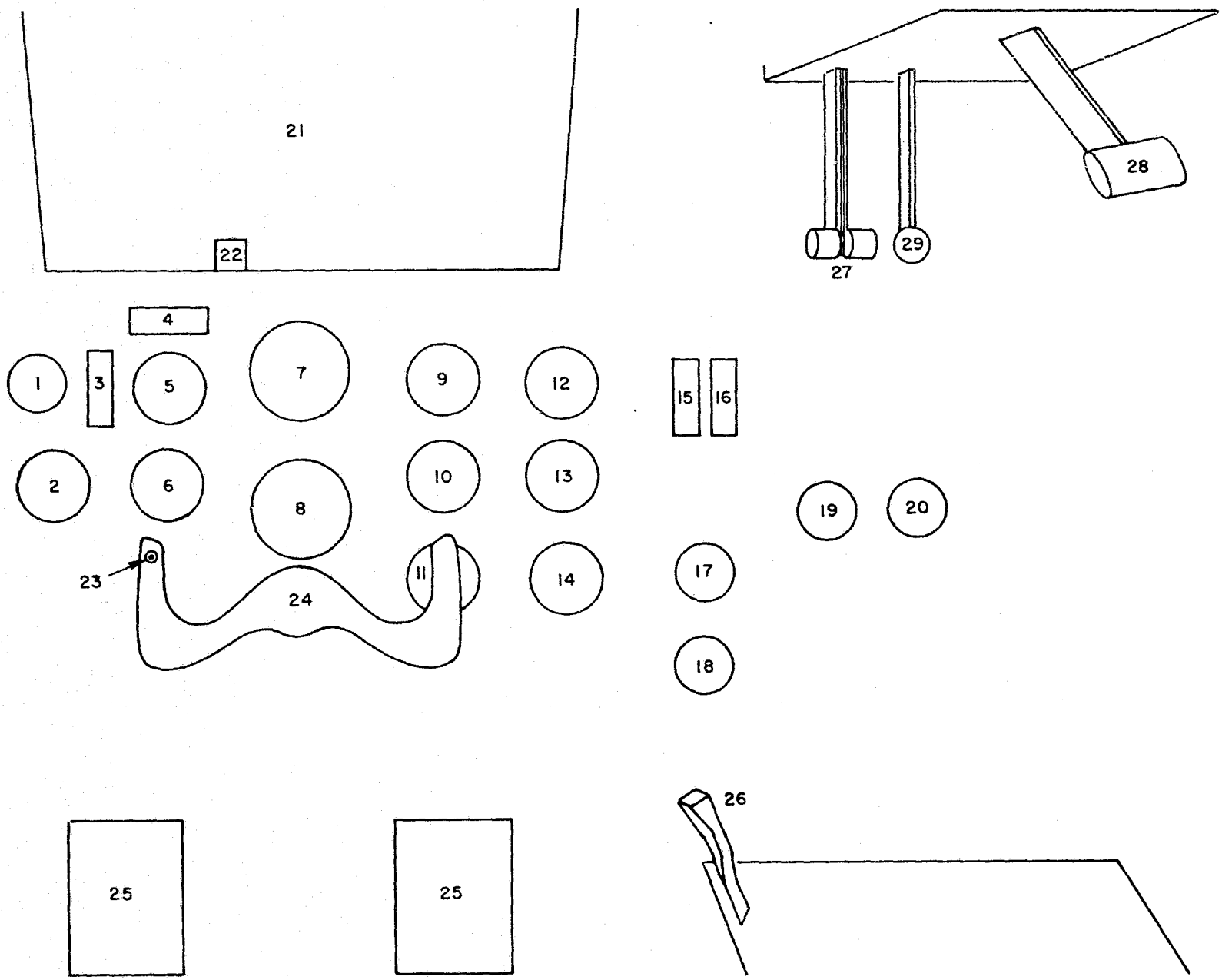

Figure II-3
Instrument Panel Layout

TABLE II-1

KEY TO INSTRUMENT PANEL LAYOUT OF FIGURE II-3

1. No. 1 engine RPM
2. Turn and bank indicator
3. Angle of attack
4. Sideslip angle
5. Indicated airspeed
6. Angle of attack
7. Attitude director indicator (includes glide slope, $\pm$ 2 deg; localizer, $\pm$ 5 deg; and fast/slow indicator)
8. Horizontal situation indicator (includes localizer data)
9. Barometric altimeter
10. Instantaneous Vertical Speed Indicator
11. Magnetic compass
12. Radar altimeter
13. Normal accelerometer
14. Elevator position indicator
15. No. 1 nozzle position indicator
16. No. 2 nozzle position indicator
17. Flap position indicator
18. Clock
19. No. 1 engine RPM
20. No. 2 engine RPM
21. Virtual image TV display
22. Angle of attack chevrons (not used)
23. Pitch trim switch
24. Control wheel
25. Rudder pedals (and brakes)
26. Direct lift or drag control lever (when used)
27. Throttles
28. Flap selector lever
29. Nozzle control lever

Figure II-4

View From the Pilot's Station

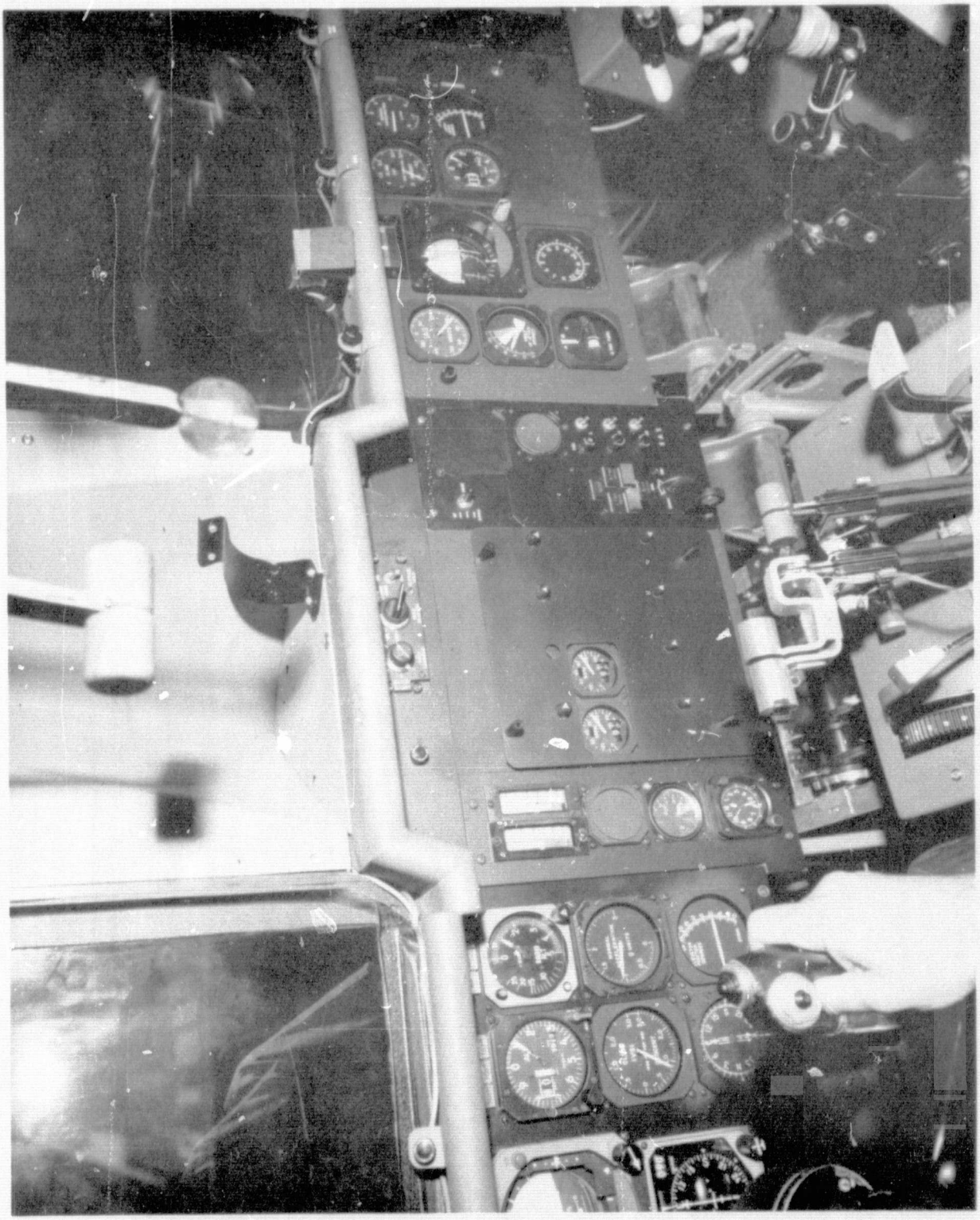

Figure II-5
Cockpit Instruments and Controls

Figure II-6. Simulator Apparatus

TABLE II-2

FSAA MOTION CAPABILITY

MOTION	DISPLACEMENT*	ACCELERATION	VELOCITY	FREQUENCY†
Roll	± 36 deg	1.6 rad/s^2	0.5 rad/s	2.1 Hz
Pitch	± 18 deg	1.6 rad/s^2	0.5 rad/s	.4 Hz
Yaw	± 24 deg	1.6 rad/s^2	0.5 rad/s	.6 Hz
Vertical	± 1.2 m (4 ft)	.30 g	2.1 m/s	.6 Hz
Longitudinal	± .9 m (3 ft)	.25 g	1.5 m/s	.8 Hz
Lateral	± 12-15 m (40-50 ft)	.30 g	5.0 m/s	.9 Hz

* Useable.

† At 30 deg phase lag without washout.

The visual scene apparatus consisted of the Ames VFA-VII Redifon system. This provided the pilot with a virtual image color TV display of a STOL runway and surrounding terrain for the purpose of heads-up navigation in the final stages of the approach.

Simulation computation was carried out entirely on an XDS Sigma 8 Digital Computer.

The runway used during the simulation is shown in Figure II-7. The touchdown zone extends from 90 - 150 m (300 - 500 ft) down the runway, indicated by the heavy lines along the runway edges. The glide slope and localizer transmitters were located 75 m (250 ft) and 640 m (2100 ft), respectively, from the touchdown end of the runway.

A simulated VASI was located on the left side of the runway near the glide slope transmitter. This VASI consisted of two lights - one upwind and the other downwind. For 1/2 deg low, the upwind light is red and the downwind light is green. The upwind light is green and the downwind light is changed to white when the airplane is 1/2 deg above the glide slope. The on-course indication is two greens. Both lights turn red or white as the deviation off course exceeds 1 deg.

D. MATHEMATICAL MODEL

The mathematical model used in this simulation was based on that described in Reference 2. Some changes were made to better serve this particular experiment. Details of the changes are given in Appendix D. Highlights of these changes are briefly outlined below:

- In the engine model, step changes in cold thrust were deleted to provide a more continuous function of thrust versus throttle position.
- Because of dynamic ground handling problems, the AWJSRA landing gear model was replaced with the BR 941S model used in the simulation of Reference 1.
- The turbulence model was also that used in previous BR 941S tests. This was for the purpose of better continuity between simulations.

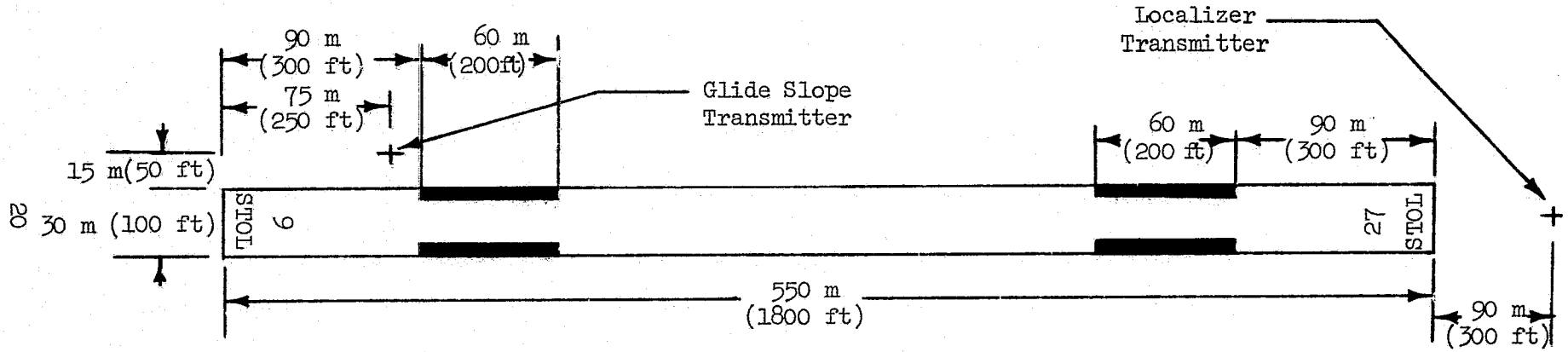

Figure II-7

Runway Geometry

- Ground effects were deleted from the basic model. In the few instances where a ground effect was evaluated the general form used in the previous BR 941S testing was employed.
- The longitudinal SAS used in the augmentor wing tests were generally similar to that used in the BR 941S testing (attitude command/ attitude hold). In doing so, the attitude control (short period) aspects were kept relatively unchanged between the two experiments.

E. SUBJECT PILOTS

A total of eight subject pilots participated in this simulator program. These pilots have diverse backgrounds but all share in currently being involved in development of STOL airworthiness standards. Also, all of the pilots have flight experience with STOL aircraft. A brief account of each pilot's background is presented in Table II-3.

F. DATA GATHERING

Several forms of data were obtained during the course of these experiments. Some were for the purpose of on-line monitoring of pilot opinion and performance while others were for analyses carried out further downstream from the actual testing. The following briefly lists and describes these data forms.

1. Pilot Evaluation Information

During simulator runs pilot ratings were requested as indicated in Section II. These ratings, along with written pilot comments, were kept as permanent records. Figure II-8 shows the evaluation sheet used for approach and landing tasks.

2. Pilot Performance Printout

For each task the pilot's relevant performance information was printed in the format shown in Figures II-9 and II-10. The first is for approach and landing or go-around and the other for takeoff. In addition, digital

TABLE II-3

SUBJECT PILOT BACKGROUND

JOHN CARRODUS ASSISTANT CHIEF TEST PILOT CAA (United Kingdom)	BRYANT CHESTNUTT FLIGHT OPERATIONS SPECIALIST FAA	LTC. ROBERT CHUBBOY (USA) R & D SPECIALIST FAA
• Some STOL experience as a certification test pilot of smaller twin turboprop types (e.g. Skyvan) plus a limited amount of heavier twin turboprop types (AVRO 748) and a jet V/STOL type (Harrier). • Limited experience in helicopters and light aircraft. • Considerable simulator experience. • Military experience as naval fighter pilot and as test pilot (primarily fighters).	• Current flight experience in conventional light twin and DHC-6. Majority of time in heavy multi-engine (DC-3, DC-4, DC-9). • Participated in STOL evaluation at NAFEC using DHC-6. • No helicopter experience. • FAA instructor and check pilot in conventional light and heavy multi-engine aircraft. Extensive experience as navigation facilities flight check pilot (DC-3 and DC-4).	• Current rotary wing and light single and twin engine fixed wing. • Extensive STOL test and operational experience (DHC-2, 4, 5, 6). • Extensive rotary wing test and operational experience in a wide range of helicopters. • Extensive research simulator experience in a wide variety of aircraft.

TABLE II-3 (Continued)

RICHARD GOUGH FLIGHT TEST PILOT FAA	GORDON HARDY RESEARCH PILOT NASA	ROBERT KENNEDY FLIGHT TEST PILOT FAA
• Current experience in conventional airplane airworthiness certification programs (DC-10, L-1011, etc.). • Research test pilot for USAF flying wide range of conventional fixed wing aircraft. (Fighter, bomber, trainer, utility, light STOL). • Limited STOL experience (YC-134, BR 941 S). • Little rotary wing experience. • Little ground based simulator experience. • R & D subject in TIFS (Concorde).	• Current flight experience largely in conventional aircraft (CV-340, CV-990, Lear Jet). • Limited experience in several STOL aircraft (DHC-5, DHC-6, AWJSRA, BR 941S) as research pilot. • No helicopter experience. • Extensive light aircraft experience. • Military experience in conventional single engine fighter/attack aircraft. • Research simulator experience in a range of handling qualities experiments (space shuttle, DHC-6, AWJSRA, etc.).	• Seven years experience as FAA flight test pilot. (Participated in STOL project at NAFEC using DHC-6 and Heliporter). • Experienced test pilot for Piasecki and Vertol in ducted fan aircraft and helicopters. • Considerable simulator experience. • Military experience in wide range of aircraft (fighter, bomber, transport, helicopter, etc.).

TABLE II-3 (Concluded)

JOHN RYAN FAA	J. P. VAN ACKER TEST PILOT CEV (France)
• Current experience as flight test pilot in NAFEC curved path MLS program. • Experienced in BR 941S and DHC-6. • Helicopter experience. • Extensive simulation experience.	• Current flight experience in military aircraft (fighter, transport) and airbus certification program. Research pilot for variable stability Mirage. • Considerable experience with Transall C160 modified for STOL operation and limited experience in BR 941S. • Military experience with fighter/attack aircraft. • Extensive simulation experience.

PILOT EVALUATION

Pilot_____ Date_____ Runs_____

Configuration_____

Pilot Ratings:	ILS	FLARE	
	_____	_____	Calm Air
	_____	_____	Turbulence/Steady Winds
	_____	_____	Turbulence/Shears

ILS Tracking

1. Evaluate task difficulty, performance, and safety margins.
2. How were the above affected by the turbulence or low visibility?
3. Describe the piloting technique used.
4. Describe any problems in trimming, tracking the ILS beam, or maintaining airspeed.

Flare and Landing

5. Evaluate task difficulty, performance, and safety margins.
6. How were the above affected by the turbulence or wind shears?
7. Describe the piloting technnique used.
8. Describe any problems encountered in the flare and landing.

General

9. What were the major factors involved in each of the ratings?
10. Add any additional comments you wish to.

Figure II-8: Pilot Evaluation Sheet

AWJSRA REAL-TIME DATA PRINTOUT

RUN NUMBER = 13 DATE: 13:39 AUG 13,'73

WEIGHT = 40000. PITCH SAS = 1 CONFIG. SAS = 0
CG = .16 YAW SAS = 1 ROLL SAS = 1

REDIFON BREAKOUT = 220.FT
GLIDE SLOPE ANGLE = 7.50 DEG

RMS UTURB = 4.41 F/S RMS VTURB = 5.00 F/S RMS WTURB = 3.00F/S

THERE WAS NO ENGINE FAILURE THIS RUN

XIC = -8105. FT YIC = 0.FT WIND = 270. DEG AT 10. KTS
HIC = 1100. FT VEQIC = 70.00 KTS
DELTA PSI = .0 DEG FLAPIC = 65.0 DEG TURB = 4.50 F/S NOZIC = 75.0 DEG

XTD = 439. HDOT = -7.5 THETA = 8.2 RPM = 89.1 NOZ = 74.1

FROM 1000 FT TO 300 FT

QUANTITY	MAX	HEIGHT	MIN	HEIGHT	MEAN	RMS DEV
LOCALIZER ERROR	.39 DEG	592. FT	-.21 DEG	300. FT	.227 DEG	.139 DEG
GLIDE SLOPE ERROR	.19 DEG	945. FT	-.00 DEG	434. FT	-.375 DEG	.377 DEG
EQUIVALENT AIRSPEED	74.95 KTS	639. FT	66.84 KTS	469. FT	70.314 KTS	1.846 KTS
VERTICAL VELOCITY	-12.87 FT/S	372. FT	-28.51 FT/S	727. FT	-19.060 FT/S	4.072 FT/S
PITCH ANGLE	-1.98 DEG	501. FT	-4.96 DEG	413. FT	-3.893 DEG	.525 DEG
ANGLE OF ATTACK	8.69 DEG	812. FT	.77 DEG	415. FT	4.669 DEG	1.693 DEG
NOZZLE DEFLECTION	74.14 DEG	1000. FT	74.14 DEG	1000. FT	74.135 DEG	.000 DEG
BANK ANGLE	2.54 DEG	966. FT	-2.16 DEG	893. FT	.390 DEG	1.081 DEG
COLUMN DISPLACEMENT	2.10 IN	830. FT	.71 IN	428. FT	1.575 IN	.200 IN
WHEEL DISPLACEMENT	14.60 IN	318. FT	-9.48 IN	685. FT	-.656 IN	3.158 IN
ENGINE RPM	91.36 PCT	392. FT	88.94 PCT	791. FT	90.187 PCT	1.472 PCT
RUDDER PEDAL DISPL.	-.28 IN	329. FT	-.30 IN	981. FT	-.286 IN	.005 IN
DELTA PSI	2.95 DEG	641. FT	-7.37 DEG	375. FT	-.608 DEG	3.048 DEG

8 13 131 5 3 4 7.5-3.0 74.63. 70.1100. 220.270.10.4.5 0.140000.0020.ND COMM
8 13 132 -3.09 .52 .38 1.08 -.61 3.04 1.57 .20 -.66 3.16
8 13 133 -.29 .00 70.31 1.85 .23 .14 -.37 .38 4.67 1.69
8 13 134 90.19 1.47 63.11 .00 74.14 .00 63.29 -7.55 439.06 2.07
8 13 135 -1.35 58.00 8.19 89.06 .00 .00 .00 .00 .009999.00
8 13 136 89.99 .00 .00 .00 .00 .00 .00 89.59 .00 .00

CARD IMAGE TAPE WRITE SUCCESSFUL

AT BREAKOUT:
RUN TIME = 49.9SEC LOC. ERROR = -.61DEG G/S ERROR = .28DEG
ALTITUDE = 208.FEET X DISTANCE FROM THRESHOLD = -1333.FEET Y DISTANCE FROM THRESHOLD = -38.FEET

FROM BREAKOUT TO 35 FT WHEEL HEIGHT

QUANTITY	MAX	HEIGHT	MIN	HEIGHT	MEAN	RMS
EQUIVALENT AIRSPEED	78.54 KTS	150. FT	64.51 KTS	59. FT	67.19 KTS	1.58 KTS
VERTICAL VELOCITY	-11.94 F/S	35. FT	-21.51 F/S	180. FT	-18.51 F/S	2.49 F/S
PITCH ANGLE	.16 DEG	35. FT	-2.96 DEG	172. FT	-2.22 DEG	.83 DEG
ANGLE OF ATTACK	8.28 DEG	98. FT	4.48 DEG	194. FT	6.36 DEG	.84 DEG
NOZZLE DEFLECTION	74.14 DEG	208. FT	74.14 DEG	208. FT	74.14 DEG	.44 DEG
BANK ANGLE	7.49 DEG	122. FT	-1.06 DEG	35. FT	2.51 DEG	2.03 DEG
COLUMN DISPLACEMENT	2.78 IN	51. FT	1.71 IN	198. FT	1.86 IN	.23 IN
WHEEL DISPLACEMENT	26.48 IN	138. FT	-21.68 IN	116. FT	-.72 IN	10.69 IN
ENGINE RPM	91.46 PCT	48. FT	89.04 PCT	208. FT	90.61 PCT	.67 PCT
RUDDER PEDAL DISPL.	.32 IN	138. FT	-.51 IN	189. FT	-.23 IN	.17 IN
DELTA PSI	1.52 DEG	49. FT	-2.69 DEG	208. FT	-.36 DEG	1.43 DEG

*******LANDING DATA

	MAX	MIN	
HDOT =	-7.07	-11.82	FT/SEC
NU =	74.14	74.14	DEG
THETA =	8.23	.21	DEG
ALFA =	14.49	5.13	DEG
RPM =	91.46	89.13	PCT
PSI =	.80	-2.55	DEG
PHI =	2.60	-3.41	DEG
DCOL =	6.96	2.26	IN

AT 35 FT WHEEL HEIGHT:
RUN TIME = 59.2 SEC X = -98. FEET Y = -15. FEET VEQ = 66.6 KNOTS
HDOT =-11.89 FT/SEC RPM = 91.43 PCT NOZZLE DEFL.=74.14DEG ALFA = 5.2 DEG
THETA = .18 DEG HEADING OFFSET= .8 DEG PHI= -1.1 DEG BETA= 2.3 DEG

AT TOUCHDOWN:
RUN TIME = 63.3 SEC X = 439. FEET Y = 2. FEET VEQ = 58.8 KNOTS
HDOT = -7.55 FT/SEC RPM = 89.06 PCT NOZZLE DEFL.=74.14DEG ALFA = 13.4 DEG
THETA = 8.19 DEG HEADING OFFSET= -1.3 DEG PHI= 2.8 DEG BETA= 1.4 DEG

NO GO-AROUND

Figure II-9: Digital Printout of Approach and Landing Performance

```
                    AWJSPA  REAL-TIME DATA PRINTOUT

 RUN NUMBER = 82                    DATE: 21:21 AUG 03,'73

 WEIGHT =  40000.                   PITCH SAS = 1      CONFIG. SAS = 0
 CG     =  .16                      YAW SAS   = 1       ROLL SAS   = 1


 REDIFON BREAKOUT =  1600.FT
 GLIDE SLOPE ANGLE =   7.50 DEG

 RMS UTURB =  .00 F/S   RMS VTURB =  .00 F/S   RMS WTURB =  .00F/S

 THERE WAS NO ENGINE FAILURE THIS RUN

 XIC =     20. FT          YIC =      0.FT        WIND =   0. DEG AT   0.  KTS
 HIC =      9. FT          VEQIC =  20.00 KTS
 DELTA PSI =     .0 DEG    FLAPIC =  30.0 DEG       TURB =   .00 F/S   NOZIC =   6.0 DEG

 XTD =    0.  HDOT =    .0  THETA =    .0  RPM =    .0  NOZ =    .0

AT ROTATION:     TIME=10.93 SEC
                 X  =     688.51 FT          VEQ   =      68.54 KTS
                 AX =      13.78 FT/SEC      DELTF =      30.12 DEG

AT LIFT OFF:
                 TIME =      12.17 SEC       X     =     838.88 FT
                 VEQ  =      75.60 KTS       THET  =      12.40 DEG
                 ALFA =      10.43 DEG       NU    =       6.00 DEG
                 Y    =       8.53 FT        PSI   =        .68 DEG
                 PHI  =        .28 DEG       BETA  =        .04 DEG

FROM START TO LIFTOFF:
                              MAX                 MIN
  THETD =                    9.91                 -.05   DEG/SEC
  THETA =                   12.40                  .25   DEG
  ALFA  =                   10.50                  .22   DEG
  NU    =                    6.00                 6.00   DEG
  PSI   =                    1.07                 -.00   DEG
  PHI   =                     .28                 -.09   DEG

DATA AT 35 FT:

                          TIME= 14.87 SEC     X= 1202. FT     HDOT= 20.77 FT/SEC
                          VEQ = 85.89 KTS     HWEEL=   35. FT

DATA FROM LIFTOFF TO 35 FT:

                              MAX                 MIN
  HDOT  =                    20.55                 4.21   FT/SEC
  VEQ   =                    85.89                75.60   KTS
  THETA =                    14.37                12.10   DEG
  ALFA  =                    10.49                 6.22   DEG


  NU    =                     6.00                 6.00   DEG
  PSI   =                     1.10                  .68   DEG
  PHI   =                      .91                  .28   DEG
  HWEEL =

DATA AT 1000 FT:

                          TIME= 35.28 SEC     X= 3981. FT     HDOT= 48.36 FT/SEC
                          VEQ = 83.59 KTS     HWEEL=  1000. FT

DATA BETWEEN 35 FT AND 1000

                              MAX                 MIN
  HDOT  =                    59.78                20.77   FT/SEC
  VEQ   =                    90.96                81.76   KTS
  THETA =                    26.57                14.44   DEG
  ALFA  =                     6.20                 1.27   DEG
  NU    =                     6.00                 6.00   DEG
  PSI   =                     6.44                 1.11   DEG
  PHI   =                     2.75                  .07   DEG
  HWEEL =

MINIMUM OBSTACLE CLEARANCE PLANE = 28.04 DEG  AT HWEEL =   997. FT
```

Figure II-10: Digital Printout of Takeoff Performance

plots were obtained of the vertical and lateral flight path. Samples of these are shown in Figures II-11 and II-12. These data were primarily for use in post simulation analyses.

3. Analog Strip Chart Recordings

For the purpose of on-line monitoring, 48 channels of analog strip chart records were taken. These records included all motion, control, and engine variables which might be necessary for either on-line or post simulation analyses.

4. Flare Maneuver Plots

A profile of each flare was recorded as an x - y plot of attitude versus altitude just prior to landing. This gave a direct measure of flare height (h_{FL}) and flare attitude ($\Delta\theta$). Samples are included in Appendix C.

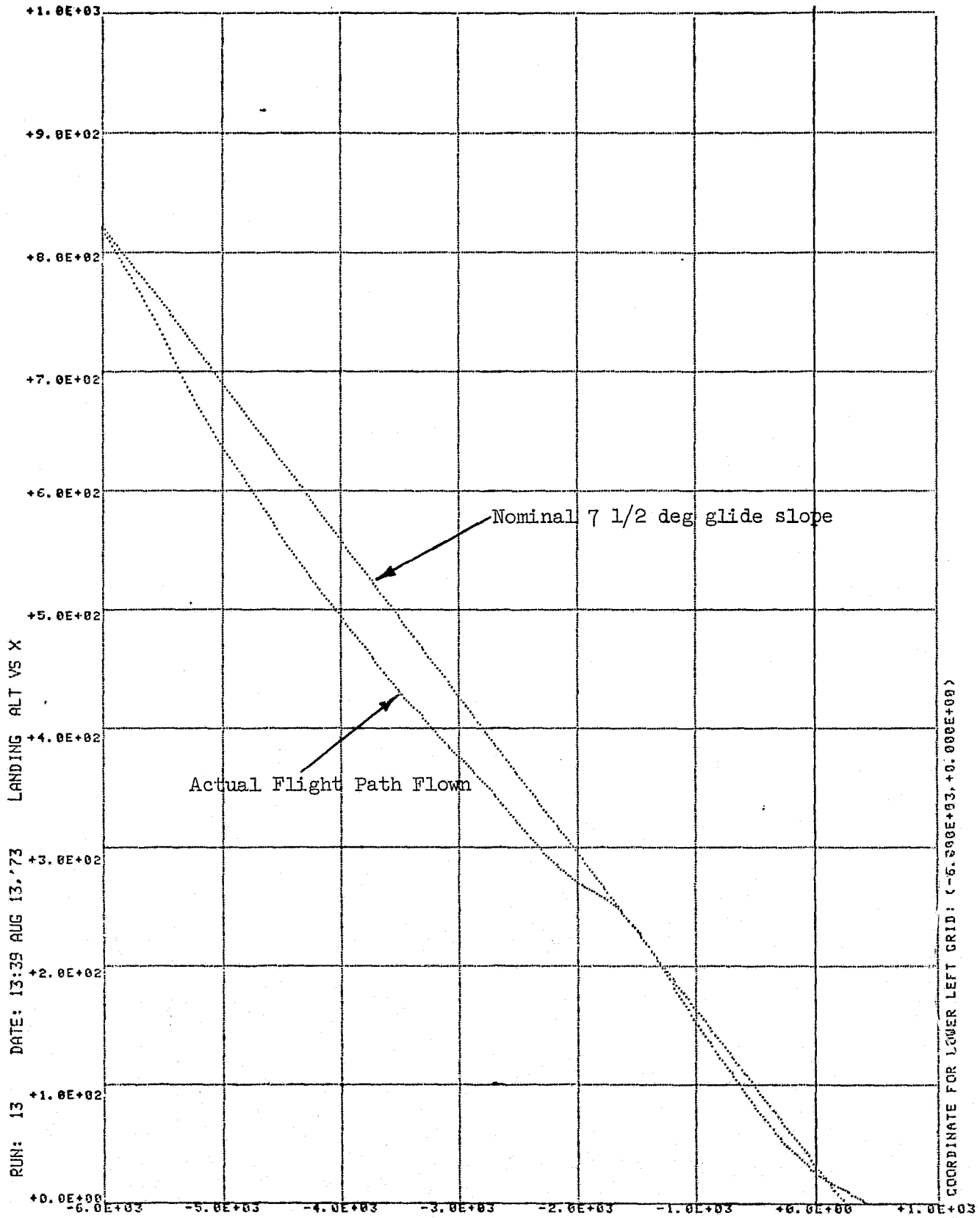

Figure II-11: Digital Plots Showing Vertical Flight Path

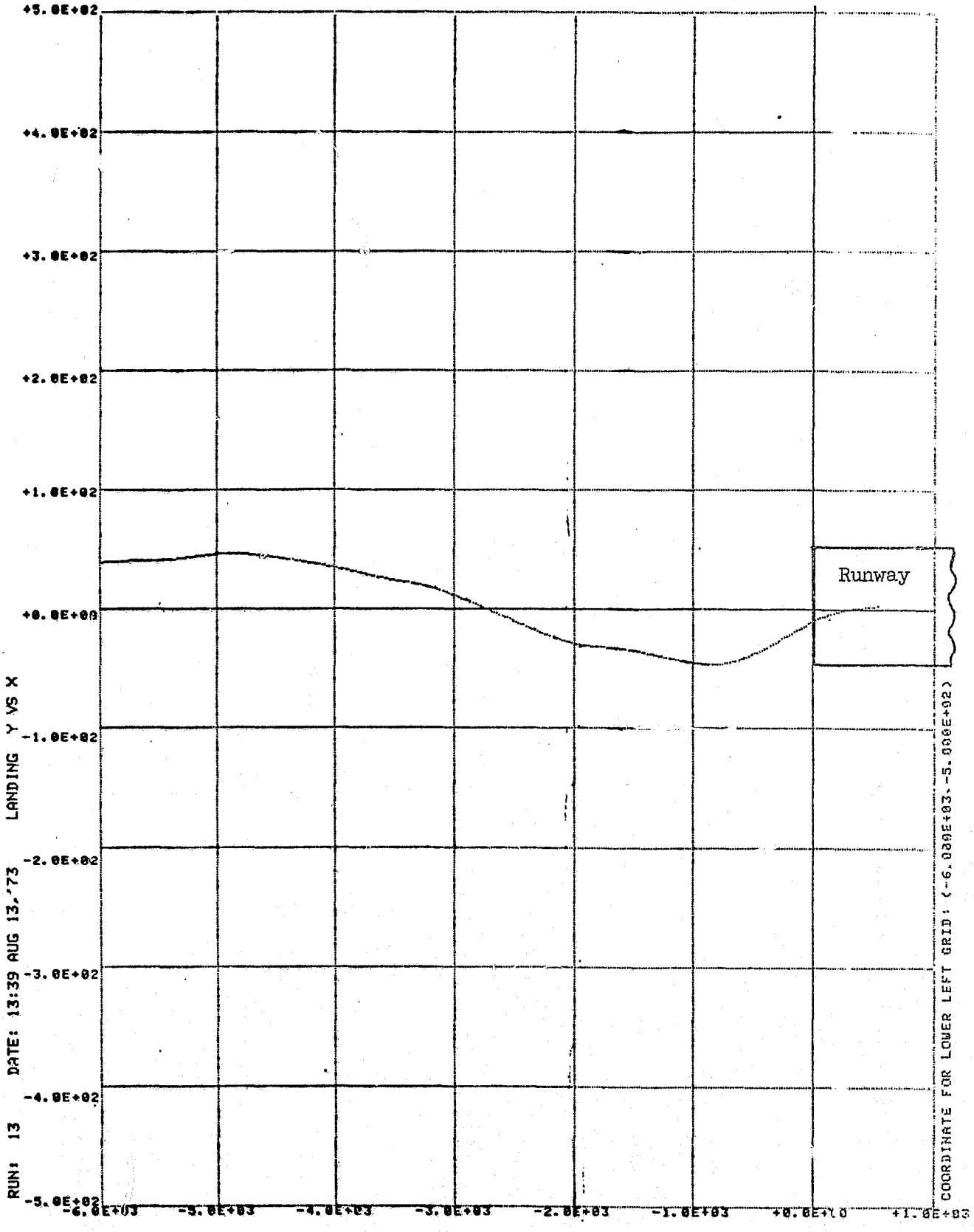

Figure II-12: Digital Plots Showing Lateral Flight Path

SECTION III

ILS TRACKING

This section presents the results obtained during the ILS tracking phase of the simulator experiment. These results consist of tabulations of data obtained plus their discussion and analysis. Results are also related to the pilot/vehicle analysis of Appendix B.

A. TABULATION OF RESULTS

1. Pilot Comments

At the end of each series of runs pilots submitted written commentary of the ILS tracking task flown. The most important value of this kind of data is the specific identification of problem areas.

The first part of Appendix E gives a summary of pilot comments which relate to the ILS tracking task. These are arranged in alphabetical order of pilots and chronological order of cases flown by each pilot.

2. Pilot Ratings

The pilot ratings assigned for the ILS tracking task are also given in Appendix E as well as being presented in summary form in Table III-1. Although the longitudinal aspects of the task were of more interest the ratings do reflect the combined three axis task (i.e., localizer and glide slope). Also, they are related to the flare task to some extent. A successful landing requires passing through a certain flight path window just prior to flare and the size of the window depends on the flare characteristics of the aircraft.

3. Measured Performance Data

A substantial number of pilot performance parameters were collected during the ILS tracking phase from 1,000 ft down to 300 ft (see Section II).

TABLE III-1

ILS PILOT RATING SUMMARY

(Calm Air/Turbulence/Turbul[illegible] Shears)

CASE	PILOT A	PILOT B	PILOT C	PILOT D	PILOT E	PILOT F	PILOT G	PILOT H
65 kt (Baseline)	3/5/4.5-5	3/4/4	3/5/5	3/3.5/3.5	4/6.5/7	3/7/- 3/4/6*	2/3.5/4.5	2/2/4
75 kt	3/5.5/-				4/6.5/7	3/5/6		
70 kt		3/3/3.5			4/6.5/7	2/5/7		
60 kt		3/6/8				2/5/8		
55 kt	4.5/7.5/-							4/5/6
55 kt, 50 deg δ_ν	6/7/8†							
2.5 sec engine lag						3/7/8		2/3/6‡
1.5 sec engine lag	2.5/5/6.5							
DLC			2/4/5					Not Available
DDC			2.5/5/6					Not Available
Nozzle (STOL)	5/6/8			5/8/-				2/4/6
Nozzle (CTOL)	5/6/7			4.5/5.5/-				
SAS Off		3.5/7/-						7/7/7
Flight Director On					3/4/4.25	3/4/5 2/3/-*		
Configuration SAS						-/6/-		

* Repeat run.
† VFR only.
‡ 3 sec engine lag used.

However, only a select few are considered to be key measures of performance. The most important of these are the resulting RMS deviations from the ILS beam, namely $\sigma_{G/S}$ and σ_{LOC}. These are of value because they describe the pilot's control structure related to flight path control (outer loops).

Other parameters describe the attitude and airspeed control (inner loop) activity. These are:

Airspeed deviation, σ_V
Mean airspeed, $\bar{V}$
Attitude deviation, σ_θ

The magnitudes of the inner loop quantities potentially tell something of the way the control loops were structured. For example, if a pilot were to exhibit a larger RMS attitude excursion than another pilot we could probably infer use of a more CTOL-like control technique.

Table III-2 shows the performance data versus pilot and configuration flown. The performance in turbulence includes both steady wind and shear cases since shears did not have any direct effect until below 200 ft.

The analysis which follows will bear more heavily on the pilot opinion data than on performance. This is due to tendency for the pilot to strive for a given level of performance even at the expense of increased workload.

B. ANALYSIS OF RESULTS

The cases flown in the approach task are best broken down into the groupings shown by the diagram in Figure III-1. Although these groups are substantially interrelated, the analysis will consider them one at a time and try to draw together the comments, ratings, and performance data.

The 65 kt case was used as a baseline case for comparison with other cases and among individual pilots. Thus, frequent reference will be made to this case in discussing such things as pilot problems, airplane characteristics, etc.

In the groupings of cases in Figure III-1 reference is made to "complementary control". This is a general term used here for throttle, nozzle, DDC, or DLC, i.e., whatever control was given to the pilot to complement his column control. The various complementary controls can be compared on the basis of:

TABLE III-2 PERFORMANCE DATA VERSUS PILOT AND CONFIGURATION FLOWN

a. GLIDE SLOPE DEVIATIONS, $\sigma_{G/S}$ (deg)

(Calm Air/Turbulence)

CASE	PILOTS							
	PILOT A	PILOT B	PILOT C	PILOT D	PILOT E	PILOT F	PILOT G	PILOT H
65 kt (Baseline)	.07/.264	.11/.404	.070/.232	.131/.353	.069/.394	.09/.282	.060/.282	.064/.322
75 kt	.090/.296				.03/.219	.080/.233		
70 kt		.101/.371			.161/.322	.068/.307		
60 kt		.063/.355				.083/.317		
55 kt	.118/.322							/.417
55 kt, 50 deg δ_ν								
2.5 sec Engine Lag						.153/.333		/.557*
1.5 sec Engine Lag	.070/.260							
DLC			.226/.248					/.351
DDC	/.264		.150/.364					/.378
Nozzle (STOL)	.14/.393			.064/.478				/.417
Nozzle (CTOL)	/.290			.241/.294				
SAS Off		.15/.439						.072/.395
Flight Director On					.124/.127	.123/.245		
Configuration SAS						/.430		

* 3 sec engine lag used.

TABLE III-2 (Continued)

b. LOCALIZER DEVIATIONS, σ_{LOC} (deg)
(Calm Air/Turbulence)

CASE	PILOTS							
	PILOT A	PILOT B	PILOT C	PILOT D	PILOT E	PILOT F	PILOT G	PILOT H
65 kt (Baseline)	.15/.511	.16/.482	.100/.550	.126/.448	.214/.457	.233/.763	.274/.423	.197/.594
75 kt	.267/.302				.19/.268	.124/.585		
70 kt		.119/.221			.122/.433	.134/.558		
60 kt		.220/.507				.180/.711		
55 kt	.09/.18							/.659
55 kt, 50 deg δ_v								
2.5 sec Engine Lag						.259/.667		/.412*
1.5 sec Engine Lag	.106/.793							
DLC			.157/.610					/.739
DDC	/.397		.15/.550					/.716
Nozzle (STOL)	.13/.513			.114/.320				/.651
Nozzle (CTOL)	/1.125			.160/.317				
SAS Off		.15/.61						.766/.717
Flight Director On					.047/.078	.603/.209		
Configuration SAS						/.486		

* 3 sec engine lag used.

TABLE III-2 (Continued)

c. Pitch Deviations, σ_θ (deg)

(Calm Air/Turbulence)

CASE	PILOTS							
	PILOT A	PILOT B	PILOT C	PILOT D	PILOT E	PILOT F	PILOT G	PILOT H
65 kt (Baseline)	.451/.714	.42/.73	.451/.923	.449/.979	.388/.644	.384/.936	.424/.777	.137/.803
75 kt	.398/.681				.26/.639	.148/.854		
70 kt		.724/.702			.884/.696	.180/1.04		
60 kt		.327/.632				.409/1.18		
55 kt	.775/1.48							/1.41
55 kt, .50 deg δ_v								
2.5 sec Engine Lag						.382/.689		/1.16*
1.5 sec Engine Lag	.448/1.36							
DLC			.831/1.265					/.870
DDC	/1.926		1.735/1.349					/1.794
Nozzle (STOL)	.73/1.373			.220/1.267				/1.32
Nozzle (CTOL)	/2.20			3.743/1.479				
SAS Off		.63/2.06						1.03/1.40
Flight Director On					.582/.784	.339/.746		
Configuration SAS						/2.247		

* 3 sec engine lag used.

TABLE III-2 (Continued)

d. Velocity Deviations, σ_V (kt)

(Calm Air/Turbulence)

CASE	PILOTS							
	PILOT A	PILOT B	PILOT C	PILOT D	PILOT E	PILOT F	PILOT G	PILOT H
65 kt (Baseline)	1.25/2.77	1.30/2.38	.986/2.72	1.37/2.79	.967/2.52	1.11/2.46	2.35/2.82	1.55/2.44
75 kt	1.18/2.23				1.02/2.08	1.06/2.48		
70 kt		1.37/2.36			1.56/2.19	1.11/2.49		
60 kt		.897/2.273				1.18/2.46		
55 kt	1.17/2.02							/2.81
55 kt, 50 deg δ_ν								
2.5 sec Engine Lag						1.20/2.37		/2.98*
1.5 sec Engine Lag	1.14/2.73							
DLC			2.57/2.96					/2.26
DDC	/2.46		1.64/3.05					/2.90
Nozzle (STOL)	1.39/3.34			.98/2.48				/2.74
Nozzle (CTOL)	/2.30			2.14/2.13				
SAS Off		1.31/3.5						1.41/2.41
Flight Director On					1.32/2.86	1.02/2.71		
Configuration SAS						/2.32		

* 3 sec engine lag used.

TABLE III-2 (Concluded)

e. Mean Airspeed, $\overline{V}$ (kt)

(Calm Air/Turbulence)

	PILOTS							
CASE	PILOT A	PILOT B	PILOT C	PILOT D	PILOT E	PILOT F	PILOT G	PILOT H
65 kt (Baseline)	64.96/65.82	68.90/68.07	65.35/66.0	65.43/65.88	66.49/65.58	65.87/65.92	67.59/66.74	66.24/66.91
75 kt	74.69/75.40			75.08/74.93	75.13/74.31			
70 kt		70.82/71.21			70.48/70.18	71.29/69.51		
60 kt		61.16/62.11				62.09/63.57		
55 kt	55.05/56.02							/55.03
55 kt, 50 deg δ_ν								
2.5 sec Engine Lag						65.59/64.55		/66.34*
1.5 sec Engine Lag	64.76/64.44							
DLC			66.01/66.03					/65.57
DDC	/65.91		65.90/66.07					/65.48
Nozzle (STOL)	64.76/65.81			65.10/66.76				/67.49
Nozzle (CTOL)	/65.37			65.43/66.39				
SAS Off		66.41/66.49						66.30/66.52
Flight Director On					67.33/65.55	64.79/65.29		
Configuration SAS						/66.81		

* 3 sec engine lag used.

Figure III-1. ILS Tracking Task Relation of Test Cases to Baseline

Sensitivity -- The acceleration per unit movement of the controller (e.g., g/in)

Direction -- The direction of the resultant force vector due to control deflection (e.g., the throttle effectively produced a force 90 deg from the flight path even though the nozzles were set at 75 deg)

Control Power -- The range of effect on steady state flight path and airspeed due to full forward or full aft control (e.g., the range from maximum rate of climb to minimum rate of climb)

Control Response -- The effective rate of buildup or decay in flight path angle following a controller input (i.e., the effect of any delays or lags).

1. Approach Speed Variation

As approach speed was decreased from 65 kt the pilot comments indicated increased workload due to:

- Sluggish throttle response
- Coupling of IAS and G/S with wrong sense
- Turn rate sensitivity to small bank angle errors.

Increasing the approach speed from 65 kt to 70 or 75 kt did not result in much change, according to most pilots. Where favorable comments were indicated they related to the airplane flying more like a conventional airplane and increased margins for maneuvering. Adverse comments had to do with the increased trim sink rate on the glide slope and its nearness to the 1,000 ft/min rule-of-thumb limit recognized by many pilots.

Pilot ratings from Table III-1 are plotted in Figure III-2 for three levels of atmospheric conditions. Although the raw ratings vary among pilots, two important trends are recognizable. The severity of atmospheric disturbances strongly influences pilot rating for a given operating condition; and, below a certain point, decreasing approach speed results in worsening pilot opinion. In order to more clearly show these features, pilot opinion

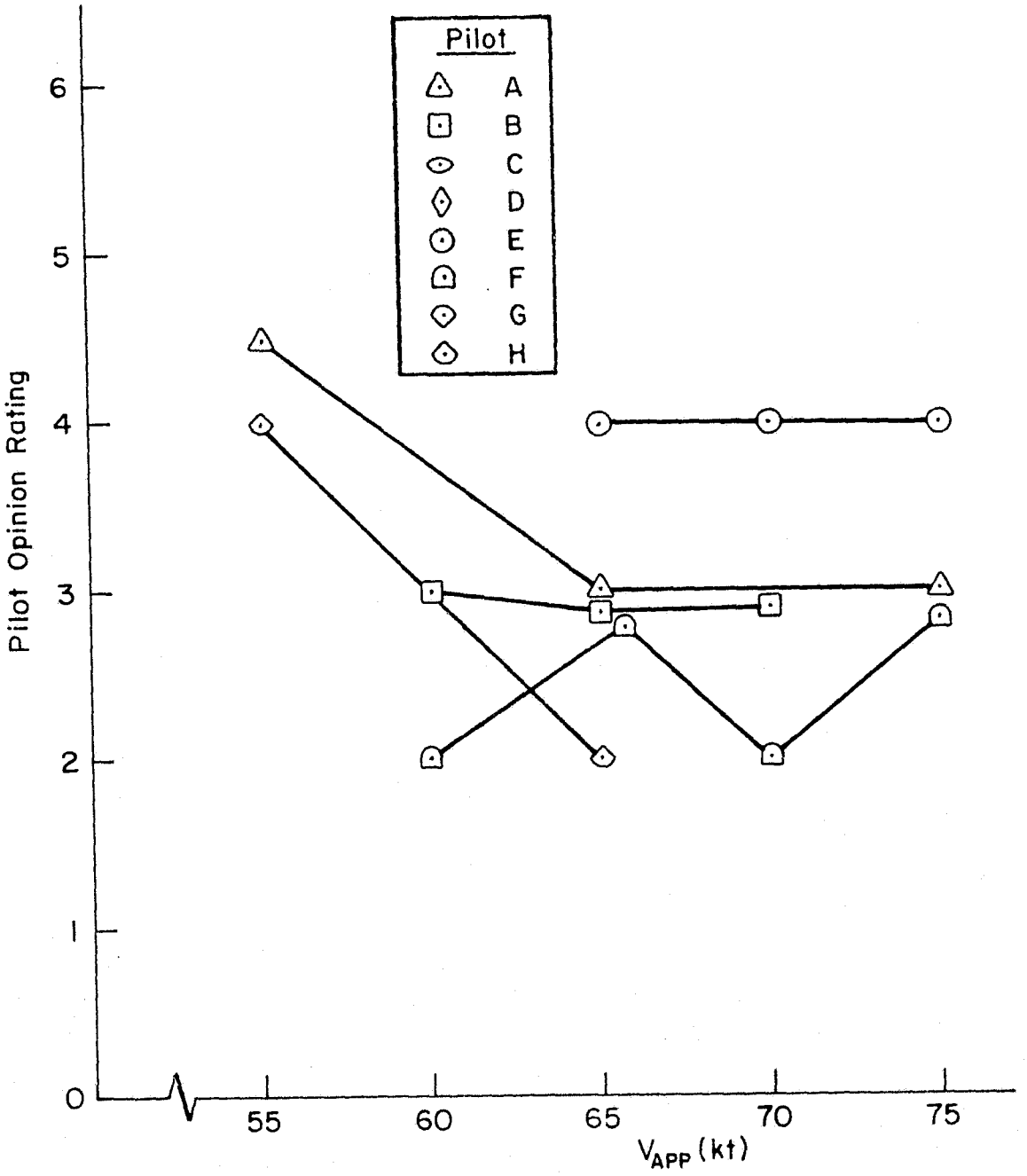

a. Calm Air

Figure III-2. Pilot Rating vs. Approach Speed

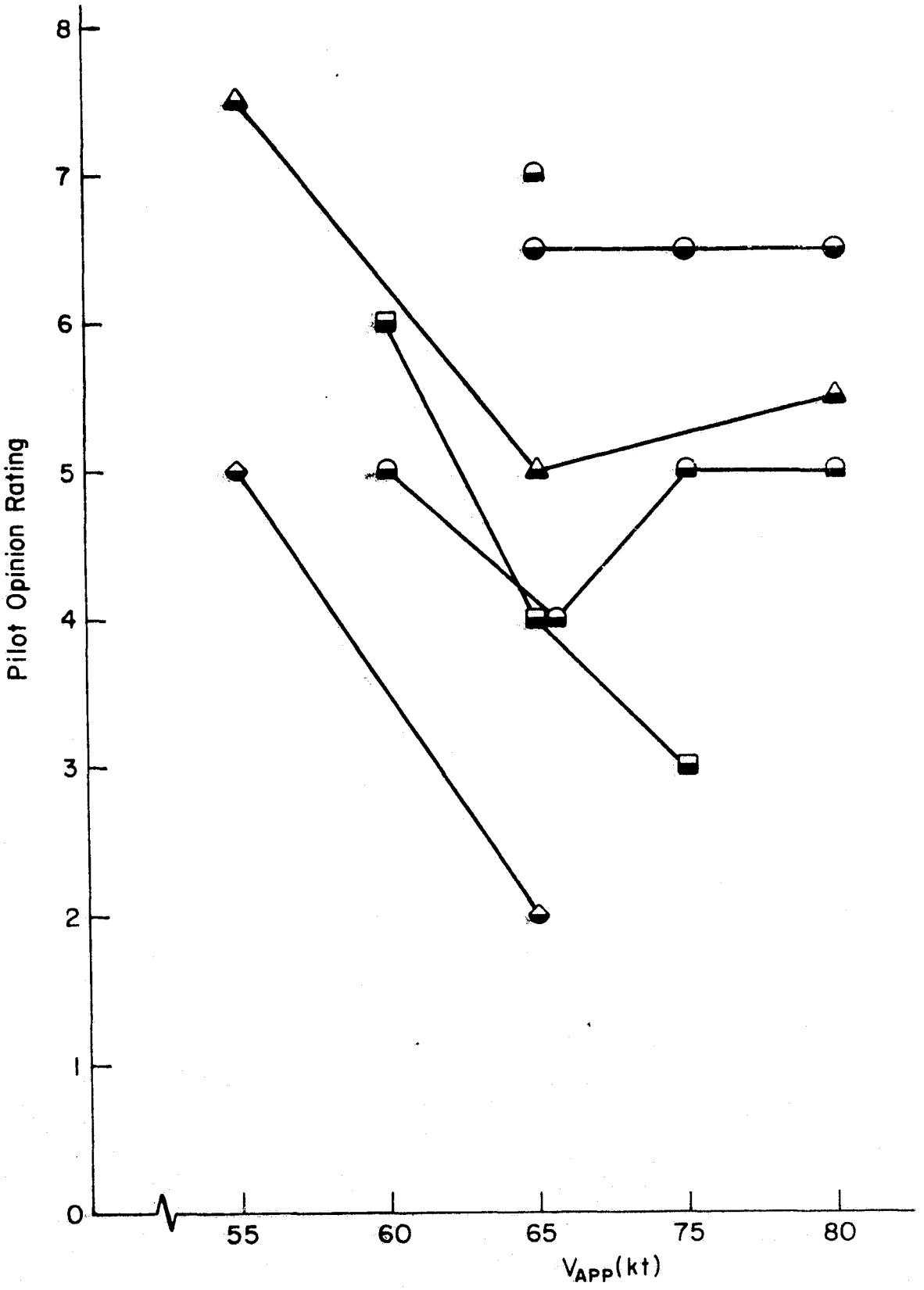

b. Turbulence/Steady Winds

Figure III-2. (Continued)

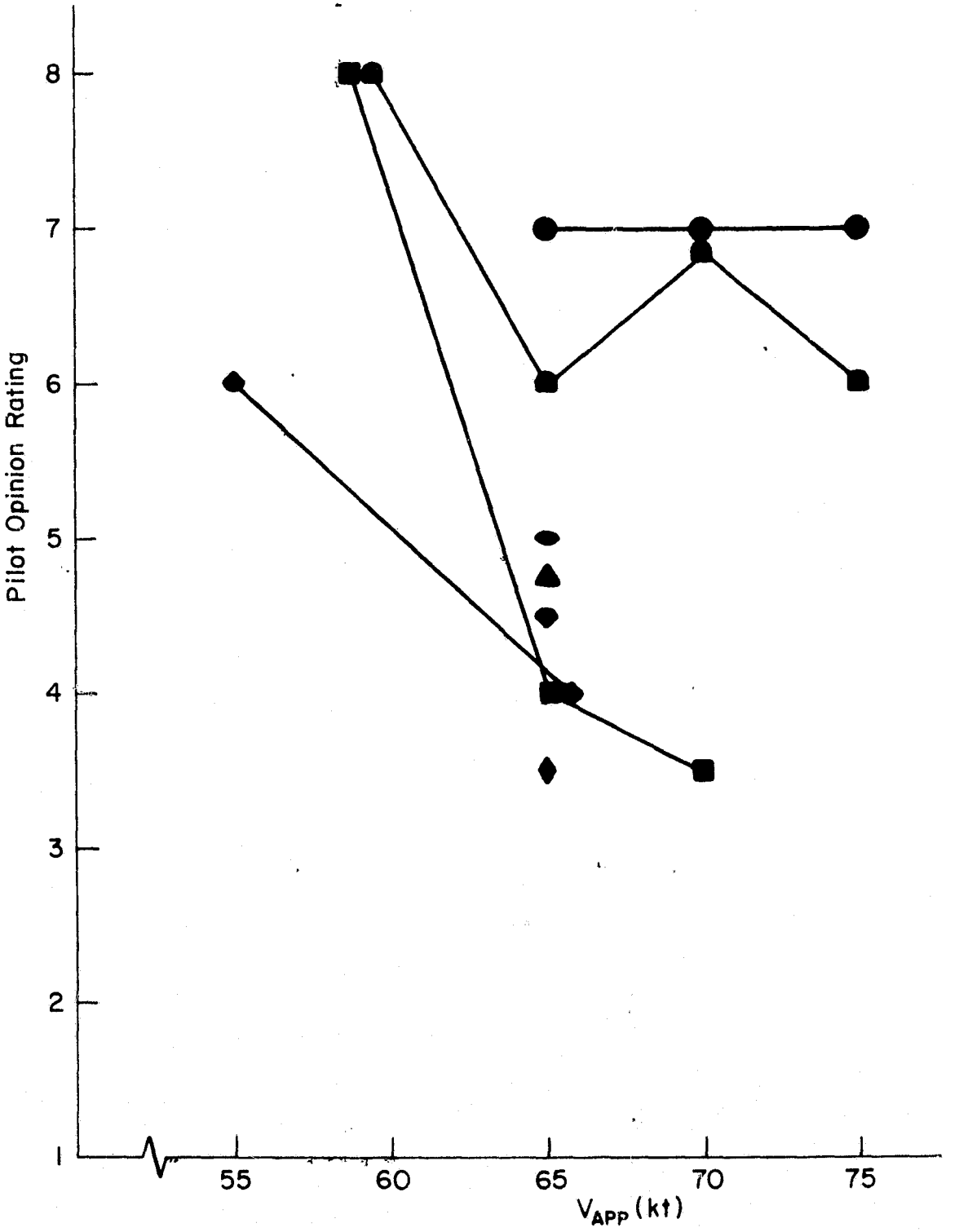

c. Turbulence/Shears

Figure III-2. (Concluded)

trends of individuals are plotted relative to a common baseline for each pilot. The baseline selected here is the 65 kt approach case. Figure III-3 shows the incremental ratings for each of the three levels of atmospheric disturbances of the previous figure. In calm air, pilot opinion deteriorates below 60 kt whereas in rough air it occurs below 65 kt. In all cases, increasing approach speed above 65 kt does not result in a significant change in pilot opinion.

Glide slope control performance, as measured by $\sigma_{G/S}$, is fairly uniform over the approach speeds tested. Deviation in calm air was normally about .07 to .10 deg and in turbulence about .2 to .4 deg. No consistent speed effect was observed. Localizer tracking performance was likewise not affected, except that angular excursions were larger. Also, no real correlation was observed between glide slope error and localizer error (that is shown in Figure III-4). Thus, the pilot apparently does not tradeoff localizer performance with glide slope performance as one might expect.

Looking at the inner loops, RMS airspeed deviations were consistently about $\pm$ 2 1/2 kt in turbulence among all pilots for all approach speeds. Mean speeds were generally 1 or 2 kt above the target speed. Attitude deviations were also consistent except for the 55 kt case where attitude excursions roughly doubled in amplitude.

Airspeed/flight path cross coupling is regarded as the prime contributor to adverse pilot ratings for decreasing approach speeds. Referring to the analysis of Appendix B, we see that the only significant feature that varies with V_{APP} is the degree of coupling as reflected by the parameter μ^{STOL}. This parameter is defined as the ratio of flight path response to throttle at constant attitude to the flight path response to throttle at constant speed. Under steady state conditions μ^{STOL} bears a direct relation to the γ - V curve.

μ^{STOL} is a convenient non-dimensional measure of flight path-airspeed cross coupling problems. A value of μ^{STOL} equal to one is considered ideal. A value less than one is generally more tolerable than a value greater than one. Examples of varying μ^{STOL} for trimming or long-term corrections are shown in Figure III-5. In these long-term cases, the γ - V curves can

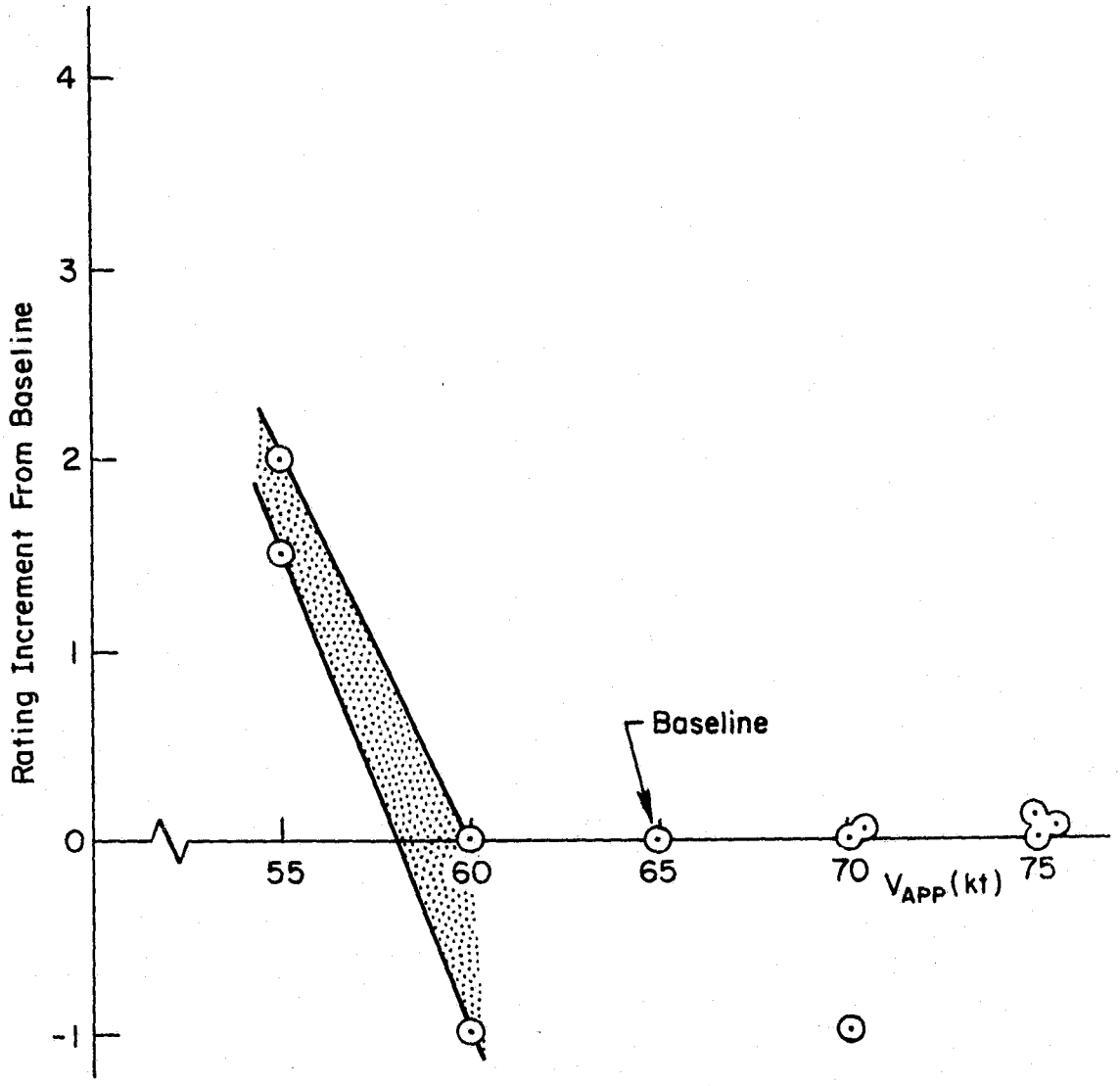

a. Calm Air

Figure III-3. Pilot Rating Variation with Approach Speed

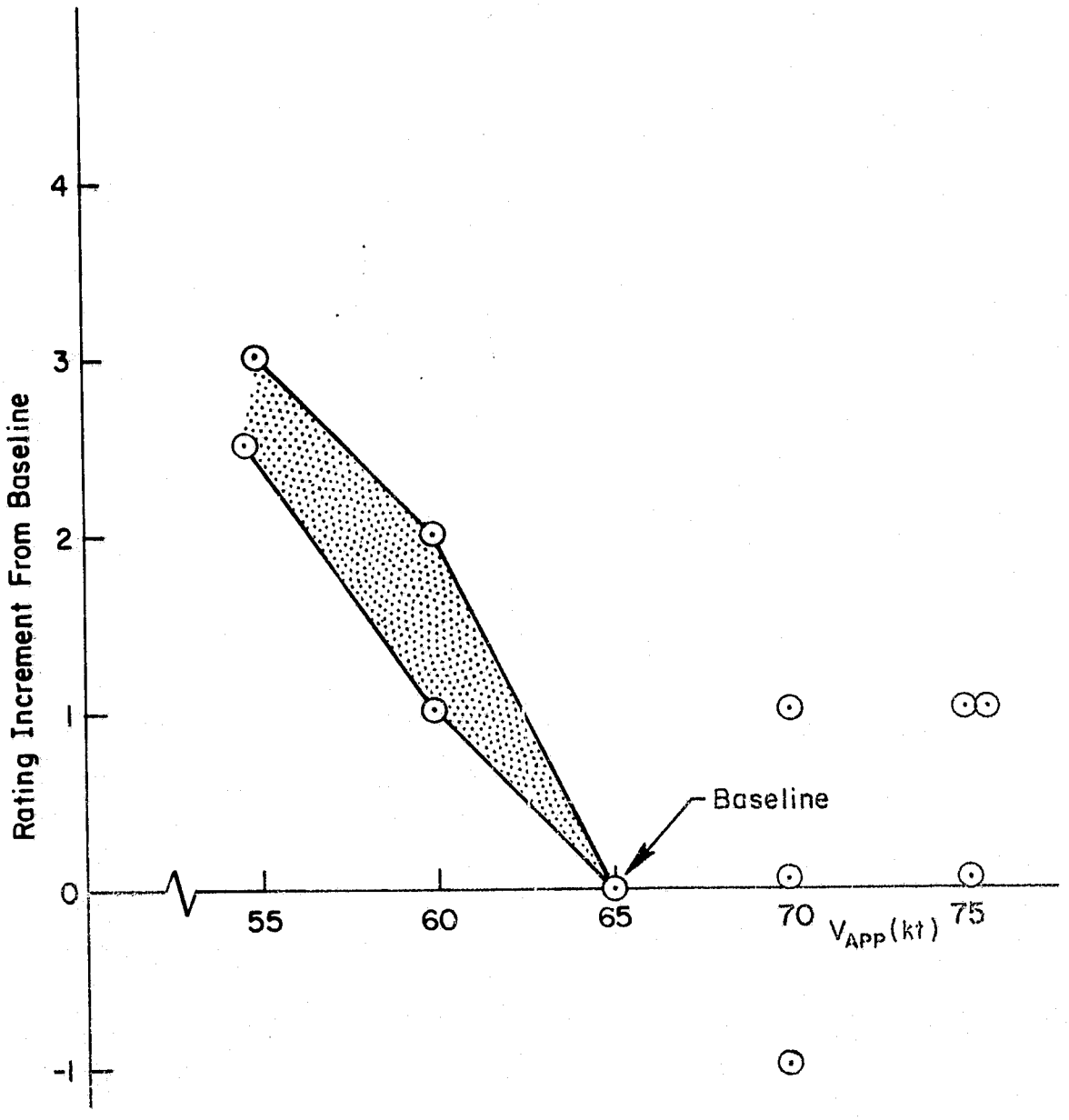

b. Turbulence/Steady Winds

Figure III-3. (Continued)

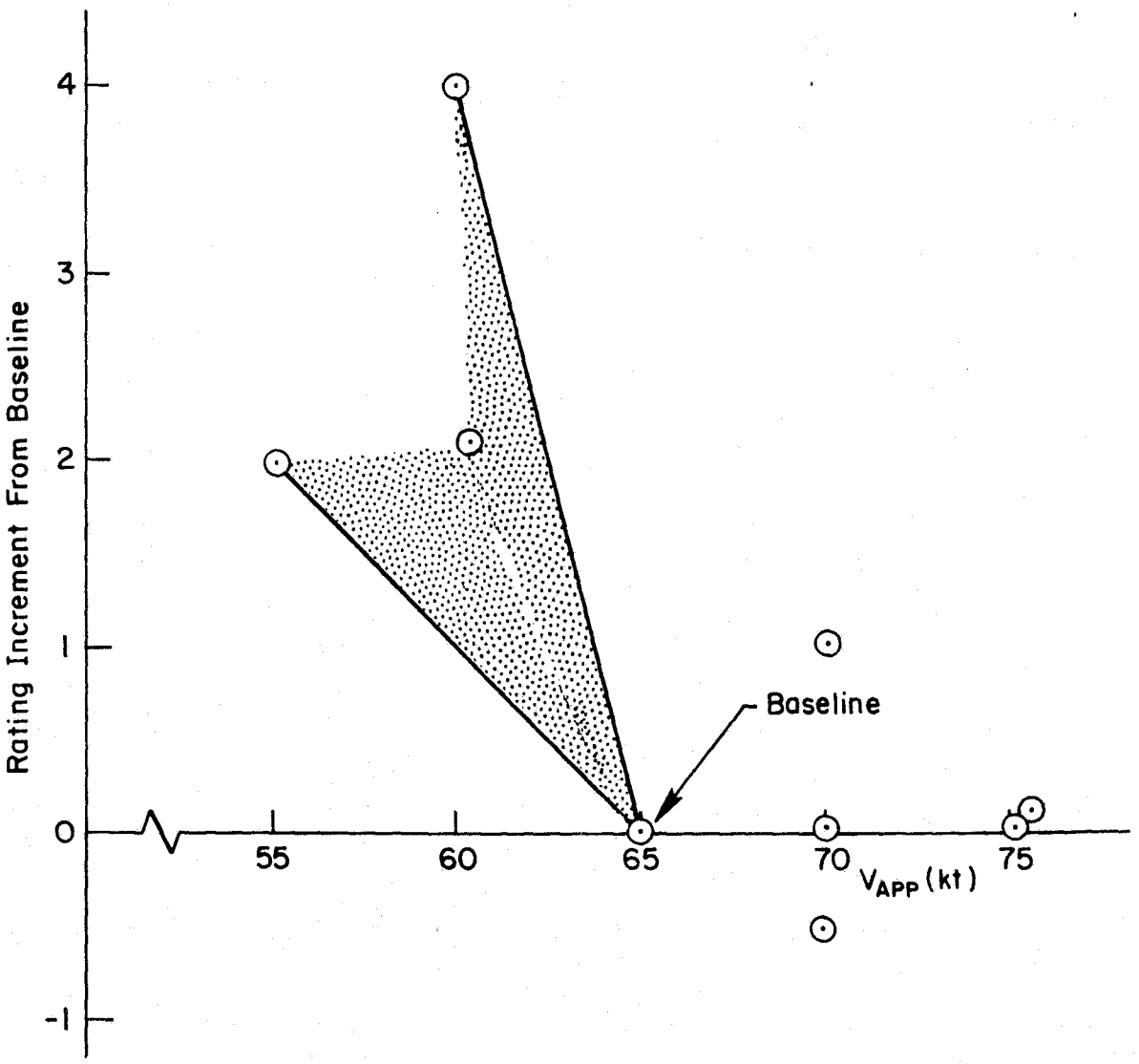

c. Turbulence/Shears

Figure III-3. (Concluded)

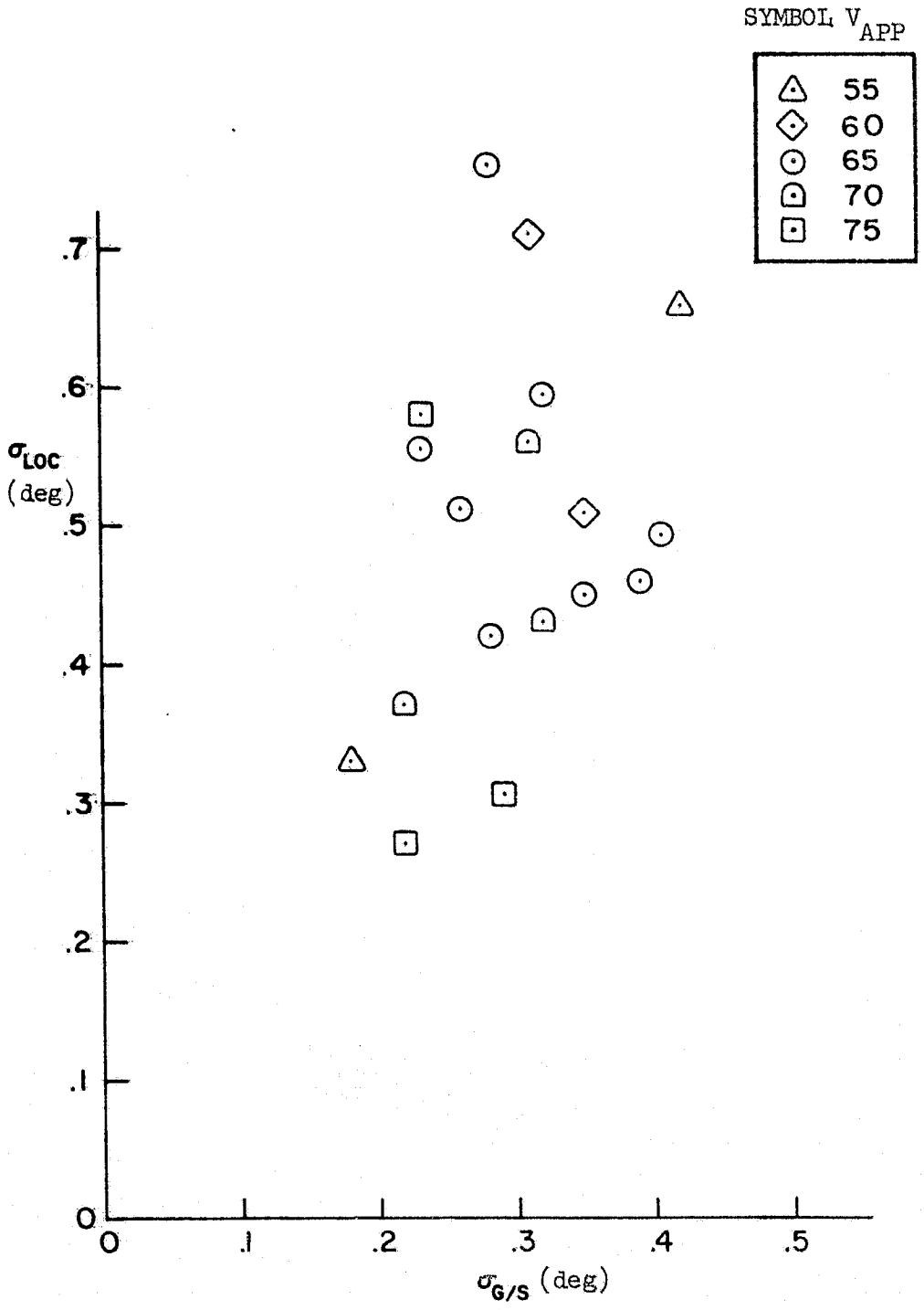

Figure III-4. Localizer Error Versus Glide Slope Error Approach Speed Varied in Turbulence

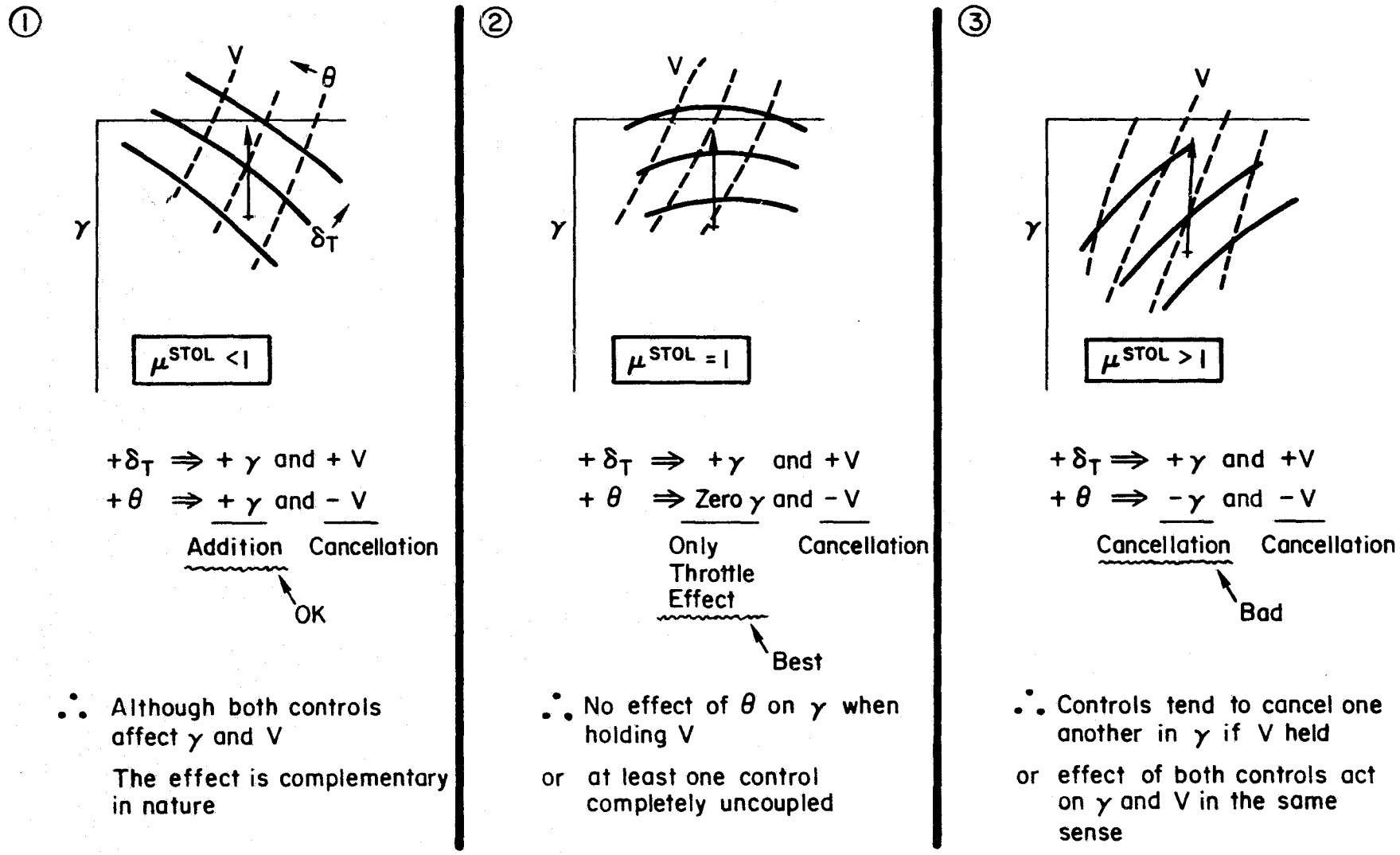

Figure III-5. Examples of Trim γ – V Cross-Coupling

Situation: Pilot Makes an Up Correction Without Changing Airspeed

be associated directly with μ^{STOL}. Short-term corrections (such as IIS tracking) in general can have a different value of μ^{STOL} than long-term corrections. The relative magnitude of short-term μ^{STOL} versus long-term μ^{STOL} can be just as important as the absolute magnitude of each. (For a further explanation of μ^{STOL} see Appendix B.) Figure III-6 shows μ^{STOL} as a function of frequency. The predominant feature shown there is the coupling variation between the low frequency trimming region and the higher frequency tracking region. This feature becomes more extreme at the lower speeds.

Sc ; pilot comments indicate that the level of acceptable cross coupling is bracketed by the 55 kt and 65 kt cases. In particular, Pilot A commented that at 65 kt the cross coupling did not cause undue problems or workload while at 55 kt he felt that the magnitude of the cross coupling effect was unacceptable. Furthermore, he remarked that at 75 kt the cross coupling was more evident than at 65 kt. (This suggests that the lower frequency μ^{STOL} was important.) Pilot H agreed with Pilot A's evaluation of coupling at 65 and 55 kt. Pilot C remarked that there was no coupling problem at 65 kt for small corrections but that it was bothersome for larger corrections.

The problem of cross coupling is also affected by wind conditions. Figure III-7 shows μ^{STOL} for the airplane flying a 65 kt approach in varying steady winds. The striking feature of this plot is the strong adverse effect of a tailwind. In fact, the 10 kt tailwind is worse than the 55 kt approach case in the region of tight glide slope tracking. This correlates qualitatively with the degree of difficulty in flying the tailwind approaches. Pilot C, in one instance, mentioned that the 10 kt tailwind would worsen his pilot rating by one unit (6 $\longrightarrow$ 7 for the 65 kt approach case in turbulence).

Thus, the approach speed variation for the AWJSRA did reveal a minimum acceptable speed (about 63 kt). Furthermore, this minimum speed seemed to be a strong function of the amount of γ - V cross coupling between the two controls, and specific pilot comments indicate that the level of coupling at 55 kt was unacceptable while the level at 65 kt was acceptable.

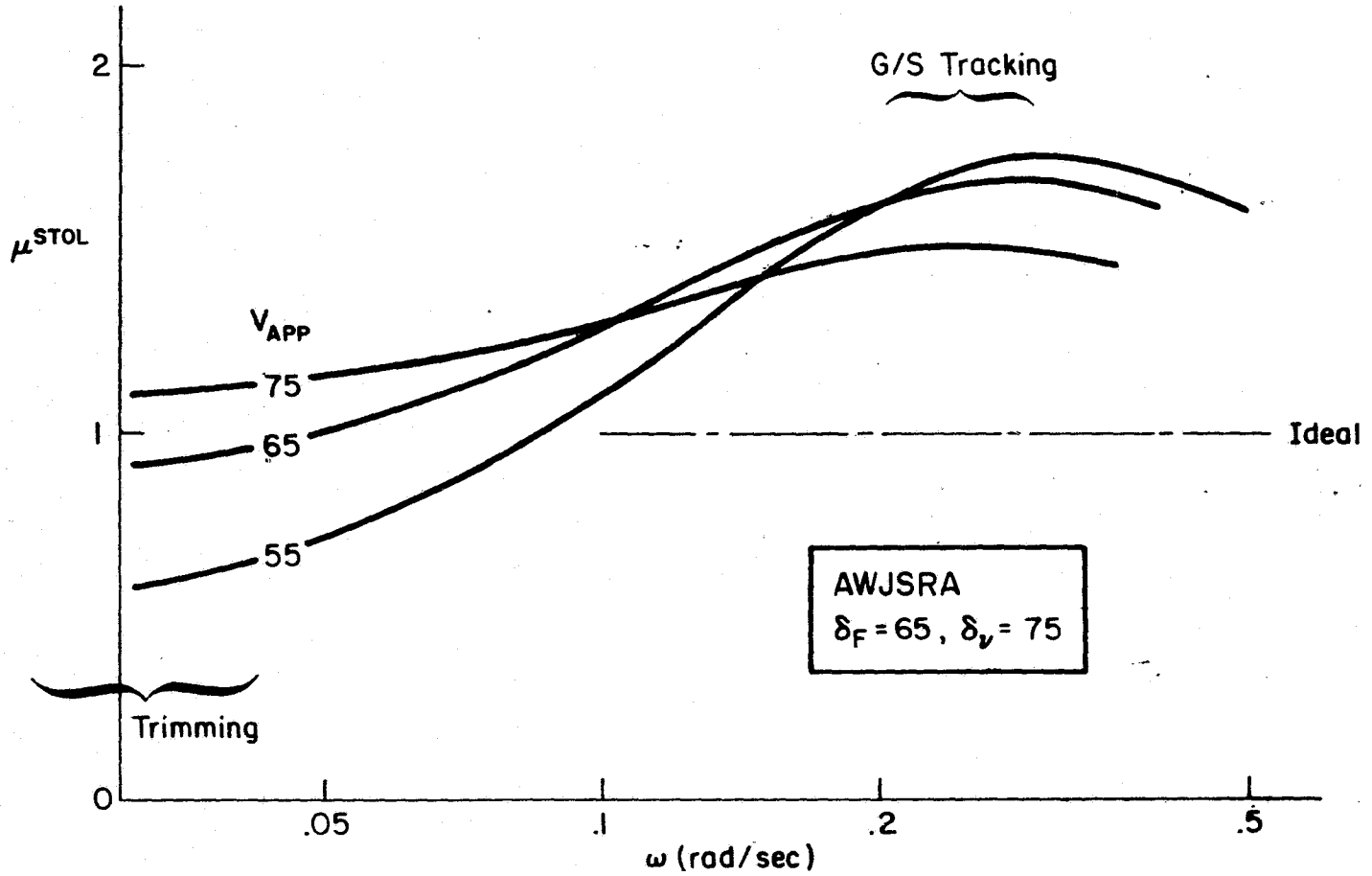

Figure III-6. G/S-IAS Coupling Parameter
Varying Approach Speed

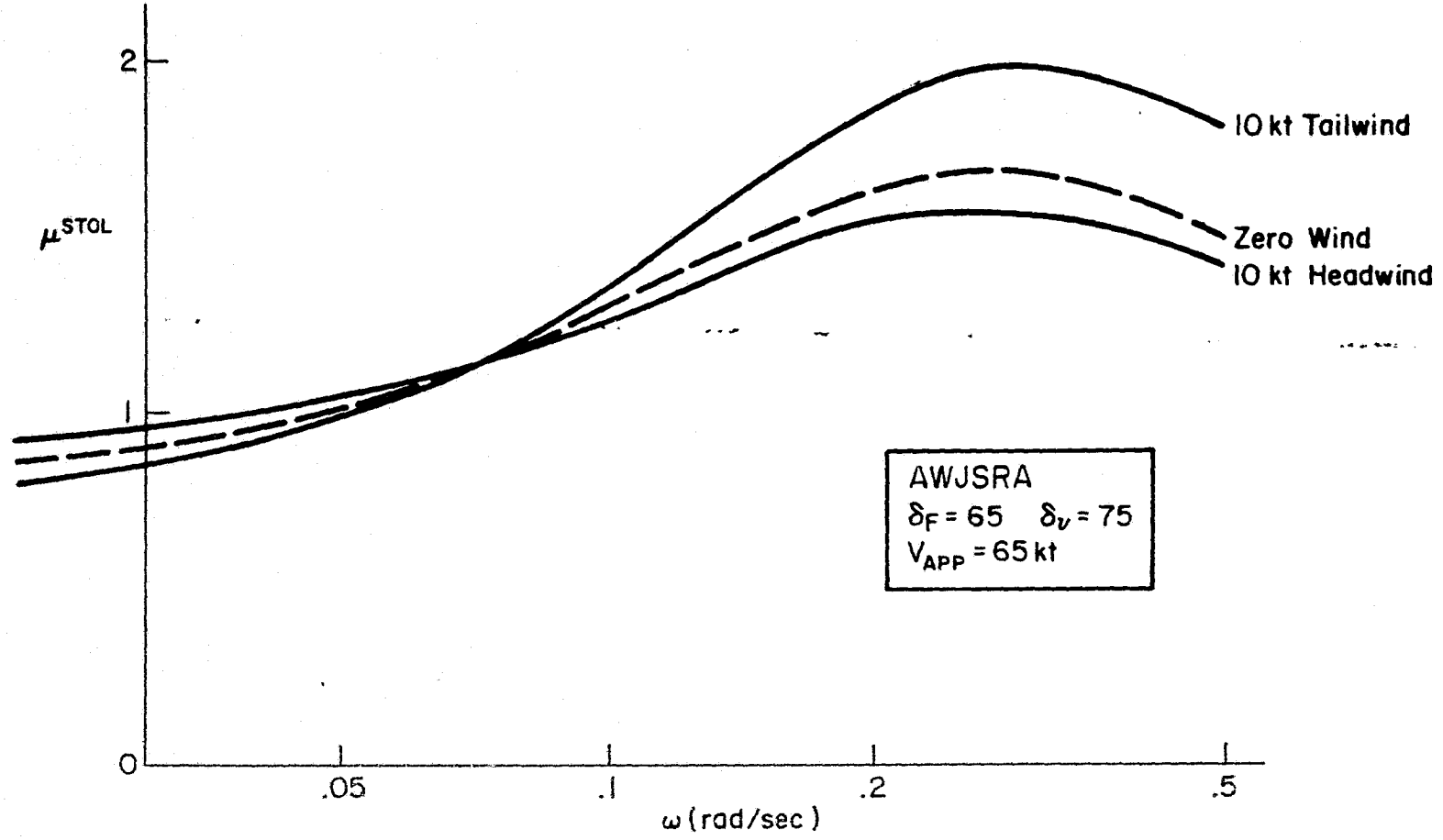

Figure III-7. G/S-IAS Coupling Parameter Varying Wind Direction

2. Airframe Natural Response Variation

This grouping really includes the airspeed variation cases as well as the 55 kt, 50 deg nozzle case shown in the organization scheme of Figure III-1. The goal here was to observe the effect of the bare airframe dynamics on flight path control as opposed to the effects of complementary control variations. This sort of distinction is not necessarily apparent to the pilot since he views more the overall aircraft responses to his control inputs.

Prior to the simulation the possible nozzle/flap/airspeed combinations of the AWJSRA model were searched to find a case which should have a relatively bad set of flight path dynamics. The worst combination appeared to be low approach speeds with reduced nozzle deflection. This resulted in pitch/elevator zeros which were oscillatory and at low frequency; consequently, holding attitude well would result in sluggish, lightly-damped flight path responses.

The "worst" case was selected to be 55 kt approach speed with 75 deg flaps and 50 deg nozzle. This case was examined briefly by Pilot A and found in fact to be unsatisfactory. His comments mention the oscillatory tendency of flight path, and in addition, poor visibility due to the large nose up attitude (θ = 7 deg) and coupling of airspeed with power in the wrong sense. Lateral-directional problems were also encountered.

3. Complementary Control Response Variation

Thrust lag was varied to determine the magnitude of effect on pilot opinion and performance. The nominal lag for the AWJSRA engine model was .7 sec. Increased values to a maximum of 3 sec were tested. The DLC case was compared with these engine lag cases as one having zero lag. The comparison was considered valid since the effective force vector acted in virtually the same direction as that of thrust (i.e., about 90 deg).

Since several pilots were involved, the results were adjusted to take into account only the incremental effects from a common baseline. Also, the following discussion considers an effective lag which includes a nominal

pilot reaction time of 0.4 sec. The effective lag is defined simply as the sum of the engine lag plus the pilot lag. This way of handling complementary control response is helpful because it is easier to relate the total pilot plus engine lag to the desired glide slope bandwidth.

The results are plotted in Figures III-8 and III-9. The first shows pilot opinion trends, the second pilot performance. As we have seen before, pilot opinion degrades before performance does. Also, the amount of lag that the pilot will tolerate is highly dependent on the level of disturbance. Good glide slope tracking ability is more essential when the atmospheric disturbances are larger.

The ILS analysis in Appendix B shows that the primary effect of varying the throttle response was on glide slope bandwidth. For the pure DLC case, the maximum bandwidth was .56 rad/sec and with the 3 sec engine lag this dropped to .22 rad/sec.

4. Complementary Control Orientation

The comparison was made between an essentially vertical thrust vector and a horizontal one. The throttle and DLC controls were the vertical controls and the nozzle and DDC the horizontal ones.

While no significant performance effect appeared, pilot opinion was influenced. Pilot C gave perhaps the clearest indication of the essential effects. In calm air both the DLC and DDC were liked (Pilot Ratings 2 vs 2.5), but in turbulence the DLC was more distinctly preferred (Pilot Ratings 4 - 5 vs 5 - 6). With DDC the pilot recognized that although horizontal response was quick, vertical response was slow to come. Also, the pilot felt that the indirect vertical response caused by a change in the drag was less appealing than the thought of direct control over vertical path (DLC). Figure III-11 shows that whether the complementary control is a DLC type or DDC, the STOL Technique is best suited for long-term corrections. On the other hand, for short-term corrections (such as ILS tracking) a CTOL technique becomes more attractive for the DDC control ($\mu^{STOL} \longrightarrow$ zero at higher frequencies). Tight tracking with the DLC control calls for a STOL technique but this will be complicated by the

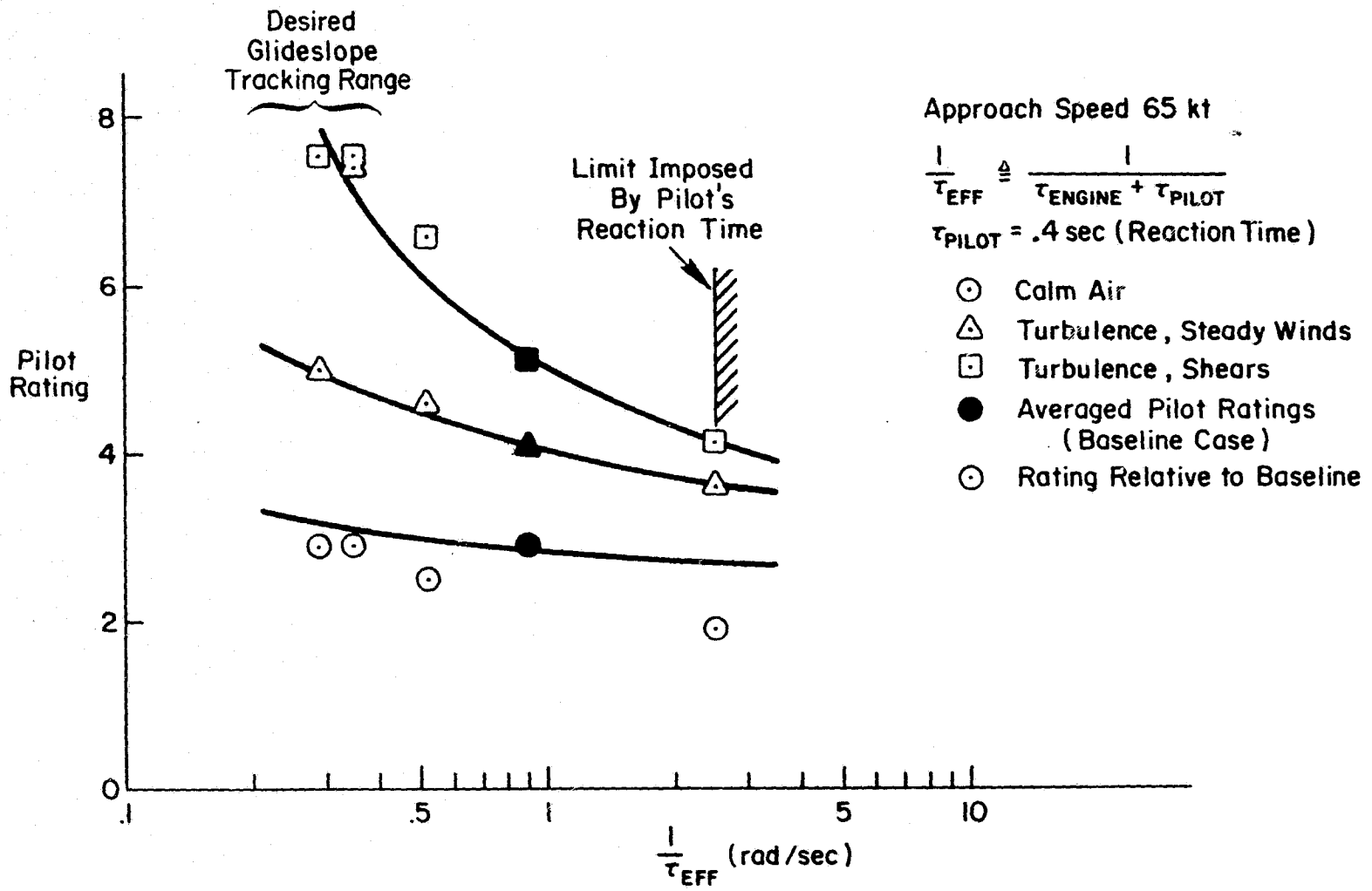

Figure III-8. Adjusted Pilot Opinion Versus Effective Frequency Response of Pilot Plus Engine

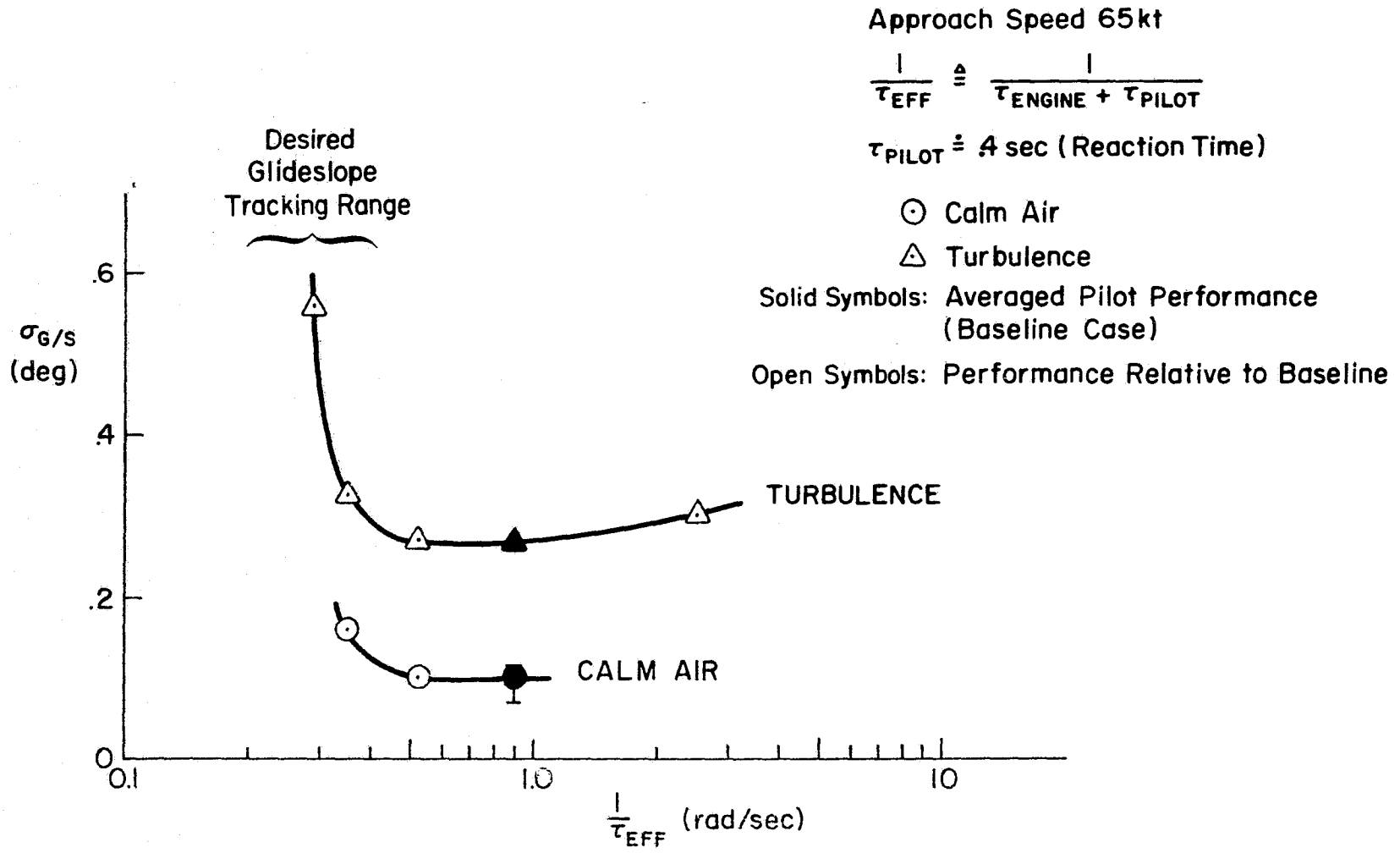

Figure III-9. Adjusted Glide Slope Tracking Performance Versus Effective Frequency Response of Pilot Plus Engine

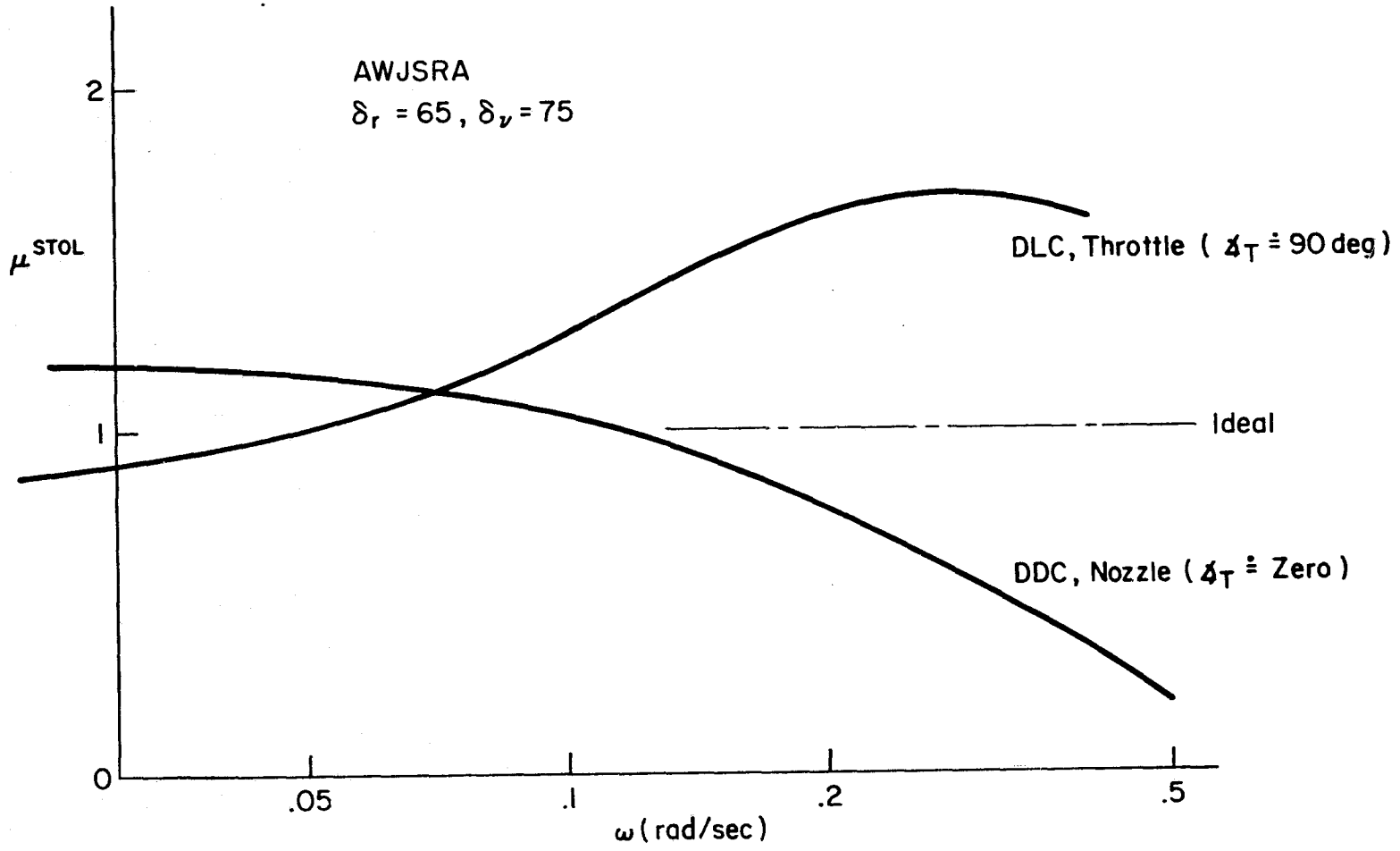

Figure III-10. G/S-IAS Coupling Parameter

$\mu^{STOL} > 1$ condition. For the cases flown which had a primarily horizontal thrust component the CTOL technique was preferred for glide slope tracking. Appendix B shows that glide slope bandwidth is heavily dependent on thrust orientation. With DDC closure of the airspeed loop is crucial for good glide slope control.

5. Piloting Technique Variation

For most of the cases run a STOL piloting technique was used. However, in a few cases a change of technique seemed attractive. As mentioned previously, the cases where this was true were those where the complementary control was primarily horizontal, i.e., DDC and nozzle. The pilot's motivation for doing so was that at least one of the controls would have a direct effect on one of the controlled variables (i.e., δ_ν or DDC $\longrightarrow$ IAS).

In terms of glide slope tracking performance, the CTOL technique appears superior for the horizontal complementary control. Also, pilot comments indicate a preference for the CTOL technique for this type of complementary control. However, in trying to use the CTOL technique the pilots consistently commented on the low attitude to flight path sensitivity. This is, of course, a fundamental characteristic of the bare airframe of any aircraft operating at a high lift coefficient since $n_{Z_\alpha} \doteq C_{L_\alpha}/C_L$ and C_{L_α} does not vary greatly.

The presence of a horizontal complementary control thus presents the pilot with a difficult situation. The STOL technique requires a good airspeed control loop to provide sufficient glide slope tracking bandwidth, but the airspeed loop must use an inferior control (attitude rather than throttle). On the other hand, the CTOL technique, which provides excellent airspeed response, forces the pilot to use a low sensitivity glide slope control (attitude). Furthermore, the CTOL technique is completely inadequate for long-term (trimming) control. For trim, the most effective control technique is flight path to DDC or nozzle and airspeed to attitude. This can be seen from the γ - V curves of Appendix A. This can also be deduced from the fact that μ^{STOL} at low frequencies is nearly equal to 1, see Figure III-10.

6. Augmentation Level Variation

The baseline case was flown with the basic augmentation (longitudinal and lateral-directional SAS) but without a flight director. Three cases were flown in which the level of augmentation was varied. These consisted of:

- All augmentation off
- Basic augmentation plus flight director
- Basic augmentation plus configuration SAS.

The object of running these cases was to gain a general appreciation of the role of augmentation in relieving pilot workload and the effects on pilot performance.

a. SAS Off. Pilot B flew the 65 kt case with SAS off through the same series of runs (calm air, turbulence, winds, shears, etc.) as with the other cases. Table III-3 summarizes the results in terms of pilot rating and performance. The interesting point here is that the main effect was on pilot rating with turbulence. The calm air pilot rating and ILS performance (both calm air and with turbulence) were only slightly degraded with the SAS off. The pilot's main complaint (SAS off) was directed toward heading control and the long delays associated with it. Such a characteristic, according to one subject pilot, is typical of other heavy STOL airplanes (e.g., the BR 941S and DHC-5).

b. Flight Director On. The baseline case was flown with the aid of a flight director designed specifically for the AWJSRA. The director provides pitch, roll, and power commands. Details of this director are presented in Reference 7.

As shown in Table III-3, two pilots flew this case. The first, Pilot F, had no previous experience with this particular flight director/airframe combination and began by tracking the flight director relatively tightly. In fact, he rated the workload about equal to the basic 65 kt case. His pilot ratings reflect this. However there is a dramatic improvement in localizer tracking performance.

TABLE III-3

SUMMARY OF AUGMENTATION EFFECTS
(65 kt Approach Case)

	PILOT RATING	$\sigma_{G/S}$	σ_{LOC}
SAS Off:			
PILOT B	3.5/7 (3/4)	.15/.44 (.11/.40)	.15/.61 (.16/.48)
Flight Director On:			
PILOT F--Tight Tracking	3/4 (3/4)	.12/.22 (.09/.28)	.07/.17 (.16/.76)
PILOT F--Loose Tracking	2/3 (3/4)	--/.27 (.09/.28)	--/.27 (.16/.76)
PILOT E	3/4 (4/6.5)	.12/.13 (.07/.39)	.05/.08 (.21/.45)
Configuration SAS On:			
PILOT F	-/6 (3/4)	--/.43 (.09/.28)	--/.49 (.16/.76)

NOTE:
- Slash separates calm air value from turbulence in steady winds.
- Parentheses indicate baseline condition for respective pilot (i.e., SAS on, flight director off, and configuration SAS off).
- Dash indicates insufficient data.

After reviewing the results, Pilot F was asked to refly the same case but to loosen up considerably on the tracking in order to reduce the workload level. His results are shown in the second set of ratings. Pilot ratings were improved by about one unit yet the improvement in localizer tracking over the baseline case was still considerable.

Pilot E, the second pilot, had considerable previous experience with this flight director. His performance was improved greatly with the flight director and at the same time, pilot ratings improved.

One of the most significant advantages of the flight director was the reduction in lateral dispersions at breakout. This eliminated last minute sidestep maneuvers and thus made the landing task easier.

c. Configuration SAS. A configuration SAS was briefly evaluated. The function of this SAS was to provide automatic speed regulation through control of the nozzles and flaps. With the configuration SAS on, the aircraft behaved like it was on the frontside of the power required curve. Thus the pilot could use a CTOL technique (i.e., $\theta \longrightarrow$ G/S). This SAS is described in Reference 7. The main interest here was the impact of failing such a SAS and requiring the pilot to revert to a STOL technique during an approach. This aspect of the experiment was not pursued more than flying just a few approaches. This was because of the recognized need for long-term pilot training before valid results could be obtained.

One negative comment made by the pilot concerned the large pitch changes required to control flight path. This was a result of the low value of n_{z_α} at this flight condition which is typical of this class of STOL airplane. This is reflected in Table III-1 by the degraded pilot opinion from baseline.

SECTION IV

FLARE AND LANDING

This section presents the flare and landing results obtained during the simulation along with an analysis of the results. The landings were generally a part of the combined approach and landing sequence. Thus the ILS tracking task and the flare and landing task were usually evaluated in conjunction with one another in a realistic way. Details of the flare and landing task were presented in Section II.

This section is broken down into two main parts. The first describes the types of data which were obtained. The second presents the numerical results and an analysis of the data. The second part is arranged in order of the various vehicle perturbations which were tested as was done in the glide slope tracking analysis of the previous section. The specific breakdown consists of:

- Approach speed variation
- Complementary control variation
- Ground effect
- Approach speed compensation for tailwinds.

A. TYPES OF DATA

The data obtained to describe flare and landing results include:

- Pilot comments
- Pilot numerical ratings
- Flare profile
- Measured touchdown performance.

1. Pilot Comments

Following each series of approach and landing runs the subject pilot prepared a written commentary of his reactions to the flare and landing task. The second part of Appendix E contains a summarized list of these

comments. The comments are arranged in alphabetical order of pilots and chronological order of cases flown by each pilot.

2. Pilot Ratings

The numerical pilot ratings which were obtained during the runs are listed in Table IV-1. Pilot ratings were given for three levels of wind severity: calm air, turbulence with steady winds, and turbulence with wind shears. In the table, each of these ratings is separated by a slash.

3. Flare Profile

A plot of attitude vs altitude (see Figure C-1) was recorded for each landing. This provided a means of observing the nature of the flare maneuver and led to the closed loop control description of the flare which is developed in Appendix C. The data presented in this report consist of averages of several representative flare profiles for a particular case. These averages are given in terms of $\Delta\theta/h_{FL}$ (flare gain) and h_{FL} (flare height).

4. Touchdown Performance Data

The touchdown sink rate, $\dot{h}_{TD}$, and the touchdown point relative to the runway threshold, x_{TD}, are the two parameters which are used to describe touchdown performance. They are plotted in a number of ways to show the problems associated with precision landings as the aircraft and atmospheric factors are varied.

B. RESULTS

1. Approach Speed Variation

The baseline approach configuration (65 kt case) provided a good starting point from which to make approach speed changes and examine the impact on flare and landing difficulties. The baseline case flare and landing pilot ratings for the 8 subject pilots had the following means and standard deviations:

MEAN	STANDARD DEVIATION	CONDITION
3.4	.7	Calm air
4.8	1.0	Turbulence and steady winds
5.7	.7	Turbulence and shears

TABLE IV-1

FLARE AND LANDING PILOT RATING SUMMARY

CASE	PILOTS							
	PILOT A	PILOT B	PILOT C	PILOT D	PILOT E	PILOT F	PILOT G	PILOT H
65 kt (Baseline)	4/5/6	4/5.25/5	3/5.5/7	4/5.5/5.5	3/4.5/5	4/6	2/3/5.5	3/4/6
55 kt	6/7.5/--							5/--/--
60 kt		4/8/8				3/6/8		
70 kt		3/4/4.5			3/4.5/5	4/7/9		
75 kt	4/5/--				4/4.5/5	3/5/7		
55 kt, 50 deg δ_ν	6.5/7/9							
1.5 - 3 sec Engine Lag	3.25/5/5.5					4/6/7		
Nozzle	4/6/8							
DDC			2.75/4.5/6					
DLC			2/4/5					
SAS Off		4/9/--						
Flight Director On						3/4/6		

Slashes separate wind conditions, i.e., calm air/turbulence with steady winds/turbulence with shears.

Thus the baseline case was considered to have marginally acceptable characteristics as defined by the pilot rating scale of Section II.

Figure IV-1 shows the effect of approach speed on the pilot ratings. There is a general deterioration in ratings as approach speed is decreased and little effect as it is increased. Straight line segments are faired to indicate these trends. The minimum acceptable approach speed (POR = 6.5 in turbulence) is between 60 and 65 kt and coincides with the minimum speed relative to the ILS tracking task.

Written pilot comments generally fit the numerical ratings. Some specific comments are worth mentioning, in particular those for the lower approach speeds examined.

At 55 kt, Pilot A complained of not having enough lift margin to cope with abuses with angle of attack reaching 20 to 23 deg. Also, the 15 deg pitch attitude at touchdown was nearly view limiting. Adequate touchdown sink rates were attainable.

Pilot B made a similar comment about margins for the 60 kt case. In addition, he recognized the need to lower the flare height as approach speed is decreased. Also, he indicated not having enough time to compensate for crosswinds prior to touchdown. He specifically termed the 60 kt case as "operationally unacceptable". His rating with turbulence was 8.

Pilot E made a short series* of calm air runs where he varied speed over a wide range to get a quick look at the gross effects. He commented on having to use increasing amounts of power at lower approach speeds. He felt this was no problem in smooth air but did not try it with turbulence.

Flare profiles were reduced for three of the pilots who concentrated on the effect of speed variation. The averages of those profiles are ploted in Figure IV-2. For the purpose of comparison the predicted "critical"† flare parameters are plotted along with the measured data.

---

* Insufficient training time was available for the various approach speeds, so the data from that series are not included here.

† A critical flare is the term coined for a flare which would result in a zero sink rate touchdown with no ballooning tendency if $C_{L_{max}}$ limits were neglected. See Appendix C for a more complete discussion.

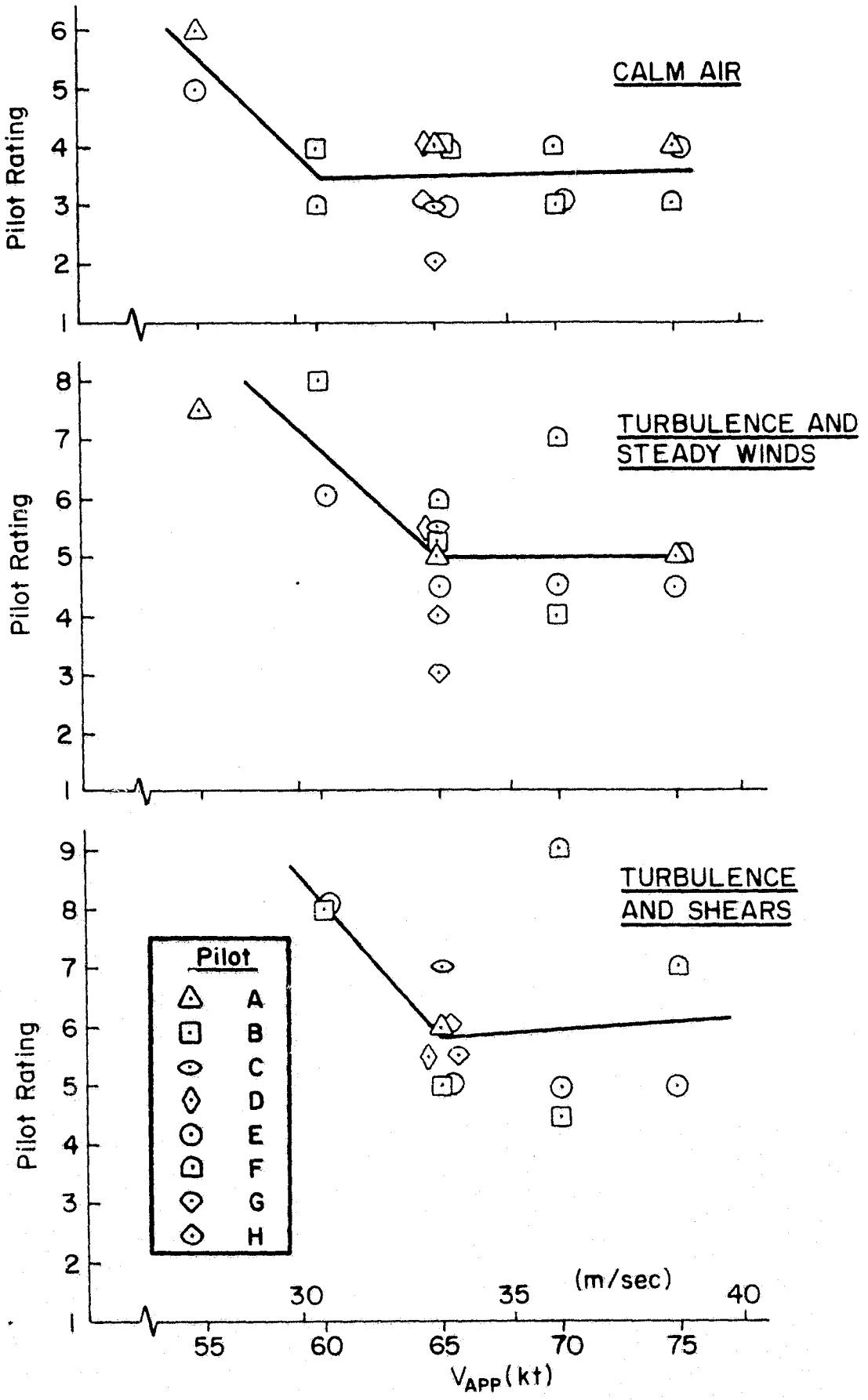

Figure IV-1. Flare Pilot Rating vs. Approach Speed

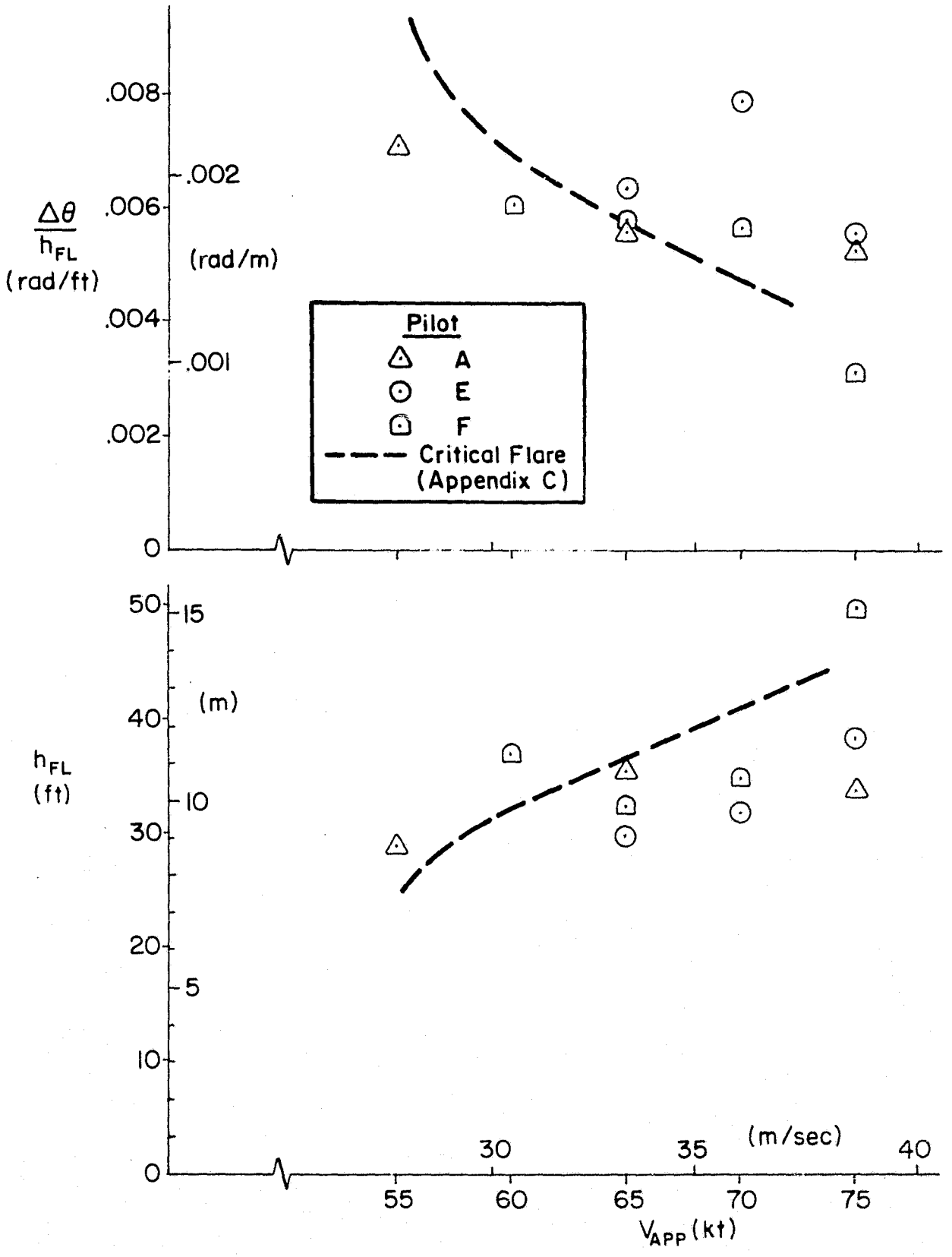

Figure IV-2. Measured Flare Profiles

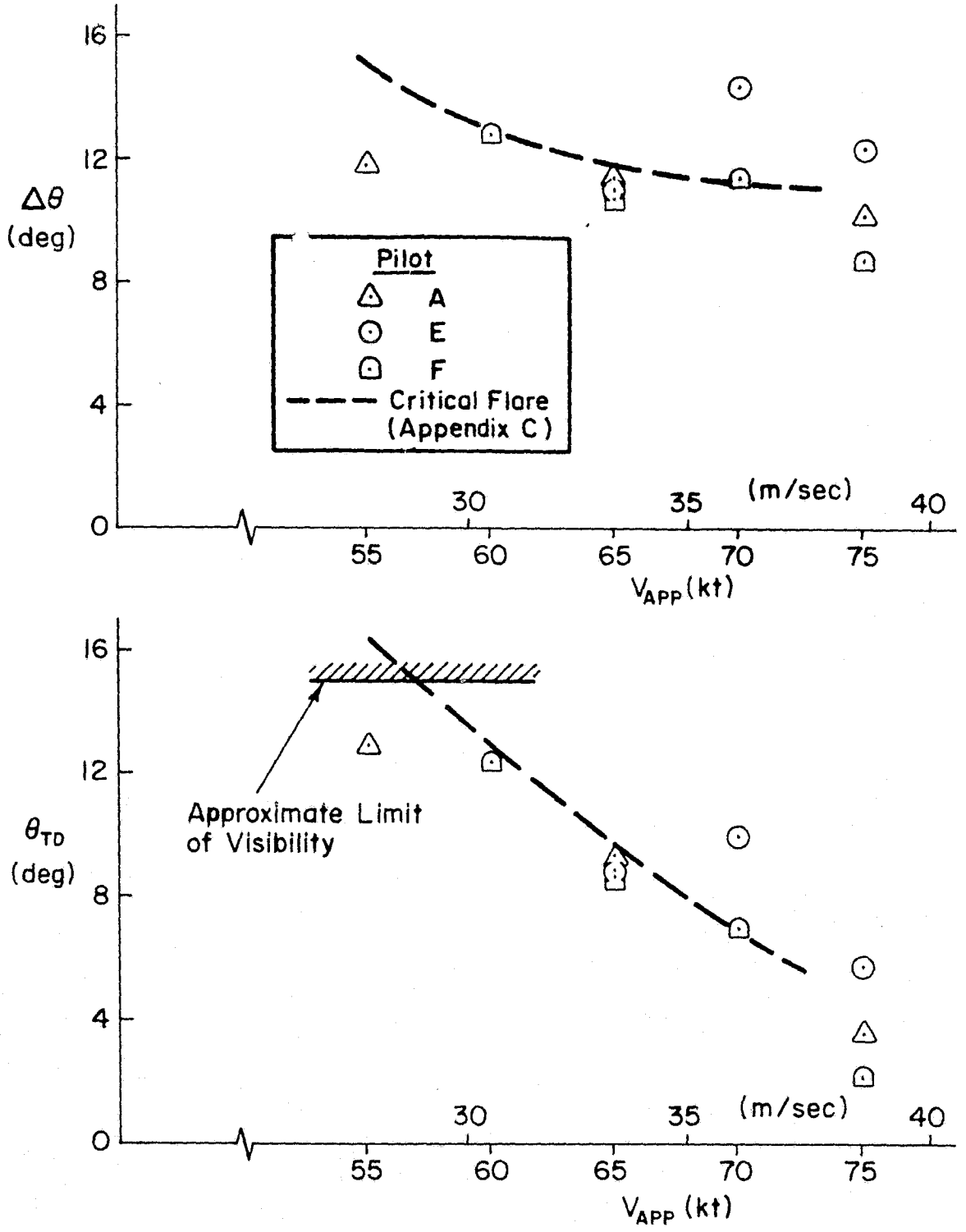

Figure IV-2 (Concluded)

The speed effect in the measured data is somewhat weaker than the theoretical case. However, at 65 kt where pilots had the most practice the profiles are all quite close to the critical flare. This strongly suggests that the simulation was, in fact, good enough to provide the pilot with sufficient visual information during flare for him to settle on the same optimized solution that would be obtained analytically.

The measured landing performance for the various approach speeds is presented in Figure IV-3. These data consist of run-by-run results of touchdown sink rate vs touchdown point. For each approach speed case the data is separated according to the level of atmospheric disturbance. The purpose of these plots is to show the data scatter and the correlation between touchdown sink rate and position.

Touchdown conditions at 65 kt are the best defined because this speed was used as a common baseline for all pilots. In calm air, we see a consistent pattern of $\dot{h}_{TD}$ vs x_{TD}, that is, hard/short landings progressing to soft landings in the touchdown zone (90 to 150 m or 300 to 500 ft) then becoming increasingly hard as floating occurs. Turbulence obscures this pattern. Also, the scatter with and without shears is about the same. These plots show a strong effect of V_{APP} on x_{TD}. Landings are shorter at slow speeds and longer at high speeds as would be expected. However, for the slow speeds it appears that the pilots had difficulty in making the touchdown zone.

The data points from Figure IV-3 are plotted in terms of cumulative distribution in Figure IV-4. These plots better indicate the sameness of data in turbulence with steady winds and turbulence with shears. More important, however, this sort of plot allows us to quantify the dispersions of sink rate and touchdown point along the runway. The 10, 50, and 90 percentile points (cumulative distribution of .1, .5, and .9) are thus plotted vs approach speed in the next set of figures.

Figure IV-5a shows the range of $\dot{h}_{TD}$ for varying approach speed and varying atmospheric distrubance. The solid lines indicate the general trends with and without turbulence. Similarly, Figure IV-5b shows the effect on touchdown point. The results of these plots are more easily viewed in Figures IV-6a and b where the faired trends are replotted to show the 10 to 90 percentile ranges on the same scale.

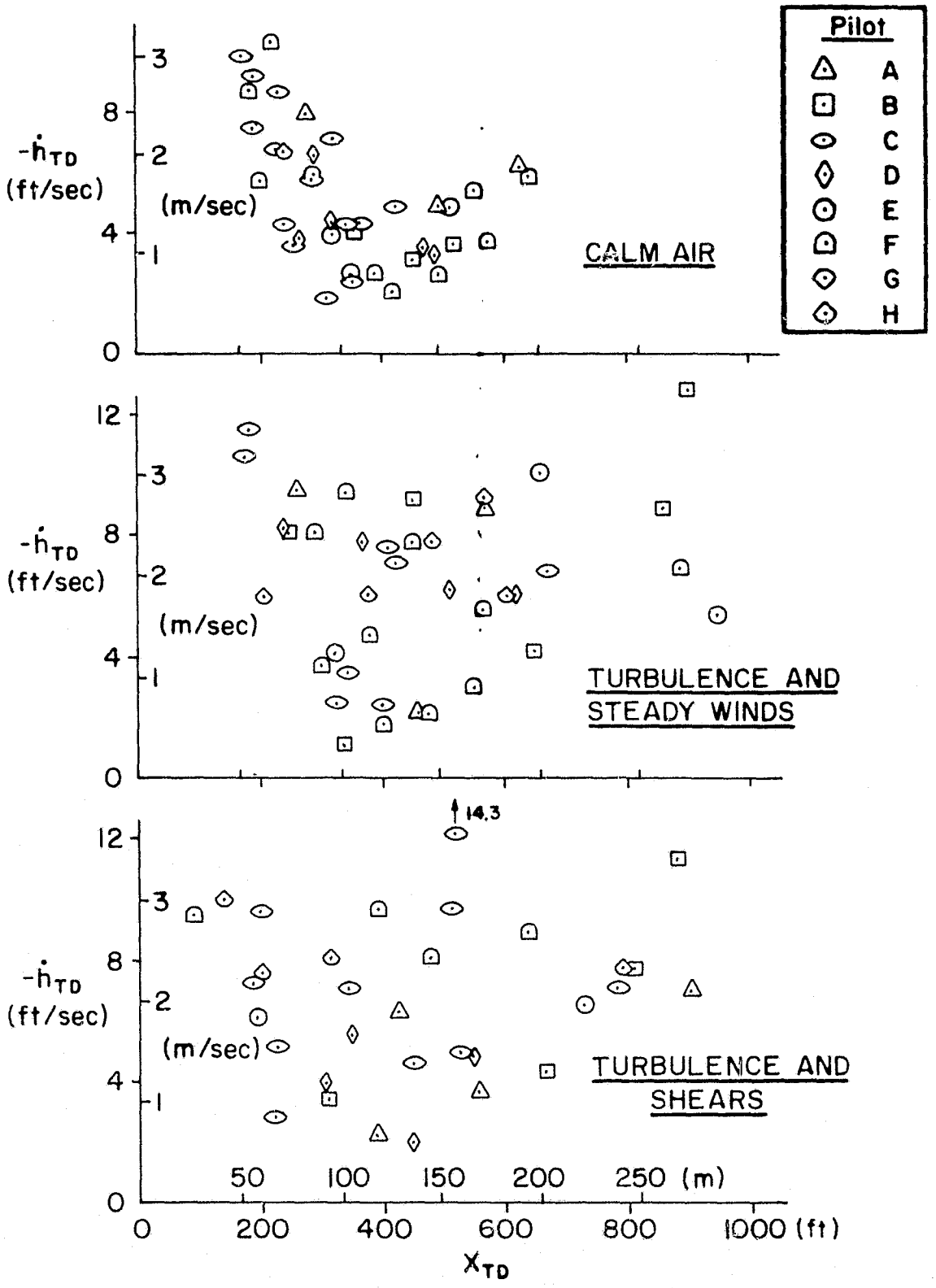

a. V_{APP} = 65 kt (Baseline Case)

Figure IV-3. Landing Performance, $\dot{h}_{TD}$ vs. X_{TD}

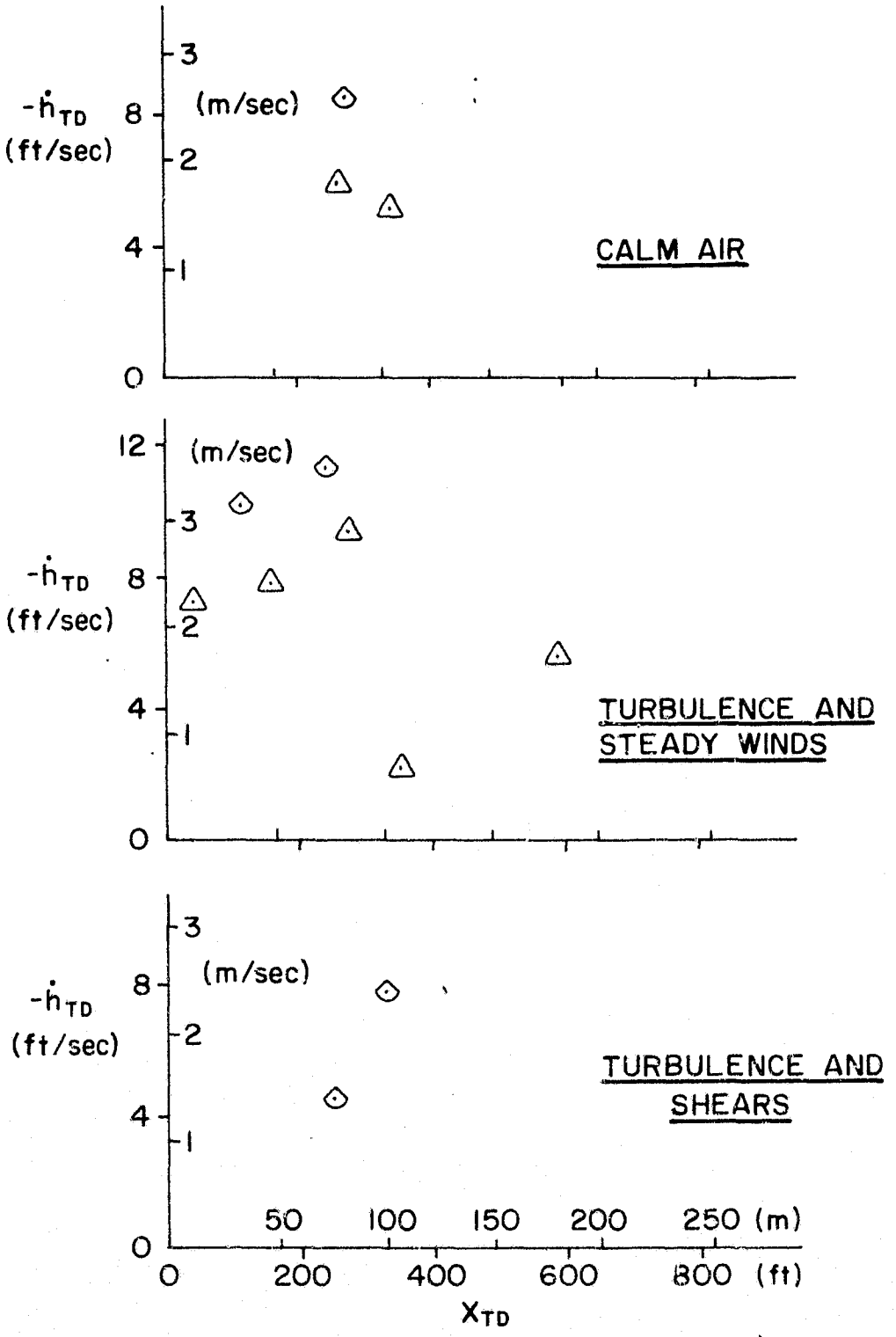

b. V_{APP} = 55 kt

Figure IV-3 (Continued)

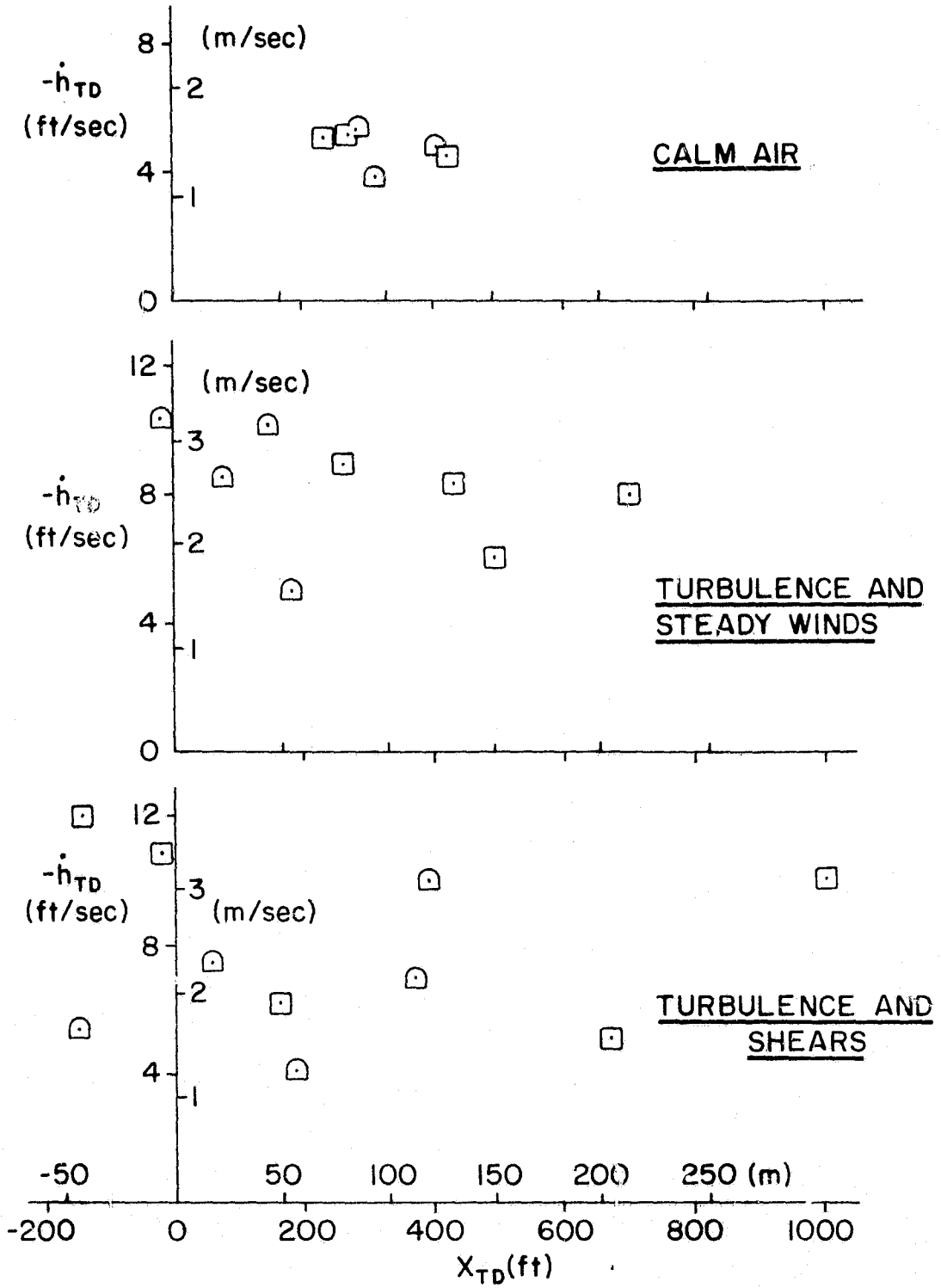

c. V_{APP} = 60 kt

Figure IV-3 (Continued)

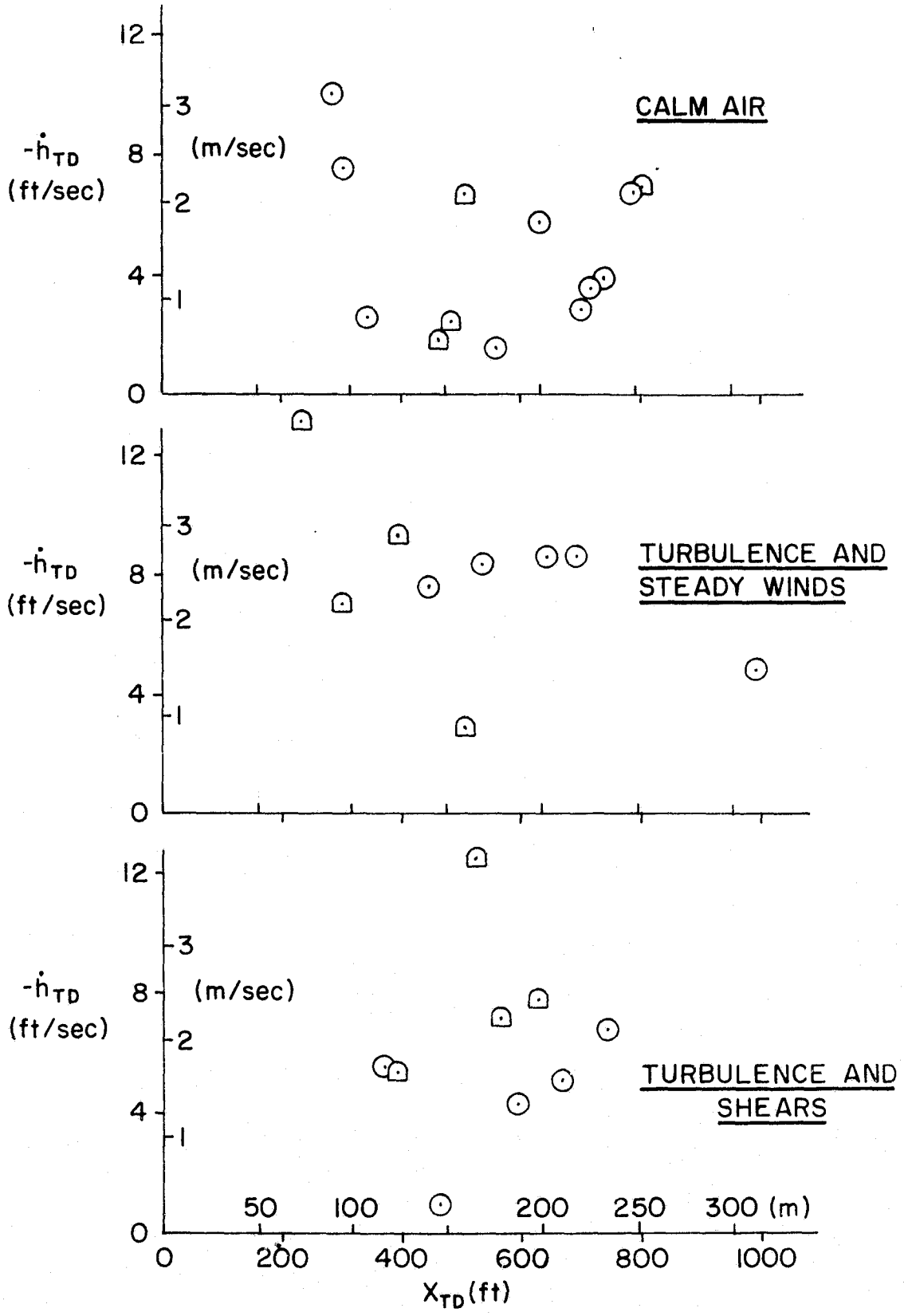

d. V_{APP} = 70 kt

Figure IV-3 (Continued)

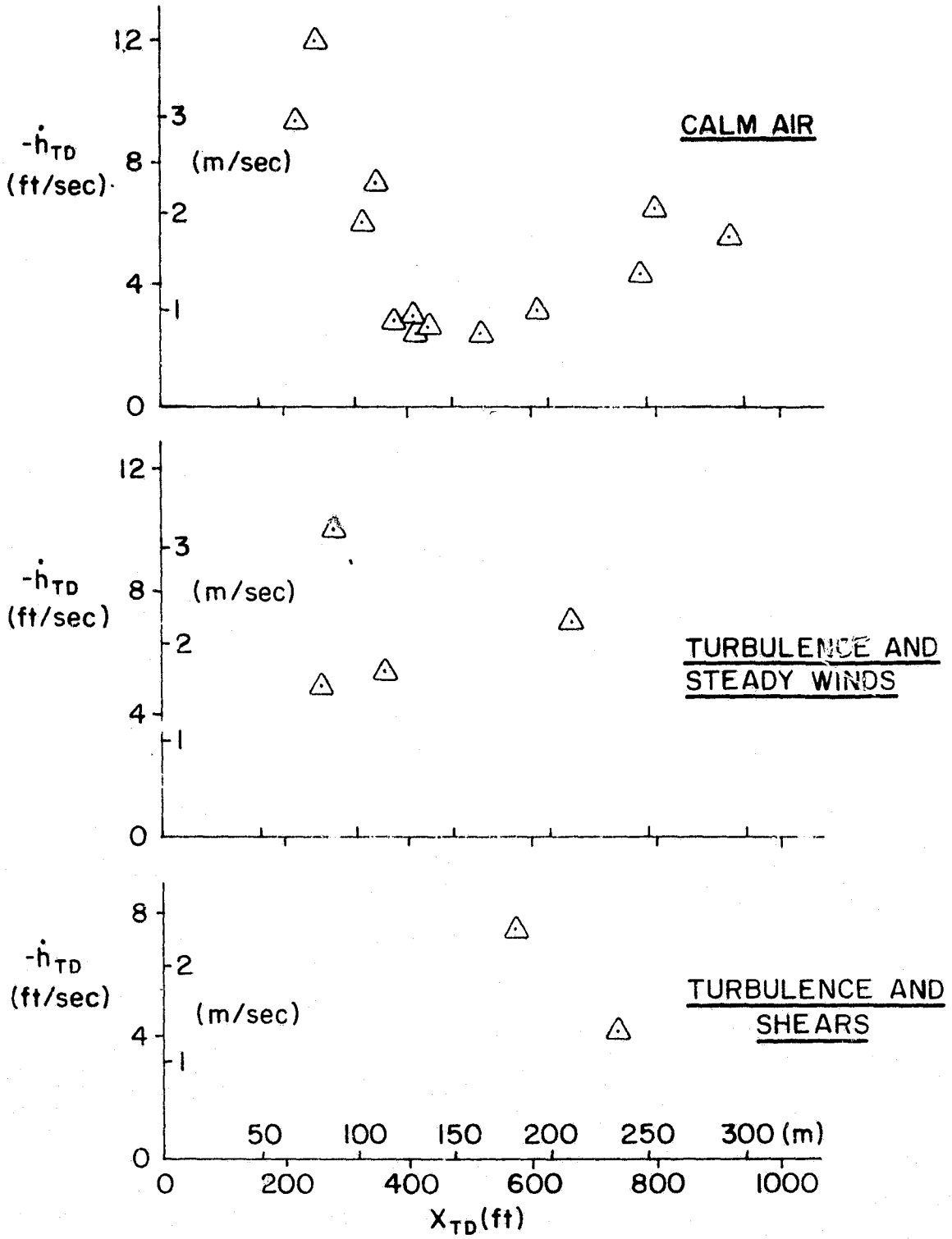

e. V_{APP} = 75 kt

Figure IV-3 (Concluded)

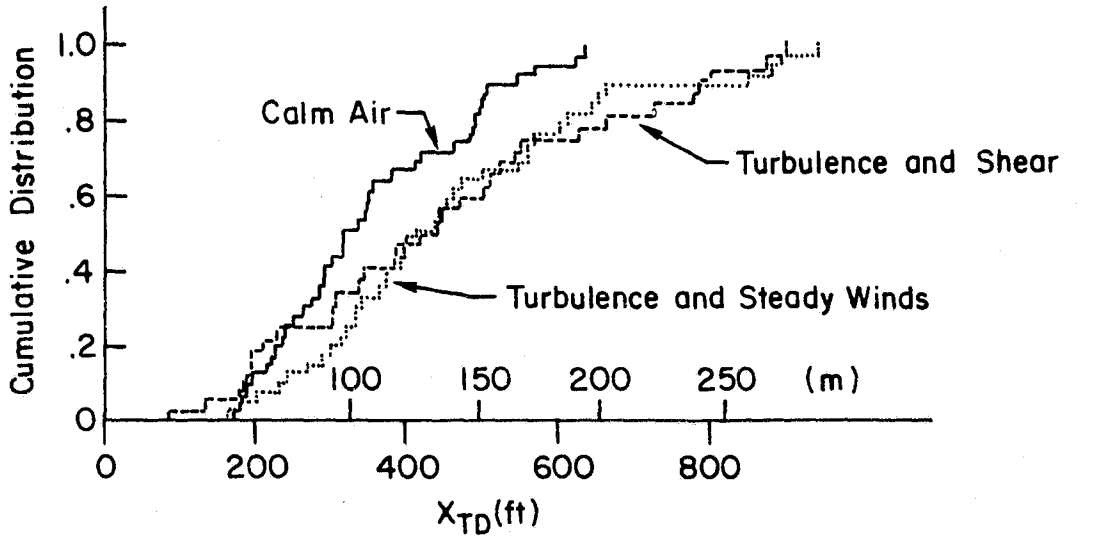

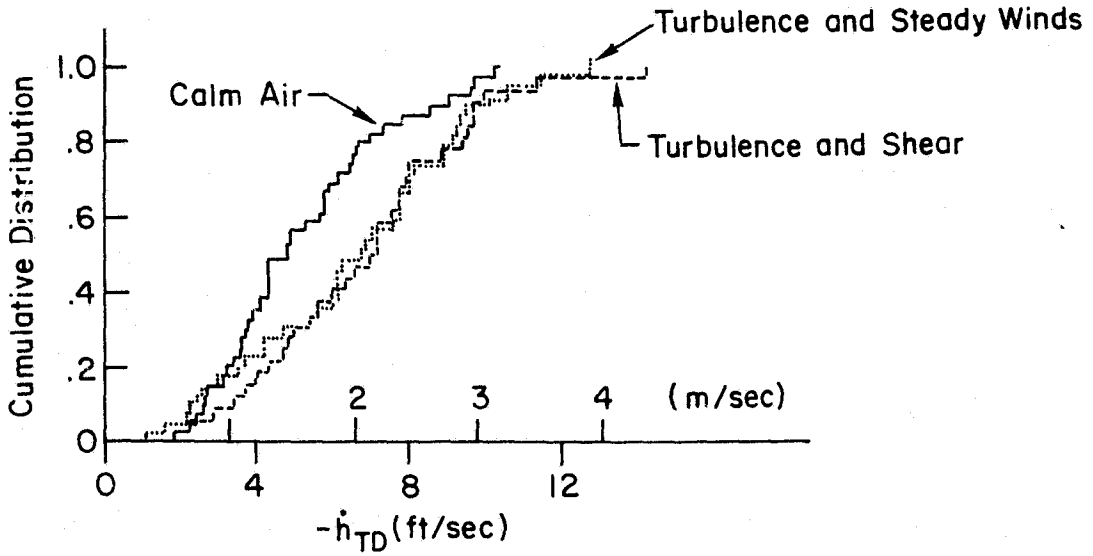

a. V_{APP} = 65 kt

Figure IV-4. Cumulative Touchdown Performance; X_{TD} and $\dot{h}_{TD}$

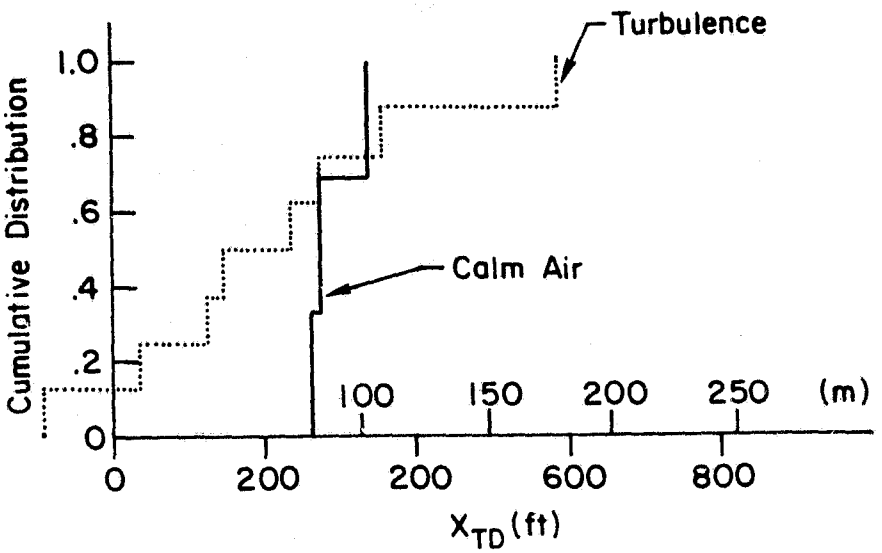

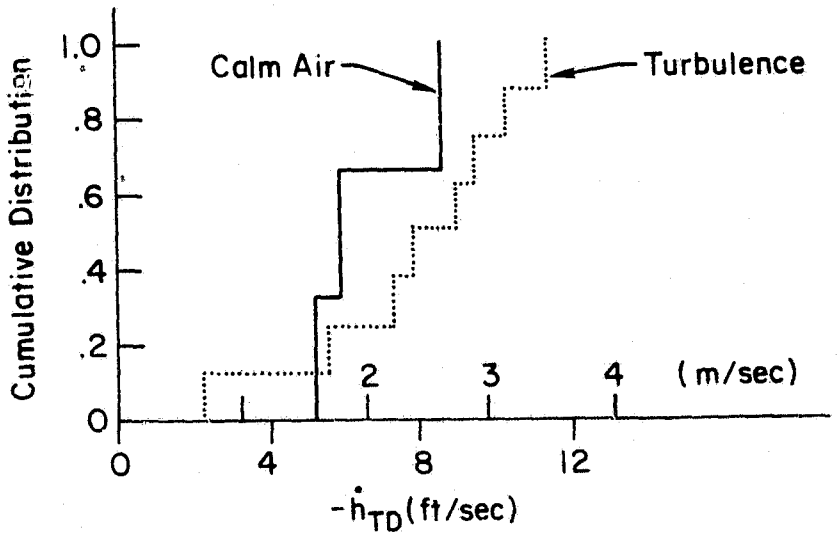

b. V_{APP} = 55 kt

Figure IV-4 (Continued)

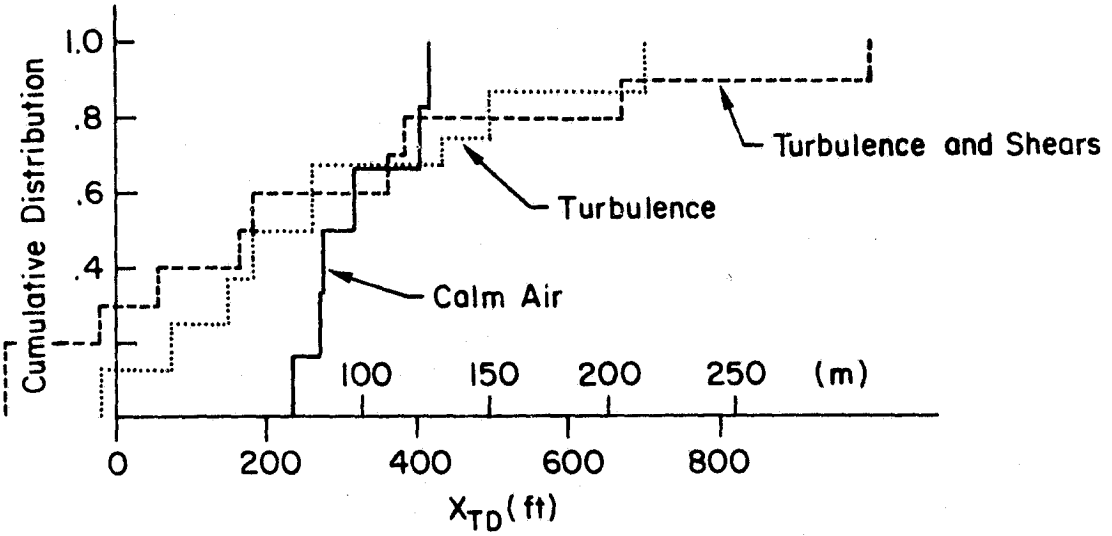

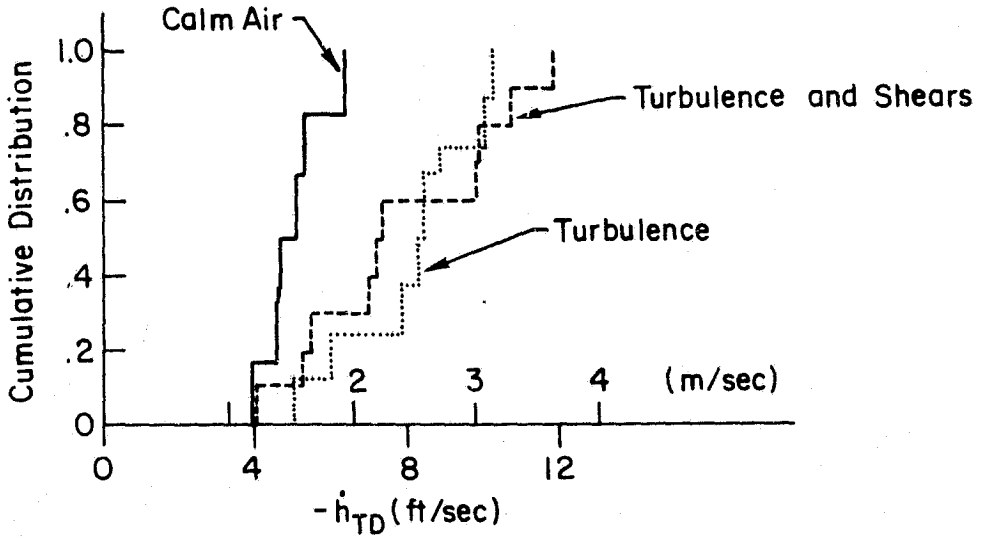

c. V_{APP} = 60 kt

Figure IV-4 (Continued)

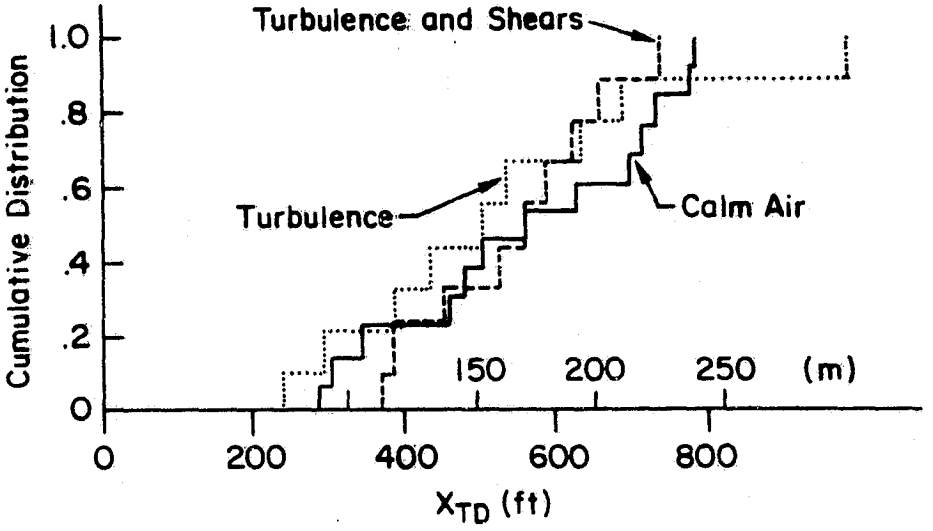

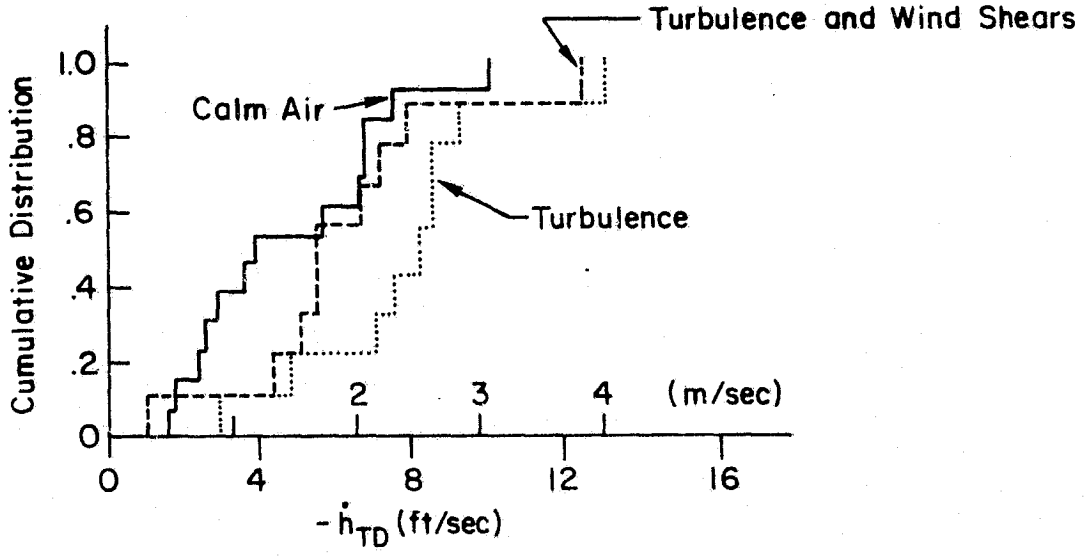

d. V_{APP} = 70 kt

Figure IV-4 (Continued)

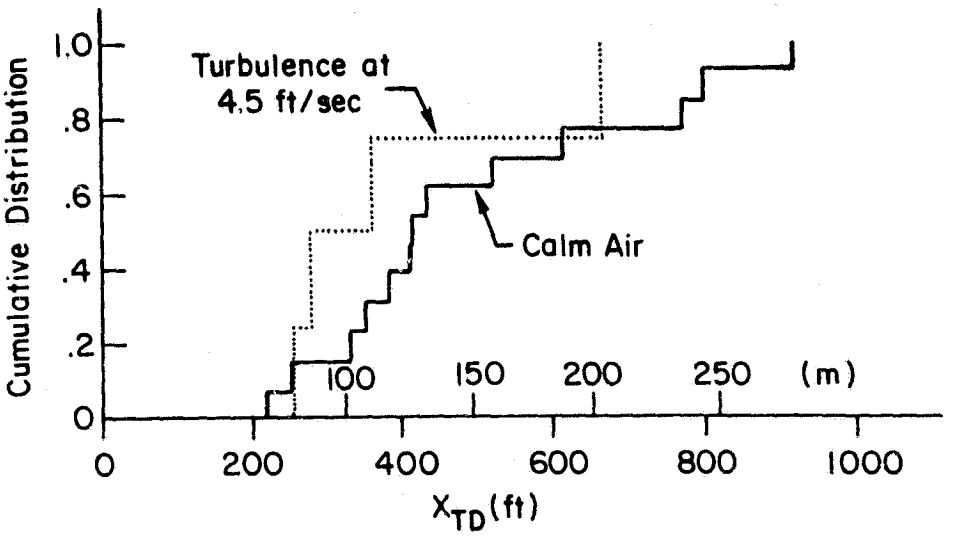

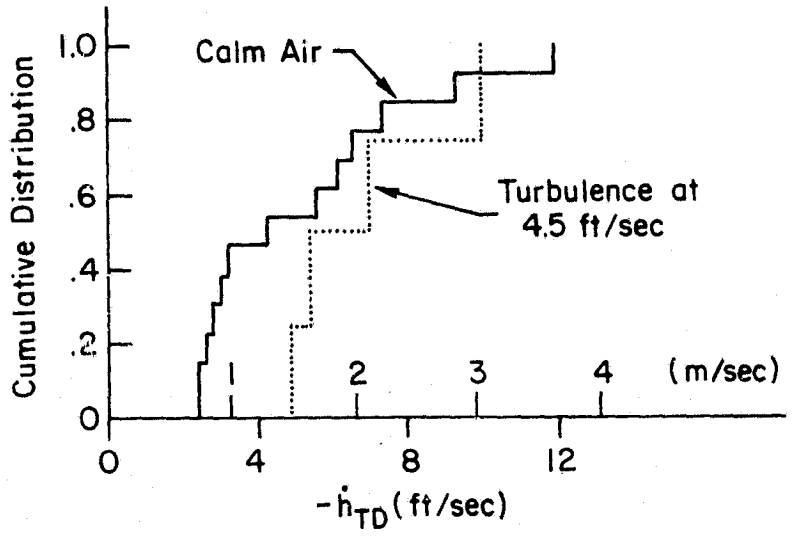

e. V_{APP} = 75 kt

Figure IV-4 (Concluded)

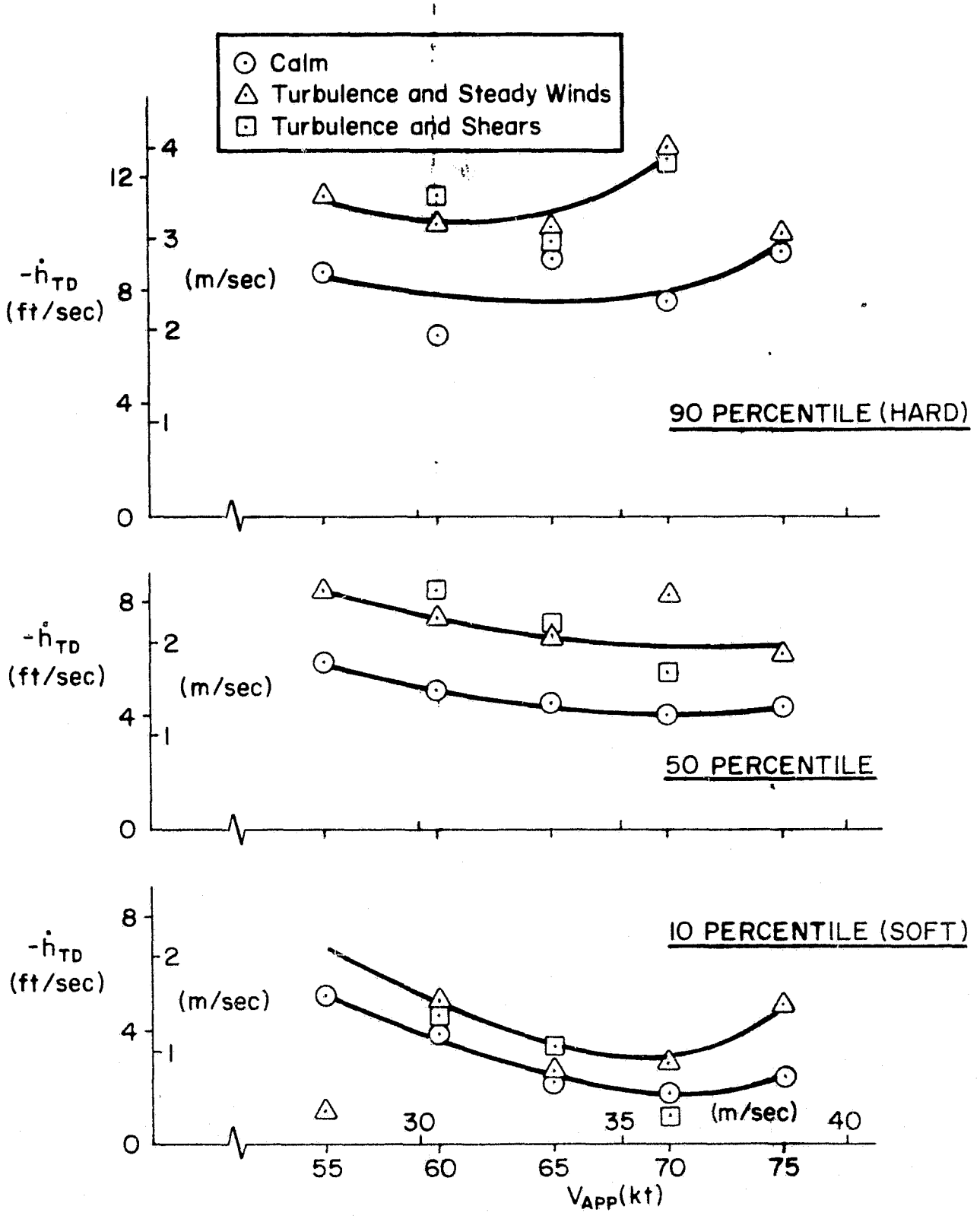

a. Touchdown Sink Rate

Figure IV-5. Landing Performance vs. Approach Speed

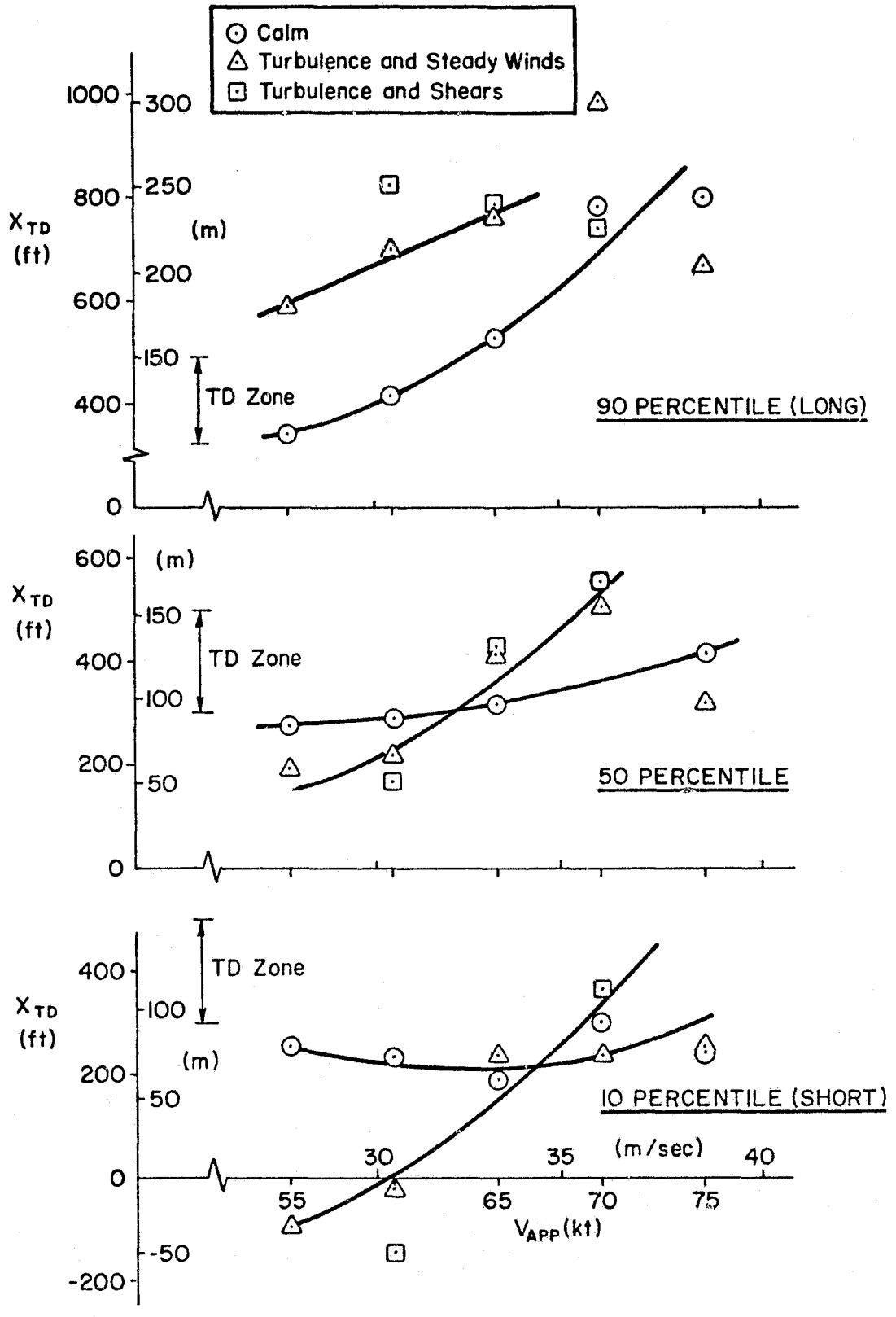

b. Touchdown Point

Figure IV-5 (Concluded)

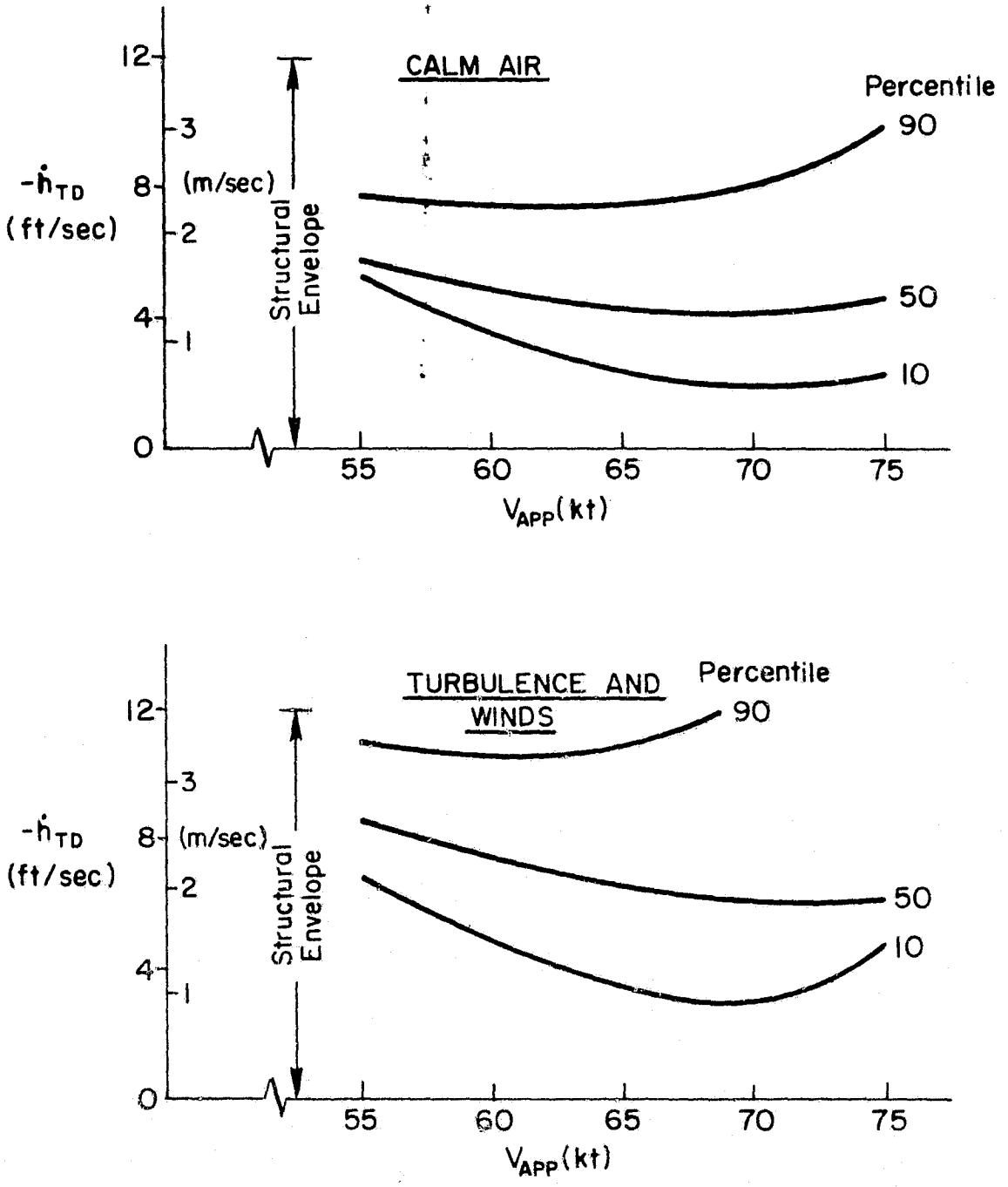

a. Touchdown Sink Rate
(Faired Lines From Fig. IV-5a)

Figure IV-6. General Effect of Approach Speed

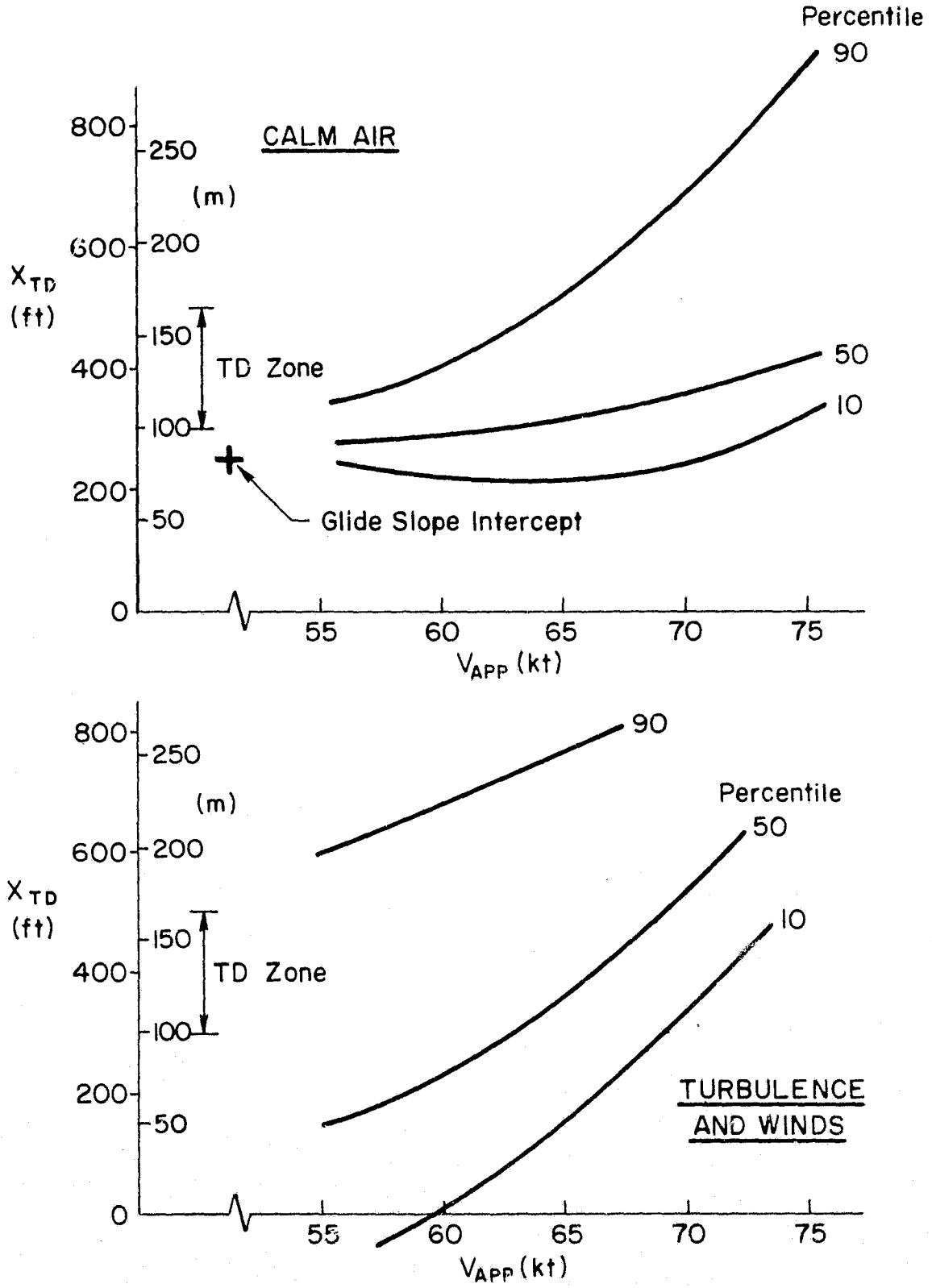

b. Touchdown Point
(Faired Lines from Fig. IV-5b)

Figure IV-6 (Concluded)

Figure IV-6a shows that at low speeds landing tends to be consistently hard while at high speeds more inconsistent with most soft but some very hard landings. There appears to be a tradeoff in the intermediate speed range. Turbulence affects this mainly by adding an incremental $\dot{h}_{TD}$ to the calm air results.

The touchdown point results (Figure IV-6b) are perhaps more interesting. In calm air at low speeds there is little touchdown point dispersion and landings tend toward the runway glide slope intercept. At higher speeds the 10 to 50 percentile range falls within the touchdown zone but some landings tend to be excessively long. Again, the intermediate speeds show a favorable tradeoff. When turbulence and winds are introduced the effect on touchdown point dispersion is disturbing. Regardless of approach speed the 10 to 90 percentile range is at least twice the length of the touchdown zone. Also, the 10 percentile line falls short of the threshold at about 60 kt.

To summarize the approach speed effect on flare and landing:

- The pilot ratings, comments, and performance were consistent with a minimum acceptable speed of slightly less than 65 kt.
- Lower approach speeds were characterized by pilots complaining of lack of safety margin and ability to cope with abuses. Performance problems seemed to be the tendency for short landings and, to a lesser degree, hard landings.
- High approach speeds did not improve ratings, in fact, performance was adversely affected (i.e., touchdowns beyond the touchdown zone and more dispersion in sink rates).

2. Complementary Control Variations

The landings made with variations in thrust lag, effective thrust angle, and piloting technique revealed a few noteworthy items. These are mainly qualitative, in the form of pilot comments. The relatively small number of landings involved limits the use of the performance data gathered.

Thrust lag seemed to be the key factor in use of throttle either just prior to or during flare. Pilot C, who made the most direct comments

concerning power to flare, allowed that the baseline thrust lag (τ = .7 sec) permitted some open loop gust compensation with power during the flare. However, he indicated that DLC (same thrust orientation as baseline but zero lag) provided a good means of flaring the aircraft in a closed loop manner. Also, he gives a better pilot rating for the DLC case.

This ties in with the flight path control and flare analysis that was done for this simulation. The nominal flare is modeled in Appendix C by using a $\Delta h \longrightarrow \theta$ feedback. At 65 kt the measured gain of this feedback gives a crossover frequency of .47 rad/sec which indicates the bandwidth desired by the pilot. In contrast, from Appendix B, the available flight path bandwidth using the nominal engine lag is .34 rad/sec. Using DLC this bandwidth goes up to .44 rad/sec which is close to that desired. This indicates that depending on power to flare hinges in part on adequate flight path control response.

In some cases the pilot was requested to flare using the nozzles. Comments mentioned difficulty due to slow flight path response. In view of the sort of analysis of the previous paragraph such a comment is not surprising. The flight path bandwidth with nozzle (or DDC) is only .09 rad/sec (speed uncontrolled).

Pilot C indicated one way of using a DDC type control in the flare was the control of speed bleed off by countering with DDC. However, he also mentioned that this could have an adverse effect on touchdown position. He gives a slightly better rating with DDC over the nominal case.

3. Ground Effect

All the approach and landing cases were nominally made without a ground effect. A short series of runs was made to get some feel for how a ground effect might influence the results.

The ground effect model used provided a simple increment of lift or drag scaled as an exponential function of height above the ground. Three parameters were used to define ground effect, K_L, K_D, and h_1 where

$$\Delta C_L = K_L e^{-h/h_1} (C_L)_{\text{zero GE}}$$

$$\Delta C_D = K_D e^{-h/h_1} (C_L)_{\text{zero GE}}$$

Thus for K_L = +.1 and h_1 = 10 ft a favorable lift ground effect of 10% was felt at touchdown while only 3.7% was felt at the scale height of 10 ft. The ground effect parameters used were:

h_1	K_L	K_D	
10 ft	ZERO	ZERO	(no effect)
10 ft	.1	ZERO	
10 ft	.2	ZERO	
20 ft	.1	ZERO	
10 ft	ZERO	-.1	
10 ft	ZERO	-.5	

The runs were made in calm air starting from 200 ft initial altitude with the baseline approach case.

The results of the ground effect tests are summarized in Table IV-2 according to pilot ratings, pilot comments, flare profile, and touchdown performance. Since the number of runs was small the results are expressed in mainly qualitative terms.

4. Approach Speed Compensation for Tailwinds

In any set of runs in this experiment the target approach speed was maintained constant regardless of the wind conditions. This meant that although V_{APP} was constant, the angle of attack and speed margins were changing with the wind. After flying a series of runs at constant V_{APP}, Hardy felt that the matter of compensation for winds with approach speed should be examined. Tailwinds in particular were singled out because they presented especially difficult piloting problems. This led to a short series of landings from 200 ft initial altitude without turbulence. The resulting tests and analysis pointed up more than just the matter of angle of attack and speed margins, it also showed that a degree of compensation in the flare maneuver was required to avoid hard landings.

Runs were started using the 65 kt case in calm air. The pilot made a few landings to provide a baseline. The next step was to provide a 10 kt

C-2

TABLE IV-2

RESULTS OF GROUND EFFECT STUDY

CASE	PILOT RATING	COMMENTS	FLARE PROFILE	TOUCHDOWN PERFORMANCE
No ground effect	3			
$K_L = .1$, $h_1 = 10$	2.5	Liked this level.	Flare started about 5 ft earlier and a little less abrupt.	Consistently good $\dot{h}_{TD}$ but mild floating tendency in a few cases.
$K_L = .2$, $h_1 = 10$	2.5	Felt that more learning would be required to judge fairly but probably would like it.	Wasn't sure how to adjust.	Strong floating tendency.
$K_L = .1$, $h_1 = 20$	2	Like this combination best.	About the same as the lower h_1.	
$K_D = -.1$, $h_1 = 10$	3		Higher flare, less abrupt.	Not much changed from baseline.
$K_D = -.5$, $h_1 = 10$	-	Unlandable, feels like an afterburner cuts in near the ground.		Extreme floating tendency.

tailwind holding the approach speed at 65 kt. Then, with this level of tailwind the approach speed was increased to 67.5 kt and finally to 70 kt. The series ended after returning to the 65 kt no wind case. The object was for the pilot to qualitatively examine the adequacy of margins with respect to the flare. At the same time flare profiles and touchdown data were recorded.

According to the pilot there was a noticeable loss of "flareability" between the zero wind and 10 kt tailwind cases. This flareability was restored as the approach speed was increased.

The analysis performed after this experiment suggested that the term flareability used by the pilot is best quantified as how insensitive an adequate break in sink rate is to a range of flare maneuvers. This is related to angle of attack or speed margins but not uniquely.

The pilot's sense of flareability agreed with the computed margins as shown in Figure IV-7. Whether the desired margin be in angle of attack or speed, or whether the margins are taken for initial trim conditions or for touchdown about 5 kt must be added to the 65 kt approach speed to compensate for a 10 kt tailwind. (On the other hand the approach speed could be decreased for a headwind.)

The actual touchdown performance for this series of runs brings to light another feature of the tailwind effect. This concerns the flare maneuver whereas the margins were related to flare potential.

The analysis methods of Appendix C can be used to show how the flare maneuver can be adjusted to compensate for winds. The adjustment is mainly to offset the variation in initial sink rate prior to flare. For the 65 kt case $\dot{h}_o$ is -4.4 m/s (-14.3 ft/s) with a 10 kt tailwind. The pilot must either start the flare higher (h_{FL}) or make the flare more abrupt $\left(\frac{\Delta\theta}{h_{FL}}\right)$.

Figure IV-8 shows the flare data from these tests along with the theoretical flare parameters for a "good landing". The open symbols are touchdowns less than 1.8 m/s (6 ft/s), the closed are harder. The dashed line is the trade-off of $\Delta\theta$ vs h_{FL} to get exactly 1.8 m/s (6 ft/s). Note first that the theoretical line generally separates the good landings from the bad. More important, this theoretical flare changes considerably with wind and only slightly with

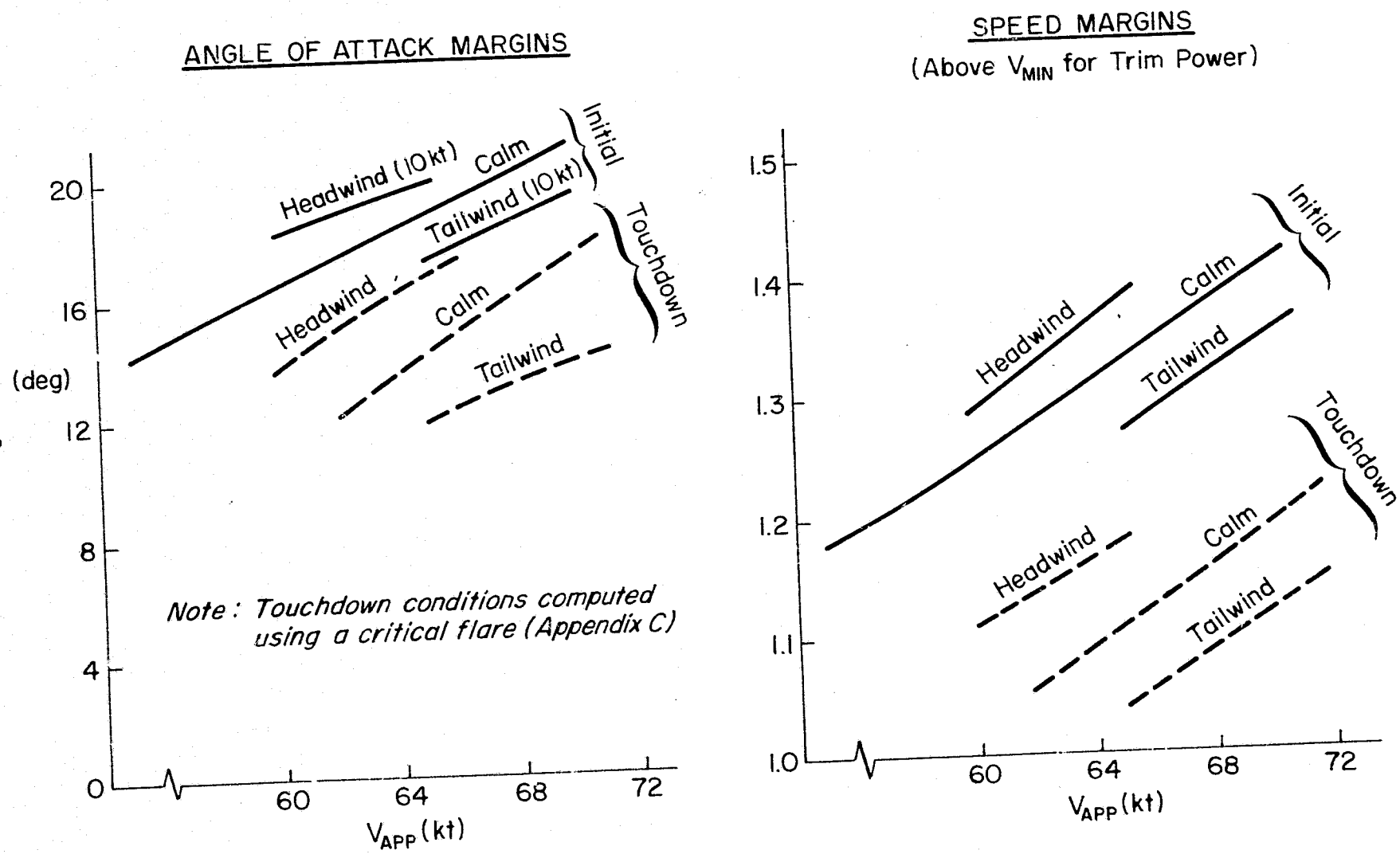

Figure IV-7. Margins vs. Approach Speed and Steady Winds

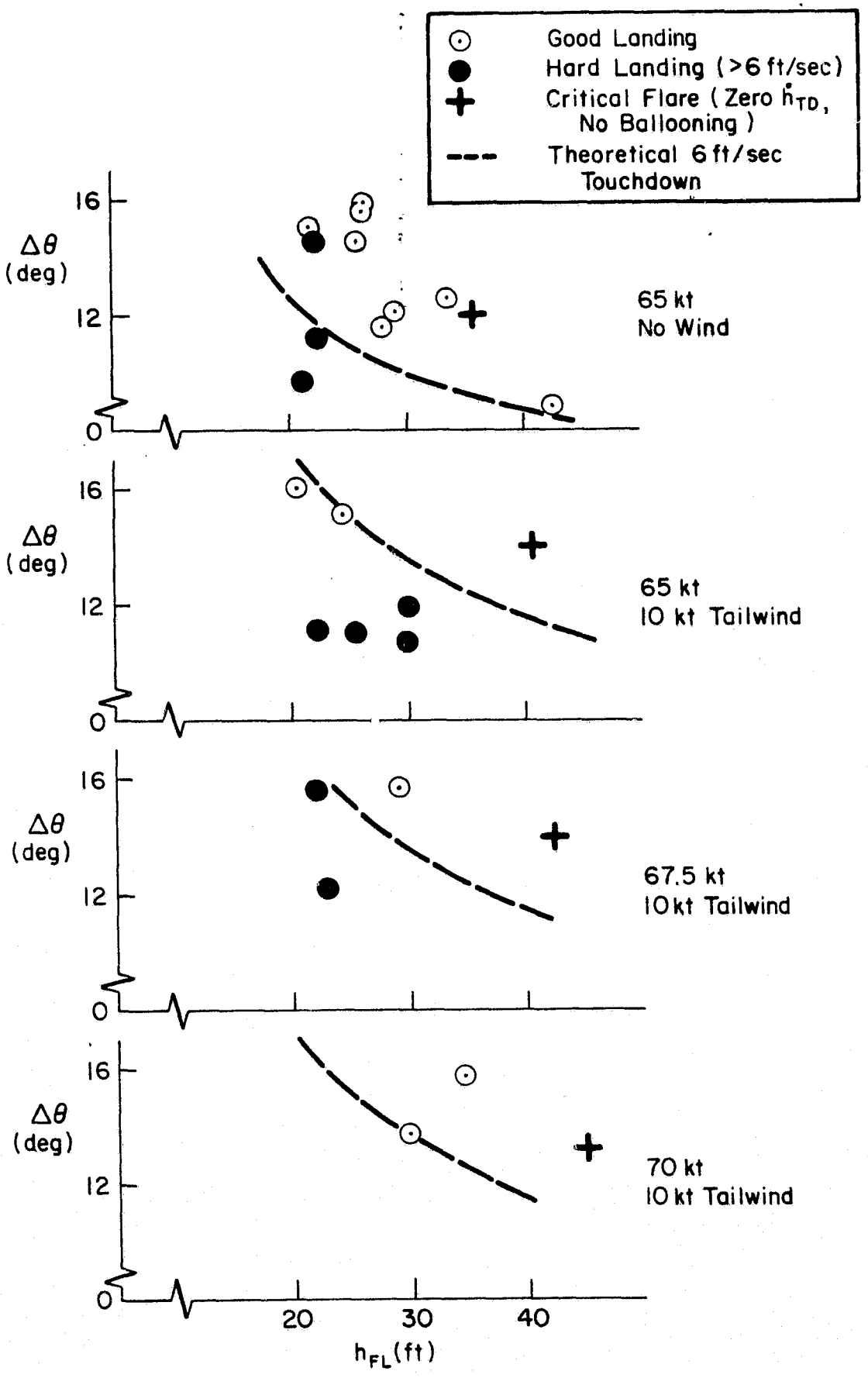

Figure IV-8. Flare Technique Used in Tailwind Experiment

approach speed. For the 10 kt tailwind, the attitude excursion must be increased about 3 - 4 deg or the flare height about 10 to 20 ft.

This part of the flare and landing experiment thus points out the degree of approach speed adjustment necessary to maintain a given speed or angle of attack margin for this airplane in the presence of headwinds or tailwinds. At the same time, a flare maneuver adjustment is required to preserve touchdown sink rate performance.

SECTION V

GO-AROUND

This section deals with the problems associated with go-arounds for the STOL aircraft simulated. A relatively small amount of simulator time was devoted to go-arounds because of the emphasis on the approach and landing tasks. Therefore, this section will be limited mainly to a qualitative discussion of pilot's observations and of the small amount of data collected. This discussion will center primarily on the problem of go-arounds involving an engine failure. As a sidelight we will also discuss continued approaches with an engine failure.

Go-arounds were conducted in two ways. A series of planned go-arounds were made by two pilots to closely examine the factors involved and to establish go-around procedures. Then, during the approach and landing tasks, pilots were forced to make unannounced go-arounds by lowering the ceiling below the decision height of 60 m (200 ft). An engine was frequently failed as the pilot applied go-around power. Unfortunately time did not permit a sufficient number of the unannounced variety of go-arounds to obtain meaningful statistics.

The general procedure established for go-arounds was:

- Reposition throttles to maximum power
- Reposition nozzles to 6 deg (fully retracted)
- Reposition flaps to 30 deg
- Climb at 75 kt unless pitch attitude exceeds 15 deg in which case increase speed to hold at 15 deg
- Maintain heading of 090 and climb to 335 m (1100 ft).

This procedure provided a starting point for examination by each pilot. Variations were tried as each pilot saw fit.

A. AEO GO-AROUNDS

Go-arounds with all engines operating were made on occasion but were universally considered to be no problem for this aircraft. Altitude losses below decision height were minimal. The mean loss was about 10 m (30 ft) with a standard deviation of about 3 m (10 ft). The procedures were different from those of a CTOL aircraft in that three distinct motions were required to reposition the throttles, nozzles, and flaps. Regardless, the task was considered easy. Thus, go-arounds with all engines operating require no further discussion here.

B. OEI GO-AROUNDS

Go-arounds complicated by an engine failure deserve a good deal of attention. This aircraft, being a twin engine design, would seem to represent something of an extreme in adverse handling and performance under engine out/maximum power conditions. It is perhaps the antithesis of the 4 engine deflected slipstream simulation of Reference 1 for which there were no asymmetries (because of propeller cross-shafting) and only a 25% loss of power (actually only 15% loss of thrust) with an engine failure.

For the AWJSRA, the single engine steady state climb performance was marginal (see Figure A-4) with a maximum flight path angle only slightly greater than 4 deg. This shortcoming was aggravated by the initial sequence of events involving execution of the go-around procedure and coping with engine failure transients. Pilot A found that the aircraft motions due to an engine failure were a confusing clue as to which engine had failed. He complained that the aircraft rolled in the opposite direction to what he expected. (i.e. loss of right engine produced a net loss of lift on the left wing because of cross-ducting yet the nose yawed to the right which is normal.) Further, he was reluctant to add go-around power because the yaw asymmetry was so difficult to control.

The single engine go-around performance measurements showed that the minimum altitudes were considerably below the decision height of 200 ft.

Also, the minimum plane penetrated* on climbout to 335 m (1100 ft) was marginal with respect to that specified in Reference 8 (i.e., 4 deg). For both of the above performance measures it was apparent that pilot technique was an important factor.

Specifically, minimum altitude for all the single engine go-arounds had an average value of about 26 m (85 ft), with a standard deviation of about 6 m (20 ft). The biggest factor in the variation observed here seemed to be the quickness of the attitude change upon go-around initiation. A rapid nose up command to +15 deg resulted in a minimum altitude of around 34 m (110 ft). Where a pilot would emphasize the acceleration to 75 kt rather than the initial rotation, altitude loss would be larger.

The minimum plane penetrated was generally about 5 deg, 1 deg less than the theoretical best for this simulation model, assuming climb at γ_{max} = 4.2 deg from h_{min} to 335 m (1100 ft).

Pilot workload probably did not adversely affect the performance measured in the simulation. However, the level of workload was high enough that pilots elected to assign the right seat man duties such as repositioning flaps and calling out airspeed. The pilot would generally prefer to handle the nozzles because of the coordination required with power and lateral-directional controls. An automatic reconfiguration scheme such as that of the BR 941S could probably remove any requirements for the second man.

C. OEI CONTINUED APPROACHES

A single engine continued approach and landing was evaluated at some length by Pilot B. Discussion of this logically follows the single engine go-around because the piloting problems are similar.

Loss of power early in the approach allowed reconfiguration. For Pilot B the desired continued approach configuration consisted of moving nozzles from 75 deg to 40 deg and leaving flaps at 65 deg. Approach speed was increased to 75 kt because of reduced margin above V_{min}. This resulted in an ILS tracking rating of 4.5 in calm air. No rating was given for

---

* The minimum plane penetrated intersects the runway at 640 m (2100 ft) from the threshold. This is the same definition used in Section VI.

turbulence conditions but the pilot termed workload as moderately high with marginal safety margins.

With the above reconfiguration flare and landing was considered more of a problem than the approach. Touchdowns were generally long. Reducing power to prevent this resulted in excessive sink rate and hard landings. A suitable compromise was not found for making a good landing in the touchdown zone. The pilot rating for flare and landing was 5.5

The above discussion applies to power losses down to an altitude of 60 m (200 ft). Below this, there was not enough time for reconfiguration. However, Pilot B found that good landings were possible by avoiding the temptation to make a large power increase and by accepting a landing short of the touchdown zone. Excessive power excited lateral-directional problems and generally resulted in an unavoidable lateral drift. If there were a "gray" area for successful landings it was for engine failures between 60 m (200 ft) and 30 m (100 ft). In that region correct pilot reaction was most critical.

SECTION VI

TAKEOFF DATA

A. TEST CONDITIONS

All takeoff tests were conducted with an aircraft gross weight of 18143 kg (40,000 lb), a flap setting of 30 deg, and a nozzle setting of 6 deg. Tests were conducted to determine the minimum takeoff velocity, the balanced field length, and the effects on takeoff performance* of V_2 and V_R abuses, engine failures, crosswinds, and turbulence. Throughout the tests, a nominal rotation speed (V_R) of 60 kt and a nominal climb speed (V_2) of 82 kt were used.

B. V_{MU} TESTING

Tests to determine the minimum takeoff velocity (V_{MU}) were conducted by rotating the aircraft as early as possible and measuring the distance to lift-off (x_{LOF}) and the velocity at lift-off (V_{LOF}). The takeoff roll was approximately 200 m (650 ft) with a minimum V_{LOF} of 62.5 kt.

C. BALANCED FIELD LENGTH

No testing was done to explicitly evaluate V_1 for this aircraft. However, the data in Figure VI-1 was computed by measuring the distance required to accelerate to V_{EC} and assuming that the aircraft decelerated at .17 g (the deceleration available from braking) to a complete stop. A pilot delay of 1 sec is included between engine failure and brake application to account for any pilot lags. Figure VI-1 indicates that V_1 is slightly greater than V_R (and would thus be set equal to V_R) and that the balanced field length is 500 m (1640 ft).

For the Breguet 941S simulation (Reference 1) it was also found that $V_1 \doteq V_R$ for balanced field length. Furthermore the OEI takeoff performance was quite insensitive to V_1. Reducing V_1 from 65 kt to 0 only increased

---

* Although the takeoff simulations were initiated with a velocity of 20 kt, all distances have been corrected to correspond to zero initial velocity.

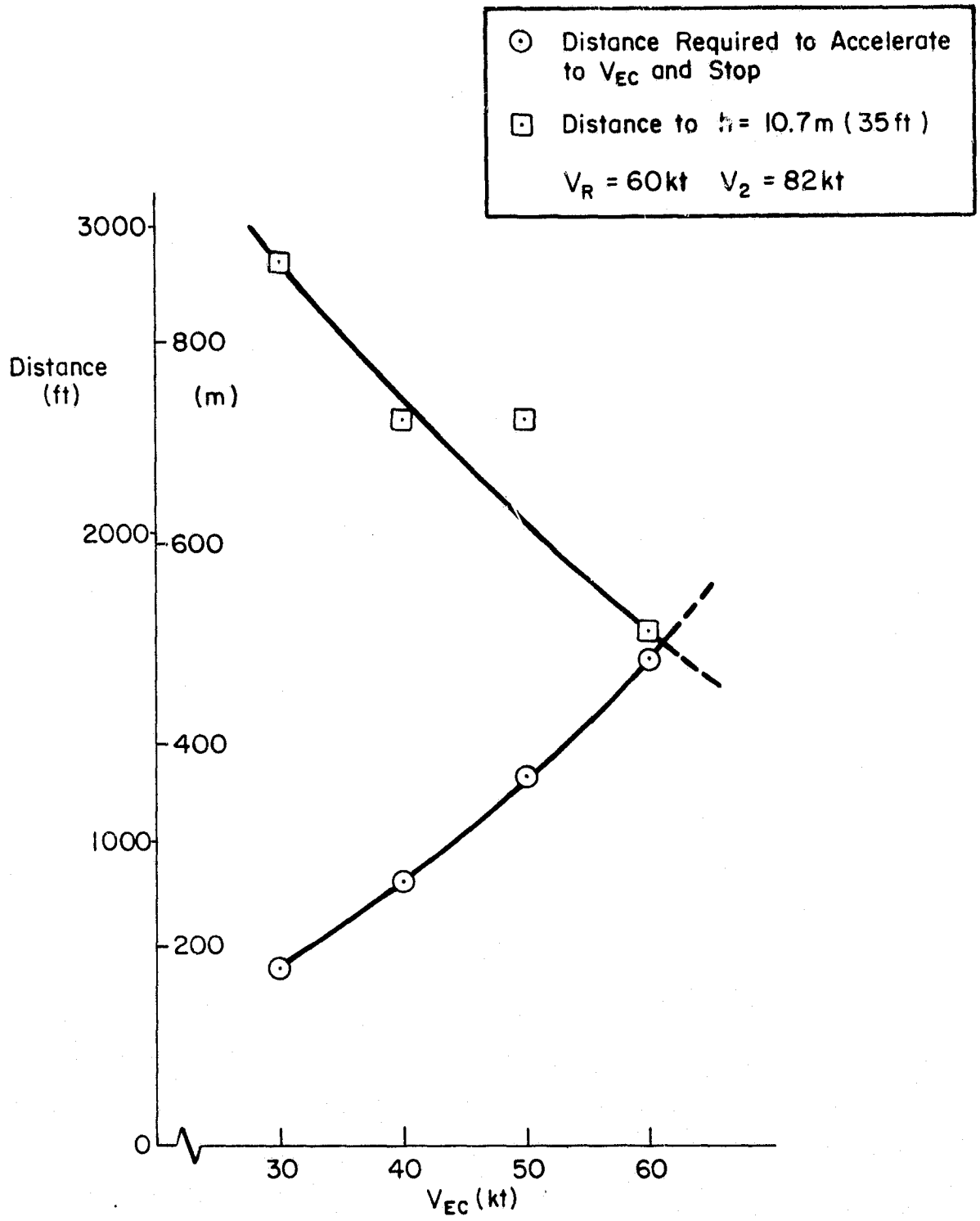

Figure VI-1. Balanced Field Test

the OEI x_{35} by 90 m (300 ft). On the other hand, the AWJSRA performance is very sensitive to V_1. A 1 kt reduction in V_1 increases x_{35} by roughly 12 m (40 ft), see Figure VI-1. The AWJSRA is sensitive to V_1 because it is a 2 engine airplane whereas the Breguet is a 4 engine airplane with cross-shafted propellers.

D. V_2 VARIATION

The OEI γ - V curve of Appendix A suggests that a lower V_2 may give better climb performance than does the nominal V_2 of 82 kt. Accordingly, a series of OEI takeoffs with a V_R of 60 kt and a V_2 of 72 kt were conducted. Figure VI-2 presents the results. The data include distance to 35 ft, x_{35}, and the minimum plane penetrated, MPP. The MPP was computed by defining a family of planes originating at a point 640 m (2100 ft) from the runway threshold (30 m [100 ft] past the upwind end of a 610 m [2000 ft] runway). MPP is the lowest plane which the aircraft would have penetrated in climbing to 300 m (1000 ft). Mathematically this can be expressed as:

$$\text{MPP} = \text{Min} \tan^{-1} \frac{h(\text{ft})}{x(\text{ft}) - 2100} \quad \text{for } h \leq 200 \text{ m (1000 ft)}$$

Also included in Figure VI-2 is the altitude at which the MPP occurred.

As can be seen in Figure VI-2, the 10 kt reduction in V_2 (from 82 to 72 kt):

- Reduced x_{35} by roughly 120 m (400 ft)
- Increased MPP by roughly 3 - 4 deg
- Had little effect on the altitude at which the MPP occurred.

Note also that the altitude for MPP is relatively low and the trim γ's for 72 and 82 kt are quite close. This implies that the increase in MPP is primarily due to the shorter time (and distance) required to accelerate to 72 kt rather than 82 kt.

Reducing x_{35} by 120 m (400 ft) is equivalent to reducing the balanced field length by 120 m (400 ft), and from Figure VI-1 it can be seen that reduction in balanced field length of 120 m (400 ft) would reduce V_1 to 55 kt.

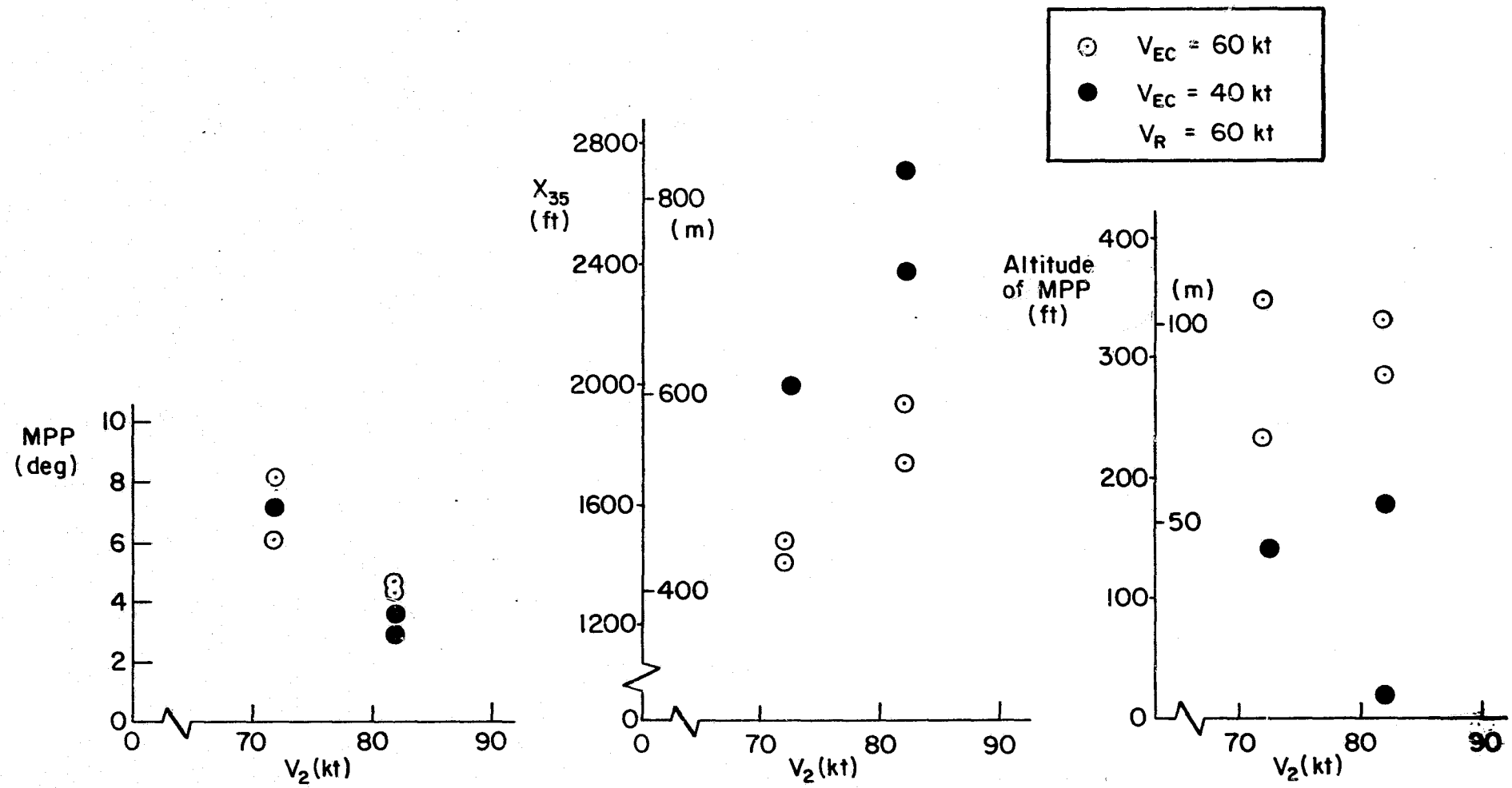

Figure VI-2. V_2 Variation

E. V_R ABUSES

A series of takeoffs were conducted with rotation speeds 10 kt above and below the nominal V_R to determine the effects of V_R abuses. In addition to V_{LOF} and x_{LOF}, the distance to a height of 10.7 m (35 ft) (x_{35}) and the velocity at a height of 10.7 m (35 ft) (V_{35}) are presented in Figure VI-3. The most significant result is that early rotation abuses actually improve takeoff performance. A 10 kt reduction in V_R results in a 30 m (100 ft) decrease in x_{LOF} and a 21 m (70 ft) decrease in x_{35}. Thus with this airplane the critical rotation abuse is a late, rather than an early, rotation. However the effects on takeoff distance are quite small in either case.

F. ENGINE FAILURES

1. Performance Effects, No Wind or Turbulence

The effects of engine failures on takeoff performance for the nominal takeoff configuration, with no wind or turbulence, is presented in Figure VI-4. As would be expected, the values of V_{LOF} and V_{35} do not vary strongly with V_{EC}, although V_{LOF} is increased by 2 - 3 kt over the average AEO value. This increase is due to the decrease in lift capability that accompanies an engine failure. More important is the relation of x_{LOF} and x_{35} to V_{EC}. A decrease of V_{EC} of 1 kt results in an increase of x_{35} and x_{LOF} of between 10 and 12 m (30 and 40 ft). Thus it is quite desirable to set V_R equal to V_1. A requirement for a margin between V_1 and V_R would significantly increase the takeoff field length requirement for this aircraft.

The minimum plane penetrated (MPP) data for AEO and OEI are presented in Figure VI-5. For OEI cases, a slight increase of MPP with V_{EC} (about .07 deg/kt) is apparent. These results also support the desirability of setting V_1 as high as possible.

The one major problem associated with OEI takeoffs was a lack of directional control associated with engine failures at speeds below 30 kt. At these speeds the rudder was not powerful enough to overcome the asymmetric thrust and the aircraft would drift laterally off the runway. Thus, the aircraft had an effective V_{MC} imposed by the lateral drift problem of roughly 30 kt.

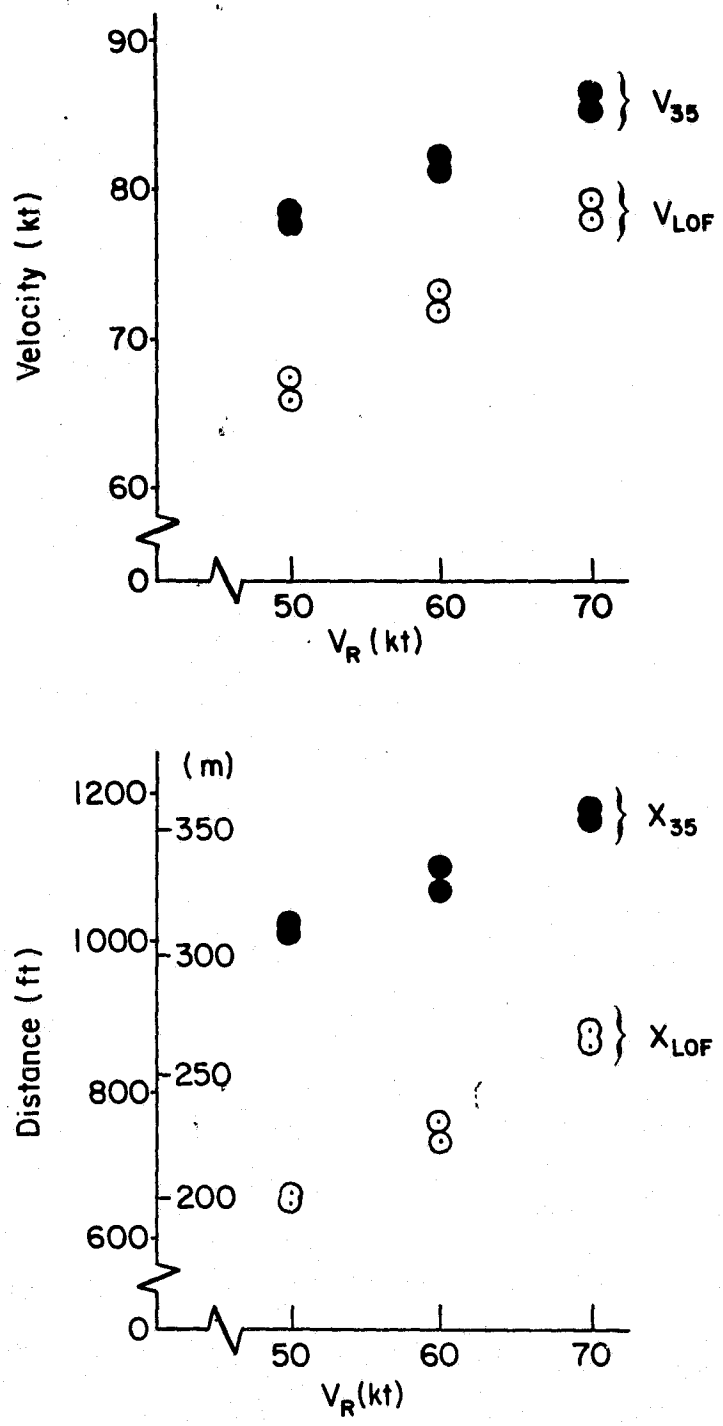

Figure VI-3. Effects of Rotation Speed

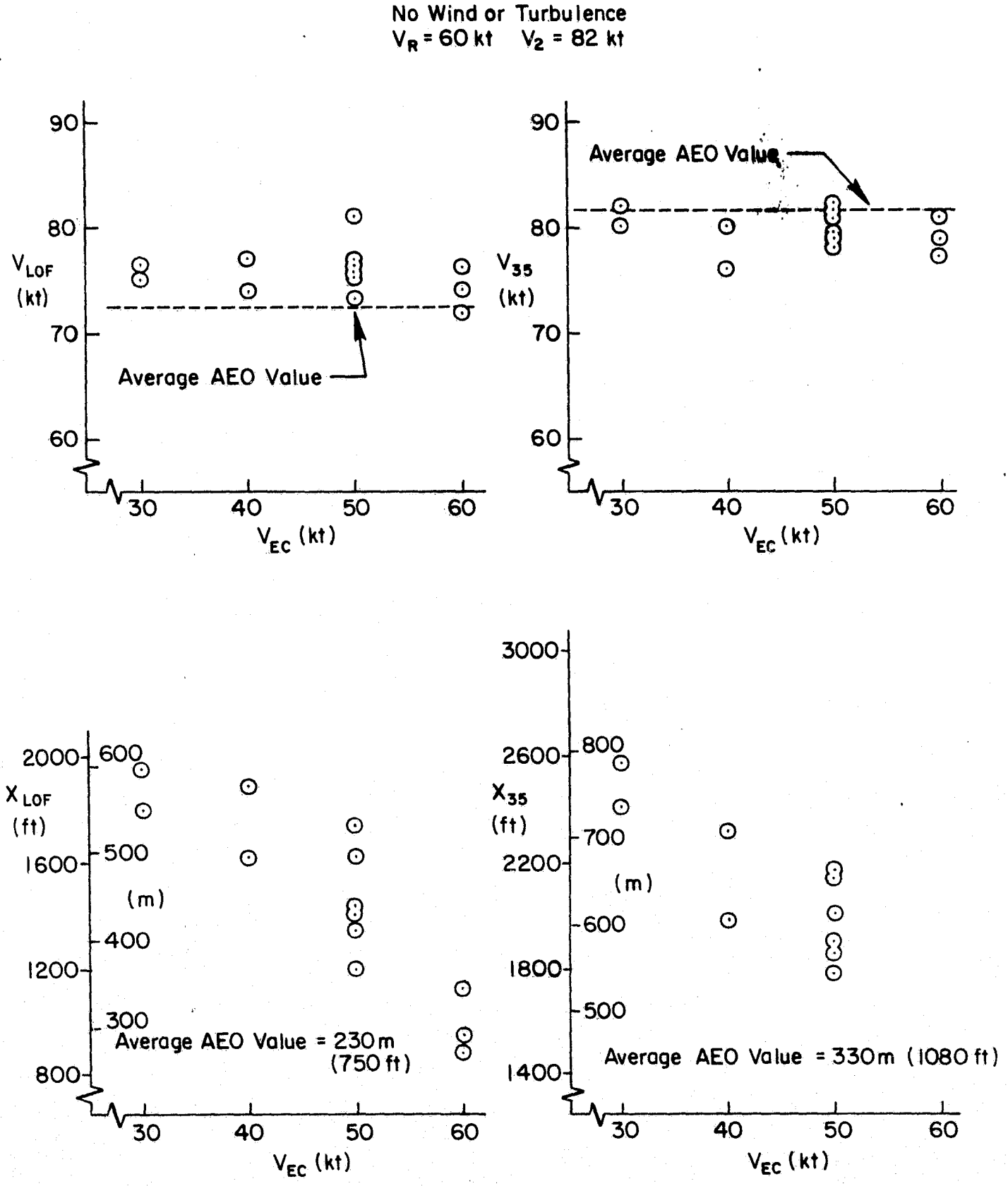

Figure VI-4. Effects of Engine Failure

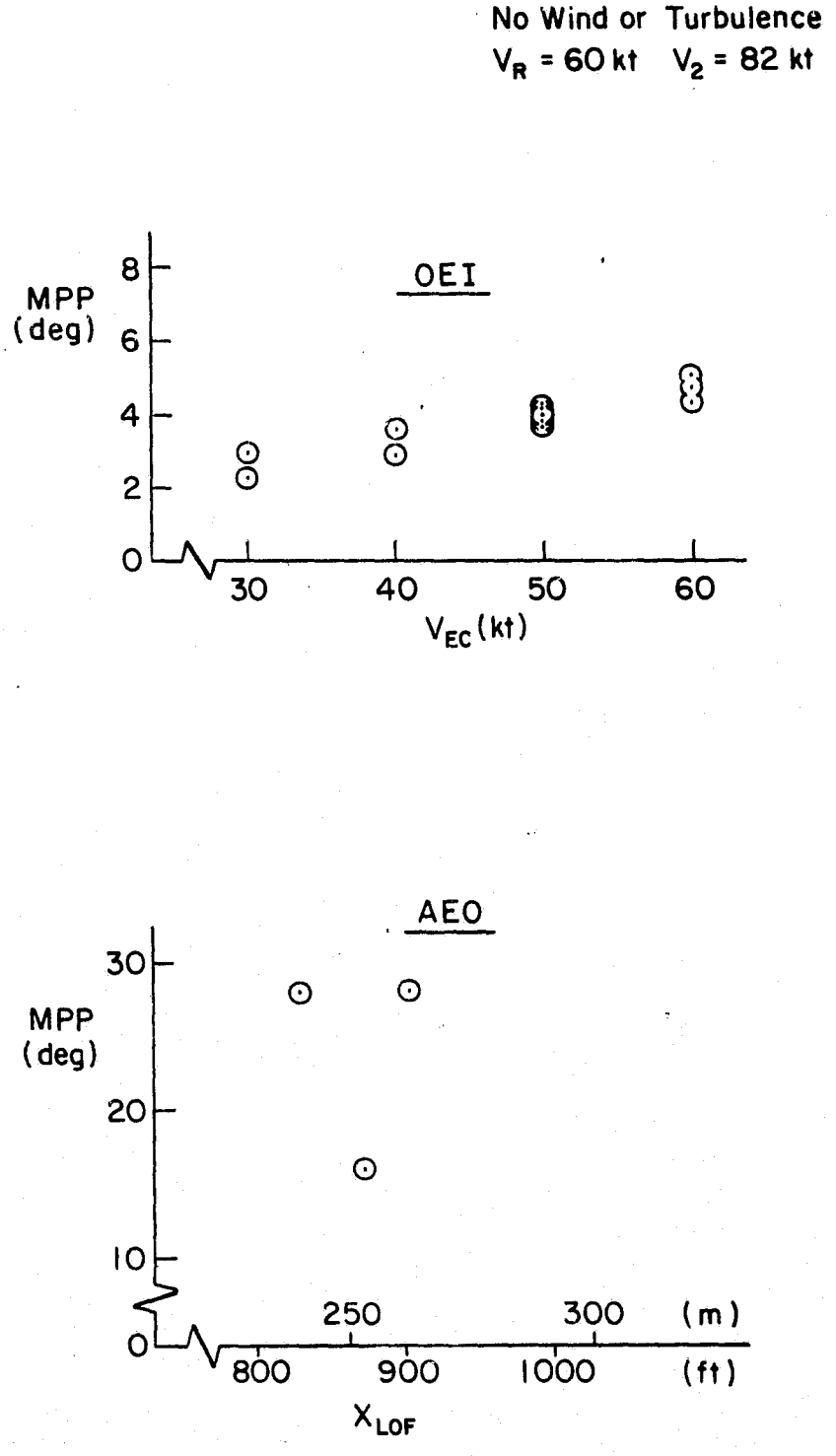

Figure VI-5. Minimum Plane Penetrated

2. Crosswind Effects

Figure VI-6 presents takeoff performance in a crosswind, with no wind average values for comparison. In general, the crosswinds did not seem to have a major influence on takeoff performance. Although directional control problems at low V_{EC} were present, the pilot did not feel as though the direction of the wind had an influence on takeoff performance. That is, there was little difference between failure of the up-wind or the down-wind engine.

3. Turbulence Effects

The effects of turbulence on takeoff performance, as seen in Figure VI-7, were not significant. Neither the velocities nor distances were affected by the existence of turbulence with a mean value of 1.4 m/s (4.5 ft/s).

G. PILOT COMMENTS

The AEO takeoffs never presented a problem to the pilots. Even in the worst abuse cases the aircraft was easy to handle. The aircraft would not lift off before it had adequate flying speed.

The OEI takeoffs did, however, present some problems with respect to lateral ground control and yaw corrections following an engine failure. The pilot comments are presented in Table VI-1.

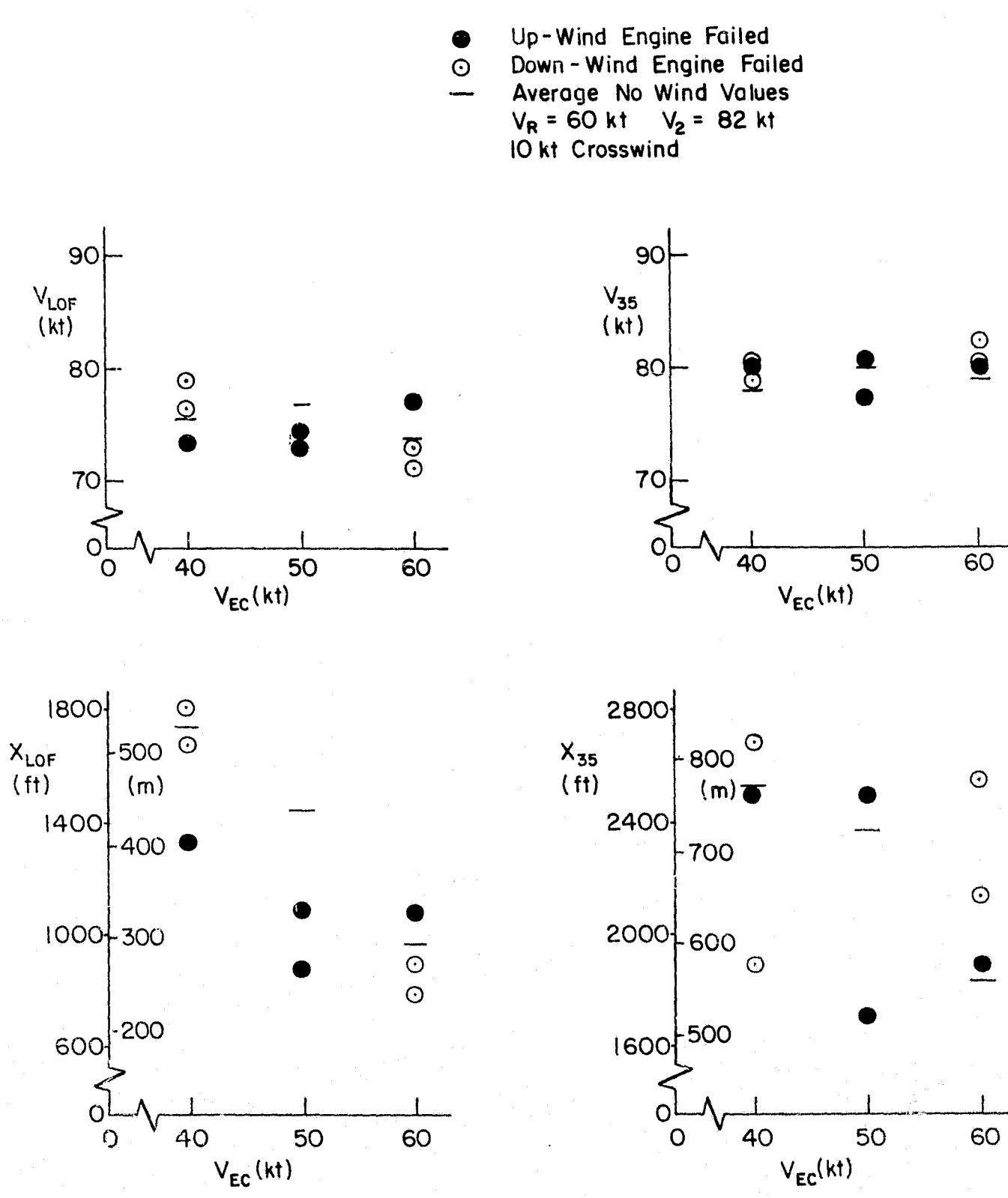

Figure VI-6. Effects of Crosswinds

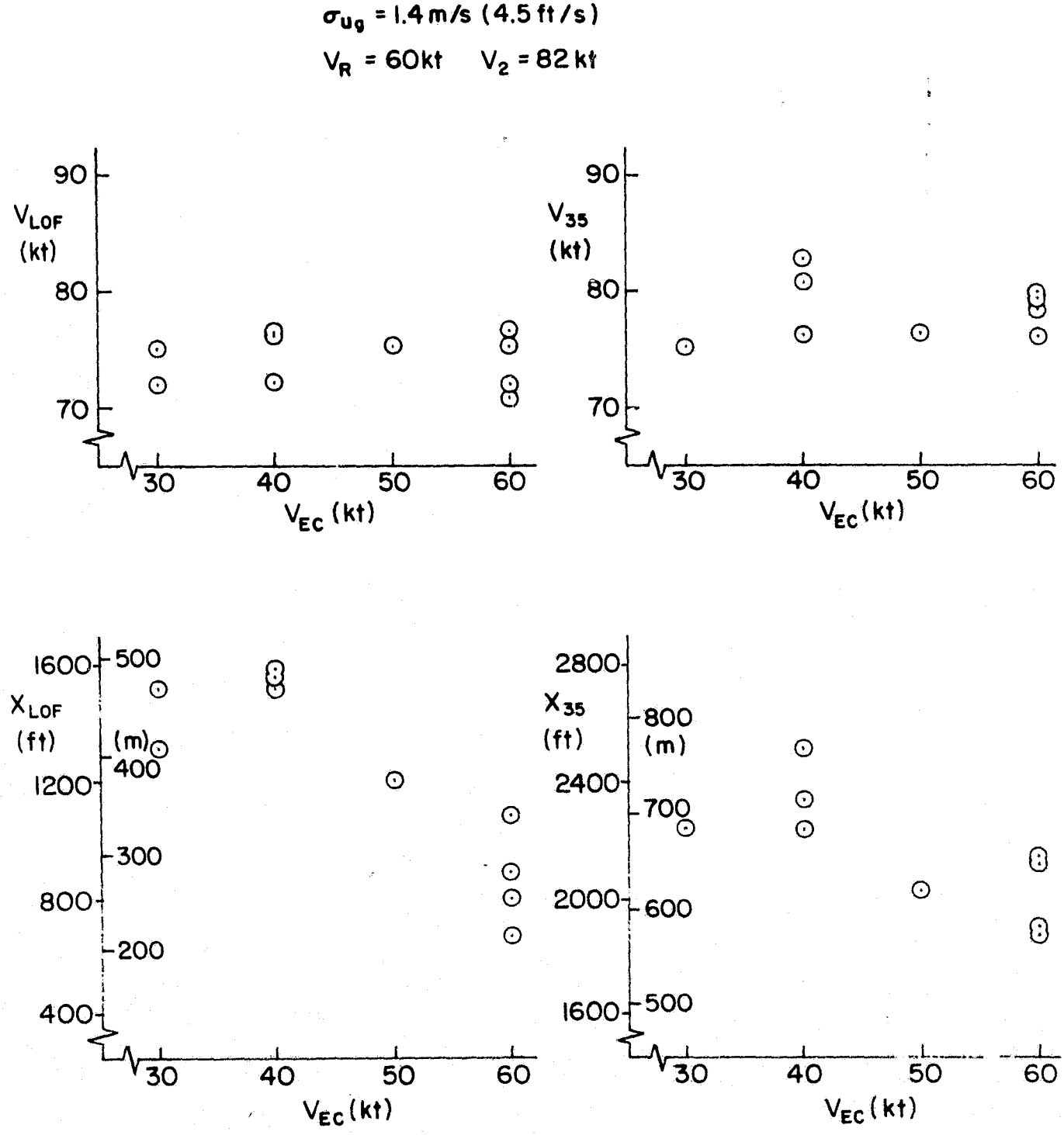

Figure VI-7. Effects of Turbulence

TABLE VI-1

PILOT COMMENTS

Pilot: F

Case: OEI Takeoff

1. Lateral control on the ground was only acceptable at the higher engine cut speeds (50 - 60 kt). No noticeable difference in difficulty when crosswinds were introduced.

2. Airplane exhibits yaw when engine is originally cut and additional correction is needed when nose wheel steering is lost after rotation, then one more correction after becoming airborne so the pilot is correcting for three distinct asymmetric conditions. Very busy.

SECTION VII
SUMMARY OF RESULTS

The following is a summary list of findings from the AWJSRA simulation experiment reported in the preceding sections and the results of analyses contained in the Appendixes. This list is arranged by task.

A. ILS TRACKING

- The 65 kt baseline case was judged acceptable for the ILS tracking task.
- For the baseline case (and in general) turbulence and winds had a major effect on pilot workload and performance.
- Decreasing approach speed (65 kt, 60 kt, 55 kt) continuously increased workload with an unacceptable level between 60 and 65 kt; performance remained unaffected for a constant level of atmospheric disturbance.
- The flight path control characteristics were analyzed in terms of bandwidth (quickness of flight path response), sensitivity (sensitivity of flight path to control movement), control power (maximum possible flight path change up and down), and cross-coupling (IAS-G/S cross-coupling).
- Decreasing approach speed affected only the cross-coupling characteristic in a significant way and the effect was adverse.
- Increasing the approach speed did not change the pilot workload from the level of the baseline case.
- From the standpoint of cross-coupling an increase in approach speed improved the short term coupling (i.e., G/S tracking) but degraded the long term (i.e., trimming).
- A tailwind had an effect equivalent to decreasing approach speed, mainly in terms of coupling.
- Varying the response time of the complementary control (e.g., throttle, DLC, etc.) is a way of changing bandwidth (quickness) without affecting coupling or any other control characteristic.

- Sluggish complementary control response became a problem in glide slope tracking as it approached the bandwidth where the pilot was apparently operating which in turn was dependent on the intensity of disturbance.
- Vertical thrust complementary controls (throttle, DLC) were judged about equal to horizontal ones (nozzle, DDC) in calm air, but in turbulence vertical control was distinctly preferred.
- Use of a horizontal complementary control (e.g., nozzle, DDC) requires speed regulation in order to achieve sufficient flight path response.
- The primary limitation in using the nozzle control of this design was the lack of control power (i.e., maximum obtainable change in steady state flight path).
- A STOL piloting technique is required for trimming regardless of complementary control orientation or response because of the small value of $\partial\gamma/\partial V$ for elevator inputs.
- CTOL technique is preferred for tight tracking with horizontal controls although analysis shows either technique is usable.
- Measures for flight path control characteristics appearing most meaningful are:

  Sensitivity -- Acceleration per unit control (e.g., $\partial n_z/\partial\delta_T$)

  Control Power -- Maximum up $\Delta\gamma$ and maximum down $\Delta\gamma$ while maintaining approach speed

  Bandwidth -- Frequency at which flight path angle lags control by 135 deg

  Cross-coupling -- Ratio of $\Delta\gamma/\delta_T$ without speed control to $\Delta\gamma/\delta_T$ with perfect speed control (i.e., μ^{STOL}).

- Attitude stability augmentation can play a dominant role in determining pilot workload but may have little effect on ILS tracking performance.
- The bare airframe was acceptable in calm air but in turbulence workload increased greatly with the main problem being lateral flight path control.

- Improved performance and pilot opinion was obtained when a flight director was introduced, the area of most improvement was lateral lineup at breakout.

B. FLARE AND LANDING

- The 65 kt baseline case had acceptable flare and landing characteristics, however disturbance intensity strongly affected pilot opinion and performance.
- Decreasing the approach speed resulted in worsening pilot opinion to an unacceptable level at slightly less than 65 kt, about the same point at which ILS tracking became unacceptable.
- As with ILS tracking, an increase in approach speed had little effect on flare and landing ratings; however, landing performance suffered.
- Landing performance was a particularly strong function of approach speed, especially in turbulence, with the most favorable combination occuring around 65 kt.
- In general, winds and turbulence had the disturbing effect of making the 10 to 90 percentile range of touchdown points twice the length of the touchdown zone regardless of approach speed used.
- Subsequent analysis has shown that glide path/touchdown zone geometry can have a significant influence on landing performance obtainable for a given airframe/flight condition combination; these factors were apparently favorable for the baseline case. They were not favorable for higher and lower speeds thus perhaps contributing to landing problems.
- Additional work should be done to investigate the compatibility of a range of STOL aircraft sizes and operating conditions with respect to glide path/touchdown zone geometry.
- The use of power alone to flare may depend primarily on a flight path control bandwidth requirement (quickness of response); this requirement may be that bandwidth required for an acceptable attitude-to-flare landing.

- Tailwinds were found roughly equivalent to decreasing approach speed with the pilot having to make adjustments in flare for touchdown sink rate performance; an increase in approach speed was required to offset losses in margin above V_{min} or α_{max}.
- A linear closed loop feedback control model was developed to analyze the flare, in particular, the relationship between the flare maneuver and the resulting touchdown performance.
- The most useful vehicle for describing flare and landing characteristics of a given configuration was a plot of touchdown performance contours as functions of flare attitude and flare height; with such a mapping the sensitivity of touchdown performance to flare maneuver was shown as well as the compatibility of the touchdown zone geometry with the airframe.
- Variations in approach speed, winds, and ground effect resulted in pilots making adjustments in their flare maneuver appropriate to optimizing landing performance; this lends additional credence to the usefulness of this simulator in flare and landing studies.

C. GO-AROUND

- AEO go-arounds presented no problems in terms of either pilot workload or performance.
- OEI go-arounds, on the other hand, did require considerable pilot skill as well as aid from the right seat occupant.
- OEI go-arounds were complicated by characteristics common in a twin engine design (i.e., thrust/lift asymmetries leading to lateral-directional difficulties) plus the STOL characteristic of required configuration changes (in this case flap/nozzle changes).
- Altitude losses with OEI were approximately 115 ft $\pm$ 20 ft and the minimum plane penetrated was about 5 deg, 1 deg less than the theoretical limit (assuming maximum climb angle from the minimum altitude).

D. TAKEOFF

- This airplane is sensitive to the choice of V_1 in terms of distance to 35 ft altitude because of the twin engine design (i.e., a large thrust decrement with loss of power).
- A requirement for a margin between V_1 and V_R would significantly increase the takeoff field length of this aircraft.
- A lower limit on V_1 was set by a V_{MCG} of about 30 ft.
- Neither crosswinds nor turbulence had a significant effect on takeoff performance.
- The airplane was forgiving to abuses of V_R and V_2.

REFERENCES

1. Stapleford, Robert L., Robert K. Heffley, John M. Lehman, and Wayne F. Jewell; A STOL Airworthiness Investigation Using a Simulation of a Deflected Slipstream Transport. Volume II: Simulation Data and Analysis (Final Report), STI TR 1014-3, Vol. II, November 1973.

2. Cleveland, William B., Richard F. Vomaske, and S. R. M. Sinclair; Augmentor Wing Jet STOL Research Aircraft Digital Simulation Model, NASA TM X-62,149, April 1972.

3. Heffley, R. K., W. F. Jewell, R. L. Stapleford, and S. J. Craig; A STOL Airworthiness Investigation Using a Simulation of a Deflected Slipstream Transport. Volume III: Breguet 941S Simulation Model (Final Report), STI TR 1014-3, Vol. III, November 1973

4. Flying Qualities of Piloted Airplanes, Military Specification MIL-F-8785B (ASG), 7 August 1969.

5. Bristol, Edgar H., "On a New Measure of Interaction for Multivariable Process Control", IEEE Transactions on Automatic Control, pp. 133-134, January 1966.

6. McRuer, Duane; Irving Ashkenas, Dunstan Graham; Aircraft Dynamics and Automatic Control, Princeton University Press, 1973.

7. Hoh, Roger H., Richard H. Klein, and Walter A. Johnson; Design of a Flight Director/Configuration Management System for Piloted STOL Approaches, STI TR 1015-3, September 1973.

8. Planning and Design Criteria for Metropolitan STOL Ports, FAA AC 150, November 1970.

9. Craig, Samuel J., Irving L. Ashkenas, and Robert K. Heffley; Pilot Background and Vehicle Parameters Governing Control Technique in STOL Approach Situations, FAA-RD-72-69, June 1972.

10. Scott, B. C., Investigation of a Curved Path Approach Using the Augmentor Wing Jet STOL Research Aircraft Simulation on the Flight Simulator for Advanced Aircraft at NASA Ames Research Center, Letter Report From FAA Flight Simulations Branch, Moffett Field, California, August 1973.

APPENDIX A

SIMULATION MODEL CHARACTERISTICS

The basic simulation model characteristics used in the analyses of this report are presented in the following pages. These characteristics include:

- Complementary control characteristics
- Dimensional airframe stability derivatives (longitudinal and lateral-directional)
- Airframe transfer functions (longitudinal and lateral-directional)
- Trim γ - V curves
- Step control input time histories (longitudinal).

All of the above were computed from the basic aerodynamic and propulsion program as given in Reference 2 with the modifications described in Appendix D.

1. COMPLEMENTARY CONTROL CHARACTERISTICS

The complementary control characteristics important to the analyses of this report consist of the relationship between the complementary control manipulator and its respective airframe stability derivatives in terms of gain and time lag. This is shown by the following block diagram:

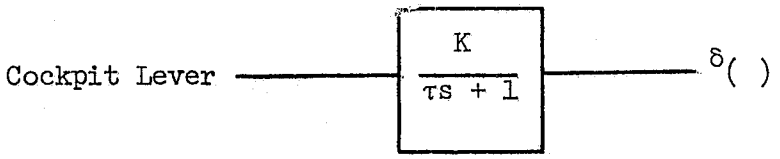

The manipulator input is defined here in terms of a linear deflection. The output units depend upon the type of complementary control used in a particular case. The factor K is simply the steady-state relationship between minipulator and complementary control. The dynamic relationship is represented by a simple first order lag. Table A-1 lists K and τ for each of the complementary controls used in this simulation.

TABLE A-1

K AND τ VALUES FOR COMPLEMENTARY CONTROLS
USED IN VARIOUS SIMULATION CASES

COMPLEMENTARY CONTROL	K	τ
Throttle		
Nominal	2.28 %/in	.5 sec (increase) 1.0 sec (decrease)
1.5 sec lag	2.28 %/in	1.5 sec
2.5 sec lag	2.28 %/in	2.5 sec
3.0 sec lag	2.28 %/in	3.0 sec
Nozzle	12.5 deg/in	Approx. zero
DDC	.05 g/in	zero
DLC	.05 g/in	zero

The nominal throttle control was distinguished by having different spool up and spool down time constants. However, for the cases where the engine lag was varied the lag was made symmetric. The nozzle was characterized by a rate limit of 60 deg/s, thus the effective lag time constant could be considered approximately zero.

2. DIMENSIONAL AIRFRAME STABILITY DERIVATIVES

The dimensional stability derivatives given in this appendix are for a body-fixed stability axis system. The derivatives as well as axis system conventions are defined in Reference 6.

The longitudinal stability derivatives corresponding to each approach case analyzed are given in Table A-2. Lateral-directional stability derivatives for three approach speeds are given in Table A-3.

3. AIRFRAME TRANSFER FUNCTIONS

The bare airframe longitudinal transfer functions are given in Table A-4 for the cases of Table A-2. Similarly, respective bare airframe lateral-directional transfer functions are given in Table A-5. SAS-on lateral-directional transfer functions are given in Table A-6. The longitudinal SAS is described in Appendix D.

4. TRIM γ - V CURVES

The steady-state flight path control characteristics for the cases flown in this simulation are shown in Figures A-1 through A-4. Case numbers corresponding to those used in the previous tables are indicated on the plots. Figures A-2 and A-3 show γ - V characteristics only about the trim condition. Figure A-4 represents the takeoff and go-around configurations. The single engine maximum power γ - V curve is also given in Figure A-4.

5. STEP CONTROL INPUT TIME HISTORIES

The altitude and airspeed responses for step inputs of column, throttle, and nozzle are shown in Figures A-5 through A-10. The cases include approach speed variations from 55 to 75 kt. Longitudinal SAS was on. The one-inch column steps correspond to a 4 deg attitude step.

TABLE A-2

LONGITUDINAL STABILITY DERIVATIVES

40,000 lb @ BS 341.2; 65 deg flaps; 75 deg nozzle; -7.5 deg glide slope

	TRIM CONDITION									
Case	1	2	3	4	5	6	7	8	9	10[1]
V_{T_o} (kt)	50	55	60	65	70	75	65	65	65	55
θ_o (deg)	2.32	1.10	-.43	-2.31	-4.40	-6.60	-2.31	-2.31	-2.31	6.70
N_H (% RPM)	93.3	92.2	91.4	91.0	90.8	90.9	91.0	91.0	91.0	90.6
( )[2]	N_H	N_H	N_H	N_H	N_H	N_H	δ_ν	DLC	DDC	N_H
	DIMENSIONAL DERIVATIVES (Stability Axis)									
X_u^* (1/s)	-.075	-.061	-.067	-.068	-.072	-.075	-.068	-.068	-.068	-.067
Z_u^* (1/s)	-.413	-.337	-.284	-.281	-.275	-.261	-.281	-.281	-.281	-.406
X_w (1/s)	.131	.142	.143	.136	.131	.133	.136	.136	.136	.153
Z_w (1/s)	-.434	-.445	-.465	-.505	-.534	-.614	-.505	-.505	-.505	-.387
g/U_o (1/s)	.382	.347	.318	.294	.272	.254	.294	.294	.294	.347
$\tan^{-1}\left[\frac{-Z_{()}}{X_{()}}\right]$ (deg)	92	92.9	90.9	89.6	87.7	85.8	-10.4	90	0	90.7
M_u^* (1/s-ft)	-.00064	-.00061	-.00054	-.00035	-.000074	.00016	-.00035	-.00035	-.00035	-.0013
M_w (1/s-ft)	.00038	-.0014	-.0023	-.0045	-.0066	-.0105	-.0045	-.0045	-.0045	-.00027
$M_{\dot{w}}$ (1/ft)	-.0054	-.0047	-.0041	-.0037	-.0032	-.0029	-.0037	-.0037	-.0037	-.005
M_q (1/s)	-.869	-.946	-1.02	-1.08	-1.14	-1.18	-1.08	-1.08	-1.08	-.983
$Z_{\dot{w}}$ (1/1)	-.0186	-.016	-.014	-.013	-.011	-.011	-.013	-.013	-.013	-.017
M_{δ_e} (1/s²-rad)	-.944	-1.14	-1.34	-1.56	-1.79	-2.02	-1.56	-1.56	-1.56	-1.16
Z_{δ_e} (ft/s²-rad)	-3.26	-3.95	-4.70	-5.5	-6.39	-7.34	-5.5	-5.5	-5.5	-3.95
$X_{()}$ (ft/s²-%)	-.053	-.098	-.034	.0161	.086	.1575	-3.69[3]	0[4]	1.61[4]	-.023
$Z_{()}$ (ft/s²-%)	-1.52	-1.96	-2.25	-2.22	-2.17	-2.13	-.677[3]	-1.61[4]	0[4]	-1.94
$M_{()}$ (rad/s²-%)	.0075	.0081	.0087	.0081	.0066	.0050	-.050[3]	0	0	.0130
$Z_w^\dagger$ (1/s)[5]	-.433	-.440	-.457	-.489	-.510	-.576	-.489	-.489	-.489	-.386

1/ 50 deg nozzle.

2/ Respective complementary control.

3/ Units are ft/s²-rad, rad/s²-rad.

4/ Units are ft/s²-in.

5/ $Z_w^\dagger \triangleq Z_w \left(1 - M_{\dot{w}}/Z_w \; Z_{\delta_e}/M_{\delta_e}\right)$

TABLE A-2 (Concluded)

TRIM CONDITIONS

Case	11	12	13	14	15	16	17
V_{T_o} (kt)	65	65	60	65	65	65	70
θ_o (deg)	-3.3	-.7	-1.42	-2.9	-2.0	-1.1	-3.3
N_H	92.0	89.8	92.2	91.5	91.0	90.1	89.8
Wind	0	0	10 kt Headwind	10 kt Headwind	10 kt Crosswind	10 kt Tailwind	10 kt Tailwind
γ_o (deg)	-6/	-9/	-6.25	-6.35	-7.4	-8.65	-8.57
( )	N_H	N_H	N_H	N_H	N_H	N_H	N_H

DIMENSIONAL DERIVATIVES (Stability Axis)

X_u^* (1/s)	-.06728	-.07463	-.06319	-.06745	-.06764	-.07286	-.07248
Z_u^* (1/s)	-.2493	-.3262	-.3079	-.2253	-.2817	-.3144	-.3052
X_w (1/s)	.1213	.1416	.13117	.1311	.1357	.1386	.1371
Z_w (1/s)	-.5206	-.4895	-.4955	-.4955	-.4984	-.4903	-.5223
g/U_o (1/s)	.294	.294	.318	.294	.294	.294	.272
$\tan^{-1}\left[\frac{-Z_{(\ )}}{X_{(\ )}}\right]$ (deg)	87.2	93.0	89.1	89.1	89.8	92.5	91.1
M_u^* (1/s-ft)	-.0001434	-.0004178	-.0003423	-.0001842	-.0003938	-.0004027	-.0002569
M_w (1/s-ft)	-.005297	-.002756	-.003623	-.003623	-.003996	-.002864	-.005436
$M_{\dot{w}}$ (1/ft)	-.003370	-.004007	-.003946	-.003430	-.003729	-.003909	-.003411
M_q (1/s)	-1.050	-1.116	-.9945	-.9945	-1.072	-1.108	-1.167
$Z_{\dot{w}}$ (1/1)	-.01208	-.01394	-.013964	-.0123	-.01315	-.01364	-.01204
M_{δ_e} ($1/s^2$-rad)	-1.538	-1.585	-1.337	-1.327	-1.525	-1.579	-1.812
Z_{δ_e} (ft/s^2-rad)	-5.513	-5.513	-4.697	-4.697	-5.378	-5.513	-6.394
$X_{(\ )}$ (ft/s^2-%)	.106	-.124	.030	.030	.006	-.103	-.046
$Z_{(\ )}$ (ft/s^2-%)	-2.17	-2.37	-1.97	-1.97	-2.23	-2.37	-2.34
$M_{(\ )}$ (rad/s^2-%)	.0062	.0059	.0070	.0071	.0083	.0055	.0047
$Z_w^\dagger$ (1/s)	-.502	-.485	-.483	-.483	-.484	-.480	-.503

6/ Not trimmed on glide slope.

TABLE A-3

LATERAL-DIRECTIONAL STABILITY DERIVATIVES

40,000 lb @ BS 341.2; 65 deg flaps; 75 deg nozzle; -7.5 deg γ_o

TRIM CONDITION

Case	2	3	4
V_{T_o} (kt)	55	60	65
θ_o (deg)	1.10	-.43	-2.31

DIMENSIONAL DERIVATIVES (Stability Axis)

Y_β (ft/s^2)	-10.4	-11.9	-13.34
L'_β ($1/s^2$)	-.0001487	.02344	.04029
N'_β ($1/s^2$)	.3836	.4617	.5450
L'_p ($1/s$)	-.5129	-.5564	-.6002
N'_p ($1/s$)	-.2433	-.2548	-.2467
L'_r ($1/s$)	.8855	.8733	.8630
N'_r ($1/s$)	-.2975	-.2794	-.2744
$Y^*_{\delta_r}$ ($1/s$)	.05012	.05465	.05924
L'_{δ_r} ($1/s^2$)	.08985	.08921	.1445
N'_{δ_r} ($1/s^2$)	-.5886	-.6896	-.806
$Y^*_{\delta_w}$ ($1/s$)	-.009684	-.01018	-.01077
L'_{δ_w} ($1/s^2$)	.3204	.3501	.3827
N'_{δ_w} ($1/s^2$)	-.03254	-.01998	-.01218

LONGITUDINAL TRANSFER FUNCTIONS

APPROACH CONFIGURATION

Case	1	2	3	4	5	6
V_{T_o} (kt)	50	55	60	65	70	75
( )	N_H	N_H	N_H	N_H	N_H	N_H
TRIM CONDITION						
DENOMINATOR						
Δ	(-.0747)(1.52)[.544;.344]	(.110)(1.43)[.789;.213]	(.435)(1.38)[.47;.15]	[.23;.138][.974;1.01]	[.19;.206][.868;1.17]	[.191;.214][.757;1.42]
ELEVATOR NUMERATORS						
$N^u_{\delta_e}$	19.236(.642)	+20.81(.723)	23.0(.806)	26.09(.889)	28.99(.961)	30.30(1.18)
$N^w_{\delta_e}$	-3.20(25.3)[.149;.392]	-3.88(27.6)[.149;.337]	-4.63(29.9)[.175;.298]	-174.62[.180;.285]	-216.14[.191;.272]	-262.09[.205;.257]
$N^\theta_{\delta_e}$	-.926[.867;.294]	-1.12[.919;.273]	-1.32[.983;.266]	-1.54(.199)(.359)	-1.77(.180)(.462)	-2.0(.157)(.494)
$N^{\dot{u}}_{\delta_e}$	3.20(-.195)(-2.50)(3.64)	3.88(-.112)(-2.71)(3.83)	4.63(-.0504)(-2.93)(4.06)	5.44(-.0282)(-3.19)(4.37)	6.32(-.009)(-3.39)(4.61)	7.26(.0174)(-3.77)(5.01)
$N^{\dot{w}}_{\delta_e}$	3.18(-.127)(-2.66)(3.75)	3.85(-.0585)(-2.84)(3.92)	4.59(-.0059)(-3.04)(4.15)	5.40(.0116)(-3.28)(4.44)	6.27(.0271)(-3.48)(4.68)	7.20(.0502)(-3.84)(5.07)
( ) NUMERATORS						
$N^u_{(\ )}$	-.0532(.140)[.811;3.25]	-.098(.314)[.85;2.53]	-.0336(.453)(2.14)(8.70)	.0161(-18.9)[.99;1.20]	.0865(-3.49)[.837;1.36]	.157(-1.92)[.71;1.62]
$N^w_{(\ )}$	-1.50(-.322)[.808;.518]	-1.93(-.274)[.90;.488]	-2.21(-.23)[.954;.482]	-2.20(-.20)(.425)(.528)	-2.15(-.147)(.281)(.725)	-2.11(-.0878)(.197)(.873)
$N^\theta_{(\ )}$	.0155[.544;.218]	.0172[.914;.230]	.0178(.146)(.427)	.0161(.103)(.830)	.0135(.0960)(1.30)	.0111(.0978)(2.25)
$N^{\dot{u}}_{(\ )}$	1.50(-.117)(.324)(1.18)	1.93(-.0505)(.383)(1.10)	2.21(-.00512)(.482)(1.03)	2.20(.0326)[.890;.858]	2.15(.0627)[.772;.995]	2.11(.0873)[.637;1.23]
$N^{\dot{w}}_{(\ )}$	1.49(-.0942)(.346)(1.16)	1.93(-.0185)(.391)(1.08)	2.20(.0291)(.486)(1.01)	2.17(.0695)[.886;.851]	2.12(.0995)[.767;.987]	2.07(.123)[.631;1.22]
ELEVATOR - ( ) COUPLING NUMERATORS						
$N^{u\,w}_{\delta_e(\ )}$	-.170[.770;16.4]	-.38(11.9)(15.8)	-.155[.602;24.9]	4.84(-22.9)	21.83(-5.66)	44.69(-3.04)
$N^{\theta\,u}_{\delta_e(\ )}$	.0493(4.25)	.109(3.33)	.0444(10.1)	-.0249(-18.5)	-.153(-2.81)	-.315(-1.23)
$N^{u\,\dot{u}}_{\delta_e(\ )}$	.169[.0337;12.9]	.377[.0476;9.94]	.154[.0282;18.1]	-.0870(-25.7)(26.8)	-.542(-11.0)(12.1)	-1.13(-8.14)(9.33)
$N^{\theta\,w}_{\delta_e(\ )}$	1.43(.0608)	2.22(.0443)	3.01(.0631)	3.47(.0702)	3.89(.0824)	4.30(.0939)
$N^{\theta\,\dot{u}}_{\delta_e(\ )}$	-1.43(.0796)	-2.22(.0654)	-2.99(.0826)	-3.44(.0877)	-3.83(.0974)	-4.23(.107)
STEADY STATE PARTIAL DERIVATIVES						
$\left[\frac{\partial \gamma}{\partial V}\right]_{(\ )}$ $\left(\frac{deg}{kt}\right)$	.53	.313	.144	.081	.026	-.051
$\left[\frac{\partial \gamma}{\partial V}\right]_{\theta}$ $\left(\frac{deg}{kt}\right)$	-.478	-.282	-.403	-.469	-.609	-.793
$\left[\frac{\partial \dot{V}}{\partial \gamma}\right]_{(\ )}$ $\left(\frac{kt}{sec}\right)$	-1.59	-1.87	-2.03	-2.18	-2.25	-2.36

TABLE A-4 (Continued)

	TRIM CONDITION					
Case	7	8	9	10	11	12
V_{T_o} (kt)	65	65	65	55	65	65
( )	δ_v	DLC	DDC	N_H δ_v = 50 deg	N_H γ = -6 deg	N_H γ = -9 deg
	DENOMINATOR					
Δ	[.23;.138][.974;1.01]	[.23;.138][.974;1.0]	[.23;.138][.974;1.0]	(-.0665)(1.56)[.586;.338]	[.184;.191][.913;1.06]	(.522)(1.45)[.387;.175]
	ELEVATOR NUMERATORS					
$N^u_{\delta_e}$	26.09(.889)	26.09(.889)	26.09(.889)	19.98(.665)	28.29(.841)	25.26(.901)
$N^w_{\delta_e}$	-174.62[.180;.285]	-174.62[.180;.285]	-174.62[.180;.285]	-3.88(28.2)[.143;.369]	-5.45(31.7)[.176;.269]	-5.44(32.6)[.189;.307]
$N^\theta_{\delta_e}$	-1.54(.199)(.359)	-1.54(.199)(.359)	-1.54(.199)(.359)	-1.14[.767;.295]	-1.52(.154)(.415)	-1.56[.969;.236]
$N^{\dot{w}}_{\delta_e}$	5.44(-.0282)(-3.19)(4.37)	5.44(-.0282)(-3.19)(4.37)	5.44(-.0282)(-3.19)(4.37)	3.88(-.162)(-2.46)(3.67)	5.45(-.0229)(-3.26)(4.40)	5.44(-.0365)(-3.12)(4.35)
$N^{\dot{\theta}}_{\delta_e}$	5.40(.0116)(-3.28)(4.44)	5.40(.0116)(-3.28)(4.44)	5.40(.0116)(-3.28)(4.44)	3.85(-.104)(-2.59)(3.77)	5.42(.00883)(-3.34)(4.46)	5.37(.0117)(-3.23)(4.44)
	( ) NUMERATORS					
$N^u_{(\ )}$	-3.69(-.142)[.995;1.08]	-.216[.944;1.03]	1.61(.0186)[.976;1.0]	-.0227(.216)(2.92)(11.6)	.106(-2.79)[.904;1.25]	-.124(.469)[.943;2.24]
$N^w_{(\ )}$	-.688(7.90)[-.219;.291]	-1.59(-.0697)(.148)(1.07)	-.446(.00427)(1.21)	-1.91(-.404)[.727;.570]	-2.15(-.145)(.284)(.678)	-2.33(-.180)(.279)(.801)
$N^\theta_{(\ )}$	-.0479[.742;.392]	.00581(.0793)(1.22)	.00181(1.61)	.0226[.586;.262]	.0134(.0932)(1.06)	.0152(.120)(.557)
$N^{\dot{w}}_{(\ )}$	.688(.0982)(2.25)(-2.43)	1.59(.0541)(.543)(.963)	.446(.398)(1.08)	1.91(-.109)(.416)(1.22)	2.15(.0520)[.826;.879]	2.33(.0154)(.411)(1.19)
$N^{\dot{\theta}}_{(\ )}$	1.14(1.31)(-1.41)(2.07)	1.57(.0955)(.505)(.969)	-.210(.507)(1.04)(-1.68)	1.89(-.0842)(.438)(1.19)	2.12(.0833)[.822;.870]	2.32(.0569)(.404)(1.13)
	ELEVATOR - ( ) COUPLING NUMERATORS					
$N^{u\ w}_{\delta_e(\ )}$	-645.21(.0752)	-79.1	280.87(.0371)	-.0879[.493;28.7]	.576(-5.03)(36.7)	-.674(6.88)(25.8)
$N^{\theta\ u}_{\delta_e(\ )}$	5.69(.508)	.336	-2.48(.490)	.0258(13.8)	-.161(-2.02)	.194(3.21)
$N^{u\ \dot{h}}_{\delta_e(\ )}$	19.9(-3.16)(4.24)	41.8	-8.68(-3.24)(4.32)	.0872[.0233;21.1]	-.572(-10.6)(11.6)	.666[.0639;8.73]
$N^{\theta\ w}_{\delta_e(\ )}$	.769(-2.0)	-2.48(.0682)	.694	2.26(.0623)	3.33(.0793)	3.73(.0578)
$N^{\theta\ \dot{h}}_{\delta_e(\ )}$	-1.51(-.763)	-2.46(.0861)	.324(-1.64)	-2.24(.0829)	-3.30(.0899)	-3.72(.0835)
	STEADY STATE PARTIAL DERIVATIVES					
$\left[\frac{\partial\gamma}{\partial V}\right]_{(\ )}$ $\left(\frac{deg}{kt}\right)$	.081	.081	.081	.447	.0663	.1044
$\left[\frac{\partial\gamma}{\partial\theta}\right]_{\theta}$ $\left(\frac{deg}{kt}\right)$	.470	-.443	.506	-.413	-.718	-.306
$\left[\frac{\partial V}{\partial\theta}\right]_{(\ )}$ $\left(\frac{kt}{deg}\right)$	-2.18	-2.18	-2.18	-1.38	-2.531	-1.84

TABLE A-4 (Concluded)

Case	13	14	15	16	17
V_{T_o} (kt)	60	65	65	65	70
Wind	10 kt Headwind	10 kt Headwind	10 kt Crosswind	10 kt Tailwind	10 kt Tailwind
( )	N_H	N_H	N_H	N_H	N_H
DENOMINATOR					
Δ	(.742)(1.115)[.217;.1930]	[.251;.1661][.989;.930]	(.873)(1.07)[.252;.181]	(.553)(1.41)[.361;.173]	[.221;.202][.934;1.10]
ELEVATOR NUMERATORS					
$N^{n}_{\delta_e}$	-.608(.805)(-40.1)	-.609(.854)(-37.8)	-.720(.870)(-35.8)	-.754(.886)(-34.1)	-.866(.988)(-32.1)
$N^{w}_{\delta_e}$	-4.63(29.6)[.1510;.310]	-4.64(32.0)[.1888;.256]	-5.31(31.8)[.179;.287]	-5.44(32.5)[.187;.301]	-6.32(34.6)[.191;.287]
$N^{q}_{\delta_e}$	-1.309(.212)(.334)	-1.311(.1583)(.392)	-1.51(.203)(.349)	-1.56[.988;.280]	-1.79(.219)(.396)
$N^{\dot{w}}_{\delta_e}$	4.63(-.0639)(-3.05)(4.17)	4.64(-.01259)(-3.23)(4.30)	5.31(-.0325)(-3.15)(4.32)	5.44(-.0361)(-3.13)(4.34)	6.32(-.0146)(-3.35)(4.60)
$N^{\dot{q}}_{\delta_e}$	4.61(-.0261)(-3.14)(4.24)	4.61(.0203)(-3.31)(4.37)	5.26(.00804)(-3.25)(4.39)	5.38(.0104)(-3.24)(4.43)	6.25(.0269)(-3.44)(4.67)
( ) NUMERATORS					
$N^{u}_{()}$	.0301(.756)(1.625)(-8.95)	.0301(.955)(1.302)(-8.86)	.00592(.872)(1.55)(-50.9)	-.103(.50)[.972;2.39]	-.0463(6.72)[.886;1.23]
$N^{w}_{()}$	-1.939(-.210)[.962;.473]	-1.942(-.1777)[.995;.428]	-2.20(-.208)[.992;.476]	-2.33(-.170)(.268)(.813)	-2.31(-.138)(.227)(.907)
$N^{q}_{()}$	.01467(.1073)(.670)	.01369(.0972)(.737)	.0165(.107)(.741)	.0147(.112)(.594)	.0125(.0875)(1.17)
$N^{\dot{w}}_{()}$	1.939(.01350)[.931;.781]	1.942(.0366)[.892;.791]	2.20(.0254)[.923;.826]	2.33(.0181)(.425)(1.16)	2.31(.0480)[.898;.896]
$N^{\dot{q}}_{()}$	1.924(.0450)[.927;.774]	1.927(.0679)[.888;.785]	2.18(.0621)[.920;.819]	2.32(.0586)(.417)(1.15)	2.29(.0893)[.897;.876]
ELEVATOR - ( ) COUPLING NUMERATORS					
$N^{n\ w}_{\delta_e\ ()}$	.1395(-13.76)(43.4)	.1397(-13.20)(45.2)	.0314(-45.0)(76.8)	-.362(9.0)(23.6)	-.298[.809;21.4]
$N^{q\ u}_{\delta_e\ ()}$	-.0394(-8.19)	-.0395(-8.19)	-.00891(-51.3)	.161(3.68)	.0829(7.46)
$N^{u\ \dot{h}}_{\delta_e\ ()}$	-.1387(-18.55)(19.54)	-.1389(-18.03)(19.02)	-.0312(-42.8)(43.9)	.395[.0565;9.81]	.289[.0403;14.5]
$N^{q\ w}_{\delta_e\ ()}$	2.61(.0678)	2.61(.0708)	3.40(.0684)	3.72(.0593)	4.21(.0665)
$N^{q\ \dot{h}}_{\delta_e\ ()}$	-2.59(.0815)	-2.59(.0847)	-3.37(.0861)	-3.70(.0831)	-4.17(.0884)
STEADY STATE PARTIAL DERIVATIVES					
$\left[\frac{\partial \gamma}{\partial ()}\right]_{()} \left(\frac{1}{kt}\right)$	.1831	.0364	.0923	.1032	.0424
$\left[\frac{\partial \gamma}{\partial ()}\right]_{\zeta} \left(\frac{1}{kt}\right)$	-.5237	-.5035	-.449	-.328	-.371
$\left[\frac{\partial V}{\partial ()}\right]_{()} \left(\frac{kt}{1bf}\right)$	-2.19	-2.50	-2.166	-1.925	-2.033

Note: The following identities hold true for stability axis transfer functions

$$N^{u}_{\delta_e} N_H = \frac{-N^{u}_{\delta_e} N_{\dot{h}}}{\cos \gamma_o} \quad \text{and} \quad N^{\theta}_{\delta_e} N_H = \frac{N^{w}_{\delta_e} N_{\dot{h}}}{U_o} = N^{w}_{\delta_e} N_{\dot{\alpha}}$$

TABLE A-5

LATERAL-DIRECTIONAL TRANSFER FUNCTIONS

Approach Configuration, SAS Off

Case	2	3	4
	TRIM CONDITION		
V_{T_o} (kt)	55	60	65
Δ	(-.218)(.640)[.285;.878]	(-.212)(.657)[.276;.923]	(-.203)(.683)[.268;.959]
	WHEEL NUMERATORS		
$N^{\beta}_{\delta_w}$	-.0097(.136)(3.39)(-6.07)	-.0101(.143)(3.91)(-5.18)	-.011(.150)(4.20)(-4.61)
$N^{p}_{\delta_w}$	.320(.045)[.221;.620]	.350(.041)[.224;.682]	.383(.038)[.222;.742]
$N^{\varphi}_{\delta_w}$	.325[.283;.630]	.353[.277;.693]	.384[.268;.752]
$N^{r}_{\delta_w}$	-.0325(-.544)(.840)(2.84)	-.020(-.597)(.834)(5.14)	-.012(-.656)(.869)(8.74)
$N^{a_y}_{\delta_w}$	-.900(-.715)(.716)(1.97)(-4.52)	-1.03(.083)(1.39)[-.232;1.37]	-1.18(.085)(1.41)[-.228;1.37]
	RUDDER NUMERATORS		
$N^{\beta}_{\delta_r}$	.050(-.271)(.965)(11.9)	.055(-.247)(.960)(12.74)	.059(-.213)(.985)(13.7)
$N^{p}_{\delta_r}$	.090(-.053)(.060)(-5.40)	.089(.055)(-.077)(-6.32)	.145(.047)(-.145)(-4.30)
$N^{\varphi}_{\delta_r}$	.167(.0009)(-2.60)	.180(-.033)(-2.77)	.251(-.125)(-2.11)
$N^{r}_{\delta_r}$	-.589(-.135)[.993;.385]	-.690(-.151)[.986;.416]	-.806(-.182)[.967;.469]
$N^{a_y}_{\delta_r}$	4.66(.587)(12.0)[-.427;.020]	5.54(-.285)(-.755)[.896;1.05]	6.50(-.223)(-.851)[.900;1.08]
	COUPLING NUMERATORS		
$N^{\beta\, p}_{\delta_w \delta_r}$	-.017(.046)(10.83)	-.020(.042)(11.8)	-.024(.038)(12.6)
$N^{\beta\, \varphi}_{\delta_w \delta_r}$	-.018(10.4)	-.021(11.3)	-.025(12.0)
$N^{\beta\, r}_{\delta_w \delta_r}$	.0073(-2.46)(3.54)	.0081(-2.52)(3.70)	.0094(-2.52)(3.76)
$N^{\beta\, a_y}_{\delta_w \delta_r}$	.571(10.4)	.822(-.0092)(2.01)	1.03(.00026)(2.02)
$N^{p\, \varphi}_{\delta_w \delta_r}$	.0244(.077)	.032(.078)	.040(.077)
$N^{p\, r}_{\delta_w \delta_r}$	-.186(0.00)(.077)	-.239(0.00)(.078)	-.307(0.00)(.077)
$N^{p\, a_y}_{\delta_w \delta_r}$	1.57(-.059)(.059)(10.9)	2.03(.042)(.907)(-1.02)	2.66(.038)(.939)(-1.04)
$N^{\varphi\, r}_{\delta_w \delta_r}$	-.186(.077)	-.239(.078)	-.307(.077)
$N^{\varphi\, a_y}_{\delta_w \delta_r}$	1.66(0.00)(10.4)	2.14(.936)(-.947)	2.80(-.963)(.966)
$N^{r\, a_y}_{\delta_w \delta_r}$	-.681(1.42)[-.248;.687]	-.822(1.51)[-.234;.693]	-1.03(1.54)[-.224;.688]

TABLE A-6

LATERAL-DIRECTIONAL TRANSFER FUNCTIONS

Approach Configuration, SAS On

	TRIM CONDITION		
Case	2	3	4
V_{T_o} (kt)	55	60	65
	DENOMINATOR		
Δ	(.009)(.563)(1.57)(3.54)(9.44)(9.63)[.501;.574]	(.0246)(.567)(1.70)(3.43)[.505;.626][.999;9.50]	(.058)(.566)(1.79)(3.31)[.495;.685][.999;9.50]
	WHEEL NUMERATORS		
$N^{\beta}_{\delta_w}$	-.0097(.109)(.402)(-4.68)(10.0)(10.2)[.993;2.95]	-.0102(.104)(.362)(-3.31)(10.0)(10.3)[.977;2.97]	-.011(-.555)(.338)(-1.81)(1.99)(3.21)(10.0)(10.5)
$N^{p}_{\delta_w}$	.320(.046)(.542)(3.52)(10.0)(10.1)[.454;.572]	.350(.042)(.552)(3.42)(10.0)(10.1)[.485;.632]	.383(.039)(.559)(3.31)(10.0)(10.2)[.495;.691]
$N^{\phi}_{\delta_w}$	.325(.549)(3.52)(10.0)(10.1)[.487;.570]	.352(.559)(3.41)(10.0)(10.2)[.507;.629]	.384(.563)(3.31)(10.0)(10.2)[.504;.688]
$N^{r}_{\delta_w}$	-.0325(1.12)(-1.19)(3.09)(10.0)(13.4)[.882;.624]	-.020(1.06)(-1.82)(2.85)(10.0)(16.5)[.865;.683]	-.0122(.648)(3.23)(-3.29)(10.0)(21.75)[.678;.743]
$N^{a_y}_{\delta_w}$	-.900(.545)(3.40)(-4.15)(10.0)[.455;.580][.994;7.48]	-1.03(.555)(3.30)(-4.01)(10.0)[.484;.640][.989;.747]	-1.18(.561)(3.29)(-3.83)(10.0)[.495;.696][.986;7.39]
	RUDDER NUMERATORS		
$N^{\beta}_{\delta_r}$	.050(.0044)(.400)(1.64)(4.00)(8.42)(10.0)(12.5)	.055(.027)(.400)(1.73)(4.00)(8.39)(10.0)(13.3)	.059(.057)(.400)(1.80)(4.00)(8.39)(10.0)(14.2)
$N^{p}_{\delta_r}$	.090(.050)(.400)(-.443)(-1.25)(4.00)(6.26)(10.0)	.089(.043)(.400)(4.00)(4.76)(10.0)[-.501;1.14]	.145(.037)(.400)(4.00)(4.31)(10.0)[.462;1.35]
$N^{\phi}_{\delta_r}$	.167(.400)(4.00)(7.21)(10.0)[.171;.539]	.180(.400)(4.00)(6.32)(10.0)[.582;.751]	.251(.400)(4.00)(6.03)(10.0)[.937;.930]
$N^{r}_{\delta_r}$	-.589(-.084)(.172)(.400)(1.56)(4.00)(8.98)(10.0)	-.690(-.094)(.185)(.400)(1.69)(4.00)(8.89)(10.0)	-.806(-.119)(.214)(.400)(1.78)(4.00)(8.85)(10.0)
$N^{a_y}_{\delta_r}$	4.66(.400)(4.00)(9.17)(10.0)[-.767;.472][.774;1.53]	5.54(.400)(4.00)(9.09)(10.0)[-.607;.632][.904;1.39]	6.50(.400)(1.14)(1.40)(4.00)(9.08)(10.0)[-.413;.904]
	COUPLING NUMERATORS		
$N^{\beta\ p}_{\delta_w\delta_r}$	-.0169(.046)(.400)(4.00)(10.0)(10.0)(10.8)	-.020(.042)(.400)(4.00)(10.0)(10.0)(11.84)	-.024(.039)(.400)(4.00)(10.0)(10.0)(12.6)
$N^{\beta\ \phi}_{\delta_w\delta_r}$	.0179(.400)(4.00)(10.0)(10.0)(10.4)	-.021(.400)(4.00)(10.0)(10.0)(11.34)	-.025(.400)(4.00)(10.0)(10.0)(12.0)
$N^{\beta\ r}_{\delta_w\delta_r}$	.0073(.400)(-2.46)(3.54)(4.00)(10.0)(10.0)	.0081(.400)(-2.52)(3.70)(4.00)(10.0)(10.0)	.0094(.400)(-2.52)(3.76)(4.00)(10.0)(10.0)
$N^{p\ \phi}_{\delta_w\delta_r}$	.024(.077)(.400)(4.00)(10.0)(10.0)	.032(.078)(.400)(4.00)(10.0)(10.0)	.040(.077)(.400)(4.00)(10.0)(10.0)
$N^{p\ r}_{\delta_w\delta_r}$	-.186(0.00)(.077)(.400)(4.00)(10.0)(10.0)	-.240(0.00)(.078)(.400)(4.00)(10.0)(10.0)	-.307(0.00)(.078)(.400)(4.00)(10.0)(10.0)
$N^{\phi\ r}_{\delta_w\delta_r}$	-.186(.077)(.400)(4.00)(10.0)(10.0)	-.240(.078)(.400)(4.00)(10.0)(10.0)	-.307(.077)(.400)(4.00)(10.0)(10.0)

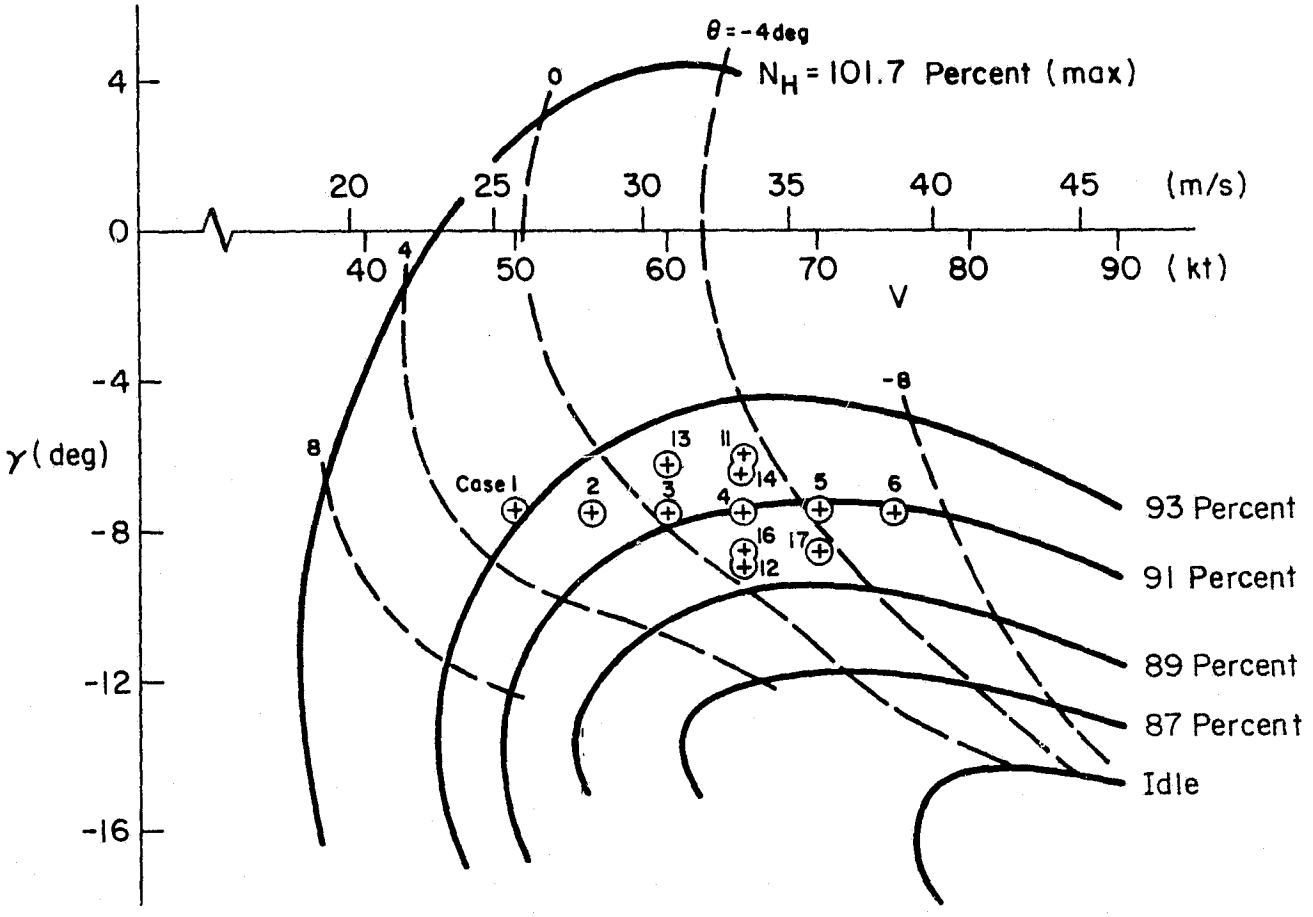

Figure A-1. γ vs. V
Approach Configuration
δ_f = 65 deg, δ_ν = 75 deg

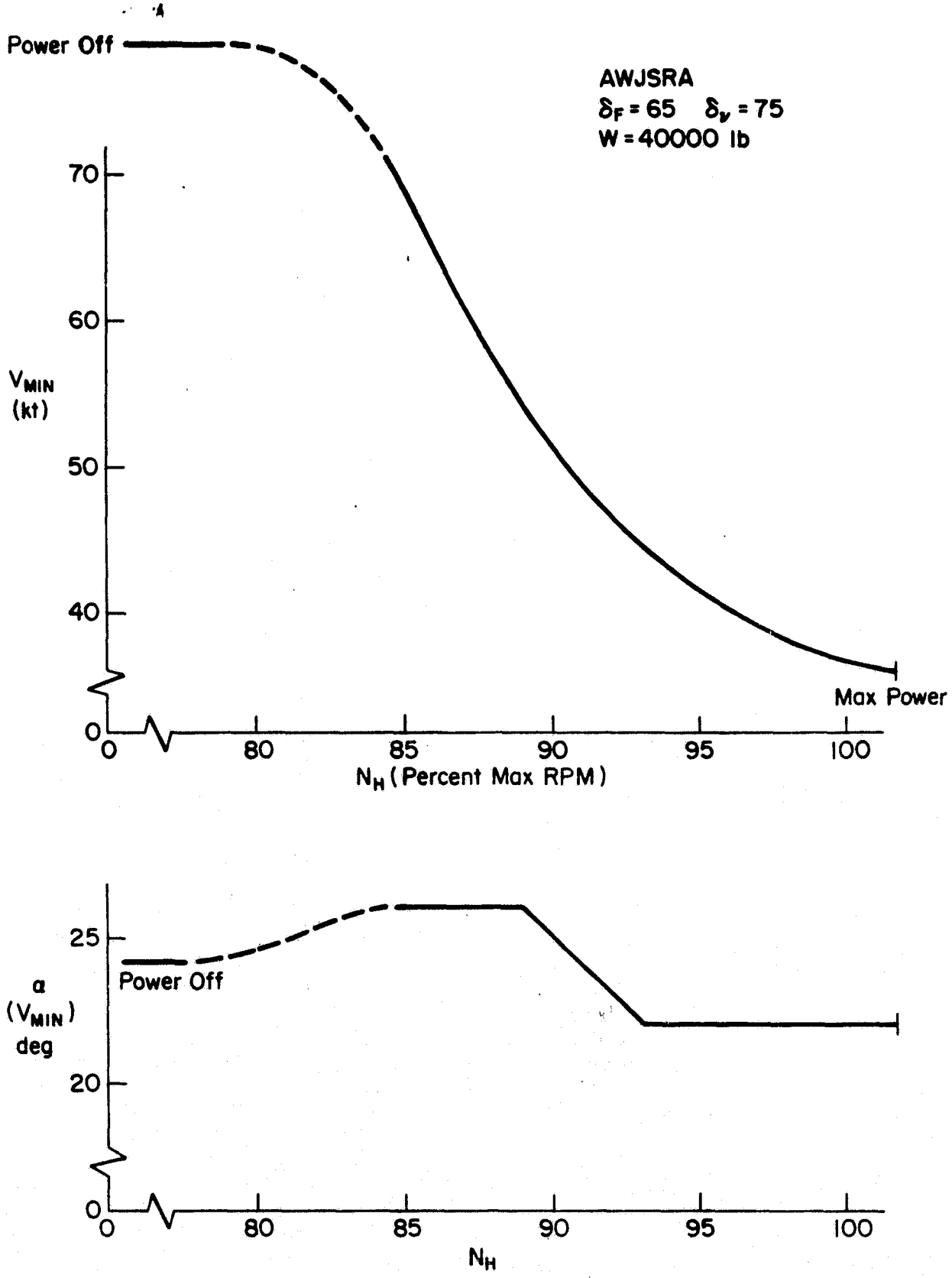

Figure A-2. Effect of Power on V_{MIN}, $\alpha(V_{MIN})$

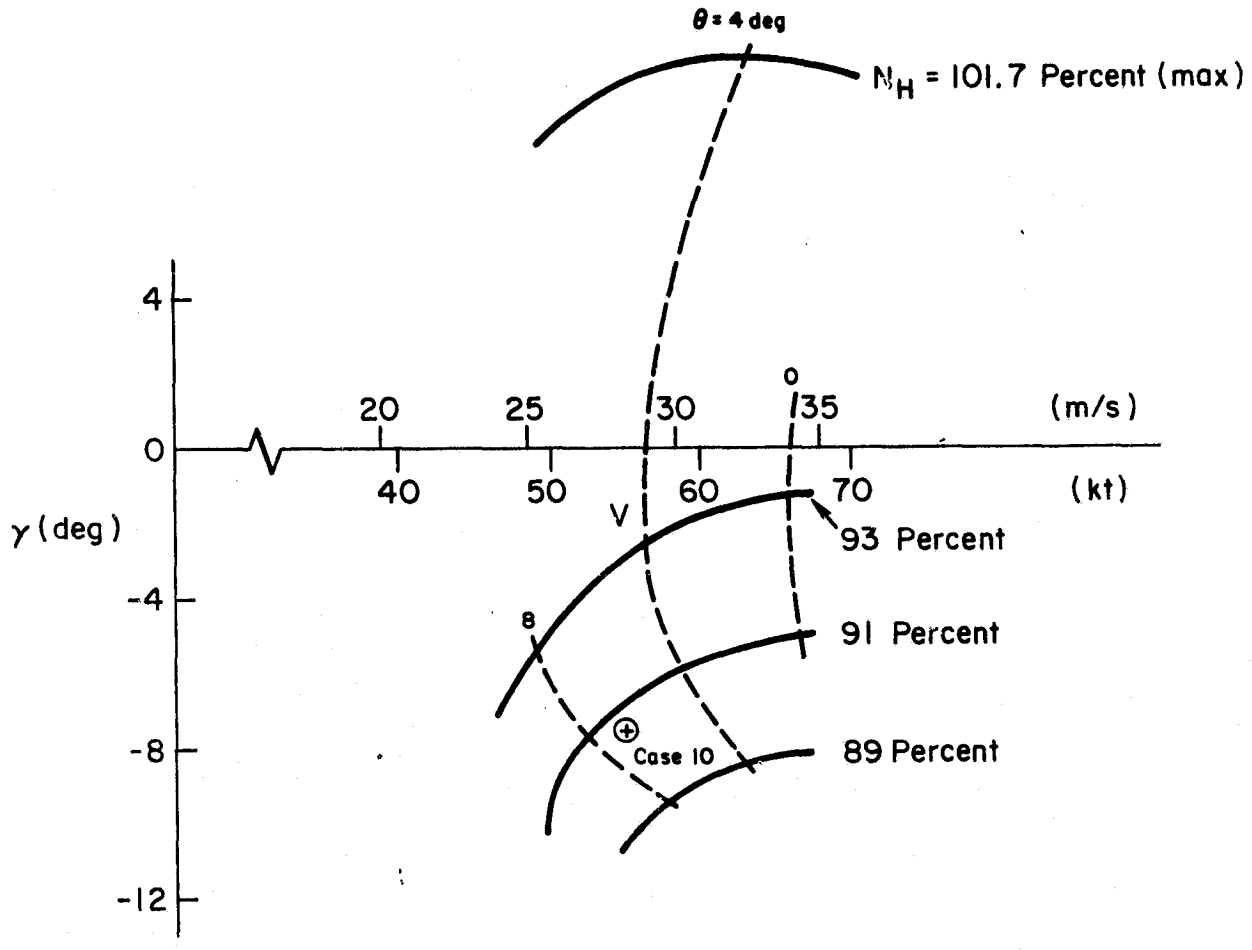

Figure A-3. γ vs. V
Approach Configuration
δ_f = 65 deg, δ_ν = 50 deg

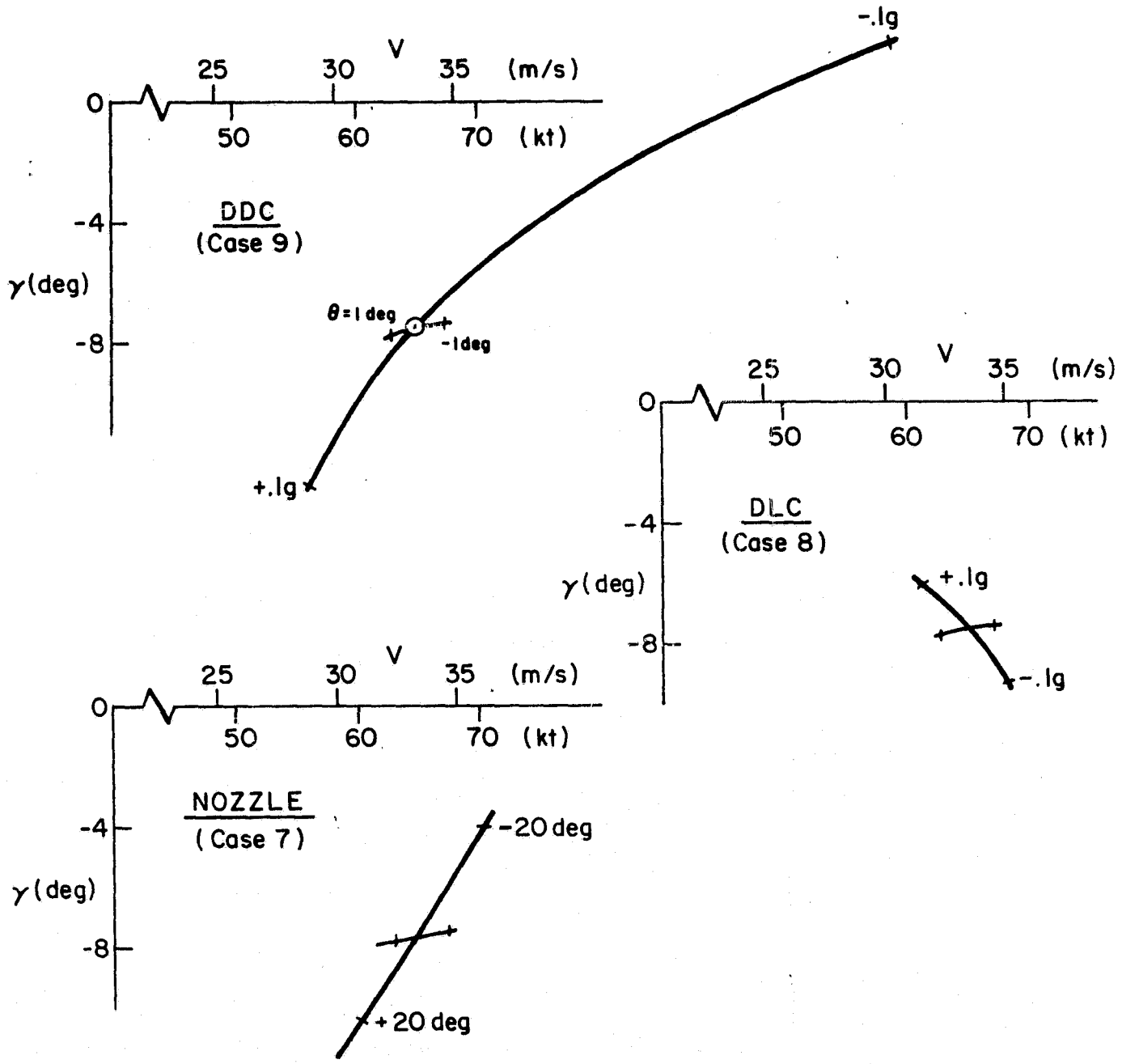

Figure A-4. γ vs. V About Trim Point for Various Controls Used
V_{APP} = 65 kt

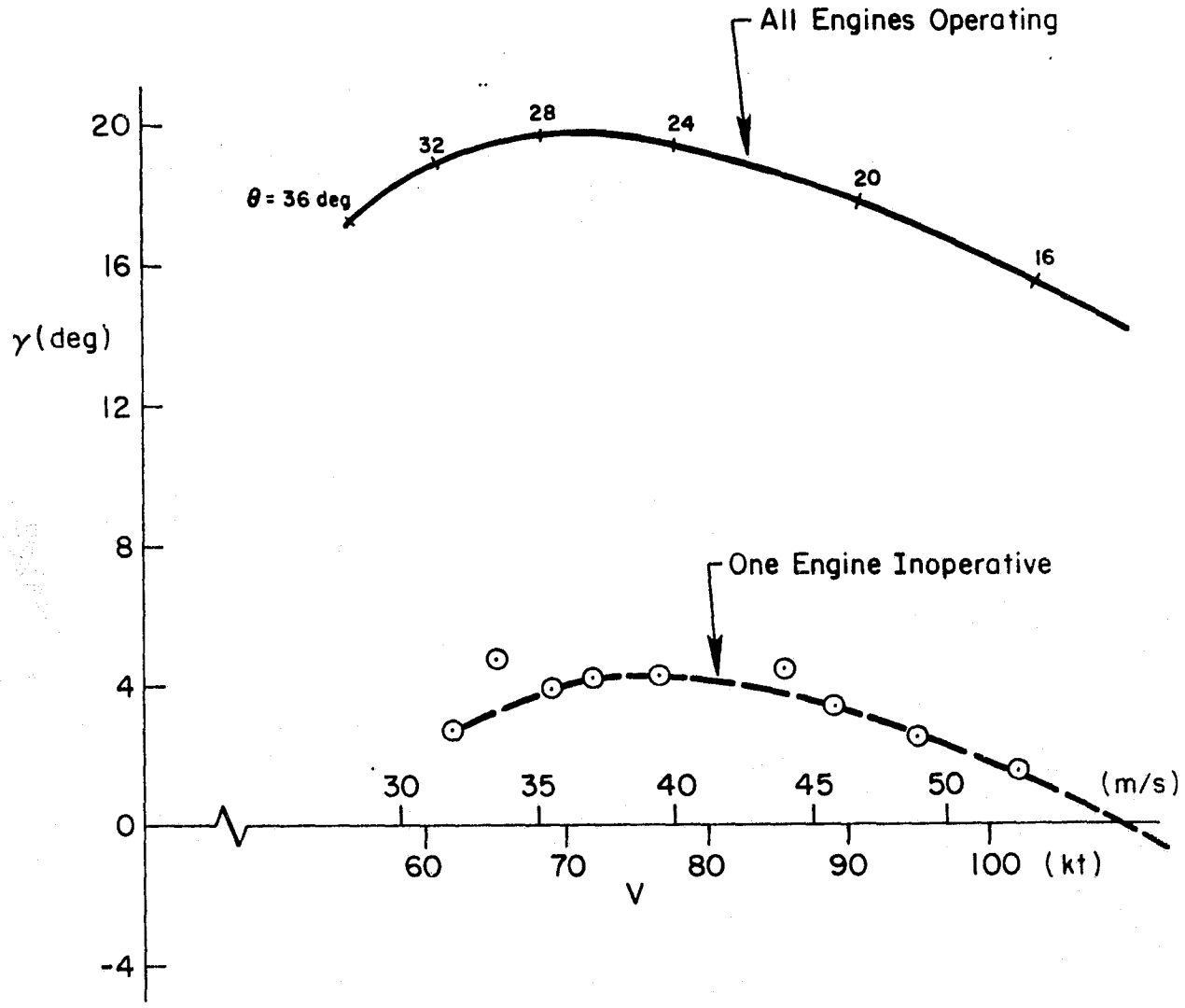

Figure A-5. γ vs. V
Takeoff Configuration: δ_f = 30 deg, δ_ν = 6 deg
Max Power (N_H = 101.7%)

Figure A-6

ALTITUDE RESPONSE TO A 1-INCH COLUMN STEP

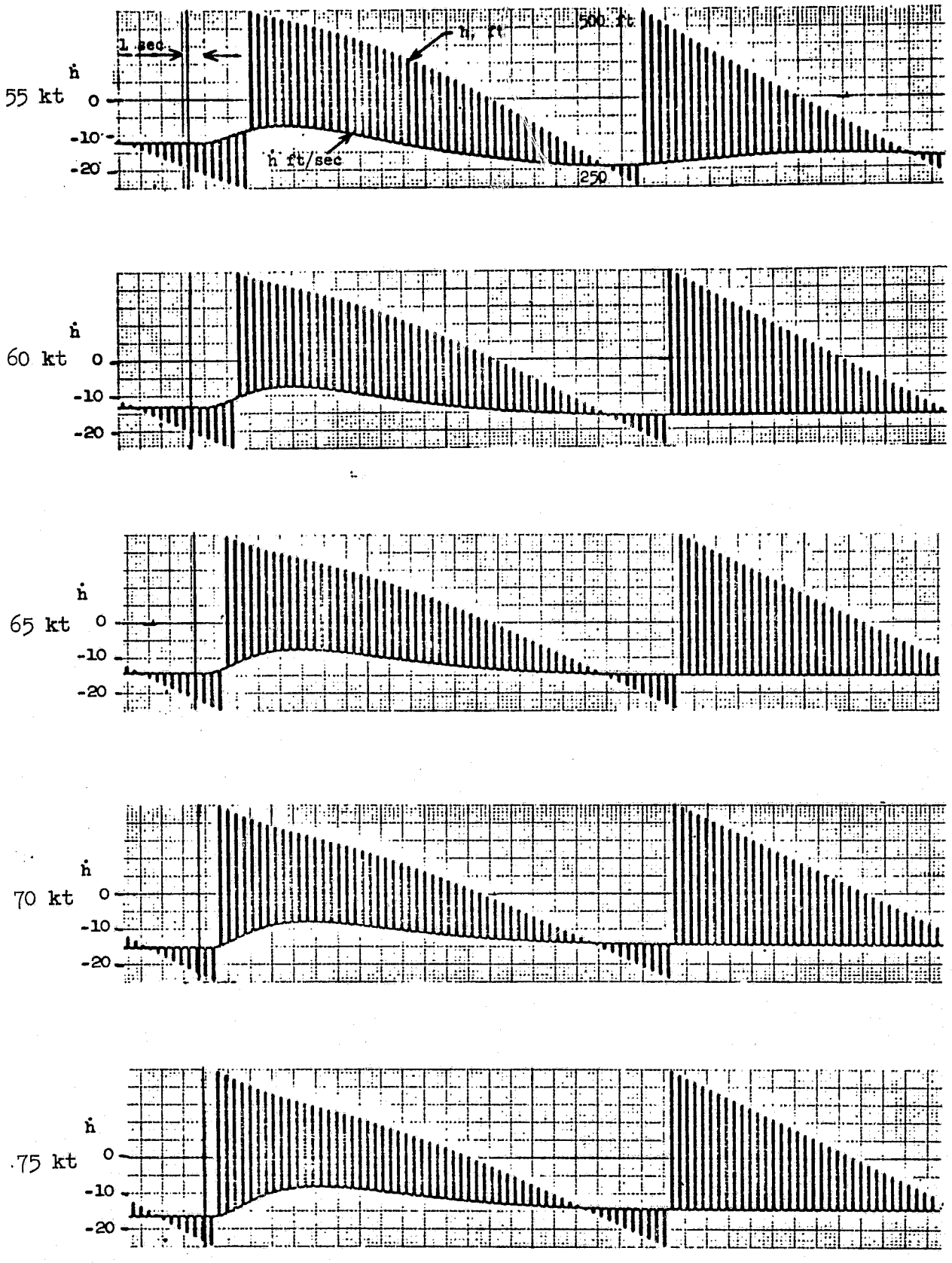

Figure A-7

SPEED RESPONSE TO A 1-INCH COLUMN STEP

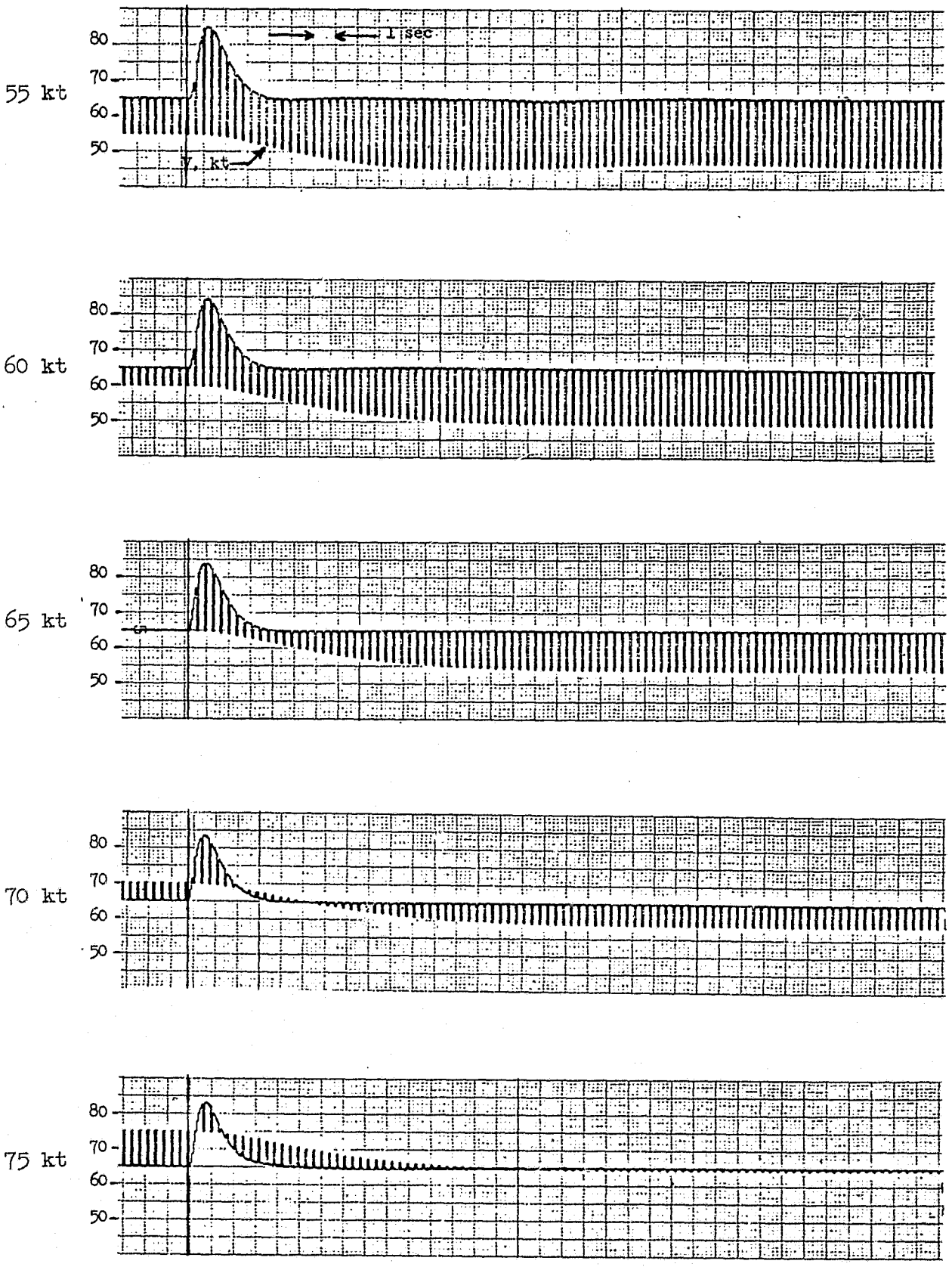

Figure A-8

ALTITUDE RESPONSE TO A 1% ENGINE RPM STEP

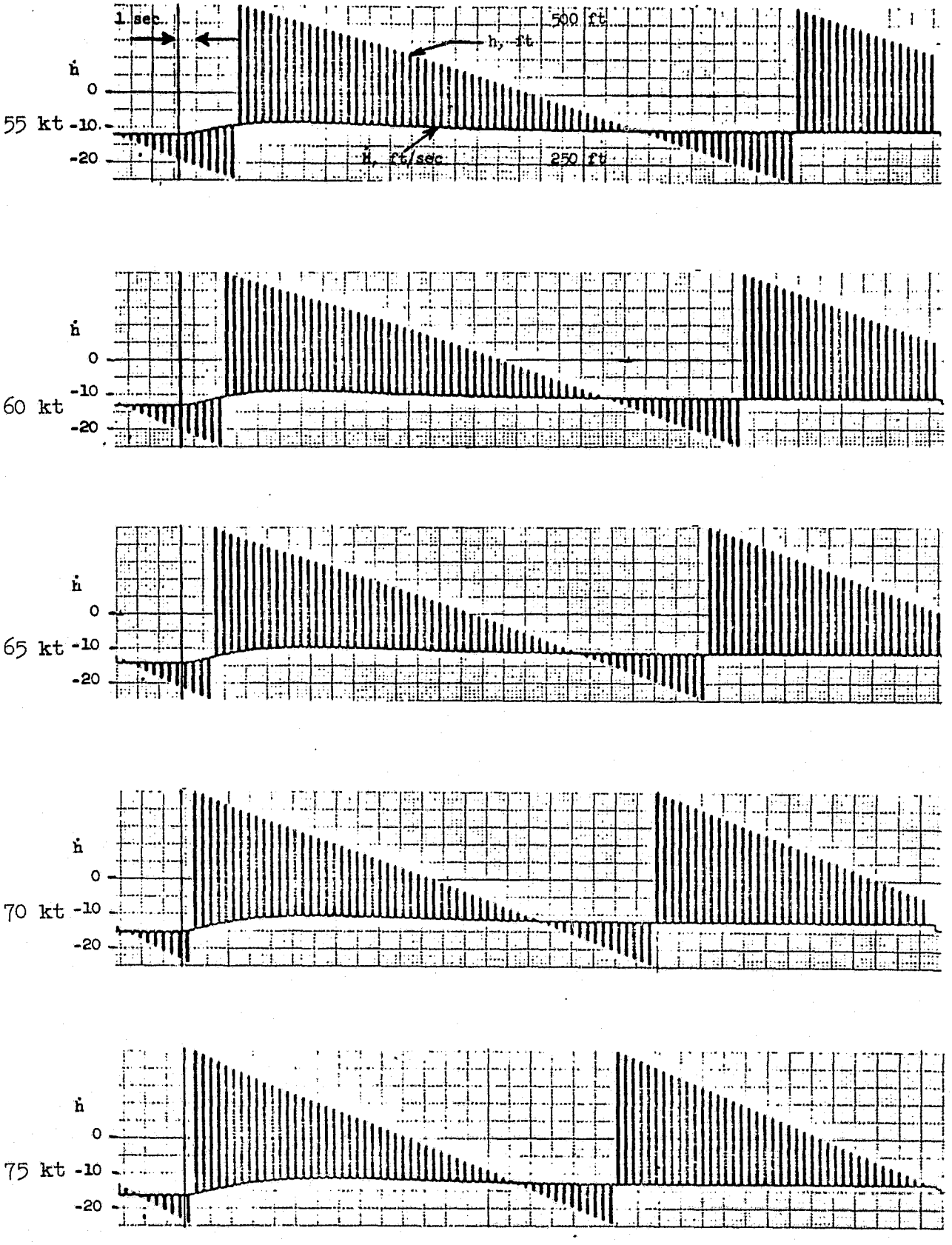

Figure A-9

VELOCITY RESPONSE TO A 1% ENGINE RPM STEP

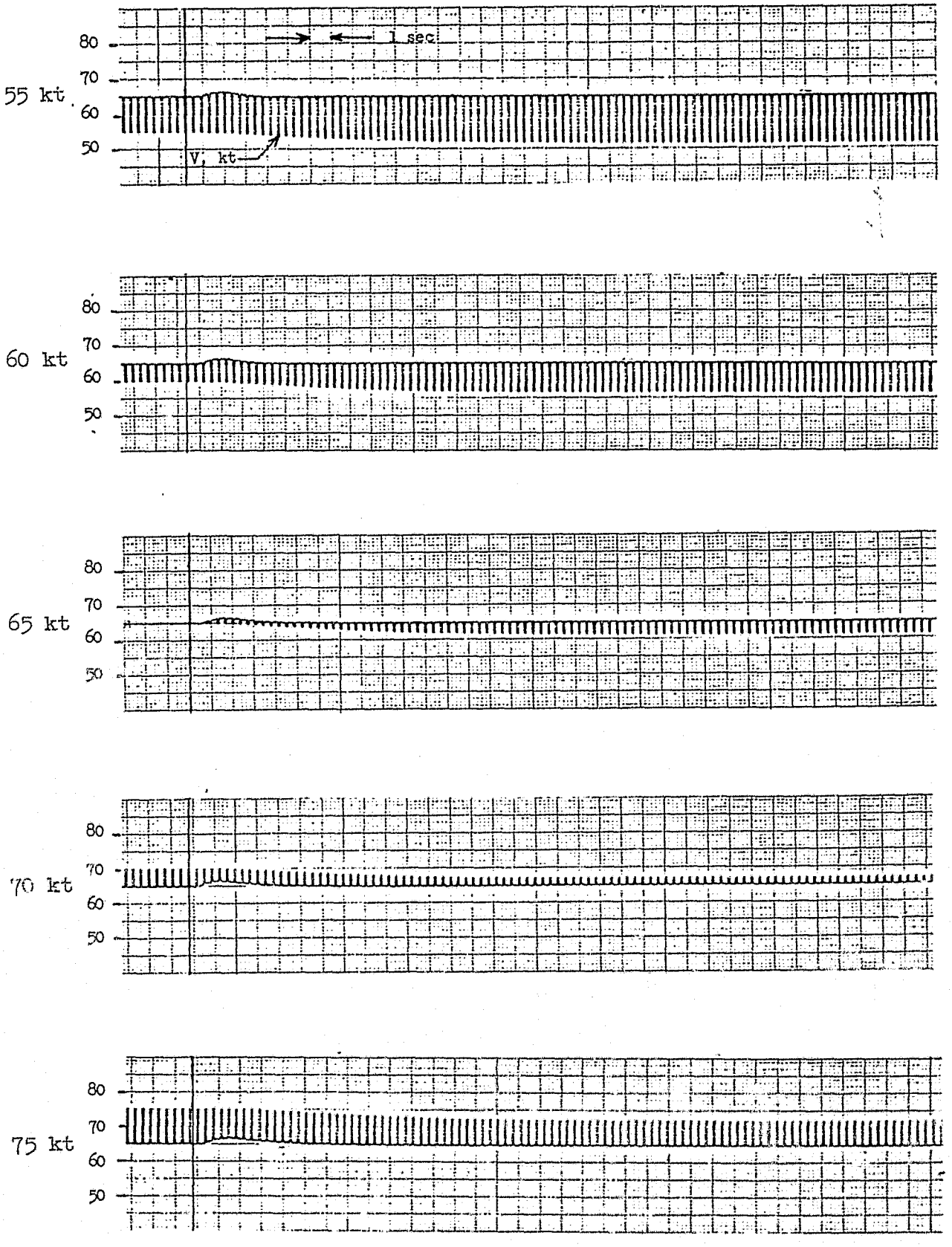

Figure A-10

ALTITUDE RESPONSE TO A +20 DEG NOZZLE STEP

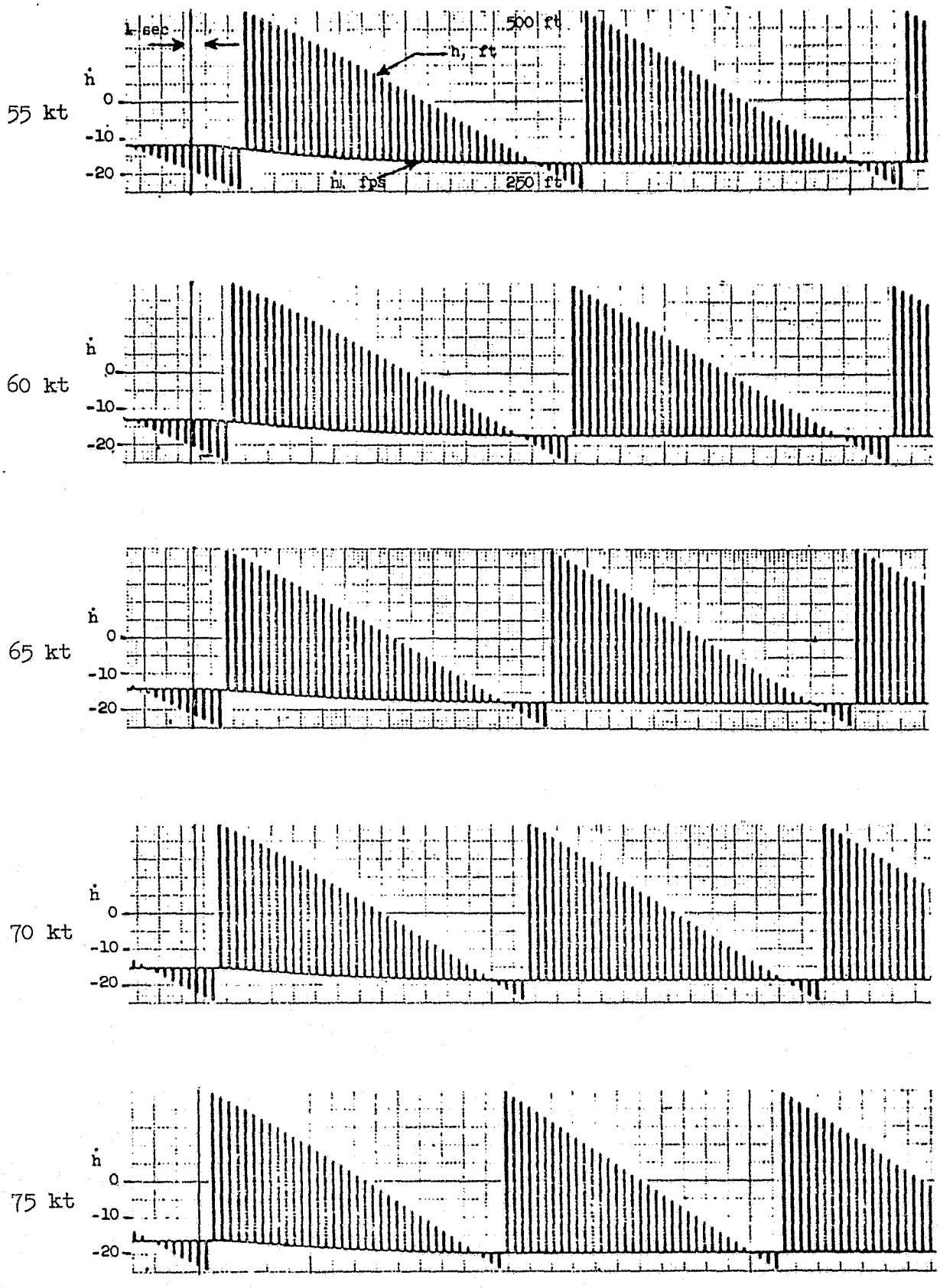

Figure A-11

SPEED RESPONSE TO A +20 DEG NOZZLE STEP

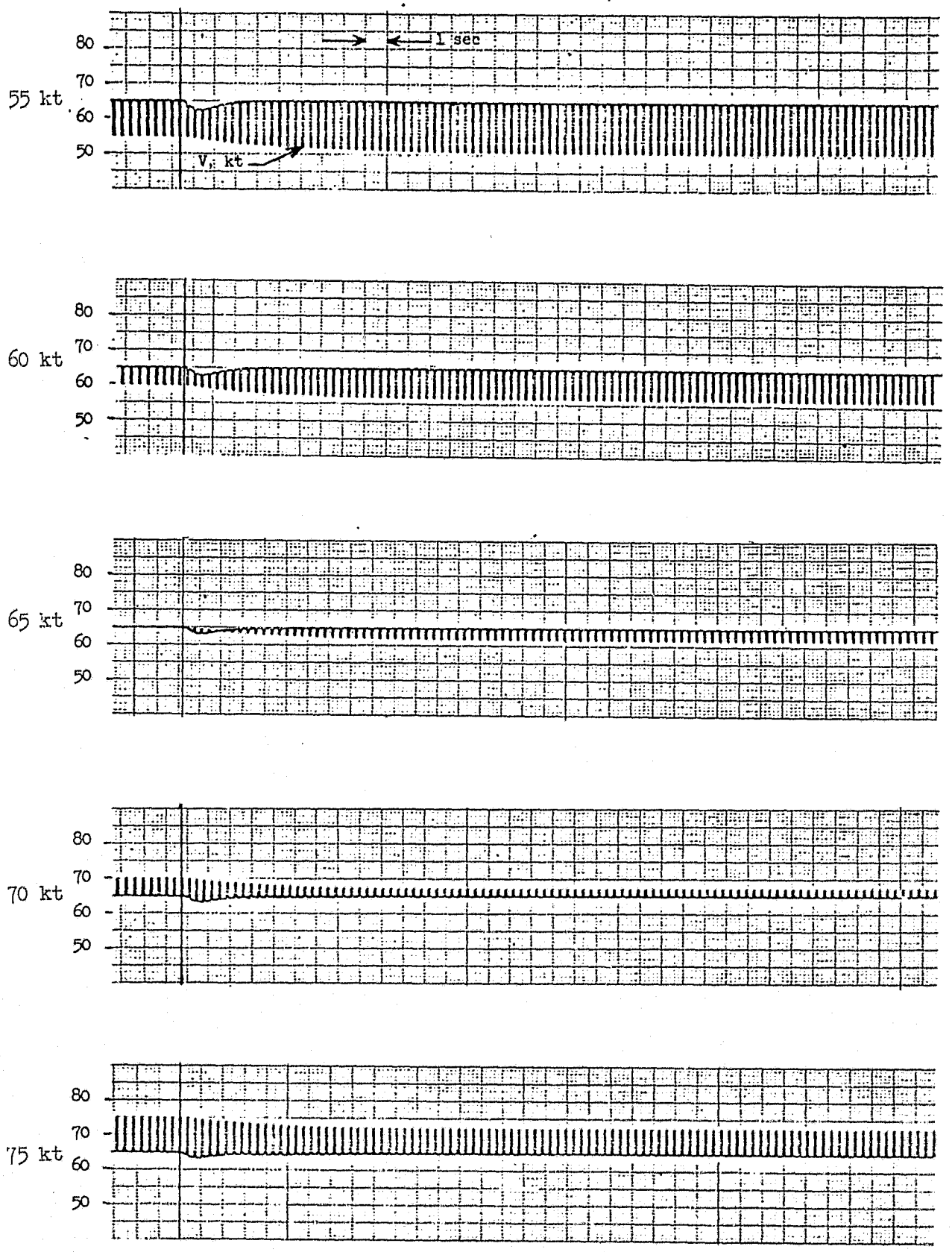

APPENDIX B

ANALYSIS OF GLIDE SLOPE TRACKING

The purpose of this appendix is to provide insights into the glide slope tracking task. This will be accomplished by describing the factors affecting the pilot's control problem in general terms and then using the AWJSRA as a specific example. The relationships introduced will be used to analyze the simulator results presented in Section III.

1. CLASSIFICATION OF KEY CONTROL FACTORS

The problem of tracking the glide slope can be described in ordinary control terms consisting of:

- Sensitivity
- Control power
- Bandwidth
- Cross coupling

Each of these is discussed below and appropriate metrics for each are defined.

a. Sensitivity

Sensitivity is the long or short term relation of aircraft response to cockpit controller motion. The sensitivity of most concern to the pilots seems to be the initial acceleration response. For throttle inputs, the total acceleration per inch of control motion will be used. Since the direction of the thrust force is also significant in glide slope tracking, the effective thrust inclination (angle between the velocity vector and the resultant thrust force) will also be considered.

Another sensitivity of possible significance is that for attitude control of flight path. This is the normal acceleration/angle of attack, n_{z_α}. This is characteristically low for STOL's because of the high lift

coefficient $\left(n_{z_\alpha} \doteq \frac{C_{L_\alpha}}{C_L}\right)$. This is why such large pitch attitude excursions are required when attempting to use a CTOL control technique.

b. Control Power

Control power defines the maximum correction that can be made with a full control input. The most appropriate measure of control power in this case is the incremental flight path angle capability for maximum and minimum control inputs. This sort of information is shown best in a γ - V or $\dot{h}$ - V plot. The parameter we shall use is $\pm \Delta\gamma$ at constant airspeed. This may be limited at lower power settings by V_{min} and, if so, will be indicated.

c. Bandwidth

Bandwidth is a general term and can be defined a number of ways. Basically though, it is a measure of how abruptly or quickly a system can be controlled while still maintaining an acceptable level of stability. For example, if the pilot tries to make glide slope corrections too rapidly he will tend to develop a flight path PIO because of overcontrol.

The measure of glide slope tracking bandwidth that seems most pertinent for STOL's is the frequency at which the $\frac{\text{glide slope}}{\text{throttle}} \cdot \left(\frac{d}{\delta_T}\right)$ transfer function has a phase lag of 135 deg with appropriate inner loops closed. The inner loops include attitude and possibly airspeed. The d/δ_T transfer function should also include engine and pilot lags. Over the range of reasonable flight path control frequencies, the transfer function is approximated by:

$$\underbrace{\frac{d}{\delta_T}\Big|_\theta}_{\theta \text{ Loop Closed}} \doteq \underbrace{e^{-\tau_p s}}_{\text{Pilot}} \quad \underbrace{\frac{1}{\tau_E \; s + 1}}_{\text{Engine}} \quad \underbrace{\frac{N^\theta_{\delta_e} \frac{d}{\delta_T}}{N^\theta_{\delta_e}}}_{\text{Airframe}}$$

where

$\omega_{BW} \triangleq$ Glide slope tracking bandwidth

$\angle \frac{d}{\delta_T}(j\omega_{BW}) = -135$ deg

This particular definition is convenient for partitioning the components involved (pilot, engine, airframe) and is easily computed. Also, the open loop natural response modes are easily shown to be the effective engine lag, $\frac{1}{\tau_{Eng}}$, and the attitude numerator zeros $\frac{1}{T_{\theta_1}}$ and $\frac{1}{T_{\theta_2}}$.

If airspeed were regulated the above would be modified by replacing $\frac{N^{\theta}_{\delta_e \delta_T}}{N^{\theta}_{\delta_e}}$ with $\frac{N^{u}_{\delta_e \delta_T}}{N^{u}_{\delta_e}}$ and recomputing ω_{BW}. These two should bracket the range of available glide slope bandwidths and the respective bandwidths will be noted as ω_{BW_θ} and ω_{BW_u}.

The adequacy of the airplane's tracking bandwidth must be judged against the pilot's desired bandwidth. If the desired bandwidth is greater than the airplane can provide, the pilot will have bandwidth related problems such as flight path PIO's. If the available bandwidth is equal to or greater than that desired, then bandwidth ceases to be a problem. We can take this further by considering the various components involved in determining bandwidth.

Let's return to the $\frac{\text{glide slope}}{\text{throttle}}$ relation which is broken down into pilot, engine, and airframe factors. For a given value of desired bandwidth there is a limit to how good any of the components need to be. For example, if the pilot and airframe components combined give a certain marginal level of response (or bandwidth) then a highly responsive engine wouldn't help. In fact, since the ultimate limit on bandwidth is the pilot ($\doteq 2.5$ rad/sec) then it is not really beneficial to have extremely quick airframe or engine response. (Also, the desired bandwidth is effectively limited by pilot response time. However for the flight path control this limit is reasonably far from the observed operating range.)

If a CTOL technique is used, a similar approach can be used to describe the flight path bandwidth potential. The following expressions show the glide slope control transfer functions using attitude as the control. The attitude control response is approximated by $\exp(-\tau_A S)$. This would vary depending on how tightly attitude is controlled. For loose attitude control $\tau_A = \frac{\sqrt{2}}{\omega_{sp}}$ and for tight control it could be neglected.

$$\left.\frac{\dot{\theta}_c}{\delta_T}\right| = e^{-\tau_p s} \quad e^{-\tau_A S} \quad \frac{N^{\dot{d}}_{\delta_e}}{N^{\theta}_{\delta_e}}$$

Constant Throttle — Pilot — Attitude — Airframe

$$\left.\frac{\dot{\theta}_c}{u}\right| = e^{-\tau_p s} \quad e^{-\tau_A S} \quad \frac{N^{u\,\dot{d}}_{\delta_T \delta_e}}{N^{u\,\theta}_{\delta_T \delta_e}}$$

Constant Airspeed — Pilot — Attitude — Airframe

Again, bandwidth would correspond to a phase lag of 135 deg.

d. Cross Coupling

In any control situation where there are several variables to be controlled and several controllers to do the job, the question of cross-coupling arises. Cross-coupling involves the relative impurity of the controls and the ability to independently modulate each of the variables without adversely affecting the others. Severe coupling greatly complicates the control problem as complex feedbacks or control cross feeds are required.

Unfortunately there are no simple measures of cross coupling. A relatively simple metric was presented by Bristol in Reference 5, however it

considered only the static or steady-state characteristics of a system. This measure was expanded to include variations with frequency and the expanded version has proven quite useful in interpreting and quantifying the cross-coupling problems encountered in STOL flight path control.

To understand this cross coupling metric it is useful to first review Bristol's original interaction measure. Assume a multivariable system with N inputs, δ_i, and N outputs, x_i. The static gains of the system can be written as a matrix K where element k_{ij} is the static gain from input δ_j to output x_i.

Bristol's interaction measure is an N x N matrix, M. Each element of M is a ratio of gain, i.e.

$$m_{ij} = \frac{k_{ij}}{\hat{k}_{ij}}$$

As notes above k_{ij} is the gain from input δ_j to output x_i. The term $\hat{k}_{ij}$ is the gain from input δ_j to output x_i when the remaining N - 1 controls are used to keep the other N - 1 outputs at zero. Thus the element m_{ij} is the ratio of the open loop gain to the gain when the other outputs are constrained to zero. Mathematically this can be written as

$$m_{ij} = k_{ij}\, k_{ji}^{-1}$$

where

k_{ji}^{-1} is an element of the inverse of K

The matrix M has several useful properties, including;

1. The elements in any row or column sum to one
2. Scaling changes of either the inputs or outputs do not affect M
3. In an uncoupled system, the elements of M are either zero or one
4. Elements much greater than one indicate severe coupling and a difficult control situation
5. Elements on the order of 0.5 indicate significant cross coupling which can fairly easily be decoupled.

This concept can be expanded to consider transfer functions instead of just static gains. This extends the utility of the coupling measure but the matrix elements become functions of frequency rather than constants. This modification does not affect the 5 properties listed above.

Let us now apply this concept to STOL flight path control. The primary outputs of concern are flight path angle, γ, and airspeed deviation, u. The control inputs are throttle, δ_T, and pitch attitude, θ. The cross coupling matrix in this case can be written as:

OUTPUT	INPUT δ_T	INPUT θ
γ	$\dfrac{\left(\frac{\gamma}{\delta_T}\right)_\theta}{\left(\frac{\gamma}{\delta_T}\right)_u}$	$\dfrac{\left(\frac{\gamma}{\theta}\right)_{\delta_T}}{\left(\frac{\gamma}{\theta}\right)_u}$
u	$\dfrac{\left(\frac{u}{\delta_T}\right)_\theta}{\left(\frac{u}{\delta_T}\right)_\gamma}$	$\dfrac{\left(\frac{u}{\theta}\right)_{\delta_T}}{\left(\frac{u}{\theta}\right)_\gamma}$

where

$\left(\frac{X}{Y}\right)_Z$ is the $\frac{X}{Y}$ transfer function for Z = 0

Because of property 1 noted above, only 1 of the 4 matrix elements is independent and the matrix can be rewritten as:

OUTPUT	INPUT δ_T	INPUT θ
γ	μ^{STOL}	$\mu^{CTOL} = 1 - \mu^{STOL}$
u	$\mu^{CTOL} = 1 - \mu^{STOL}$	μ^{STOL}

The notation μ^{STOL} and μ^{CTOL} was chosen to reflect the STOL and CTOL piloting techniques, i.e.

STOL: $\gamma \longrightarrow \delta_T$, $u \longrightarrow \theta$

CTOL: $\gamma \longrightarrow \theta$, $u \longrightarrow \delta_T$

From here on we will concentrate on the function μ^{STOL} and its interpretation. It can be expressed quite simply as a ratio of numerator and coupling numerators.

$$\mu^{STOL} \triangleq \frac{\left(\frac{\gamma}{\delta_T}\right)_\theta}{\left(\frac{\gamma}{\delta_T}\right)_u} = \frac{\left(\frac{u}{\theta}\right)_{\delta_T}}{\left(\frac{u}{\theta}\right)_\gamma} = \frac{N^u_{\delta_e} \; N^\theta_{\delta_e \delta_T}}{N^\theta_{\delta_e} \; N^u_{\delta_e \delta_T}}$$

While the above expression is valid at all frequencies, the dc value can be defined in terms of slopes from γ - V plots.

$$\mu^{STOL}_{\omega=0} = \frac{\left(\frac{\partial \gamma}{\partial V}\right)_\theta}{\left(\frac{\partial \gamma}{\partial V}\right)_\theta - \left(\frac{\partial \gamma}{\partial V}\right)_{\delta_T}}$$

This shows that the dc value of μ^{STOL} is one when the constant power curve is horizontal, $\left(\frac{\partial \gamma}{\partial V}\right)_{\delta_T} = 0$, or the constant attitude curve is vertical, $\left(\frac{\partial \gamma}{\partial V}\right)_\theta = \infty$. Unfortunately, the γ - V plot does not define μ^{STOL} at frequencies other than zero.

We will now discuss the various interpretations of μ^{STOL}. By definition, μ^{STOL} is the ratio of the γ/δ_T transfer function when airspeed deviations are ignored ($\theta = 0$) to that when airspeed is constrained (by a $u \longrightarrow \theta$ feedback or a $\delta_T \longrightarrow \theta$ crossfeed). This function is important to the pilot because his airspeed regulation may vary. For small flight path corrections, airspeed deviations may be within the pilot's indifference

threshold so he'll take no corrective action. However, for large flight path corrections, the pilot may have to adjust his pitch attitude to avoid excessive airspeed deviations.

The function μ^{STOL} defines the changes in the γ/δ_T response which result from the addition of airspeed regulation. A value of μ^{STOL} much different than one indicates a significant effect of airspeed control. Furthermore, a variation of μ^{STOL} with frequency indicates the γ/δ_T time response changes shape as well as amplitude. This is graphically demonstrated in Figures B-1 and B-2.

At 55 kt, μ^{STOL} has a peak of 1.75 at 0.3 rad/sec and goes to 0.5 at low frequency. In the γ/δ_T time responses, this is manifested by a larger initial response without airspeed regulation but a reduced steady-state response. Flight path control at 55 kt should be difficult because:

- Poor γ/δ_T response without airspeed regulation -- initial peak is approximately 2.6 times the steady-state value
- Airspeed regulation drastically alters γ/δ_T response -- flight path and airspeed control are strongly coupled.

Furthermore, Figure B-2 illustrates the improvement in flight path control with increasing airspeed and the connections between time responses and μ^{STOL}.

Another interpretation of μ^{STOL} is related to the control crossfeeds required to decouple the responses. Assume the pilot uses (or tries to use) the cross control technique indicated in the sketch below.

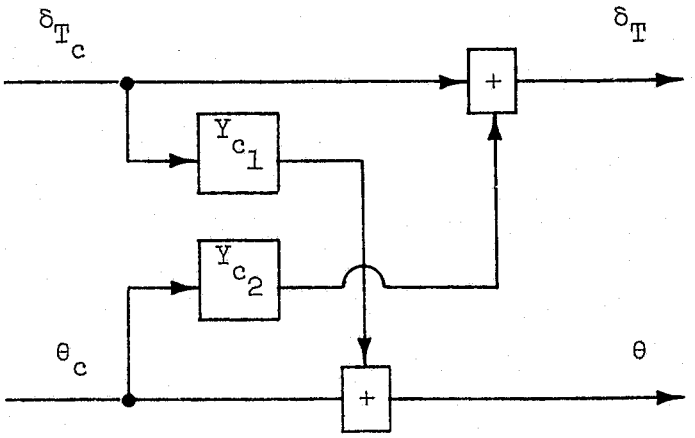

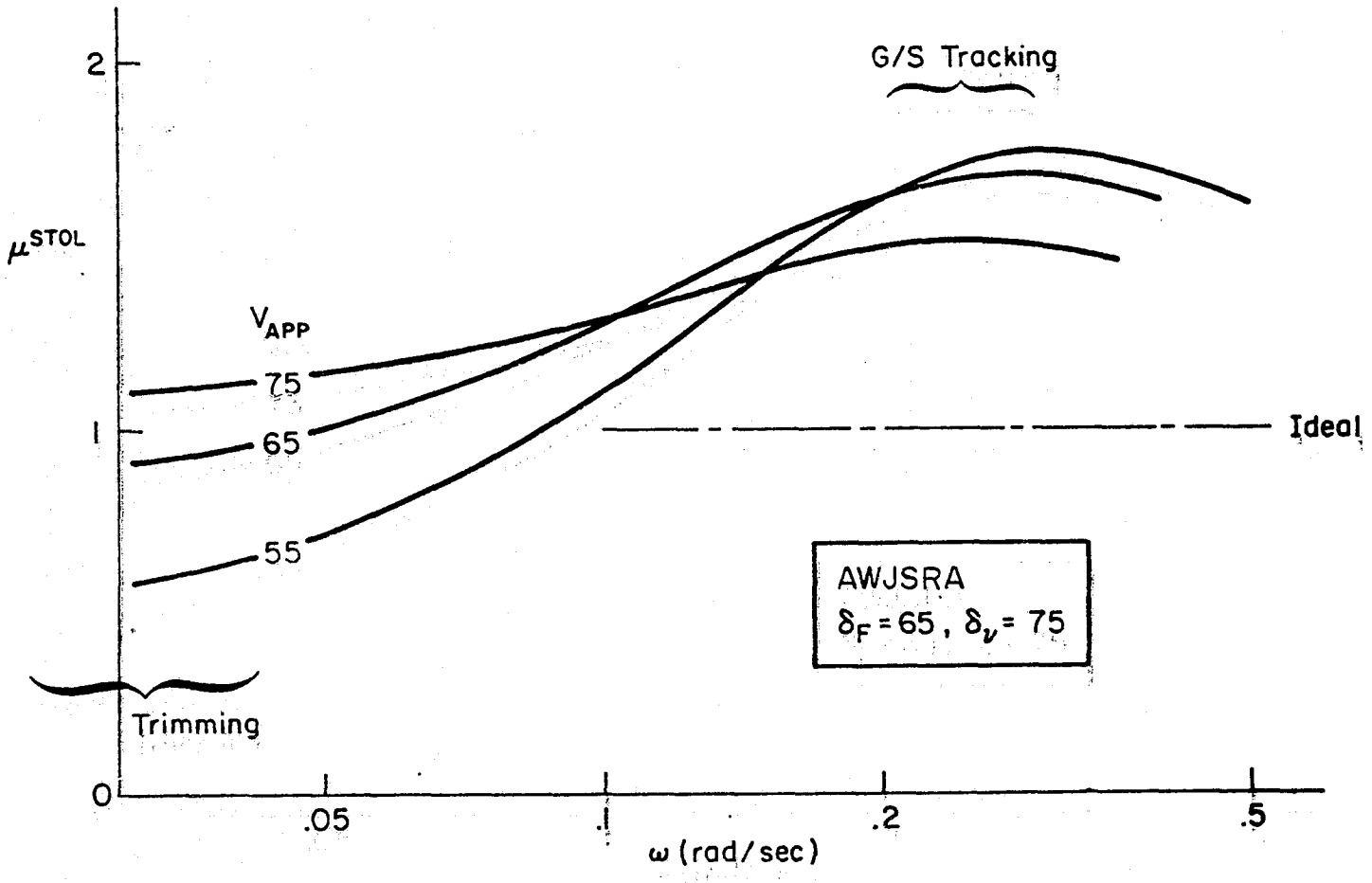

Figure B-1. G/S-IAS Coupling Parameter Varying Approach Speed

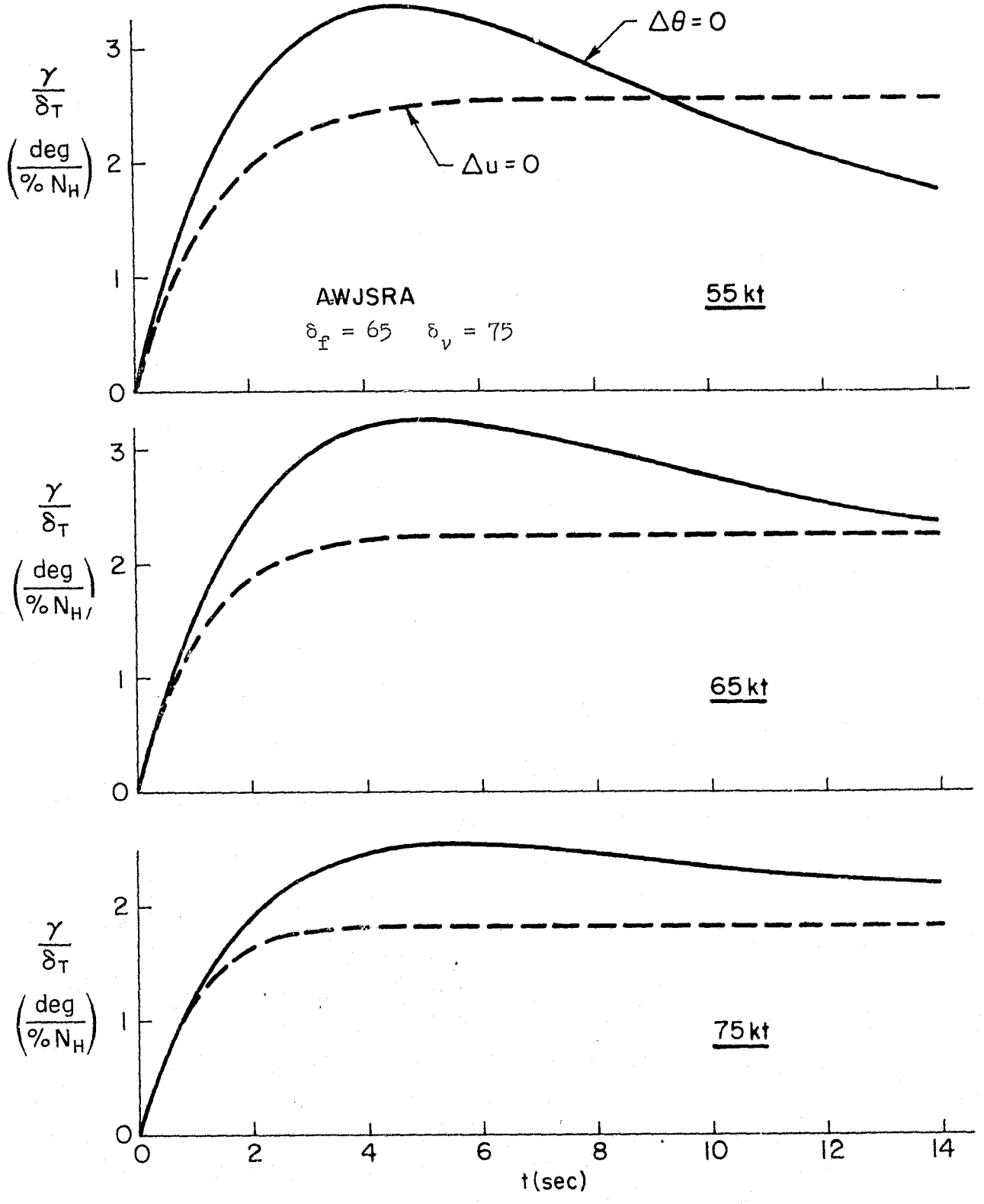

Figure B-2. Comparison of Flight Path Response to Throttle Step Attitude vs Airspeed Constraint

If Y_{c_1} is adjusted so that $u/\delta_{T_c} = 0$ and Y_{c_2} is adjusted so that $\gamma/\theta_c = 0$, then

$$Y_{c_1} Y_{c_2} = \frac{\mu^{STOL} - 1}{\mu^{STOL}}$$

Thus when $\mu^{STOL} = 1$, at least one of the decoupling crossfeeds is zero.

Table B-1 summarizes the interpretations of μ^{STOL} relative to STOL flight path control. This table discusses separately the low frequency interpretations relative to trim problems and the higher frequency ones relating to glide slope tracking. The comments in Table B-1 are based on the above theoretical considerations and correlations of μ^{STOL} with pilot comments from the AWJSRA simulation.

Table B-2 summarizes the key flight path and airspeed control parameters introduced in this part. This will form the basis of the analysis of the Augmentor Wing simulator model.

2. ANALYSIS OF AWJSRA

The key control factors presented in the preceding part will now be examined for the simulator model used along with some discussion of possible implications.

Table B-3 is a list of flight path control characteristics for the cases run during the simulation. It addresses the effects of approach speed variations, complementary control variations, steady winds, and pilot technique. Control sensitivity is given in $\frac{\partial n}{\partial \delta_T}$ (g/in) for STOL technique (along with the effective direction of control) and $\frac{\partial n_z}{\partial \alpha}$ (g/rad) for CTOL technique. Control power, independent of technique, is given in terms of incremental flight path angles up and down. Bandwidth is given not only for STOL vs CTOL techniques but also for no speed regulation vs perfect regulation. Finally, STOL coupling is tabulated for steady state (trimming) and $\omega = .3$ rad/sec (tight tracking). CTOL coupling is a simple function of this, i.e., $\mu^{CTOL} = 1 - \mu^{STOL}$.

TABLE B-1

INTERPRETATION OF μ^{STOL}

	GENERAL	LOW FREQUENCY ($0 < \omega < .05$ rad/sec)	PATH MODE FREQUENCIES ($.1 < \omega < .5$ rad/sec)
$\mu^{STOL} \doteq 1$	• IAS and G/S are easily decoupled. • γ/δ_T responses are independent of $u \longrightarrow \theta$ feedback and conversely u/θ responses are independent of $\gamma \longrightarrow \delta_T$ feedback. • The STOL piloting technique is most appropriate.	• Should trim sink rate with power and speed with attitude. • Minimum number of control iterations to retrim IAS or rate of descent without affecting the other.	• Short term glide slope tracking easily accomplished using only power.
$\mu^{STOL} \doteq 0$	• Same comments as for $\mu \doteq 1$ if change from STOL to CTOL piloting technique.	• Same as $\mu \doteq 1$ except pilot should trim sink rate with attitude and speed with power.	• Short term glide slope tracking easily accomplished using only attitude.
$\mu^{STOL} \doteq .5$	• IAS and G/S can be decoupled with a complementary use of controls. • Either throttle or attitude may be used for the initial correction.	• Trim takes a combination of both controls. • Should make only partial retrim with first control iteration.	• Glide slope tracking requires simultaneous manipulation of both controls to minimize IAS variation.
$\mu^{STOL} > 1$	• IAS and G/S not easily decoupled. • Both attitude and throttle act in a similar way on IAS and G/S. • Initial correction of G/S must be with throttle • Reverse control sense problems exist.	• Trim takes a combination of both controls. • Should overtrim with first control iteration. • Certain combinations of off-nominal γ - V conditions difficult to correct (e.g., high-fast and low-slow)	• Glide slope tracking requires manipulation of both controls in order to minimize IAS variation. • Certain combinations of off-nominal γ-V conditions difficult to correct in short term. • Reverse control sense problems especially confusing because of time element.

TABLE B-2

KEY FLIGHT PATH AND AIRSPEED CONTROL PARAMETERS

PARAMETER	DESCRIPTIVE TERM	SOURCE	SIGNIFICANCE	FORMAL DEFINITION
$\frac{\partial n_z}{\partial \delta_T}$	Short term throttle ⟶ flight path sensitivity.	Controller Geometry.	Important if STOL technique employed. Can be a factor in flight path PIO if too high.	$-\frac{1}{g} Z_{\delta_T}$ (g/in)
n_{z_α}	Short term attitude ⟶ flight path sensitivity.	Lift curve slope, lift coefficient.	Important if CTOL technique employed. Normally low for STOL aircraft.	$-\frac{U_o}{g} Z'_w$ (g/rad)
$\pm \Delta\gamma$ (or $\Delta\dot{h}$)	Long term control power.	Thrust-to-weight and lift-to-drag ratios.	Determines level of error that is correctable.	At V_{APP}, $\gamma(\delta_T = \max) - \gamma(\delta_T = \text{trim})$ and $\gamma(\delta_T = \min) - \gamma(\delta_T = \text{trim})$. Similarly for $\dot{h}$.
$\omega_{BW_\theta}^{STOL}$	Maximum obtainable flight path bandwidth with the attitude loop closed when using a STOL piloting technique.	Airframe, engine, pilot response.	Indication of pilot/vehicle bandwidth capability without airspeed regulation for STOL technique.	Frequency at which open loop phase = -135 deg for: $\frac{d}{\delta_T} = \underbrace{e^{-\tau_p s}}_{\text{Pilot}} \underbrace{\frac{1}{\tau_E s + 1}}_{\text{Engine}} \underbrace{\frac{N^u_{\delta_e} d_{\delta_T}}{N^\theta_{\delta_e}}}_{\text{Airframe}}$
$\omega_{BW_u}^{STOL}$	Maximum obtainable flight path bandwidth with the airspeed loop closed when using a STOL piloting technique.	Airframe, engine, pilot response.	Indication of pilot/vehicle bandwidth capability with airspeed regulation for STOL technique.	Same as above except airframe component is: $\frac{N^u_{\delta_e} d_{\delta_T}}{N^u_{\delta_e}}$
$\omega_{BW_{\delta_T}}^{CTOL}$	Maximum obtainable flight path bandwidth with the throttle fixed when using a CTOL piloting technique.	Airframe, pilot response.	Indication of pilot/vehicle bandwidth capability without airspeed regulation for CTOL technique.	Frequency at which open loop phase = -135 deg for: $\frac{d}{\theta_c} = \underbrace{e^{-\tau_p s}}_{\text{Pilot}} \underbrace{e^{-\tau_A s}}_{\text{Attitude}} \underbrace{\frac{N^d_{\delta_e}}{N^\theta_{\delta_e}}}_{\text{Airframe}}$
$\omega_{BW_u}^{CTOL}$	Maximum obtainable flight path bandwidth with the airspeed loop closed using a CTOL piloting technique.	Airframe, pilot response.	Indication of pilot/vehicle bandwidth capability with airspeed regulation for CTOL technique.	Same as above except airframe component is: $\frac{N^u_{\delta_T} d_{\delta_e}}{N^u_{\delta_T} N^\theta_{\delta_e}}$
μ_o^{STOL}	Control/response coupling for glide slope tracking	Static lift and drag derivatives, thrust angle.	Indication of level of cross coupling problem and of proper control technique (CTOL vs STOL)	$\frac{\frac{d}{\delta_T}\Big\|_{\theta = \text{const}}}{\frac{d}{\delta_T}\Big\|_{u = \text{const}}} = \frac{N^\theta_{\delta_e} d_{\delta_T} N^u_{\delta_e}}{N^\theta_{\delta_e} N^u_{\delta_e} d_{\delta_T}} = (s = 0)$
$\mu_{.3}^{STOL}$	Control/response coupling for glide slope tracking.	Static lift and drag derivatives, thrust angle.	Same as above except pertains to tight ILS tracking. Significant differences between μ_o and $\mu_{.3}$ also indicate problems.	Same as above except evaluated at $s = .3j$ rad/s.

TABLE B-3
AWJSRA SIMULATION

V_{APP} (kt)	CASE	COMPLEMENTARY CONTROL	SENSITIVITY			CONTROL POWER[2]		BANDWIDTH				COUPLING	
			STOL[1]		CTOL			STOL		CTOL		STOL[3]	
			$\frac{\partial n}{\partial \delta}$ (g/in)	@ χ_δ (deg)	n_{z_α} (g/rad)	$\Delta\gamma_{max}$ (deg)	$\Delta\gamma_{min}$ (deg)	Constant θ (rad/s)	Constant u (rad/s)	Constant δ_T (rad/s)	Constant u (rad/s)	μ^{STOL} (ω = 0)	μ^{STOL} (ω = .3)
65	Baseline	Throttle	.16	89.6	1.69	11.7	-6.3[4]	.34	.36	.48[7]	[5]	.86	1.68
55	Low Approach Speed	Throttle	.14	92.9	1.27	11.3	-5.3[4]	.34	.33	.52[7]	[6]	.48	1.75
60		Throttle	.16	90.9	1.44	11.9	-5.8[4]	.34	.35	.48[7]	[6]	.74	1.71
70	High Approach Speed	Throttle	.15	87.7	1.87	11.0	-6.9[4]	.33	.38	.48[7]	[5]	.97	1.57
75		Throttle	.15	85.8	2.27	10.3	-7.6[4]	.33	.42		[5]	1.07	1.48
65	Horizontal Thrust Component	Nozzle	.016	-10.4	1.69	4.1	-4.5	.09	.35	.48[7]	.36	1.2	.54
65		DDC	.05	0	1.69	---	---	.091	.35	.48[7]	.35	1.2	.54
65	Vertical Thrust Component	DLC	.05	90	1.69	---	---	.44	.56	.48[7]	[5]	.86	1.68
65	τ_E = 1.5 s	Throttle	.16	89.6	1.69	11.7	-6.3[4]	.28	.26	.48[7]	[5]	.86	1.68
65	τ_E = 2.5 s	Throttle	.16	89.6	1.69	11.7	-6.3[4]	.24	.21	.48[7]	[5]	.86	1.68
65	τ_E = 3 s	Throttle	.16	89.6	1.69	11.7	-6.3[4]	.22	.17	.48[7]	[5]	.86	1.68
65	10 kt Headwind	Throttle	.17	92.5	1.65	10.5	-7.4[4]	.32			[5]	.92	1.57
65	10 kt Crosswind	Throttle	.16	90.1	1.64	11.7	-6.3[4]	.34	.36	.48	[5]	.83	1.69
65	10 kt Tailwind	Throttle	.16	88.4	1.63	12.9	-5.1[4]	.35	.37		[6]	.77	1.97
55	δ_v = 50 deg	Throttle	.14	90.7	1.11	16.7	-2.4[4]	.36	.33		[6]	.49	1.68

1/ Sensitivity at effective control thrust inclination, χ_δ.

2/ At constant airspeed.

3/ $\mu^{CTOL} = 1 - \mu^{STOL}$

4/ V_{min} limited.

5/ u ⟶ δ_T loop unstable.

6/ Reverse sense u ⟶ δ_T control must be used.

7/ No DC gain, initial flight path change washes out.

a. Baseline Case

The 65 kt baseline case demonstrates several flight path control characteristics typical of a large STOL aircraft. Beginning at the left we see that the flight path control sensitivity using throttle (STOL technique) is .16 g/in acting nearly normal to the flight path. Based on experiments from Reference 9 and other sources, this level of gain is near optimum. On the other hand, the flight path control sensitivity using attitude (CTOL technique) would be considered low. More than 5 deg of attitude change would be required to get the equivalent of 1 inch of throttle.

Flight path control power would seem adequate for the 7.5 deg glide slope since the "up" increment available would more than allow for a positive rate of climb and the maximum "down" would give almost 1600 ft/min rate of descent.

Bandwidth of the baseline case, using a STOL technique, is nearly independent of whether speed is regulated. The adequacy of this level of bandwidth depends on how quickly corrections are desired. This could depend on choppiness and intensity of turbulence or on particular terminal time constraints such as a last-second maneuver to reach the flare window. Generally speaking, a bandwidth of around .3 rad/s is considered marginal. It is important to add that the bandwidth could be increased by pilot lead but only at the cost of added workload.

If the CTOL piloting technique is used for the baseline case, a difficult situation arises. The bandwidth without speed control is relatively high. However, there is no dc gain. Thus the flight path change that takes place initially soon washes out due to a change in airspeed. If the pilot tries to reduce the speed variation by closing a loop through the throttle an instability will result. The primary cause of such difficulties is the inability of the near vertical thrust vector to influence the horizontal velocity.

Coupling of airspeed and flight path for the baseline case is indicated by the μ^{STOL} parameter evaluated at steady state ($\omega = 0$) and at a point in the vicinity of tight glide slope tracking ($\omega = .3$ rad/s). $\mu_o^{STOL} = .86$

indicates that trimming can fairly easily be accomplished with a STOL technique. However, the $\mu_{.3}^{STOL} = 1.68$ indicates coupling problems while tightly tracking the glide slope. This value for $\mu_{.3}^{STOL}$ indicates that both the throttle and attitude controls have the same relative effect on glide slope and airspeed, adding power or raising the nose causes the airplane to initially go up and slow down. Thus, we could expect difficulties in correcting a high-fast or low-slow condition.

b. Approach Speed Variation

Decreasing approach speed, according to Table B-3, does little to STOL flight path sensitivity, control power, or bandwidth. (We have already seen that use of a CTOL technique with thrust control is impractical.) The coupling characteristics, however, do change. μ_{o}^{STOL} becomes smaller and $\mu_{.3}^{STOL}$ slightly greater. Thus coupling in trimming and tracking are not only worse in an absolute sense, but the relative difference between trimming and tight tracking is greater.

As approach speed is increased the bandwidth is slightly improved if airspeed is regulated. Beyond 70 kt coupling is greater than one at $\omega = 0$ as well as $\omega = .3$, thus while coupling is unfavorable at both points (> 1), the nature of the coupling is the same.

c. Complementary Control Variation

If the vertical thrust control is replaced by a horizontal one (i.e., nozzle or DDC) then a CTOL piloting technique is possible. However, whether a STOL or CTOL technique is used, the speed must be regulated. The coupling parameter μ_{o}^{STOL} indicates that trimming still requires a STOL technique. In the tight tracking range $\mu_{.3}^{STOL} \doteq .5$ means that either technique can be used equally well. The preferred technique would probably be CTOL because of the direct effect of the horizontal control on airspeed.

Changes in engine response affect only the bandwidth. The longer engine lags of 2.5 to 3 s degrade the bandwidth to around .2 rad/s. DLC should be recognized as equivalent to an improvement in engine lag with improvements in bandwidth to around .5 rad/s. The bandwidth change due to speed regulation is affected by engine lag. For short lags a speed loop improves bandwidth

by as much as .1 rad/s while for the very long lags a speed loop actually degrades bandwidth.

d. Wind Variations

Winds appear to be largely equivalent to changing approach speed since only the coupling is affected. A 10 kt headwind is about the same as increasing approach speed 5 kt. Likewise, a 10 kt tailwind is equivalent to a 5 kt lower approach speed except that $\mu_{.3}^{STOL}$ is even worse.

APPENDIX C

ANALYSIS OF THE FLARE AND LANDING

The object of this appendix is to describe an approach for analyzing the flare in general, and then to apply it to the AWJSRA simulation in particular. This should provide background for the analysis of simulator results given in Section IV.

1. FLARE MODEL STRUCTURE

The flare maneuver can be approximated as a closed loop control phenomenon. The following block diagram illustrates the essential loop structure.

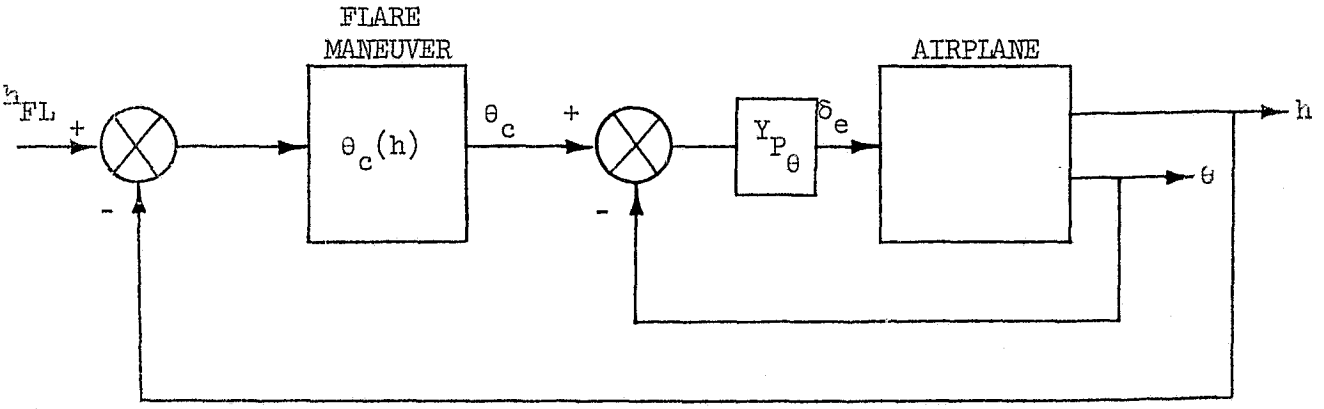

In simple terms, the pilot provides an attitude command that is a function of altitude. This function, whatever it is, we shall call the flare maneuver. If we make certain assumptions concerning this flare maneuver and the airplane, the problem can be described in terms of a linear feedback control system and analyzed as such. The following paragraphs set forth this way of describing and analyzing the flare and landing.

The linear flare and landing block diagram is shown below for the typical situation in which attitude control has a much greater bandwidth than the flight path response:

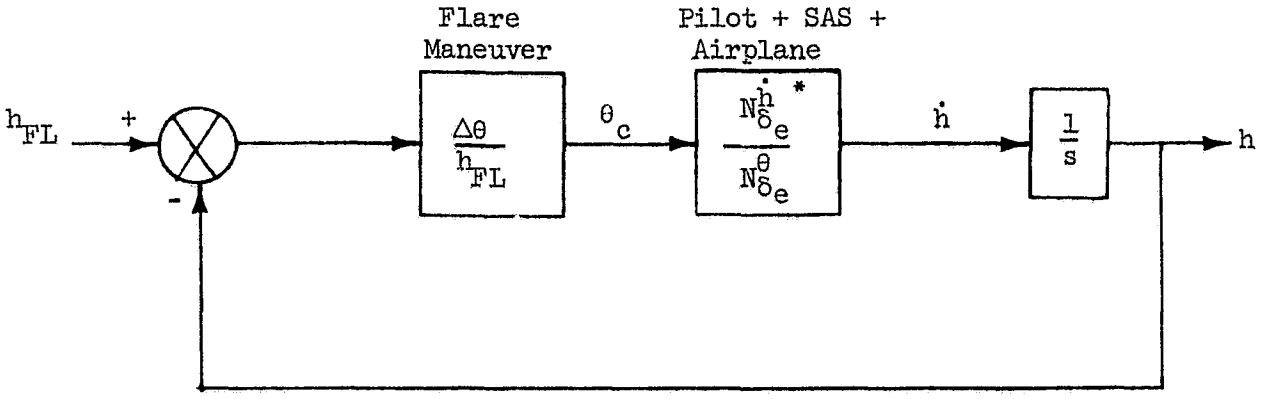

With initial conditions $h = h_{FL}$, $\dot{h} = \dot{h}_o$, and $\theta = \theta_o$ the pilot begins his flare by pitching the airplane proportionally to decreasing altitude until, at touchdown, $\theta = \theta_o + \Delta\theta$. Thus the flare maneuver could be shown by the following sketch:

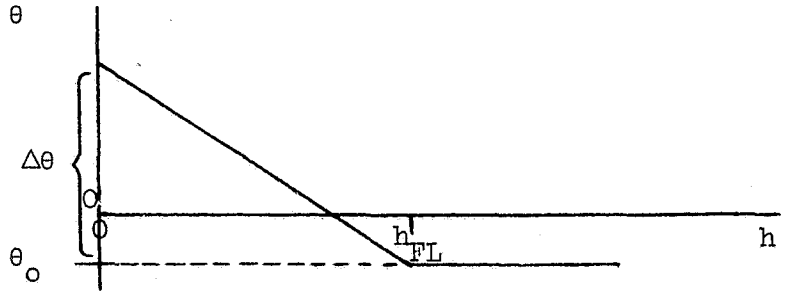

This model of the flare maneuver is based largely on observation of both simulator and actual flight results. Samples of θ versus h during flare are shown in Figure C-1. These are highly representative of calm air flares after an adequate period of learning to fly and land the airplane in a normal manner.

On the question of the use of linear equations of motion we can ultimately rely only on direct comparison with a solution using the full blown non-linear aerodynamics. But in general, as long as angle of attack and speed changes are reasonably small a linear solution is valid. We shall see that one of the qualities of an acceptable flare is to stay in what amounts to a linear aerodynamics range.

---

* The airplane dynamics are linearized about the approach speed and flight path angle.

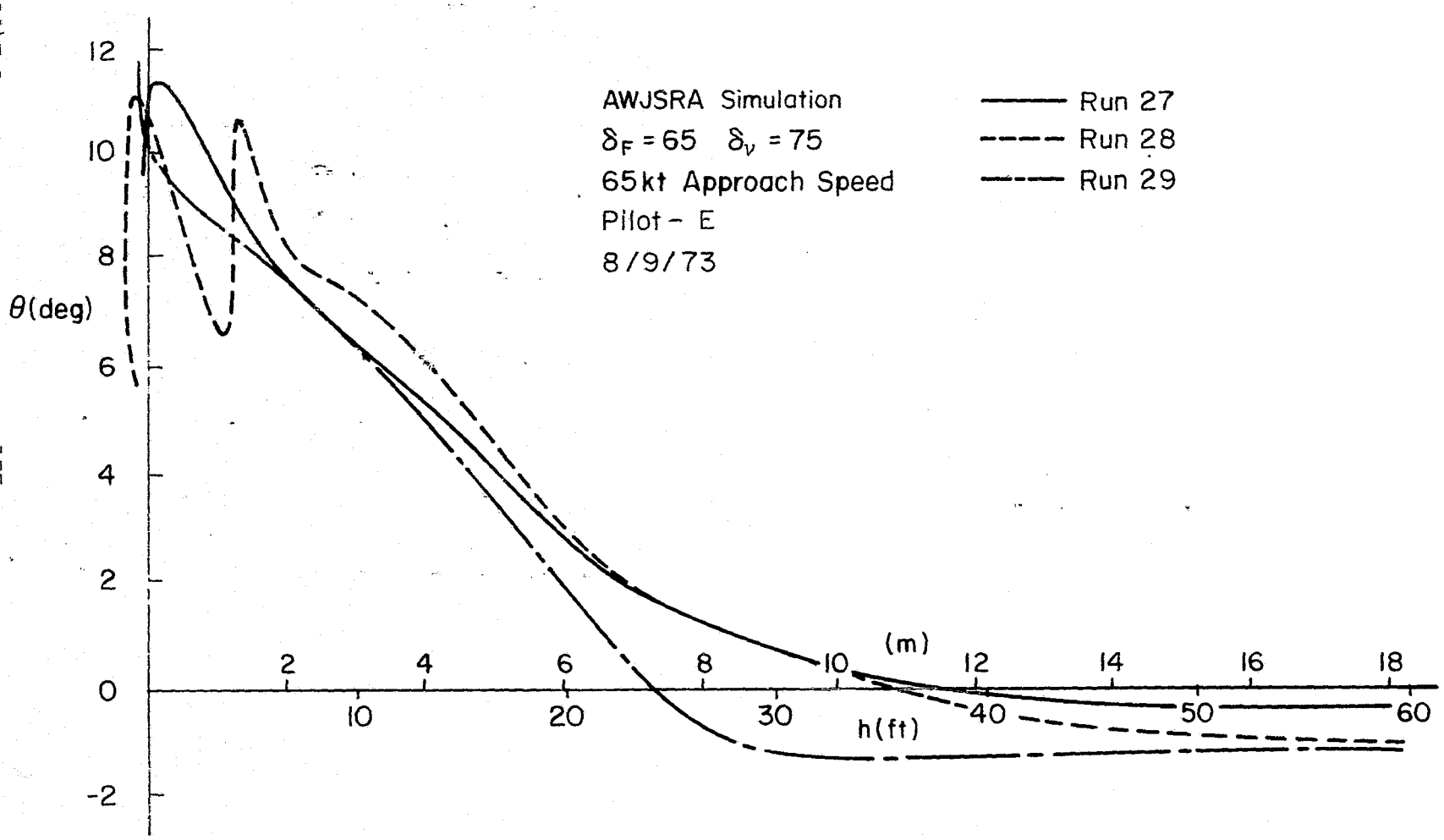

Figure C-1. Typical Flare Profiles – Calm Air

Referring back to the linear block diagram we see that the parameters describing the flare consist of:

- Gain, $\frac{\Delta\theta}{h_{FL}}$
- Amplitude, h_{FL} (or $\Delta\theta$)

The values of these parameters are set by the pilot during his learning phase for a particular airplane and flight condition. This was observed directly in simulator training sessions prior to formal testing. In fact, one strong indicator of learning level for the landing was the consistency in θ versus h profiles. The possible factors which combine to set these flare parameters for the pilot are discussed shortly.

2. DYNAMICS OF THE FLARE

Starting with the simple block diagram shown previously, we can procede to express the fundamental relationships involved in the flare. These relationships consist of the closed loop response of sink rate, angle of attack, airspeed, and position along the runway. These are all described as closed loop time responses below.

From the block diagram, the closed-loop characteristic equation can be seen to be

$$0 = \Delta_{CL} = s\, N^{\theta}_{\delta_e} + \frac{\Delta\theta}{h_{FL}}\, N^{\dot{h}}_{\delta_e}$$

Simplifying this by eliminating all high frequency roots (> short period)

$$\Delta_{CL} \doteq s\left(s + \frac{1}{T_{\theta_1}}\right)\left(s + \frac{1}{T_{\theta_2}}\right) - \frac{\Delta\theta}{h_{FL}}\, Z_{\alpha}\left(s + \frac{1}{T_{h_1}}\right)$$

$$= \left(\frac{1}{T_{FL}}\right)\left[\zeta_{FL},\ \omega_{FL}\right]$$

where

$$\frac{1}{T_{FL}} \doteq \frac{-\frac{\Delta\theta}{h_{FL}} Z_\alpha}{\frac{1}{T_{\theta_1}}\frac{1}{T_{\theta_2}} - \frac{\Delta\theta}{h_{FL}} Z_\alpha} \cdot \frac{1}{T_{h_1}} \doteq \frac{1}{T_{h_1}}$$

$$\omega_{FL}^2 \doteq -\frac{\Delta\theta}{h_{FL}} Z_\alpha + \frac{1}{T_{\theta_1}} \cdot \frac{1}{T_{\theta_2}}$$

and

$$2\zeta_{FL}\omega_{FL} = \frac{1}{T_{\theta_1}} + \frac{1}{T_{\theta_2}} - \frac{1}{T_{FL}}$$

In physical terms the mode at $\frac{1}{T_{FL}}$ corresponds to the flight path divergence (if negative) associated with the backside of the $\dot{h}$ versus V curve. Since this is usually a long time constant compared with the duration of the flare it can be considered zero. The oscillatory mode represents the dominant flight path change. The frequency, ω_{FL}, describes the abruptness of flare and the damping, ζ_{FL}, describes the oscillatory tendency (i.e. ballooning).

The motion quantities themselves can be easily expressed in terms of their closed loop time response. In fact the touchdown conditions themselves can be so expressed. Flare height can be found from:

$$h_{FL} = \mathcal{L}^{-1} \frac{-\dot{h}_o N_{\delta_e}^{\theta}}{s\left(s N_{\delta_e}^{\theta} + \frac{\Delta\theta}{h_{FL}} N_{\delta_e}^{\dot{h}}\right)} \qquad \text{at } t = t_{TD}$$

$$= \mathcal{L}^{-1} \frac{-\dot{h}_o\left(\frac{1}{T_{\theta_1}}\right)\left(\frac{1}{T_{\theta_2}}\right)}{(0)\left(\frac{1}{T_{FL}}\right)[\zeta_{FL},\ \omega_{FL}]} \qquad \text{at } t = t_{TD}$$

Touchdown quantities can be evaluated from:

$$\dot{h}_{TD} = \mathcal{L}^{-1} \frac{\dot{h}_o N^{\theta}_{\delta_e}}{s N^{\theta}_{\delta_e} + \frac{\Delta\theta}{h_{FL}} N^{\dot{h}}_{\delta_e}} \qquad \text{at } t = t_{TD}$$

$$= \mathcal{L}^{-1} \frac{\dot{h}_o \left(\frac{1}{T_{\theta_1}}\right)\left(\frac{1}{T_{\theta_2}}\right)}{\left(\frac{1}{T_{FL}}\right)[\zeta_{FL}, \omega_{FL}]} \qquad \text{at } t = t_{TD}$$

$$V_{TD} = V_o + \mathcal{L}^{-1} \frac{-\dot{h}_o \frac{\Delta\theta}{h_{FL}} N^{u}_{\delta_e}}{s\left(s N^{\theta}_{\delta_e} + \frac{\Delta\theta}{h_{FL}} N^{\dot{h}}_{\delta_e}\right)} \qquad \text{at } t = t_{TD}$$

$$= V_o - \mathcal{L}^{-1} \dot{h}_o \frac{\Delta\theta}{h_{FL}} \left\{X_\alpha - g \cos\gamma_o\right\} \frac{\left(\frac{1}{T_{u_1}}\right)}{(0)\left(\frac{1}{T_{FL}}\right)[\zeta_{FL}, \omega_{FL}]} \qquad \text{at } t = t_{TD}$$

$$\alpha_{TD} = \alpha_o + \mathcal{L}^{-1} \frac{-\dot{h}_o \frac{\Delta\theta}{h_{FL}} N^{\alpha}_{\delta_e}}{s\left(s N^{\theta}_{\delta_e} + \frac{\Delta\theta}{h_{FL}} N^{\dot{h}}_{\delta_e}\right)} \qquad \text{at } t = t_{TD}$$

$$= \alpha_o - \mathcal{L}^{-1} \dot{h}_o \frac{\Delta\theta}{h_{FL}} \frac{[\zeta_w, \omega_w]}{(0)\left(\frac{1}{T_{FL}}\right)[\zeta_{FL}, \omega_{FL}]} \qquad \text{at } t = t_{TD}$$

$$x_{TD} = C + \frac{V_o}{\sin\gamma_o} \mathcal{L}^{-1} \frac{\dot{h}_o \frac{\Delta\theta}{h_{FL}} N^{\gamma}_{\delta_e}}{s^2\left(s N^{\theta}_{\delta_e} + \frac{\Delta\theta}{h_{FL}} N^{\dot{h}}_{\delta_e}\right)} \qquad \text{at } t = t_{TD}$$

$$= C + V_o \frac{\Delta\theta}{h_{FL}} \left\{ - Z_\alpha + g \sin \gamma_o \right\} \mathcal{L}^{-1} \frac{\left(\frac{1}{T_{\gamma_1}}\right)}{(0)^2 \left(\frac{1}{T_{FL}}\right) [\zeta_{FL}, \omega_{FL}]} \quad \text{at } t = t_{TD}$$

where C = constant equal to touchdown x without a flare

An example application of the above is shown in Figure C-2. A family of touchdown conditions is shown for a typical flare gain of $\frac{\theta}{h_{FL}} = .005$ rad/ft. However, instead of plotting the variables versus t_{TD} they are plotted versus h_{FL} to avoid the less important time aspect.* The main Features of Figure C-2 are the following:

- Flare below a certain h_{FL} results in a hard landing.
- If the h_{FL} is too high, an overshoot tendency exists with a larger and rapidly building angle of attack. This is also the point at which speed rapidly bleeds off.
- The allowable range of h_{FL} to meet given $\dot{h}_{TD}$ and x_{TD} constraints can be readily evaluated.

A second variable is added in Figure C-3. Here we see the effect of both gain, $\frac{\Delta\theta}{h_{FL}}$, and amplitude, h_{FL}. This illustrates the strong effect of high gain on floating and ballooning if the flare is a little too high. On the other hand, too low a gain results in hard landings unless the flare is started quite high.

The goodness of the simple linear analysis is shown in Figure C-4. Here the $\frac{\Delta\theta}{h_{FL}} = .005$ case is compared to the conditions calculated, using the actual simulator model with an analog pilot performing the nominal flare maneuver. The comparison is good up to the point of floating which is adequate for the purposes of our analysis.

3. PILOT ADJUSTMENT OF FLARE PARAMETERS

The ideas presented to this point allow us to now describe the pilot's rationale in choosing his flare parameters (gain and amplitude). This will

---

* These curves can also be interpreted as the trajectory starting at the flare height and continuing to the ground. For example, $\dot{h}_{TD}$ vs h_{FL} is also $\dot{h}$ vs $h_{FL} - h$.

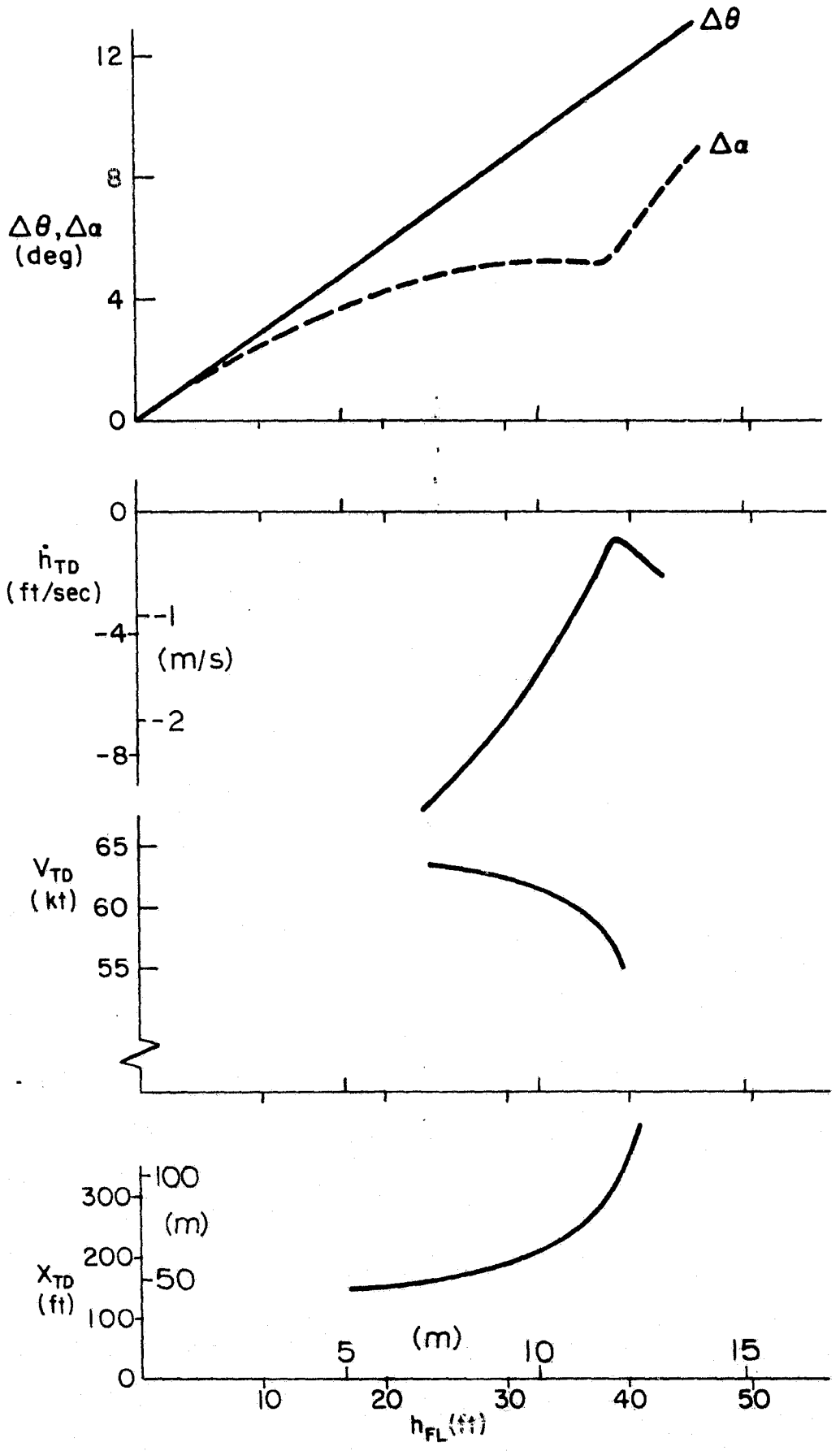

Figure C-2. Landing Conditions vs. Flare Height; $\Delta\theta/h_{FL}$ = .005 rad/ft

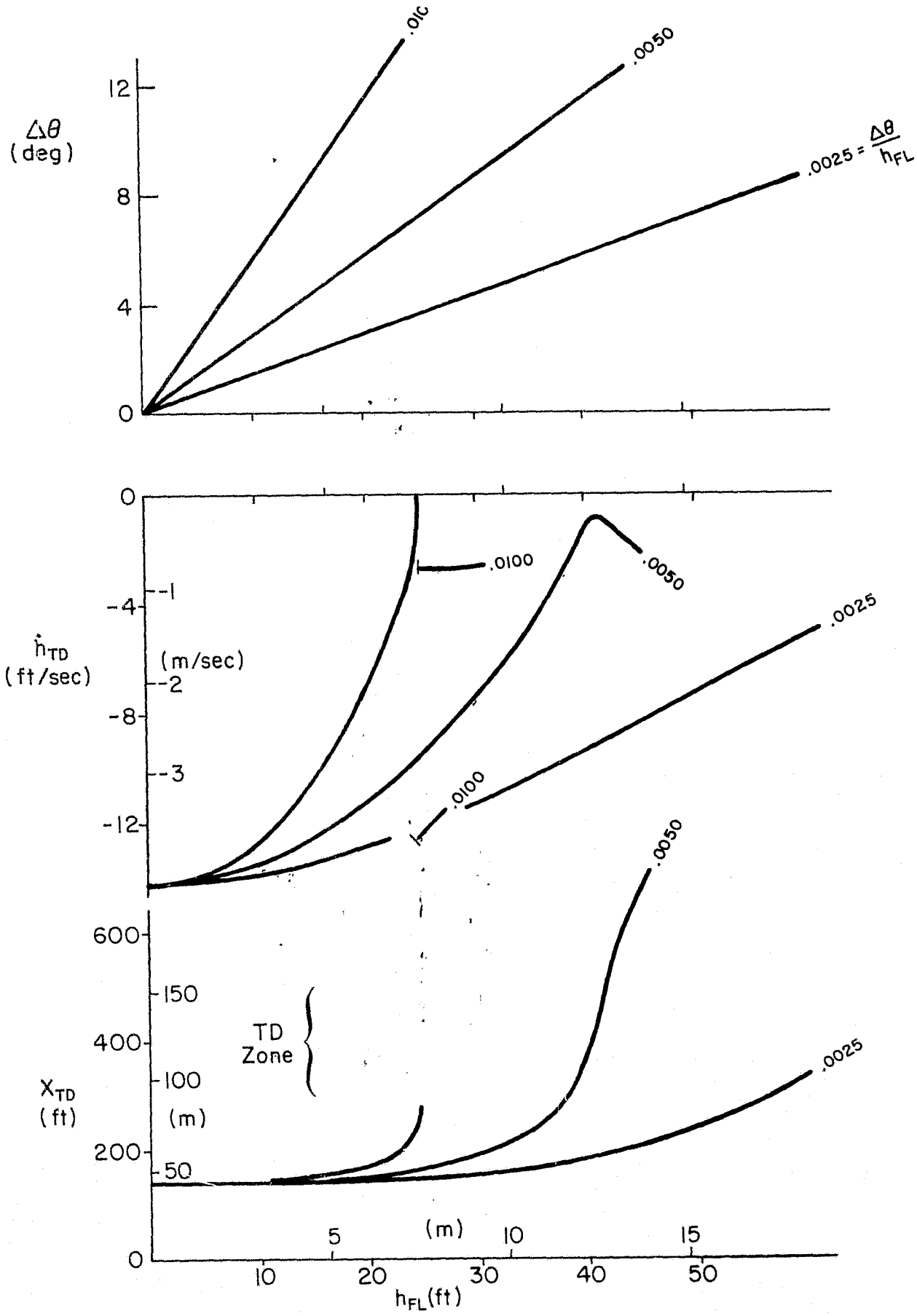

Figure C-3. Linear Flare Solution for Varying h_{FL} and $\Delta\theta/h_{FL}$

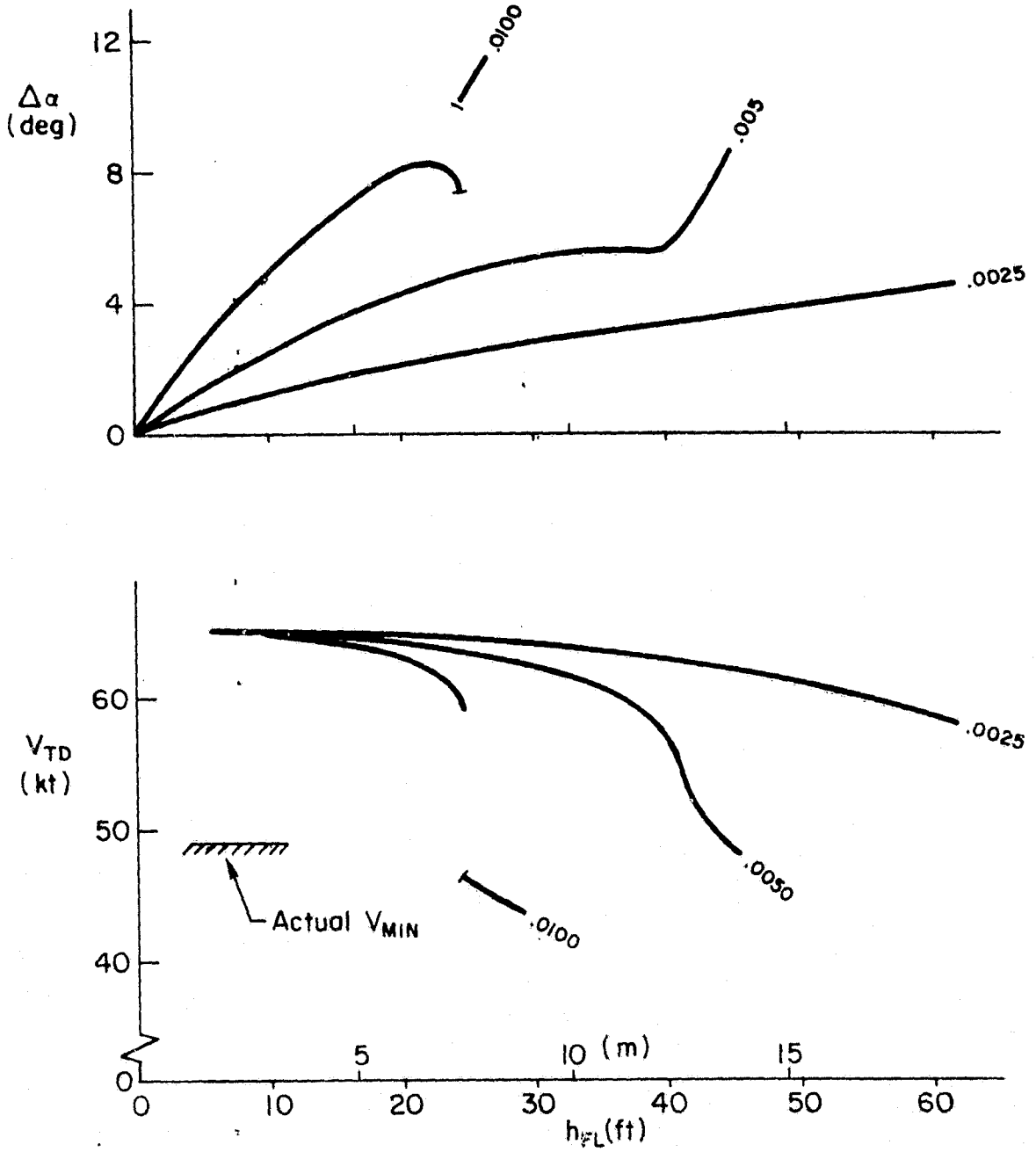

Figure C-3. (Concluded)

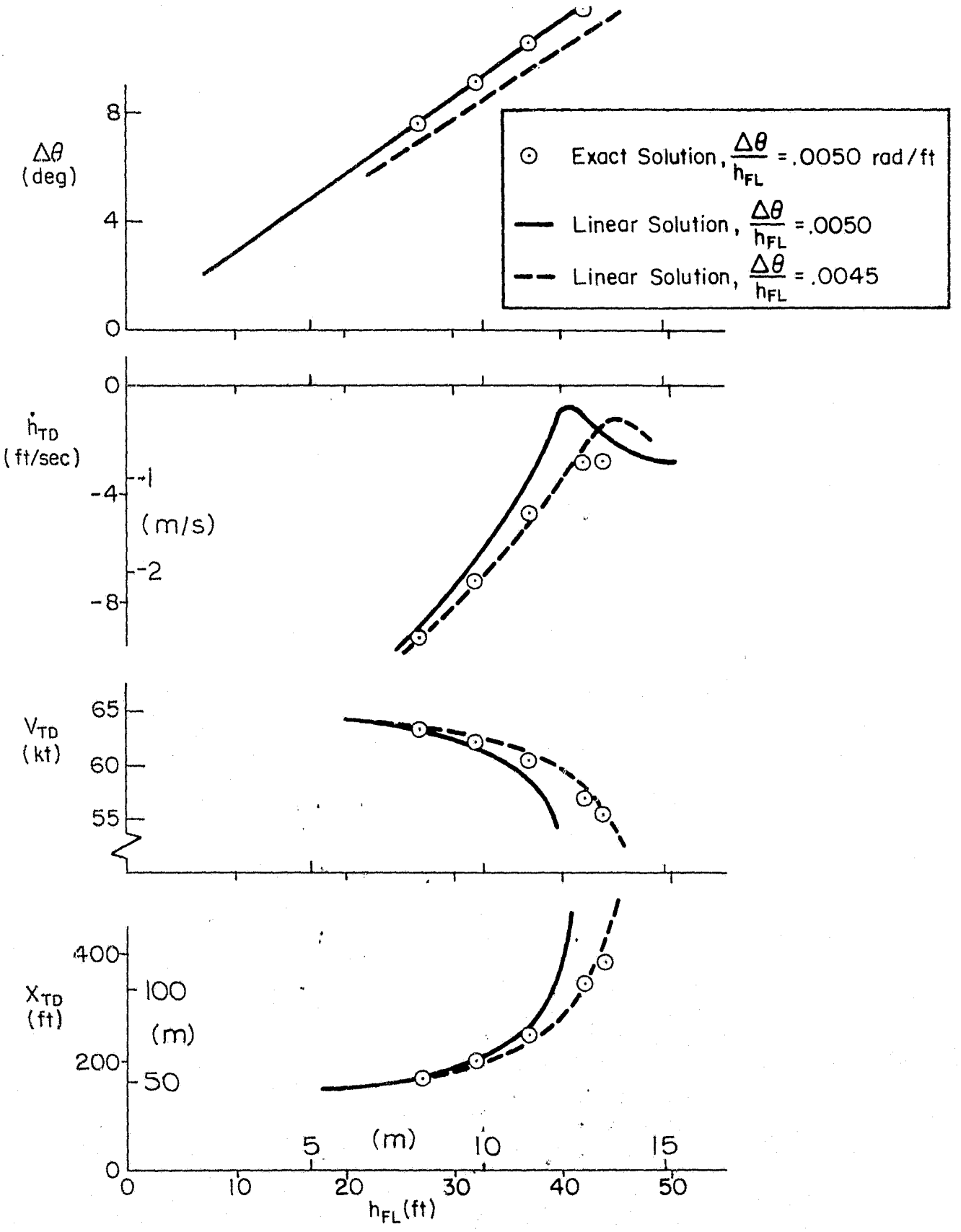

Figure C-4. Comparison of Linear Analysis to Exact

in turn set the stage for setting forth criteria by which to judge the acceptability of flare characteristics for a particular airplane and flight condition.

The upper limit of usable flare gains is set by the tendency to float if flared just a little too high or to hit hard if flared a little too low. Stated another way, only a relatively small range of flare altitudes result in an acceptable landing if the gain is too high. Figure C-3 illustrates the sensitivity of touchdown sink rate to flare height at high gains.

On the other hand, low gains lead to unrealistic flare heights. The trick then is to find a gain that results in an acceptable touchdown sink rate over a reasonable range of flare altitudes, i.e., it is a tradeoff of sensitivities.

There are other considerations to complicate the choice of flare parameters. Visibility is an important one. Since the flare parameters $\frac{\Delta\theta}{h_{FL}}$ and h_{FL} are totally visual, heads-up relationships, the pilot must be able to judge both from flare initiation to touchdown. The most limiting factor is the nose-up attitude at which the pilot loses sight of the runway, thus losing both height and attitude cues. This is more of a problem in a simulator where there is no visibility to the side which can serve as an alternative to visibility over the nose. Therefore, a $\Delta\theta$ limit enters the flare parameter tradeoff problem.

Runway touchdown point is a highly important factor, especially with STOL aircraft. This, then, will be considered in the tradeoff leading to a choice of flare parameters. However, ballooning is almost synonymous with long landings. Thus avoidance of the former takes care of the latter. Short landings are an important limiting factor and are controlled mainly by keeping the flare height high enough.

Another constraint viewed by the pilot is the angle of attack margin from stall during his flare. This translates into how much flare control he has remaining to cope with disturbances. Specific requirements on angle of attack margin are probably difficult for the pilot to formulate without having considerable experience with a particular case involving a range of adverse factors. Other factors no doubt exist when optimizing a flare

technique. However, based on simulator observations those mentioned above are the most important ones.

Figure C-5 shows an example of the relationship of flare parameters to landing characteristics for the AWJSRA at 65 kt. The boundaries shown are defined by specific numerical values depending upon the pilot's criteria for a successful landing.

4. CRITERIA FOR GOOD LANDING CHARACTERISTICS

In light of what has been discussed above, the factors which determine an easy-to-land airplane are straight forward:

> About an easily repeated range of flare parameters, the resulting range of touchdown conditions must be acceptable.

As an example, let's say the pilot can easily start a flare at 35 ft $\pm$ 5 ft and end with an attitude excursion of 10 deg $\pm$ 2 deg time after time. If this range of flare gains and amplitude results in touchdowns within specified limits of sink rate and distance along the runway in the presence of expected disturbances then we must conclude that the airplane has good landing qualities. If, on the other hand, hard short landings or long floating landings can occur then the airplane must be judged bad.

The important point here is that the closed loop analysis of the flare as presented above describes the landing characteristics of a particular airplane and can pinpoint the qualities which make it good or bad.

5. FACTORS INVOLVED IN FLARE AND LANDING

Based on the relationships developed to describe the flare maneuver and the characteristics important to the pilot, we can set forth a summary of some of the important quantities involved. At the same time we will define some relationships which prove useful in analyzing the data obtained in the experiment.

a. Flare Gain, $\frac{\Delta\theta}{h_{FL}}$ -- the commanded attitude relative to altitude during the flare. The desired value is probably established in the pilot's

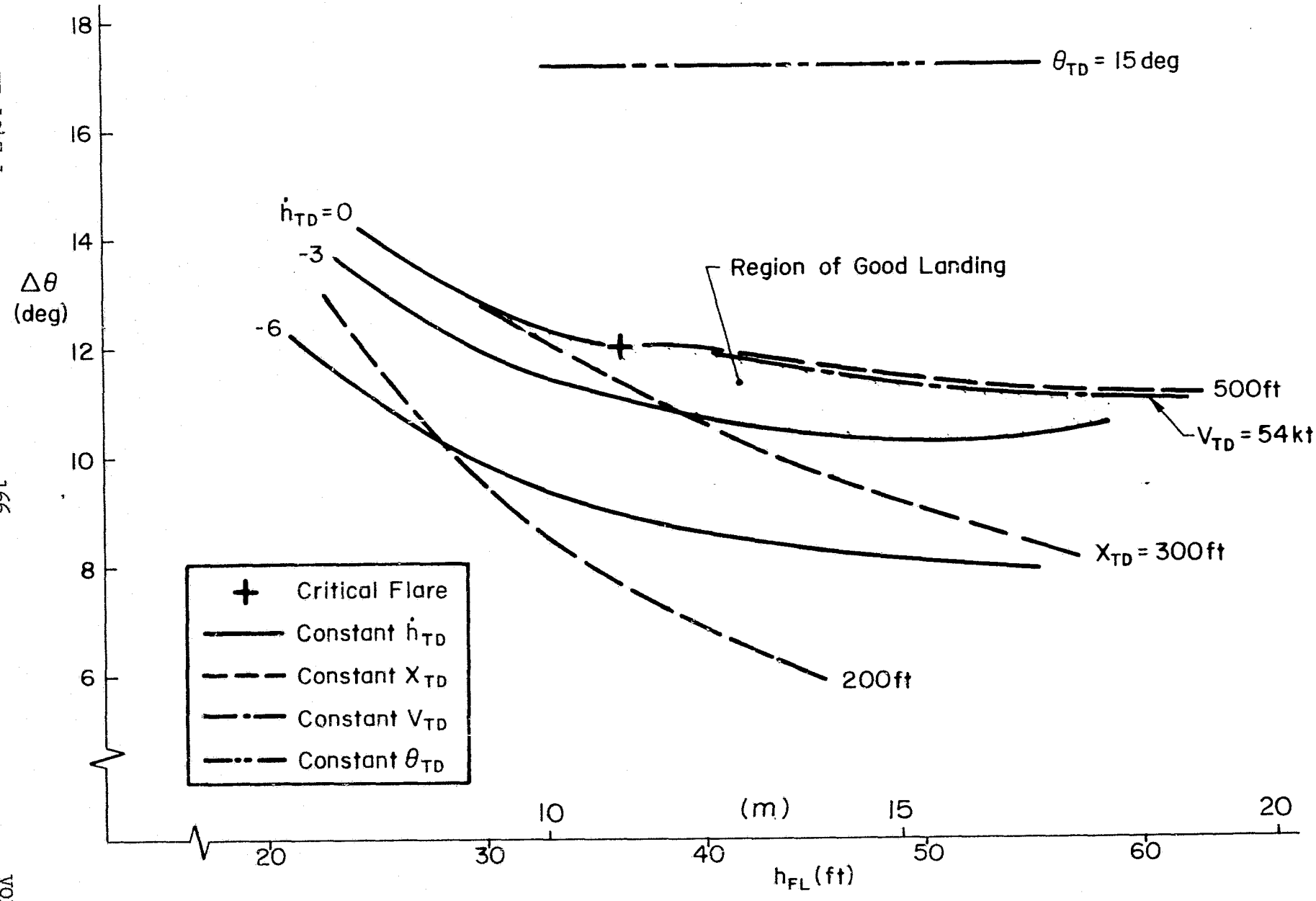

Figure C-5. Touchdown Performance Vs. Flare Parameters; V_{APP} = 65 kt

learning phase. The magnitude has a strong effect on closed loop bandwidth of the flare maneuver, i.e. how quickly disturbances may be compensated for. The parameter can be measured directly from a θ versus h history.

b. Flare Amplitude, h_{FL} -- The effective altitude at which the flare is begun. This is also determined in the pilot's learning phase. h_{FL} combined with $\frac{\Delta\theta}{h_{FL}}$ determines touchdown conditions. This parameter can also be measured directly.

c. Attitude Numerator Roots, $\frac{1}{T_{\theta_1}}$ and $\frac{1}{T_{\theta_2}}$ -- determined primarily by the 4 stability derivatives X_u, X_w, Z_u, and Z_w. The combination of these roots strongly determines the closed loop bandwidth obtainable without ballooning.

d. Sensitivity of Flight Path to Attitude, Z_α -- the product of heave damping, Z_w, and airspeed. This is the controlled element gain in the flare feedback loop.

e. Closed Loop Natural Frequency in Flare, ω_{FL} -- the result of closing the flare loop with gain $\frac{\Delta\theta}{h_{FL}}$. This indicates the abruptness of "turning the corner" during flare and is some indication of bandwidth. $\omega_{FL}^2 \doteq -\frac{\Delta\theta}{h_{FL}} Z_\alpha + \frac{1}{T_{\theta_1}} \frac{1}{T_{\theta_2}}$

f. Closed Loop Damping Ratio in Flare, ζ_{FL} -- related to the ballooning tendency. $\zeta_{FL} \doteq \frac{\frac{1}{T_{\theta_1}} + \frac{1}{T_{\theta_2}}}{2\,\omega_{FL}}$

g. Net Attitude Excursion, $\Delta\theta$ -- a measure of flare maneuver amplitude.

h. Critical Closed Loop Natural Frequency in Flare, $\omega_{FL_{crit}}$ -- determined by finding the largest $\frac{\Delta\theta}{h_{FL}}$ for which the airplane does

not quite balloon (i.e., $\dot{h}$ never becomes positive regardless of flare height). This appears to correspond closely to the actual flare maneuvers. $\omega_{FL_{crit}} \doteq \left[5 \frac{1}{T_{\theta_1}} \frac{1}{T_{\theta_2}} \left(\frac{1}{T_{\theta_1}} + \frac{1}{T_{\theta_2}} \right) \right]^{1/3}$ *

i. Critical Flare Height, $h_{FL_{crit}}$ -- the height at which the critical flare must be started and appears to correspond to measured flare heights. $h_{FL_{crit}} \doteq -\frac{\pi}{2} \frac{\dot{h}_o}{\omega_{FL_{crit}}}$

j. Critical Flare Gain, $\left. \frac{\Delta\theta}{h_{FL}} \right|_{crit}$ -- the gain used in the critical flare. $\left. \frac{\Delta\theta}{h_{FL}} \right|_{crit} \doteq \frac{\omega^2_{FL_{crit}}}{-Z_\alpha}$

6. ANALYSIS OF THE SIMULATION MODEL

The approach developed previously will now be applied to the AWJSRA model used in the experiment. The main goal will be to show the general relations between the flare maneuver and the resulting touchdown performance. In particular we will illustrate the effect of approach speed and the effect of surface winds.

The 65 kt baseline case was described previously in Figure C-5. There we saw that for various specified touchdown conditions we could plot the flare required in terms of $\Delta\theta$ and h_{FL}. The regions of particular interest are those in which the conditions prescribed by the piloting task are met. These regions must reasonably consist of:

- Sink rate at touchdown better than 6 ft/sec and, if possible, better than 3 ft/sec.
- Touchdown point inside of marked touchdown zone, 300 ft to 500 ft beyond runway threshold.

---

* This expression uses the following approximation for the overshoot of a step input to a second order system: $\frac{X_{max}}{X_{steady\ state}} = \frac{.1}{\zeta}$ This approximation gives reasonable results for $.15<\zeta<.5$.

- Airspeed at touchdown at some margin above V_{min} to allow for tailwind gusts, roughly 5 kt.
- Attitude at touchdown which allows ground visibility, roughly 15 deg for this simulation.
- Some level of dynamic stability in the basic pilot/vehicle flare feedback loop.

For the 65 kt case, Figure C-5 shows a range of flare maneuvers which could meet the requirements. The effect of reducing the approach speed by 5 kt is shown in Figure C-6. While the range of flares which meet the sink rate requirement has actually expanded slightly, we find the touchdown point is much more a problem. In fact, at this speed the airplane reaches the touchdown speed margin of 5 kt (i.e. 5 kt above V_{min} for approach power setting) at the same time it enters the touchdown zone. Noting that x_{TD} and V_{TD} track one another, Figure C-7 shows this effect of approach speed more clearly.

Since this is the product of a linear solution, the low speed margin results may not be accurate, however the trend probably remains. That is, for a relatively small change in approach speed the useable touchdown zone can change drastically. Also, we see that there can be an important relation between a particular airplane and the specific runway/glide slope geometry. For example, the runway layout used in this experiment was well suited to the AWJSRA flying a 7.5 deg glide slope at 65 kt. Desired sink rates and touchdown points were compatible. However another airplane may require a different distance between glide slope/runway intercept and the touchdown zone for the same compatibility between $\dot{h}_{TD}$ and x_{TD} (and V_{TD}).

Steady wind conditions present a different type of problem. First, a significant adjustment in flare is required for a "good" landing. Second an adjustment in approach speed is required to offset a loss in margin above V_{min}.

Figure C-8 shows a plot of touchdown performance versus flare parameters for a 10 kt tailwind at 65 kt. The main difference between this and the zero wind condition is a net shift upward of $\Delta\theta$ for the region of good

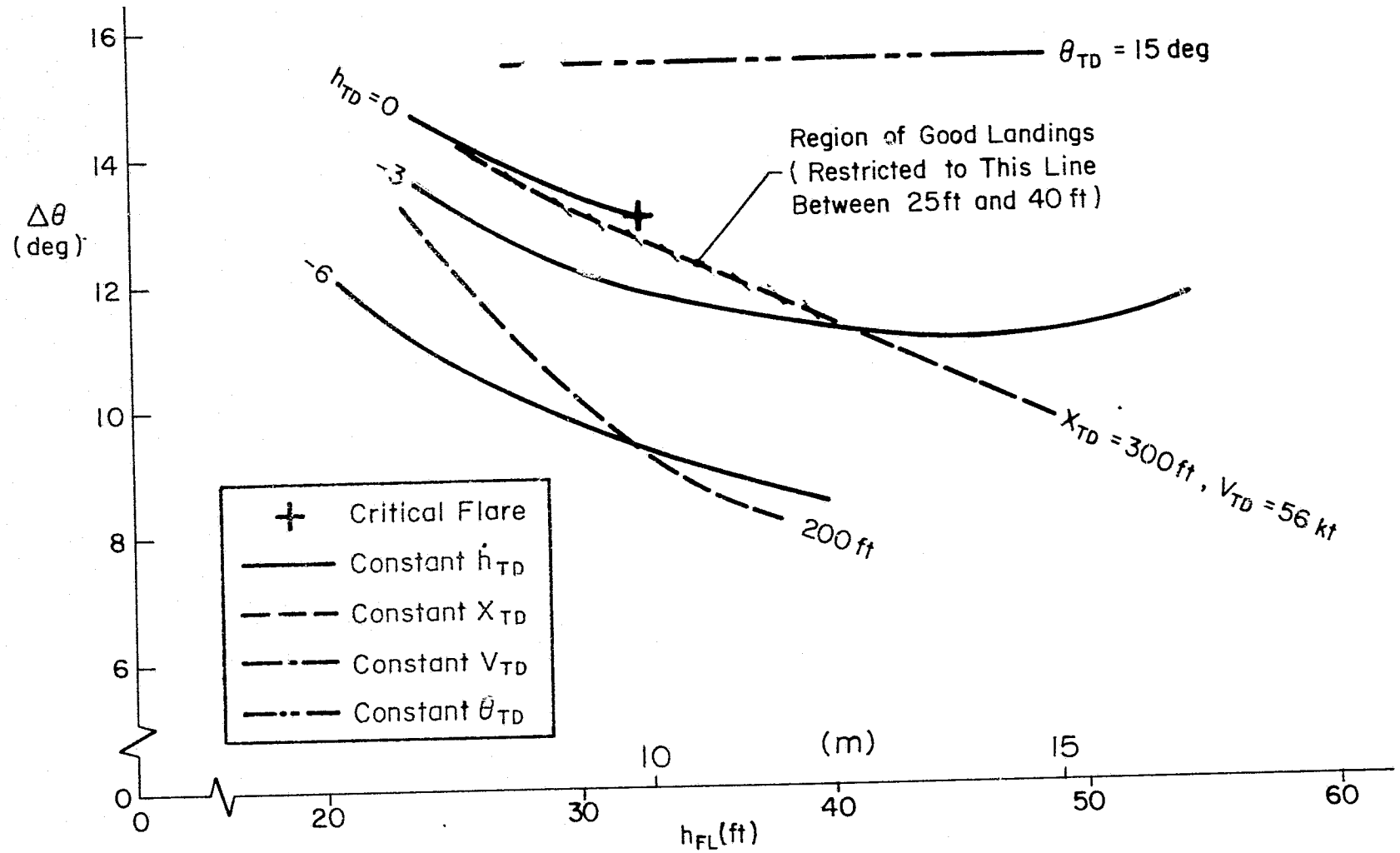

Figure C-6. Touchdown Performance Vs. Flare Parameters; V_{APP} = 60 kt

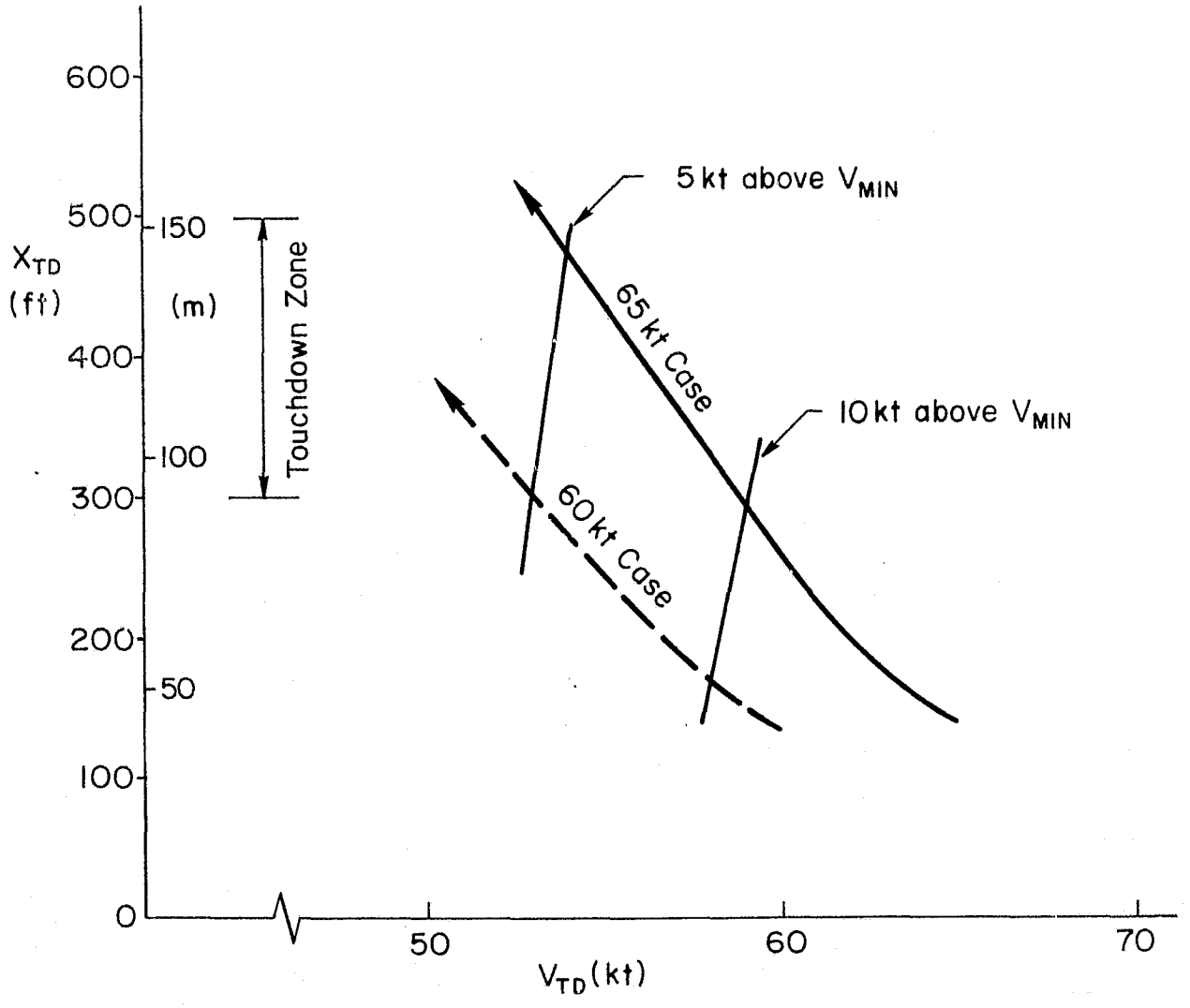

Figure C-7. Touchdown Point Vs. Touchdown Airspeed Approach Speed Effect

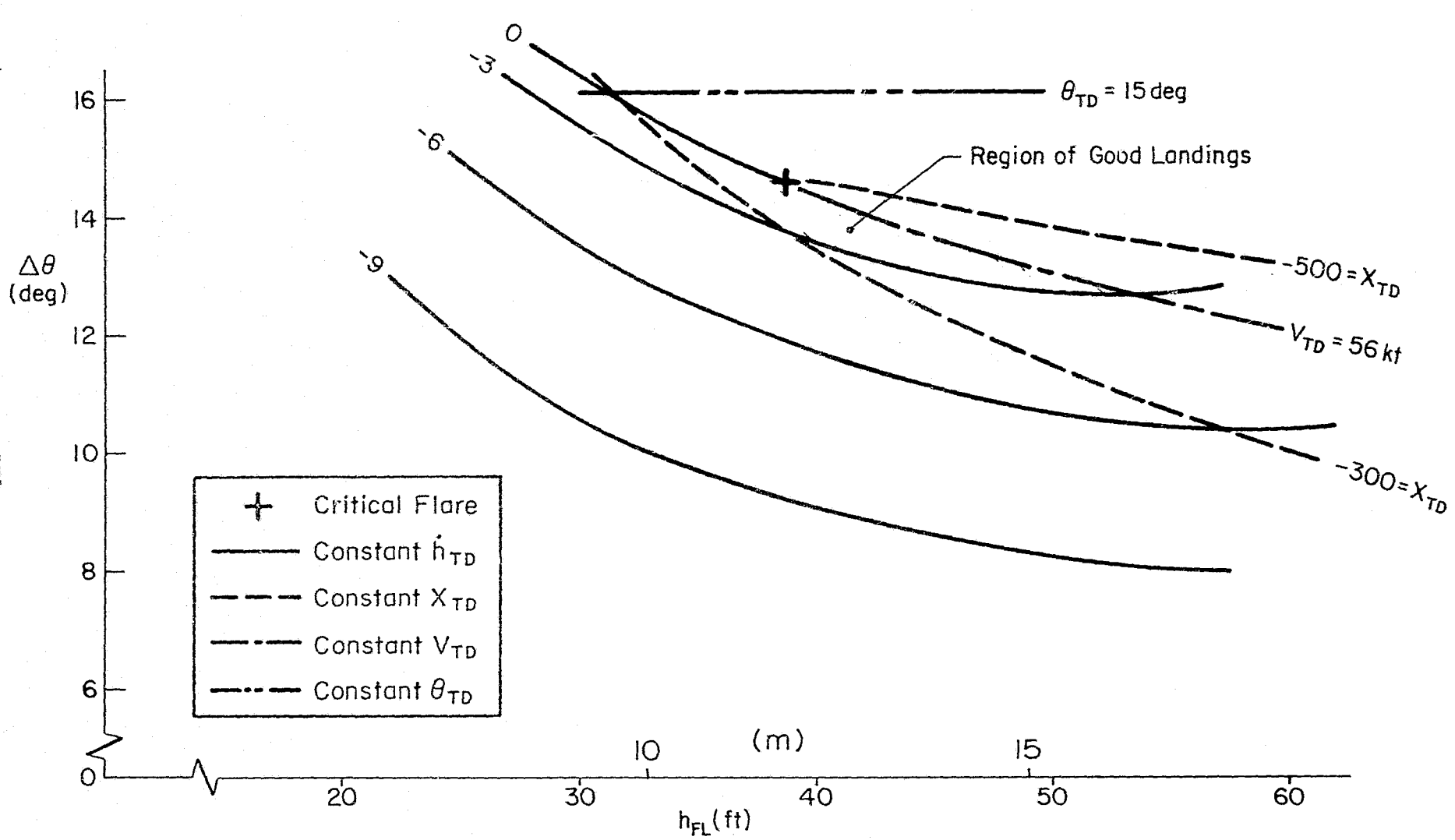

Figure C-8. Touchdown Performance Vs. Flare Parameters
V_{APP} = 65 kt with 10 kt Tailwind

landings. This amounts to 3 deg in $\Delta\theta$ and 4 deg in terms of θ_{TD}. As Figure C-8 shows, this difference could account for a significant difference in both $\dot{h}_{TD}$ and x_{TD}. Also, the same 5 kt margin above V_{min} (for approach power) is encountered earlier in the touchdown zone.

In view of the approach speed effect shown earlier, it appears that the tailwind effect on speed margin and touchdown attitude could be countered by an increase in V_{APP}. Then the end of the touchdown zone could be reached without airspeed becoming too low and touchdown attitudes would be more reasonable.

APPENDIX D

MATHEMATICAL MODEL

This appendix in combination with Reference 2 describes the mathematical model used in this simulation.

The basic AWJSRA simulation model is described in Reference 2. The changes made to the basic model include:

- Minor alteration of the engine model
- Addition of a turbulence model
- Modification of the ground effect model
- Modification of the landing gear model
- Addition of a longitudinal SAS, automatic speed control (configuration SAS), and an approach flight director
- Addition of a direct lift or direct drag control.

These changes are discussed in the following pages.

1. ENGINE MODEL CHANGES

The engine model was altered to allow a variation in thrust response time as required by the experiment and to remove non-linearities in cold thrust which seemed to present unnecessary control problems.

The thrust response was controlled by τ_2 (see Reference 2) for engine acceleration and τ_3 for deceleration. These were simply reset to the desired engine lag.

Two 230 lb cold thrust steps occurred in a normal throttle operating range for this experiment (90.6% N_H and 91.8%). Because these had the effect of sharply increasing throttle sensitivity in this range they were simply deleted. The resulting overall performance change was negligible.

2. TURBULENCE MODEL

The turbulence model used during these tests was designed to generate the spectra given by the Dryden form of the continuous random gust model given in Section 3.7.2.1 and 3.7.5 of Reference 4. Wideband Gaussian noise sequences, generated internally in the program were filtered to produce the required spectra. The spectra are functions of the scale lengths L_w, L_u, and L_v defined in Table D-1.

During the tests, the nominal turbulence level was set such that the standard deviation of the u gusts (σ_{u_g}) was 4.5 ft/sec. Figure D-1 indicates the probability of exceeding a given σ_{u_g} turbulence level on an average day as a function of σ_{u_g} ($\sigma_{u_g} \geq 4.5$ ft/sec 10% of the time). A sample time history of the turbulence is shown in Figure D-2.

3. GROUND EFFECT

The ground effect on the basic wing body aerodynamic force and moment coefficients (described in Reference 2) was not used during the simulation. A simplified ground effect model expressed as:

$$\Delta C_{L_{GE}} = K_L \, C_{L_{WB}} \, e^{-h/h_1}$$

$$\Delta C_{D_{GE}} = K_D \, C_{L_{WB}} \, e^{-h/h_1}$$

was used to provide ground effects where K_L, K_D, and h_1 are constants and are chosen to provide possible variations in lift and drag. This exponential model was used only for ground effect tests. During all other runs, K_L and K_D were zero.

4. LANDING GEAR

The landing gear model of Reference 2 was replaced by that of Reference 3. This allowed a reasonable level of pilot abuse at touchdown, mainly that connected with side loads on the landing gear.

TABLE D-1

TURBULENCE PARAMETERS

I	$100 < h < 1750$	$L_w = h$ $L_v = L_u = 145\ (h)^{1/3}$ ft
II	$h \leq 100$	$L_w = 100$ ft $L_u = L_v = 671.35$ ft

Note: For all conditions $\sigma_{u_g} = \sigma_{v_g}$ and $\sigma_{w_g} = \sigma_{u_g} \sqrt{\frac{L_w}{L_u}}$

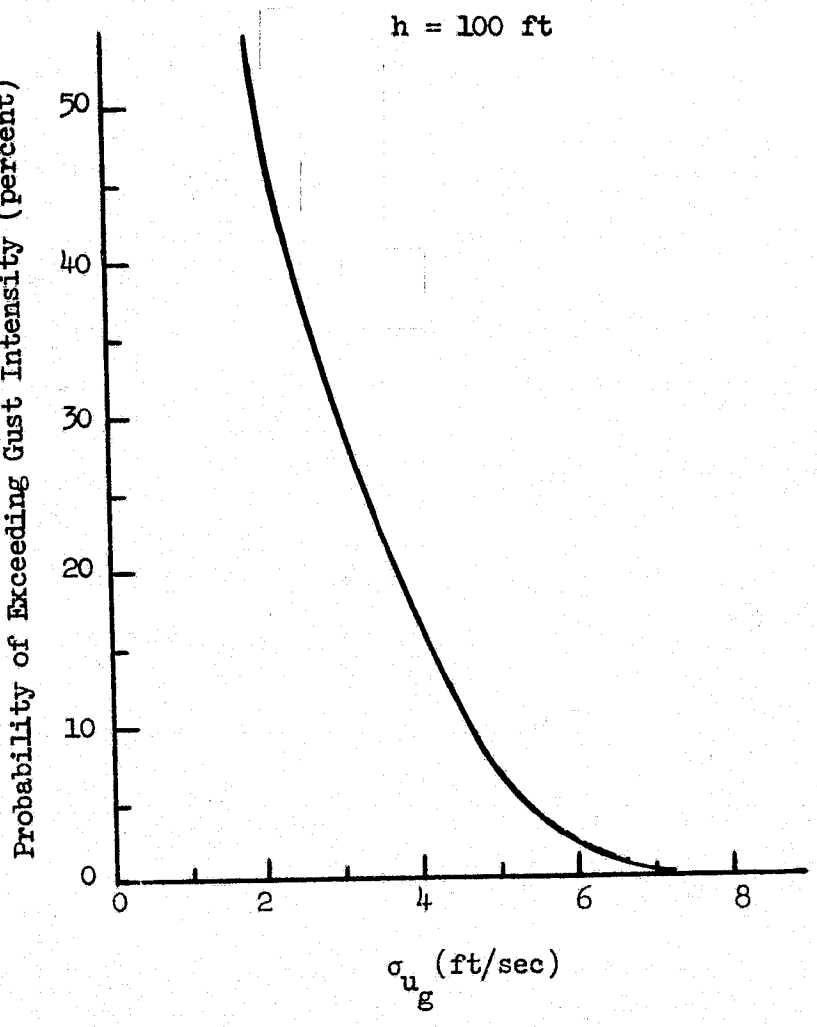

Figure D-1 . Turbulence Distribution

Notes:
1. $\sigma_u = \sigma_v$ Nominal Value = 4.5 ft/sec

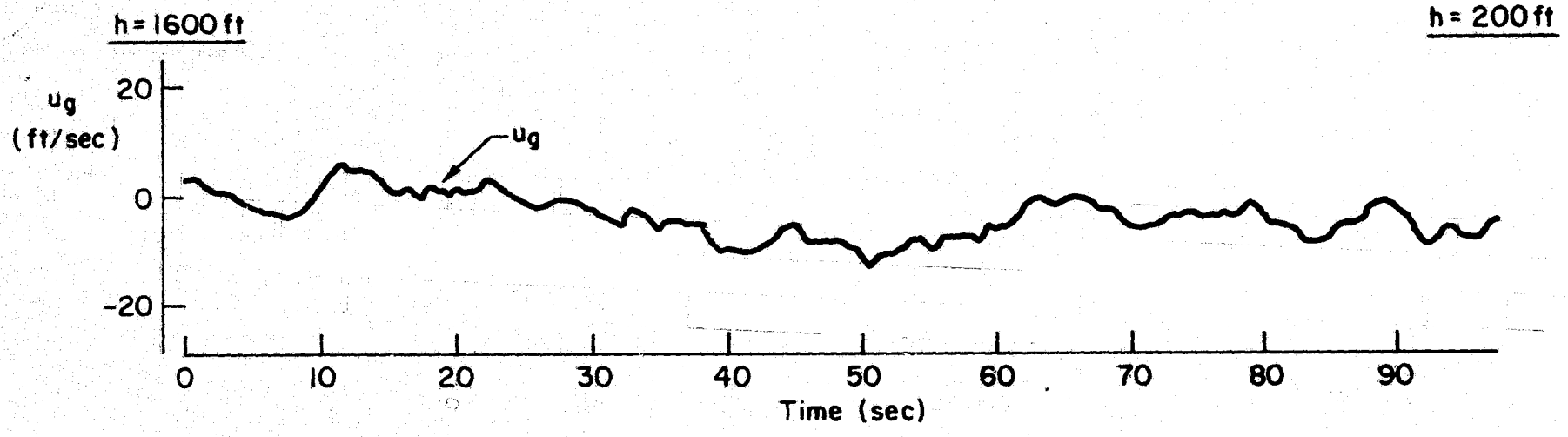

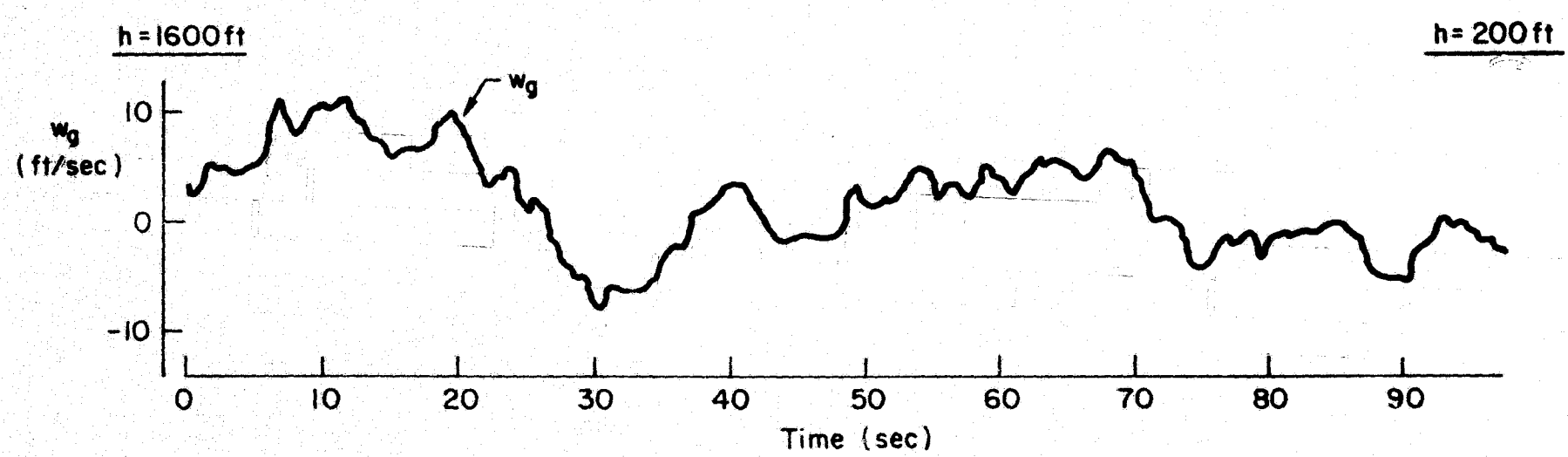

Figure D-2. Typical Turbulence Time History

A minor change was made in brake pedal scaling. Brakes began operating at 20% pedal deflection, increasing linearly to maximum at 67.5% deflection.

5. LONGITUDINAL CONTROL SYSTEM

The longitudinal control system was modified to accommodate an attitude command/attitude hold augmentation system. Also, for some limited testing a configuration SAS (automatic flap and nozzle positioning with desired speed) and a flight director were added.

The longitudinal SAS is described in Figure D-3. It is similar to the one used in the deflected slipstream STOL tests of Reference 1. Also, the feel system was modified to give a linear force gradient of 5 lb/in with 2 lb breakout force.

The configuration SAS and flight director are described in detail in Reference 7.

6. DIRECT LIFT/DRAG CONTROL

An additional complementary control was added to allow for certain idealized alternatives for the normal throttle or nozzle control. This additional control consisted of the speedbrake lever on the center console commanding a linear function of lift or drag about a neutral operating point. The commanded increment of ΔC_L or ΔC_D was simply added to the C_L and C_D of the basic aerodynamic model.

EDCOL = 4.0 deg/in
T_{COL} = .05 sec
K_{COL} = -100 ft/sec
K_c = 1.5 deg/deg
q_o = 12.2 lb/ft^2
$T_{E_{SAS}}$ = .05 sec
GDF11 = -1.5
W_{WO} = .001 rad/sec
K_{QB} = -.75 deg/deg/sec
K_{THET} = -1.5 deg/deg

Figure D-3

LONGITUDINAL ATTITUDE COMMAND SAS

APPENDIX E

SUMMARY OF PILOT COMMENTS

At the end of each series of runs, the pilot submitted a written commentary of his reaction to the ILS tracking and flare and landing tasks flown (see Section II-B). This appendix is a summarized list of these comments. Table E-1 pertains to the ILS tracking task and Table E-2, to the flare and landing task. Emphasis was given to defining the problem areas noted by each pilot and to retaining each pilot's exact words and phrasings where possible. The comments are arranged in alphabetical order by pilots and chronological order by cases flown by each pilot. A dash for the pilot rating indicates that the particular configuration was not tested.

TABLE E-1

SUMMARY OF PILOT COMMENTS ON IIS TRACKING

PILOT	DATE	CASE	COMMENTS
A	8-1-73	65 kt	1. No problem in smooth air. 2. Turbulence increased G/S workload considerably and IAS workload slightly. 3. Raw G/S used in preference to VASI because former gave earlier info [rate information]. 4. Localizer task no problem if attention given but longitudinal workload resulted in localizer being ignored for long periods--thus heading errors. This resulted in oscillating localizer tendency because of high turn rate to bank angle sensitivity. 5. Lags in power response were of no concern since corrections made slowly. 6. Positive thrust ⟶ loss of IAS relation did not cause undue problems or workload at the magnitude experienced.
		Pilot Ratings Calm Air: 3 Turbulence: 5 Turbulence/Shears: 4.5-5	
	8-2-73	65 kt 1.5 sec T_{ENG}	1. Increased lag not detected. Differences in ratings from baseline case should not be considered significant and are probably due to factors other than increased lag (e.g. learning).
		Pilot Ratings Calm Air: 2.5 Turbulence: 5 Turbulence/Shears: 6.5	
	8-2-73	55 kt	1. Larger thrust changes required for G/S errors. There was reluctance to make these changes so G/S tracking was poor. 2. Thrust effect on IAS more noticeable. Large $\Delta\theta$ (thus forces and retrimming) required to hold IAS. Result: sloppy IAS control. Sense of the thrust ⟶ θ effect caused confusion and had to be thought out consciously. This magnitude of effect is unacceptable.
		Pilot Ratings Calm Air: 4.5 Turbulence: 7.5 Turbulence/Shears: --	

TABLE E-1 (Continued)

PILOT	DATE	CASE	COMMENTS
A (Cont.)	8-2-73 (Cont.)	55 kt (Cont.)	3. High workload in pitch resulted in poor scan of heading and localizer with result of small bank errors rapidly producing large heading errors. A good flight director and/or lateral attitude stabilization could resolve this.
	8-3-73	75 kt	1. No problems in smooth air. 2. IAS holding thought to be more difficult in turbulence than at 65 kt and secondary effect of power more evident.
	8-3-73	65 kt G/S $\longrightarrow \delta_\nu$ IAS $\longrightarrow \theta$	1. Found to be similar to DDC case. Nozzle has little effect on G/S but immediate effect on IAS. 2. Large lag in G/S control resulting in sloppy holding. 3. Nozzle $\longrightarrow$ G/S authority low. On occasion a large power increase was used to prevent a crash into the undershoot in a shear.
	8-3-73	65 kt G/S $\longrightarrow \theta$ IAS $\longrightarrow \delta_\nu$	1. Nozzle fairly good control of IAS but large $\Delta\theta$ required for G/S control led to poor performance. The $\theta \longrightarrow$ IAS effect was countered instinctively with nozzle although IAS holding was still poor. 2. In one shear even a late power application failed to prevent a crash. 3. As with other cases, localizer suffered as a result of high longitudinal workload. Improved lateral SAS would probably improve ratings by 1.

Pilot Ratings
Calm Air: 3
Turbulence: 5.5
Turbulence/Shears: --

Pilot Ratings
Calm Air: 5
Turbulence: 6
Turbulence/Shears: 8

Pilot Ratings
Calm Air: 5
Turbulence: 6
Turbulence/Shears: 7

TABLE E-1 (Continued)

PILOT	DATE	CASE	COMMENTS
A (Cont.)	8-3-73	55 kt 50 deg δ_ν	1. Very poor visibility on approach (θ = +7 deg). 2. Very sloppy directionally with considerable adverse yaw. 3. Heave oscillation developed when correcting G/S in turbulence and shears. 4. Effect of power on IAS in wrong sense. 5. Large power changes required for G/S control.
	8-3-73	65 kt DDC IAS ⟶ DDC G/S ⟶ θ (CTOL Technique)	1. Main feature was very bad control of G/S with pitch attitude. Large $\Delta\theta$ for even small corrections to $\dot{h}$. G/S generally very sloppy. 2. Strong IAS effect from pitch control but because the sense of θ ⟶ IAS was correct and corrected with drag lever almost instinctively, the IAS holding was not too much of a problem. 3. Drag lever was good IAS control although authority [sensitivity] seemed lower than expected from initial control power measurements.
	8-3-73	65 kt DDC STOL Technique	1. This technique worse than CTOL [for this configuration]. 2. Drag lever had virtually no effect on G/S but affected speed strongly. Large pitch changes then required to hold IAS. These would, in turn, couple back to the G/S. 3. The lag in terms of G/S correction seemed enormous and a tendency toward pitch oscillation was noticed.
B	8-7-73	65 kt	1. No real problem in calm air. Good response to pitch and power. Fairly comfortable conditions. 2. Turbulence introduced additional workload requiring constant monitoring of power and IAS. 3. Tendency to get high on G/S was a constant problem in turbulence--reluctant to reduce power. No real problem, however, and improved greatly with piloting skill.

Pilot Ratings

Calm Air: 6
Turbulence: 7
} VFR Only
Turbulence/Shears: 8

Pilot Ratings

Calm Air: 3
Turbulence: 4
Turbulence/Shears: 4

TABLE E-1 (Continued)

PILOT	DATE	CASE	COMMENTS
B (Cont.)	8-10-73	65 kt SAS Off	1. Biggest problem in lateral-directional. Must stop on a heading and settle out even though it is the wrong heading. 2. Not acceptable for IFR under any conditions.
Pilot Ratings Calm Air: 3.5 Turbulence: 7 Turbulence/Shears: --			
	8-10-73	60 kt	1. Little or no problem in calm air. ILS tracking was as easy as at 65 kt. 2. G/S tracking became much more of a problem with turbulence and winds due to sluggish response to power changes and IAS fluctuation (± 8 kt). Had a tendency to track high. 3. Sometimes it flew as if there were a SAS failure. Would require very precise piloting at all times--operationally unacceptable.
Pilot Ratings Calm Air: 3 Turbulence: 6 Turbulence/Shears: 8			
	8-13-73	70 kt	1. Close to conventional aircraft except for steep approach angle.
Pilot Ratings Calm Air: 3 Turbulence: 3 Turbulence/Shears: 3.5			
	8-9-73	75 kt OEI Approach	1. Calm air G/S tracking had minor deficiencies with IAS ± 5 kt holding capability. G/S relatively easy in calm air but some problem with power change in turbulence. Tracking was mostly high since too much power had to be pulled off to recapture from above. More than adequate power available for recapture from below. G/S tracking moderately high in turbulence.
Pilot Ratings Calm Air: -- Turbulence: 4.5 Turbulence/Shears: --			

TABLE E-1 (Continued)

PILOT	DATE	CASE	COMMENTS
C	8-6-73	65 kt	1. Small power corrections led to minor IAS variations which were easily managed with θ. Larger G/S deviations and corresponding power corrections caused bothersome cross coupling.
			2. Get the feeling that thrust control is too sensitive.
			3. In turbulence the primary problem is due to above cross coupling. Expected throttle sensitivity problem did not materialize--especially if IVSI monitored during large corrections.
			4. Shears made no real difference in tracking ILS.
			5. IAS bug is quite useful. Sensitivity of ± 4 kt too much, ± 8 kt was quite sensible.
			6. No problem in trimming or tracking ILS under any condition.
			7. At no time during ILS tracking was there a feeling of having a safety margin problem.
	8-7-73	65 kt Nozzle and Throttle	1. In calm air, nozzles provide excellent glide path control. Sense is correct with respect to G/S correction for both nozzle and column.
			2. In turbulence, workload is increased but no indication of inadequate authority.
			3. In the presence of shears, pilot opinion worsens because of having to use both nozzles and power for G/S correction. Given greater authority the pilot rating would probably improve by one except for the strong tailwind.
			4. Full aft nozzles and low power on these runs combine to give one a feeling of going along for the ride--most uncomfortable.
			5. For the strong tailwind or for a shear which results in a substantial increase in IAS G/S tracking is rated 7. If an IAS error were permitted to persist the rating may fall in the minimal acceptable range -- 6.5 or slightly better.
			6. Use of nozzles for glide path control is favored over power because it is the more sensible and there is less cross coupling.

Pilot Ratings

Calm Air: 3
Turbulence: 5
Turbulence/Shears: 5

Pilot Ratings

Calm Air: 3
Turbulence: 4.5
Turbulence/Shears: 6

TABLE E-1 (Continued)

PILOT	DATE	CASE	COMMENTS
C (Cont.)	8-7-73 (Cont.)	65 kt Nozzle and Throttle (Cont.)	7. Use of nozzles over power has one serious drawback--engine failure. One tends to move nozzles in response to the sudden G/S error which is probably wrong. Perhaps training would help overcome this. 8. The use of two controls for vertical path control has serious certification implications if neither is able to handle the total approach task.
	8-8-73	65 kt DDC	1. In calm air excellent for G/S control. Authority more than adequate and sense correct. 2. In turbulence increased workload. In retrospect pilot rating should be comparable to tracking with nozzle. 3. In the presence of shears the improvement in authority [over nozzles] did not alter the prior rating [with nozzles]. Even though only one control was required [DDC] tailwinds and shears required maximum DDC authority. 4. One gets the feeling of having to wait for things to happen. Horizontal accelerations and decelerations are felt but the vertical response is slower to be realized. 5. At this point indirect vertical response caused by a change in the drag appears less appealing than the thought of direct control over vertical path [DLC].
	8-8-73	65 kt DLC	1. Workload in ILS tracking task characterized as outstanding in calm air, great in turbulence. 2. This DLC performs as the pilot expects it to, i.e.: • Direct effect on G/S error • Minimum cross coupling • Excellent response for handling shears and gusts and making last minute corrections prior to landing.

Pilot Ratings
Calm Air: 2.5
Turbulence: 5
Turbulence/Shears: 6

Pilot Ratings
Calm Air: 2
Turbulence: 4
Turbulence/Shears: 5

TABLE E-1 (Continued)

PILOT	DATE	CASE	COMMENTS
D	8-2-73	65 kt	1. Tracking the IAS using pitch was quite difficult and caused the most problems during ILS tracking. 2. Localizer tracking was easier than IAS tracking. 3. Tracking the G/S using power was the easiest task during the approach. 4. Safety margins were not a worry and the A/C had adequate performance.
			Pilot Ratings Calm Air: 3 Turbulence: 3.5 Turbulence/Shears: 3.5
	8-2-73	65 kt G/S $\longrightarrow \delta_v$ IAS $\longrightarrow \theta$	1. Gross and frequent pitch changes made airspeed control difficult. 2. The IVSI was used to set required power. 3. Nozzles were used through full range of travel. However, G/S tracking was difficult due to slow, sluggish response. 4. Localizer tracking degraded due to attention being diverted to other tasks causing problems staying on course. 5. Performance was poor and the safety margins seemed dangerous. Turbulence made the task very difficult.
			Pilot Ratings Calm Air: 5 Turbulence: 8 Turbulence/Shears: --
	8-3-73	65 kt G/S $\longrightarrow \theta$ IAS $\longrightarrow \delta_v$	1. Seems better than using G/S $\longrightarrow \delta_v$ and IAS $\longrightarrow \theta$.
			Pilot Ratings Calm Air: 4.5 Turbulence: 5.5 Turbulence/Shears: --
E	8-9-73	65 kt	1. Without turbulence high scan requirement increases pilot rating. 2. With turbulence workload becomes marginal and shears make the workload too high.
			Pilot Ratings Calm Air: 4 Turbulence: 6.5 Turbulence/Shears: 7

TABLE E-1 (Continued)

PILOT	DATE	CASE	COMMENTS
E (Cont.)	8-13-73	70 kt	1. Very similar to 65 kt case. 2. No need to increase speed over nominal for tailwind.
			Pilot Ratings Calm Air: 4 Turbulence: 6.5 Turbulence/Shears: 7
	8-14-73	75 kt	1. Tracking the same as 70 kt.
			Pilot Ratings Calm Air: 4 Turbulence: 6.5 Turbulence/Shears: 7
	8-17-73	65 kt with Flight Director	1. Flight director really helps. Provides an order of magnitude difference in workload. This director is not optimal but is very good. May need to be modified slightly to take more account of margins.
			Pilot Ratings Calm Air: 3 Turbulence: 4 Turbulence/Shears: 4.25
F	8-2-73	65 kt	1. In calm air no difficulty except that pilot must be careful about power setting prior to flare. 2. Turbulence increases tracking task dramatically to an unacceptable level. Response to power is immediate and easy to over-control.
			Pilot Ratings Calm Air: 3 Turbulence: 7 Turbulence/Shears: --

TABLE E-1 (Continued)

PILOT	DATE	CASE	COMMENTS
F (Cont.)	8-6-73	65 kt 2.5 sec τ_{ENG}	1. Degraded response appealing for VFR calm air conditions. Throttle action appeared smoother. 2. In turbulence and shear the tracking task was less precise with excursions in sink rate. 3. Primary technique was G/S with power and IAS with attitude using IVSI as primary instrument to pick up turbulence and shears and as an indicator that power was set correctly prior to flare. Use of this latter instrument produced a scan problem. 4. Cues used for power setting information are IVSI response, engine sound, and mechanical feel of throttle position. 5. The worse tracking errors get, the harder it is to return to an acceptable approach. 6. Least attention focused on localizer because of other workload. Willing to accept lateral lineup maneuvering after breakout although it has resulted in some go-arounds. NOTE: These comments generally apply to the previous case also.
	8-9-73	65 kt	1. No additional comments with respect to approach cases. Comments of previous flights apply.
	8-10-73	60 kt	1. The tailwind case presents the most difficulty. If a pilot has a fly down signal he will pull power but tends to gain speed which compounds his difficulties since he must fly down even faster. An attitude change greater than 10 deg was once made to recapture 60 kt approach speed.

Pilot Ratings

Calm Air: 3
Turbulence: 7
Turbulence/Shears: 8

Pilot Ratings

Calm Air: 3
Turbulence: 4
Turbulence/Shears: 6

Pilot Ratings

Calm Air: 2
Turbulence: 5
Turbulence/Shears: 8

TABLE E-1 (Continued)

PILOT	DATE	CASE	COMMENTS
F (Cont.)	8-13-73	70 kt	1. The required sink rate was 925 fpm; any fly down signal near the end of the approach required a sink rate in excess of 1000 fpm.
			Pilot Ratings Calm Air: 2 Turbulence: 5 Turbulence/Shears: 7
	8-14-73	75 kt	1. The general impression was that the aircraft could be more easily maneuvered to save a less than optimum approach. 2. The aircraft felt further away from the limits and more extreme maneuvers were acceptable. 3. The required sink rate was 1000 fpm; this sink rate was close to the limit of acceptability. The difference between 800-900 fpm is not so great as the difference between 900-1000 fpm and even more concern develops above 1000 fpm.
			Pilot Ratings Calm Air: 3 Turbulence: 5 Turbulence/Shears: 6
	8-16-73	65 kt with Flight Director	1. Performance was definitely superior to tracking without flight director. 2. The workload remains high because of very sensitive power and localizer command bars. These require the pilot to close very tight loops and make almost continuous power and lateral changes. 3. The improved ratings reflect the pilot's awareness that he is always very close to where he wants to be.
			Pilot Ratings Calm Air: 3 Turbulence: 4 Turbulence/Shears: 5
	8-17-73	65 kt with Flight Director	1. Large improvement on lateral flight path control which allowed the pilot to relax on the lateral needle.
			Pilot Ratings Calm Air: 2 Turbulence: 3 Turbulence/Shears: --

TABLE E-1 (Continued)

PILOT	DATE	CASE	COMMENTS
F (Cont.)	8-17-73	65 kt Configuration SAS Only	

Pilot Ratings
Calm Air: --
Turbulence: 6
Turbulence/Shears: --

G	8-17-73	65 kt	1. Calm air was easy. No problems with adequate performance. 2. In turbulence tracking became more difficult and the workload was excessive in shears. Safety margins were borderline for the final portion of the approach/flare in turbulence/shears. 3. A flight director would be a real help and possibly a must for this aircraft; it would improve the ILS tracking rating. 4. Main problem was to arrive at DH on G/S and aligned so as not to make further adjustments and maneuvering. Was reluctant to transition to visual scene and stayed on instruments longer than necessary.

Pilot Ratings
Calm Air: 2
Turbulence: 3.5-4.0
Turbulence/Shears: 4.5

H	8-7-73	65 kt	1. In calm air the aircraft is easy to fly. 2. In turbulence there appears to be no interaction between speed and trajectory control for small corrections. This lack of interaction makes the aircraft easy to fly. 3. Wind shears were easily controlled by adjusting power although below 100 ft it was difficult to remain exactly on glide path. For headwinds the error is acceptable.

Pilot Ratings
Calm Air: 2
Turbulence: 2
Turbulence/Shears: 4

	8-8-73	65 kt All SAS Off	1. The main problem is in the lateral control, especially in turbulence; constant attention is needed to keep the wings level. 2. With all SAS off the aircraft is unacceptable and is rather unstable. 3. With roll and yaw SAS on the aircraft would be uncomfortable but acceptable from the safety point of view.

Pilot Ratings
Calm Air: 7
Turbulence: 7
Turbulence/Shears: 7

TABLE E-1 (Continued)

PILOT	DATE	CASE	COMMENTS
H (Cont.)	8-8-73	65 kt 3.0 sec T_{ENG}	1. Below the glide slope the tendency is to overcorrect with power when the pilot wants to come back quickly; it is then difficult to get the power set correctly and the aircraft back on the glide path. 2. Nearing landing, the pilot is unable to get enough power on command and the situation further deteriorates with still more power being required. This is unacceptable.
Pilot Ratings Calm Air: 2 Turbulence: 3 Turbulence/Shears: 6			
	8-8-73	65 kt G/S ⟶ δ_ν IAS ⟶ θ	1. Works satisfactorily for small corrections but large corrections require great nozzle changes. 2. To hold speed constant, pitch attitude must be changed markedly which is somewhat annoying. 3. Would have preferred a control with more authority.
Pilot Ratings Calm Air: 2 Turbulence: 4 Turbulence/Shears: 6			
	8-9-73	55 kt	1. There was a noticeable speed instability. Pitch attitude changes to maintain speed were greater here than at 65 kt. 2. Errors in glide path took longer to correct and required greater power changes. On some occasions the power was reduced to 89% making the margin to V_{min} very small. 3. There is a marked cross coupling between the (G/S ⟶ δ_{N_H} and IAS ⟶ θ), which leads to a great increase in workload.
Pilot Ratings Calm Air: 4 Turbulence: 5 Turbulence/Shears: 6			
	8-9-73	65 kt DDC STOL Technique	1. All approach cases were successfully flown.

TABLE E-1 (Concluded)

PILOT	DATE	CASE	COMMENTS
H (Cont.)	8-9-73	65 kt DDC IAS ⟶ DRAG G/S ⟶ θ (CTOL Technique)	1. This technique better with DDC than the STOL technique. 2. The control is acceptable.
	8-9-73	65 kt DLC G/S ⟶ DLC IAS ⟶ θ	1. Control suffers from lack of authority. 2. Control is easy to use.

TABLE E-2

SUMMARY OF PILOT COMMENTS ON FLARE

PILOT	DATE	CASE
A	8-1-73	65 kt

Pilot Ratings

Calm Air: 4
Turbulence: 5
Turbulence/Shears: 6

COMMENTS

1. In smooth air no real problem though h and $\dot{h}$ estimation poor at the start (these improved markedly during this series of runs).
2. Turbulence and shears produced problems in heave due to large power changes required just prior to or during the flare. The result was an oscillatory heave tendency which could be damped to some extent but only at the expense of runway [X_{TD}].
3. Even without shear, the touchdown point and flare profile were critically dependent on power setting at flare initiation.
4. There was a reluctance to make a power change because of the heave oscillation tendency and this tendency was considered to be due largely to thrust lag [overall lag in heave response due to power change]. This lag cannot be tolerated in a tight control loop as in the flare though it can be perfectly acceptable in the approach.
5. Crosswinds produced no real problems. Drift kicked off slowly starting at flare initiation. On occasion workload of decrab resulted in insufficient attention to pitch thus heavy touchdowns.
6. Lateral offsets at breakout (200 ft) could be corrected with surprising ease with the lateral field of vision being the limiting factor.
7. There was no problem of overcontrolling pitch in the flare. The ADI was not generally used in the flare.
8. The flare height was reduced from 50 ft to 30-35 ft.
9. At the correct trim power setting margins available in flare were thought to be low considering abuses such as a late hard flare. The controllability safety margin was inadequate considering the oscillatory situation.
10. The outstanding feature which would prevent certification would be the thrust lag/heave oscillation problem.

TABLE E-2 (Continued)

PILOT	DATE	CASE	COMMENTS
A (Cont.)	8-2-73	65 kt τ_E = 1.5 sec	1. Any difference in ratings between this and previous case are not considered significant. Learning curve is one explanation.

Pilot Ratings
Calm Air: 3 - 3.5
Turbulence: 5
Turbulence/Shears: 5.5

	8-2-73	55 kt	1. There just wasn't enough lift margin to cope with any abuse cases. A long hard flare at about 30 ft generally gave acceptable sink rates but pitch attitude at touchdown was high (15 deg + and almost view limiting). Angle of attack reached was 20-23 deg indicating little margin.
			2. The vertical eye distance travelled when lowering the nosewheel indicated a much longer arm than claimed (22 ft).

Pilot Ratings
Calm Air: 6
Turbulence: 7 - 8
Turbulence/Shears: --

	8-3-73	75 kt	1. The much greater margin available led to a complete flare and prolonged float.
			2. Previous cases (65 kt) might have required less accurate height judgment towards the end of the flare as there was no requirement to feel your way onto the ground following a complete flare.
			3. In the turbulence cases there seemed to be a definite improvement in height estimation and there were fewer prolonged floats.
			4. Power setting at flare initiation was still critical.

Pilot Ratings
Calm Air: 4
Turbulence: 5
Turbulence/Shears: --

	8-3-73	65 kt Nozzle Using STOL and CTOL Techniques	

Pilot Ratings
Calm Air: 4
Turbulence: 6
Turbulence/Shears: 8

TABLE E-1 (Continued)

PILOT	DATE	CASE	COMMENTS
A (Cont.)	8-3-73	55 kt δ_ν = 50 deg	1. Very poor view -- +7 deg θ during approach and +15 deg at touchdown.

Pilot Ratings
Calm Air: 6.5
Turbulence: 7
Turbulence/Shears: 9

	8-3-73	65 kt DDC
B	8-7-73	65 kt

1. Smooth air task is relatively easy and straight forward with good repeatability.
2. More precise use of power required in flare and landing with turbulence and shears with considerable pilot workload. Very tight use of power since any power change will produce unpredictable results in touchdown sink rate and distance. The problem appears to be caused by the power lag in combination with an unreasonable sensitivity to small power changes.
3. Flare was initiated at 50 ft with a smooth and steady (firm) pitch up to approximately 12 deg. 12 deg was maintained until touchdown; never attempting to reduce pitch attitude during the flare although there is quite often the urge to do so.

Pilot Ratings
Calm Air: 4
Turbulence: 5 - 5.5
Turbulence/Shears: 5

	8-7-73	65 kt All SAS Off

Pilot Ratings
Calm Air: 4
Turbulence: 9
Turbulence/Shears: --

TABLE E-2 (Continued)

PILOT	DATE	CASE	COMMENTS
B (Cont.)	8-10-73	60 kt	1. The flare and landing in calm air was also as easy as 65 kt provided a slight flare adjustment from the 65 kt case is made. The flare must be initiated approximately 15-20 ft lower and the pitch up maneuver must be smooth and rapid. Good safety margins; pilot workload minimal. 2. There was very little or no safety margin in flare and landings with turbulence and winds. The pilot does not have adequate time to compensate for cross winds prior to touchdown. 3. With turbulence and shears the sink rate was very difficult to control. The response was too sluggish which made it impossible to maintain good control during the flare. 4. Would require very precise piloting at all times - operationally unacceptable.
			Pilot Ratings Calm Air: 4 Turbulence: 8 Turbulence/Shears: 8
	8-13-73	60 kt	
			Pilot Ratings Calm Air: -- Turbulence: 6 Turbulence/Shears: --
	8-13-73	70 kt	1. Very close to a conventional aircraft; knew exactly when the airplane was ready to touch down.
			Pilot Ratings Calm Air: 3 Turbulence: 4 Turbulence/Shears: 4.5

TABLE E-2 (Continued)

PILOT	DATE	CASE	COMMENTS
C	8-6-73	65 kt	1. Flaring with constant thrust gave critical and inconsistent performance in calm air. By using a slight power increase prior to, during, or immediately following flare, the sink rate is broken nicely. 2. With turbulence the workload is significantly higher, but the power response is excellent permitting gust compensation during and following the flare. The increases in pilot ratings is primarily related to the reluctance to pull power off during and following the flare. 3. There was an inability or reluctance to reduce power in the flare when shears are present. The apparent ground speed with tailwind causes one to fly beyond the touchdown zone. 4. Safety margin awareness occurred during the landings with tailwind when insufficient elevator authority remained to ease the nose down. 5. Airspeed became quite low on flare -- two occasions it was less than 45 kt. 6. On one crosswind landing full rudder travel was used. 7. Piloting technique was based on closed loop with visual scene for flare and power/attitude control following flare, minimum repeatable sink rate when attitude was stabilized appeared to be about 3 fps. 8. The only real problem was the high rate of closure with the touchdown zone in a tailwind; for a STOL runway performance was not adequate.

Pilot Ratings

Calm Air: 3
Turbulence: 5.5
Turbulence/Shears: 7

TABLE E-2 (Continued)

PILOT	DATE	CASE	COMMENTS
C (Cont.)	8-7-73	G/S ⟶ δ_ν (in ILS tracking) G/S ⟶ δ_T (in flare) IAS ⟶ θ	1. Shift from nozzles to power as the flare window is approached; there is no reason to hasten the transition from nozzles to power. Some care must be exercised to preclude over-controlling power. 2. Primary difficulty is hitting the flare window consistently (poor tracking performance) which in turn causes a wide variation in nozzle/throttle settings which defeat consistent landing performance. This problem is aggravated by adding too much power in the flare which at times causes the aircraft to hang uncomfortably above the runway. 3. The tailwind again is the least tolerable; killing off 10 kt tailwind seems almost impossible. 4. Power response is excellent and permits most shears to be handled readily. 5. A heads-up energy indication would be helpful in power management in and following the flare.
	8-8-73	G/S ⟶ Direct Drag Control IAS ⟶ θ	1. Excellent for flare when pilot hits the window. Control can be used to maintain IAS and thus sustain lift or increase IAS though the latter is a questionable action since it would adversely affect landing performance. 2. Some very slight improvement over basic machine with nozzles, but limited authority still requires the use of power under high rate conditions. 3. Maximum drag did result in better control of tailwinds and shears. On several occasions the flare window was missed but an acceptable landing was still possible principally because the power was not changed.

Pilot Ratings

Calm Air: 3
Turbulence: 5
Turbulence/Shears: 6.5 - 7

Pilot Ratings

Calm Air: 2.5 - 3
Turbulence: 4.5
Turbulence/Shears: 6

TABLE E-2 (Continued)

PILOT	DATE	CASE	COMMENTS
C (Cont.)	8-8-73	G/S ⟶ Direct Lift Control IAS ⟶ θ	1. DLC provides a good means of flaring the aircraft. 2. There can be no question that the direct lift control simulated performs as the pilot expects it. 3. Provides excellent response for handling shears and gusts and making last minute corrections prior to touchdown.

Pilot Ratings
Calm Air: 2
Turbulence: 4
Turbulence/Shears: 5

D	8-2-73	65 kt	1. The flare and landing was quite easy in calm air. Performance was adequate and fairly consistent; it seemed to improve with practice. The safety margin seemed adequate. 2. In turbulence, flare and landing became harder - however performance was still adequate although there was less precision. 3. A slight increase in power (1%??) about 45 ft seemed to help. 4. A fairly slow and smooth pitch rate at about 45 ft was used. The high pitch angle did not cause a problem. Runway scene was used to start flare. 5. The yellow 'bug' light on the radar altimeter provides reassurance that the flare should be initiated. 6. The VASI light was extremely useful for getting into the slot. 7. There was no problem in recognizing a good flare attitude but there was some very minor uncertainty about where the touchdown would occur.

Pilot Ratings
Calm Air: 4
Turbulence: 5 - 6
Turbulence/Shears: 5 - 6

	8-3-73	G/S ⟶ δ_ν IAS ⟶ θ^ν	1. The flare and landing were the hardest tasks because of the slow flight path response. 2. Sometimes it was impossible to land unless the power was reduced. (It was not supposed to be used other than to establish trim power). During one flare it was necessary to switch to power after full aft nozzle failed to stop the sink rate. 3. Turbulence made flare and landing hopeless.

Pilot Ratings
Calm Air: 6
Turbulence: 9.5 - 10
Turbulence/Shears: --

TABLE E-1 (Continued)

PILOT	DATE	CASE	COMMENTS
D (Cont.)	8-3-73	G/S → θ IAS → δ_ν	
Pilot Ratings Calm Air: -- Turbulence: 7.5 Turbulence/Shears: --			
E	8-9-73	65 kt	1. Used θ for primary flare control, some help with throttle. 2. Difficult to control X and ḣ on the simulator -- probably due to poor visual cues.
Pilot Ratings Calm Air: 3 Turbulence: 4.5 Turbulence/Shears: 5			
	8-13-73	70 kt	1. Pretty much the same as 65 kt. Better flareability in the tail-wind case though no need to increase speed over nominal for tail-wind.
Pilot Ratings Calm Air: 3 Turbulence: 4.5 Turbulence/Shears: 5			
	8-14-73	75 kt	1. Smooth air flare is a little harder because of the tendency to float. 2. For rough air flare, the tendency to float is lost in the turbulence noise.
Pilot Ratings Calm Air: 4 Turbulence: 4.5 Turbulence/Shears: 5			

TABLE E-2 (Continued)

PILOT	DATE	CASE	COMMENTS
E (Cont.)	8-14-73	Calm Air Varying Approach Speed Approach From 200 ft Altitude Initial Condition	1. At 75 kt a slight tendency to float. Looks like by reducing power slightly the problem could be overcome. 2. Both 65 kt and 70 kt feel pretty good in smooth air. I get the feeling that there is not too much reserve at 65 to handle disturbances. 3. 55 kt and 60 kt require increasing amounts of power in the flare to be comfortable. Really no problem in smooth air. 4. 50 kt is beginning to feel marginal even with power addition during flare. Flare is almost totally being done with power.
			Pilot Ratings Calm Air: 75 kt: 4 50 kt: ~ 6
F	8-2-73	65 kt	1. Pilot must be extra careful of where he has placed his power prior to flare. If he is tracking a fly down signal late in the approach and does not kill off the extra sink rate prior to the flare, he is apt to hit hard, or conversely, to over-fly the touchdown zone if he adds power to fly up.
			Pilot Ratings Calm Air: 4 Turbulence: 6 Turbulence/Shears: --
	8-6-73	65 kt Degraded Engine Response (2.5 sec lag)	1. In calm air the task appears less consistent than the ILS tracking. 2. Most importantly, the pilot must have the proper precise power setting needed to assure that the flare, touchdown sink rate, and touchdown distance come out right. 3. Turbulence and shears have a marked adverse effect on the pilot's ability to perform consistently in either TD sink rate or zone because of his condition and position when entering the flare. 4. Technique used was to set RAD ALT DH to 50 ft and then, based on power setting and/or IVSI sink rate and visual cues just prior to flare, to play both rate and degree of rotation during the flare. Also it was necessary after the flare to see whether a power reduction might be necessary to prevent over flying the touchdown zone. This is most difficult in shears since the pilot has only vague cues to help him know to set power to stop the sink rate.
			Pilot Ratings Calm Air: 4 Turbulence: 6 Turbulence/Shears: 7

TABLE E-2 (Continued)

PILOT	DATE	CASE	COMMENTS
F (Cont.)	8-6-73 (Cont.)	65 kt Degraded Engine Response (2.5 sec lag) (Cont.)	5. Flare and landing difficulties are compounded when having to do much of a maneuver to line up after breakout. The drift correction for crosswind is particularly difficult because you have only a few seconds to sort it out. 6. By far the largest problem is to get enough information on what to do with power. If the pilot has too much power in the flare and over flies the touchdown zone he loses some of the reference to the runway and must use up many feet of runway as he gently reduces power and plays with his flare -- a bad place to be.
	8-10-73	60 kt	1. If pilot is faced with a fly down signal he pulls power but tends to gain speed which compounds his difficulties since he must fly down even faster. 2. Major difficulty was a tendency to land short and hard.
	8-13-73	70 kt	1. At this speed you tend to overfly the touchdown zone and the pilot tends to pull power very slowly in his attempt to feel for the ground in his flared attitude. Most landings were long and some touchdown sink rates exceeded 10 fps. 2. Flare and landing is more difficult at this speed if you are trying to hit the touchdown zone. Pilot must flare and learn to pull just the right amount of power in order to hit touchdown zone. This was not the case at 60 or 65 kt.

Pilot Ratings

Calm Air: 3
Turbulence: 6
Turbulence/Shears: 8

Pilot Ratings

Calm Air: 4
Turbulence: 7
Turbulence/Shears: 9

TABLE E-2 (Continued)

PILOT	DATE	CASE	COMMENTS
F (Cont.)	8-14-73	75 kt	1. Technique for flare and landing changed on this flight resulting in a consequent improvement in consistent performance. a. Old Technique: Nose high (10-12 deg) flare and trying to correct overshooting touchdown zone by reducing power after the flare. Very difficult due to poor depth perception (visibility over nose and tendency to land hard if 'bit' [about 1%] too much throttle is removed). b. New Technique: Flare higher (70 deg on RAD ALT) and flare enough to reduce $\dot{h}$ to acceptable level. Nose up attitude 2-4; no power corrections needed - adjusted $\dot{h}$ with θ. 2. Ratings at this speed are generally slightly better than at 60 or 65 kt due to a. The changed flare technique b. A general impression that I could more easily maneuver the airplane to save a less than optimum approach.
	8-16-73	65 kt with Flight Director	1. The slightly better rating for turbulence was a result of flying consistently to a good window for landing. 2. Power command of the Flight Director flies the pilot to his window with a close to proper power setting for landing.
G	8-17-73	65 kt	1. No difficulty in calm air. 2. Performance/safety margins were satisfactory in turbulence provided aircraft was aligned on glide slope and speed prior to decision height. If abused, final adjustments were necessary which unbalanced the approach in a critical stage. This was even more critical when shears were present.

Pilot Ratings

Calm Air: 3
Turbulence: 5
Turbulence/Shears: 7

Pilot Ratings

Calm Air: 3
Turbulence: 4
Turbulence/Shears: 6

Pilot Ratings

Calm Air: 2
Turbulence: 3
Turbulence/Shears: 5.5

TABLE E-2 (Concluded)

PILOT	DATE	CASE	COMMENTS
H	8-6-73	65 kt	1. The calm air flare rather difficult. It is possible to detect an error and to correct it mainly by using power. The great change in pitch makes the maneuver difficult to do precisely and the result is just acceptable. 2. Flare is initiated from a very low height (30 to 40 ft). 3. Power is a very important parameter. Minus 1% error leads to a hard landing, +2% you never land. This is not too satisfactory.
	8-9-73	55 kt	1. Flares were found to be somewhat more difficult than at 65 kt.

Pilot Ratings

Calm Air: 3
Turbulence: 4
Turbulence/Shears: 6

Pilot Ratings

Calm Air: 5
Turbulence: --
Turbulence/Shears: --

GPO 855-923